Interactions of the Totten Glacier with the Southern Ocean through multiple glacial cycles (IN2017-V01):Post-survey report

14th January – 5th March 2017.

L.K. Armand, P.E. O'Brien and On-board Scientific Party*.

(* L. Armbrecht, H. Baker, A. Caburlotto, T. Connell, D. Cotterle, M. Duffy, S. Edwards, D. Evangelinos, J. Fazey, A. Flint, A. Forcardi, S. Gifford, L. Holder, P. Hughes, K-A. Lawler, J. Lieser, A. Leventer, M. Lewis, T. Martin, N. Morgan, A. Lopez Quiros, K. Malakoff, T. Noble, B. Opdyke, R. Palmer, R. Perera, V. Pirotta, A. Post, R. Romeo, J. Simmons, D. Thost, S. Tynan and A. Young)

Published by Research School of Earth Sciences, College of Science, The Australian National University, Canberra, ACT, Australia.

Acknowledgements
We thank the Marine National Facility, the IN2017-V01 scientific party-led by the Chief Scientists L.K. Armand and P. O'Brien, MNF support staff and ASP crew members led by Capt. M. Watson for their help and support on board the RV *Investigator*.

This Project is supported through funding from the Australian Government's Australian Antarctic Science Grant Program (AAS #4333) and the Australian Research Council's Discovery Projects funding scheme (DP170100557).

Preferred Citation:
L.K. Armand, P.E. O'Brien and On-board Scientific Party. 2018. Interactions of the Totten Glacier with the Southern Ocean through multiple glacial cycles (IN2017-V01): Post-survey report, Research School of Earth Sciences, Australian National University: Canberra, http://dx.doi.org/10.4225/13/5acea64c48693

Front cover photo. The RV *Investigator* sailing past an iceberg in East Antarctic waters during Expedition IN2017-V01. Photographer: D. Thost/MNF.

CONTENTS

SECTION 1. Introduction and Mission

INTRODUCTION

The Sabrina Sea Floor Survey was a major marine geoscience expedition to the Antarctic margin which took place between 14 January and 7 March 2017. It sailed on the Australian Marine National Facility vessel *RV Investigator*. This document describes survey activities, data collected on the ship and important metadata. Some preliminary results are included and the location of samples and data sets reported for future use. The report also provides information on data ownership and acknowledgement for future use and publication. It is intended as an aid to future research and use of results and has not been rigorously edited and peer-reviewed.

DATA MANAGEMENT

MNF equipment

All raw and processed data acquired by MNF equipment on MNF voyages will be archived by MNF data support staff in the enduring CSIRO Data Access Portal, https://data.csiro.au. Metadata records will be made publicly available at http://www.marlin.csiro.au. Processed data and data products will be made publicly available through Data Trawler http://www.cmar.csiro.au/data/trawler/index.cfm, the MNF web data access tool http://www.cmar.csiro.au/data/underway/, and/or from national or world data centres most suitable for the dissemination of particular data types.

All Metadata entries should list this requested acknowledgement statement where the data is presented or published.

> *"We thank the Marine National Facility, the IN2017-V01 scientific party-led by the Chief Scientists L.K. Armand and P. O'Brien, MNF support staff and ASP crew members led by Capt. M. Watson for their help and support on board the RV Investigator"*

User supplied equipment

Data acquired with user-supplied equipment on MNF Granted Voyages must also be managed in compliance with the MNF Data Management Policy.

All raw data and other material collected or worked upon by researchers on board is to be suitably described and included in the voyage record. Metadata records and raw or processed data are to be made available on the ship network for backup and to be included in the End of Voyage Archive.

Raw data must be provided to the MNF for archiving if it is not archived in a domain-specific international repository. The data must be made publicly available as soon as possible following a voyage and at most within 12 months of voyage completion.

CORE REPOSITORIES

Sediment cores acquired during the survey are archived at the Geoscience Australia marine sediment sample repository, Symonston, Australian Capital Territory. All samples taken on board are listed in Appendix 1.

RESEARCH PUBLICATIONS AND ACKNOWLEDGEMENTS

Records of publications and information products arising from MNF Voyages should be supplied to the MNF in an appropriate format as soon as possible after completion.

The MNF must be acknowledged in all research publications derived from research performed and data collected on the MNF with the following statement:

> *"The authors wish to thank the CSIRO Marine National Facility (MNF) for its support in the form of sea time on RV Investigator, support personnel, scientific equipment and data management. All data and samples acquired on the voyage are made publicly available in accordance with MNF Policy."*

SPONSORSHIP ACKNOWLEDGEMENTS

Marine National Facility

The MNF must be acknowledged in all research publications derived from research performed and data collected on the RV *Investigator* with the following statement:

> *"The authors wish to thank the CSIRO Marine National Facility (MNF) for its support in the form of sea time on RV Investigator, support personnel, scientific equipment and data management. All data and samples acquired on the voyage are made publicly available in accordance with MNF Policy."*

Australian Antarctic Division (AAS #4333)

The Australian Antarctic Division one of two major supporters of the science underpinning this research mission. The grant title is entitled "*Interactions of the Totten Glacier with the Southern Ocean through multiple glacial cycles*" and the PI's are: Armand, L.K. O'Brien, P., Post, A., Goodwin, I., Opdyke, B., Leventer, A., Domack, E., Escuita-Dotti, C. & DeSantis, L.
All research published through the support of this grant should be acknowledged with the following statement:

> *"This Project is supported through funding from the Australian Government's Australian Antarctic Science Grant Program (AAS #4333)".*

Australian Research Council Discovery Project (DP170100557)

The Australian Research Council is the second of the two major supporters of the science underpinning this research mission. The grant title is entitled "*Applying multidisciplinary methods to resolve past Antarctic sea-ice extent.*" and the PI's are: L. Armand, S. George, S. Belt, P. Heraud, C. Bowler, & J. Beardall.

The ARC recommends following one of the following formats for appropriate acknowledgment of the support provided to research undertaken through this grant dependent on circumstance and content.

> *"This research was funded by the Australian Government through the Australian Research Council (DP170100557)."*

However, in cases where the material or publication contains a message or view which could possibly be interpreted as being that of the ARC, and which has not been officially endorsed by the ARC as such, the following form of attribution is required:

> *"This research was supported by the Australian Government through the Australian Research Council's Discovery Projects funding scheme (DP170100557). The views expressed herein are those of the authors and are not necessarily those of the Australian Government or Australian Research Council."*

International Program Support

Three additional international Antarctic programs supported the mobilisation of personnel and equipment for the voyage, and the research undertaken post-cruise. These include the following:

1. **Italian Antarctic program support PNRA TYTAN Project** (PdR 14_00119) Project Title: Totten Glacier dYnamics and Southern Ocean circulation impact on deposiTional processes since the mid-lAte CeNozoic (TYTAN). Researchers involved: F. Donda & A. Carburlotto.
2. **Spanish Ministry of Economy and Competitivity (MINECO)** (CTM2015-60451-C2-1-P & CTM2015-60451-C2-2-P)**.** Project Title: The Tasman and Drake gateways and the Antarctic Circumpolar Current: origin, evolution and its effect on climate and Antarctic ice sheet evolution and Geodynamic Evolution of the Tasman

and Drake Gateways: onshore-offshore tectonic correlation of continental margins and oceanic basins. Lead Researcher: C. Escutia-Dotti.

3. **United States National Science Foundation's Polar Program - Antarctic Integrated System Science.** #1143834, 1143836, 1143837, 1143843, 1313826. Project Title: *Totten Glacier System and the Marine Record of Cryosphere - Ocean Dynamics*. Researchers involved: A. Leventer, D. Blankenship, G. Domack, S. Gulick, B. Huber, A. Orsi, & A. Shevenell.

Other Australian Program Support

Smaller projects have attracted funding to support research activities post-cruise these include the following:

1. **Australian and New Zealand IODP Committee (ANZIC) Special Analytical Support Grant**. Project Title: *Using ancient phytoplankton communities and genes to illuminate future ocean responses*. Researchers involved: L. Armand, L. Armbrecht, M. Ostrowski, & S. George.
2. **Australian Antarctic Division Australian Antarctic Science Grant** (#4320). Project Title: *Characterising East Antarctic seabed habitats.* Researchers involved: Post, A.L., & Smith, J.
3. **Australian Antarctic Division Australian Antarctic Science Grant** (#4419). Project Title: *Response of the Totten Glacier to past climate warming.* Researchers involved: Noble, T., Armand, L., Chase, Z., & Halpin, J.

VOYAGE PARTICIPANTS

Science Party

Associate Professor Leanne Armand, Macquarie University, Co-Chief Scientist
Dr Philip E O'Brien, Macquarie University, Co-Chief Scientist
Dr Alix Post, Geoscience Australia
Dr Bradley Opdyke, Australian National University
Prof Amy Leventer, Colgate University, USA
Megan Duffy, Colgate University, USA.
Dr Andrea Caburlotto, Istituto Nazionale di Oceanografia e di Geofisica Sperimentale (OGS) Italy.
Roberto Romeo, Istituto Nazionale di Oceanografia e di Geofisica Sperimentale (OGS) Italy
Diego Cotterle, Istituto Nazionale di Oceanografia e di Geofisica Sperimentale (OGS) Italy
Dr Taryn Noble, University of Tasmania
Dr Linda Armbrecht, Macquarie University
Vanessa Pirotta, Macquarie University
Amaranta Focardi, Macquarie University
Kelly-Ann Lawler, Macquarie University
Liam Holder, Australian National University
Rushi Perera, Australian National University
Dr Sarah Tynan, Australian National University
Adrian López-Quirós, University of Granada, Spain
Dimitrios Evangelinos, University of Granada, Spain
Jack Simmons, University of Wollongong

CSIRO-Marine National Facility Personnel

Stuart Gifford, Taroona High School, Tasmania
Asaesja Young, Communications/Photographer
Mark Lewis, SIT support – Deck Mechanic
Jason Fazey, SIT support – Deck Mechanic
Tara Martin, GSM support
Stewart Edwards, GSM support
Karl Malakoff, DAP support
Hugh Barker, DAP support
Peter Hughes, Hydrochemistry support
Rod Palmer, SIT support
Nicole Morgan, SIT support

ASP Officers and Crew
Michael Watson, Master
Roderick Quinn, Chief Officer
Adrian Koolhof, Second Officer
Andrew Roderick, Third Officer
Gennadiy Gervasiev, Chief Engineer
Sam Benson, 1st Engineer
Ian McDonald, 2nd Engineer
Damian Wright, 3rd Engineer
Shane Kroncamp, E/Engineer
Jonathan Lumb, Chief Integrated Rating
Dean Hingston, IR
Christopher Dorling, IR
Murray Lord, IR
Matthew McNeill, IR
Kel Lewis, IR
Darren Kapon, IR
Rebecca Lee, Chief Cook
Matthew Gardner, Cook
Alan Martin, Chief Steward
Emma Lade, Steward

AIMS, CONTEXT AND SUMMARY

Aims

The primary aims of the Sabrina Seafloor Survey were:

1. To improve the understanding of the interactions of the Totten Glacier with the Southern Ocean over multiple glacial cycles.
2. Improve understanding of benthic habitats in the area by collecting multibeam, subbottom profiler data and sediment data.

The interpretation of the sediments was to be enhanced by additional water sampling for a variety of palaeoceanographic, microbiological, genomic and geochemical that would enable hydrochemical characterisation.

The aims were to be achieved by systematic mapping and sampling of key areas on the continental slope between 113°E and 122°E (Fig. 1A). Provision was made in the voyage plan to also survey and sample an area on the continental shelf in the case the shelf was ice free as occurred in the summer of 2015-2016 (Fig. 1B). However, such low sea ice extent was not repeated in 2016-2017 so the survey concentrated on the slope.

A

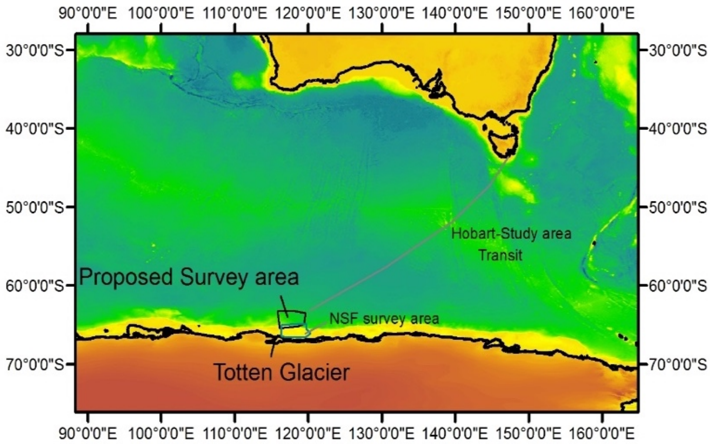

B

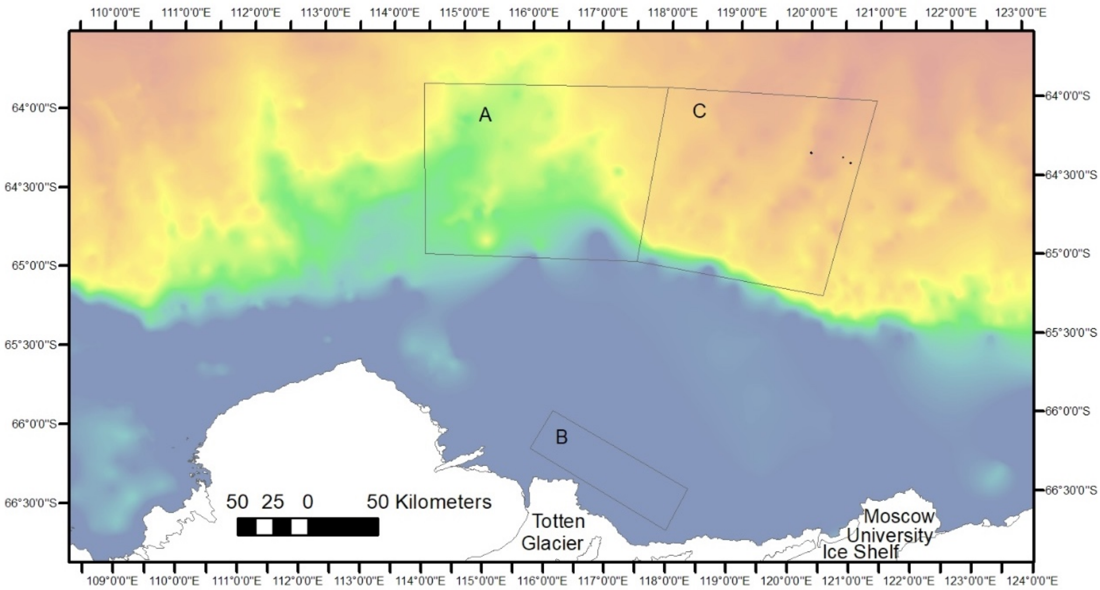

Figure 1. Location of the Sabrina Coast and planning areas for the Sabrina Seafloor Survey. *A) Sabrina Coast relative to Australia. B) Planned survey areas. Area B was added in case the shelf was ice-free and was not visited. Bathymetry from IBSCO.*

Sea floor surveying methods used comprised multibeam bathymetry, subbottom profilers, and seismic reflection profiling to give integrated acoustic imagery of sea floor sediments. Sediments were sampled using a kasten corer, piston corer and multicorer. In addition to sediment samples, the water column was sampled by CTD cast, sampling from the underway sampling lines and plankton net hauls to provide oceanographic and biological information to assist in calibrating sediment sample analysis. The ship's underway oceanographic sensors were also logged as was the gravity meter.

The habitat mapping component was to be achieved using the multibeam bathymetry and sediment samples with the addition of sea floor video tows in likely significant areas which were shallow enough to be reached by the equipment available.

Context
The understanding of climate processes and the trajectory of possible future changes and their impacts is partly dependent on insights from palaeoclimate records. The Intergovernmental Panel on Climate Change (IPCC) reports devote a chapter to the palaeoclimate record and its implications for understanding natural variability and processes of change (Masson-Delmotte et al., 2013). Our awareness of abrupt climate change is almost entirely dependent on palaeo records from ice and sediment cores (Alley et al., 2003).

Quantifying the amount and rate of sea level rise associated with global warming also depends on understanding how key parts of the Antarctic Ice Sheet respond to warming. There is still significant uncertainty in this field. The IPCC AR5 Sea Level Chapter (Church et al., 2013) states "Significant challenges remain in the process-based projections of the dynamical response of marine-terminating glaciers and marine-based sectors of the Antarctic ice sheet." and "There is currently low confidence in projecting the onset of large-scale grounding line instability in the marine-based sectors of the Antarctic ice sheet." Ice sheet response to climate forcing can be elucidated by examining how the ice sheet has behaved in the past. In spite of significant effort, AR5 Palaeoclimate chapter expresses only medium confidence in estimating the contribution of Antarctic ice melt to sea levels during the last major warm episode, the Last Interglacial. Their specific comment is: "In summary, no reliable quantification of the contribution of the Antarctic ice volume to LIG sea level is currently possible" (Masson-Delmotte et al., 2013).

The Totten Glacier is recognised as potentially the largest drainage system in East Antarctica most sensitive to climate change (e.g. Aitken et al., 2014, Pritchard et al., 2009). It is the downstream end of a vast subglacial basin, the Aurora Basin, most of which is below sea level (Roberts et al., 2011, Young et al., 2011). This subglacial topography suggests that rapid retreat of the Totten grounding line into the Aurora Basin could see rapid draw down of ice with a sea level effect equivalent to the whole of the West Antarctic Ice Sheet (Blankenship, pers. comm. 2011). The understanding of the Totten Glacier's behaviour in response to global warming has all the uncertainties listed by IPCC AR5. The importance of the Totten Glacier and Aurora Basin in understanding ice sheet behaviour and sea level change is such that a series of multinational research programs are under way. An airborne geophysical program has been mapping the geometry of the bed of the ice sheet in the Aurora Basin and the Totten Glacier (Young et al., 2011) and a marine survey by the US NSF vessel the NB Palmer mapped and sampled the continental shelf in early 2014 (NBP 1402 Scientific Party, 2014).

Surveys of the sea floor seaward of outlet glaciers can be used to understand ice behaviour. Mapping and dating of sea floor landforms on the shelf the downstream end of outlet glaciers can indicate how rapidly the glacier retreated after the Last Glacial Maximum (e.g. Cofaigh et al., 2008, Mackintosh et al., 2011, Smith et al., 2011). Sediments on the continental slope can record timing of ice advances and retreats and contain evidence of the oceanic water masses in contact with the sediments and the ice during these episodes (Weber et al., 2011). The slope can preserve sedimentary records of multiple glacial cycles, whereas the shelf typically retains only the post-LGM record. Studies of rapidly retreating outlet glaciers in the Amundsen Sea have shown a major role for a warm water mass known as Modified Circumpolar Deep Water (MCDW) which flows onto the shelf from the deep ocean and enhances melting (Jenkins et al., 2010, Smith et al., 2011, Pritchard et al., 2012). This process has also been suggested as a cause of rapid melting of the Totten Glacier (Pritchard et al., 2012, Williams et al., 2011). Pritchard et al., (2012) invoke changes in the circum-Antarctic wind field and its effects on upwelling around the continent as the cause of Totten Glacier rapid basal melting. Gwyther et al. (2014) and Khazendar et al. (2013) argue that this enhanced melting is the result of complex interactions between oceanic and shelf water masses and the base of the ice. They suggest that the melting is strongly modulated by cold High Salinity Shelf Water formed in polynyas to the east of the Totten Glacier and channelled by local bathymetry to the base of the glacier. These studies rely heavily on satellite observations and bathymetry of the regions. Gwyther et al. (2014) relied on GEBCO bathymetry for oceanographic models with 1 km grid resolution. The GEBCO grid has 2 ship tracks in the critical 150 km by 200 km area seaward of the Totten Glacier, meaning that most of the grid is a "best guess".

Marine geoscience surveys to the area can help resolve the likely processes by obtaining better bathymetry and collecting sediment cores that contain records of polynya activity, current strength over time and the likely source of water masses at locations across the shelf and slope. In particular, sediment cores can answer the question; will a warmer climate produce more polynyas which will then suppress basal melting of the Totten Glacier?

SUMMARY OF IN2017-V01

Transits

The *RV Investigator* departed Hobart at 1800 AEST on 14 January 2017. This represented an 8 hour delay on advice from the Master that leaving on time would see us encounter 11 m waves and high winds, making for minimal progress for significant fuel expenditure. Rough seas were encountered for the first two days. The rest of the transit south was uneventful with multibeam, sub-bottom profiler and gravity data collected and laboratories set up. Areas of interesting multibeam data were noted around the mid ocean ridge and the abyssal plain north of Antarctica where unprocessed backscatter images suggested current scouring and reworking of the sea floor. The NE corner of the survey area was reached on 20 January 2017.

The return transit commenced on 24 February with vessel following an easterly course to 122°53′ E, 65°23′ S where a CTD cast was completed to repeat a station visited by a previous US survey. The RV *Investigator* then headed for Hobart, attempting to follow a track adjacent to but not overlapping with, the outward transit. Bad weather was encountered on 1 and 2 March causing the vessel to alter course to the NW into the weather for 12 hours to allow the system to pass.

The RV *Investigator* arrived in Hobart on 5 March 2017.

Sabrina Coast Slope Area A

Systematic E-W multibeam and sub-bottom profiler lines were collected in Area A in order to obtain good quality multibeam backscatter data and readily interpretable sub-bottom profiler lines. About 2000 km of straight lines were collected across the area. Seismic reflection lines were also shot W-E shot on 22 January and 24 January. Seismic was interrupted by whale approaches on several occasions. CTDs were deployed at coring sites and to sample a fresh water plume from a large iceberg. Two camera tows were conducted in the SW corner of Area A in waters less than 2000 m deep. The kasten, piston and multicores were successfully collected at 2 sites though deployment of the piston corer for the second time resulted in damage to the trigger mechanism requiring repair and modification. From 25 January onwards, SE to S winds pushed pack ice into the central part of Area A, preventing further southerly extension of the survey and overlapping with planned sample sites. After coring on 31 January, operations moved east to Area C.

Sabrina Coast Slope Area C

The vessel collected multibeam and sub-bottom profiler data along the northern edge of the survey area then headed south along the eastern edge of Area C to attempt to reach the shelf edge. The SE corner of the area was reached on 2 February but sea ice prevented access to the upper slope and shelf edge. Further multibeam and sub-bottom surveying continued in area C with seismic shot on 4 February. Another piston core deployment resulted in damage to the system on 5 February so further surveying, CTDs and plankton net deployments took place

while the piston corer was repaired. The piston corer was successfully deployed on 6 February and seismic line 9 shot. Kasten and multicores were collected on 7 February before the vessel headed south to again test the edge of the sea ice for access to the shelf. February 8 and 9 were the first days where bad weather strongly curtailed the program, but we were still able to finish off mapping of area C. Multiple kasten cores were attempted in the floor of submarine canyons. Two recovered successions featuring diatomaceous sediments while 2 others recovered nothing. Abrasion of the core barrel suggested sand in these locations.
Several attempts to reach the shelf and upper slope failed because of persistent pack ice cover but on 20 February, ice cleared sufficiently from the area around 120° E for the vessel to proceed on to the shelf, collect a number of CTD casts and also deploy the sea floor camera on four occasions on the upper slope. Further CTDs, seismic lines, kasten cores and piston cores were collected in Area C before one last incursion into Area A was attempted. For Area C, 1821 km of straight multibeam and sub-bottom profiler lines were surveyed. A single kasten core was collected in Area A on 24 February before the vessel departed the survey area.

HIGHLIGHTS

The RV *Investigator's* first geoscience-focused, Antarctic research mission*, Interactions of the Totten Glacier with the Southern Ocean through multiple glacial cycles*, has re-established Australia's scientific and cooperative international commitment to understanding future climate change from the geological record. The mission achieved all aims in producing: the first detail seafloor map of the Sabrina coast slope north of the Totten Glacier; identifying major canyons and regionalised sediment deposits from the Totten Glacier and Aurora Basin; recovered both long and short cores that will enable biological, geological and geochemical analyses that can provide insights to past environmental and climatological states continuously over the last ~350 thousand years and other Epochs of time; video of seafloor environments, oceanographic characterisation of the warm water masses going onto and cool water masses coming off the continental shelf.

Piggyback Project, Polar Cell Aerosol Nucleation (PCAN)
The piggyback project, *Polar Cell Aerosol Nucleation*, has been successful in doubling the available atmospheric measurement data in the East Antarctic sea ice region. The instrumentation deployed on this mission represent the first of their kind in this region, including size distribution and chemical composition of atmospheric aerosols, cloud measurements and atmospheric mercury concentrations and speciation. These measurements will enable insight into aerosol sources and chemistry and help understand seasonal changes and weather and climate drivers for a region of the world plagued by a dearth of atmospheric data and thus poorly represented in climate models. Aerosol data also will contribute directly to major projects with collaborators at NOAA (USA) and PSI (Switzerland). Measurements of aerosol optical depth contribute directly to the Marine Aerosol Network component of NASA's global AERONET program.

LIST OF MISSION RECORDS ON THE RV *INVESTIGATOR*

i. First dedicated Antarctic geoscience mission by RV *Investigator*.
ii. First seismic survey by RV *Investigator* in collaboration with the Italian Antarctic Program (PRNA) and Instituto Nazionale di Oceanografia e di Geofisica Sperimentale OGS, Italy.
iii. First use of drone for PR purposes on mission (by Doug Thost).
iv. First inclusion of a CSIRO Educator at Sea (Stuart Gifford, Taroona High School, TAS.).
v. Longest RV *Investigator* mission to date: 53 days at sea.
vi. Record for consecutive number of days spent in science operations: 38 days.
vii. Longest RV *Investigator* mission to operate below 60° S = 39 days and 16 hours.
viii. Second longest berth-to-berth distance: 8300 nm (record is Heard Island IN2016-V01: 8755nm).
ix. Most southerly position: 65°46.6' S, 120°24.0' E.
x. Coldest Air temp: -6.5 °C.
xi. Coldest water temp: -1.6 °C.
xii. Highest winds encountered: Beaufort scale Force 11 (56-63 knots) representative of very high seas, violent storm.

xiii. Total number of meters of the seafloor recovered: 70 m and counting.
xiv. Longest piston core recovery from 18-m barrel: 16 m 28.5 cm.
xv. Longest piston core recovery from 15-m barrel: 13 m 60.3 cm.
xvi. Longest Kasten core recovery from 3-m barrel: 2.65 m.
xvii. Longest Kasten core recovery from 4-m barrel: 3.38 m.
xviii. Longest consecutive run of successful multicores: 4
xix. Longest camera tow duration: 55 minutes on the seafloor.
xx. Deepest seafloor mapped: 4236 m.
xxi. Shallowest seafloor mapped: 430m.
xxii. Total area mapped: 44,000 km^2 science ops. (Close to the size of Tasmania) ~130,000 km^2 with transits.
xxiii. Longest seismic line without whale interruptions: 66.207 km
xxiv. Most Pollywogs initiated by King Neptune to Red Nose Order on RV *Investigator* mission: 22
xxv. First time L. Armand is Chief Scientist.
xxvi. 28.98 m in 10 Kasten cores, 0.65m^3, 440.38 kg kept
xxvii. 67.43 m in 6 piston cores (proposed 2-4), 0.706 m^3
xxviii. 9.47 m in 5 multicores 0.07 m^3 14.76 kg
xxix. Total sediment 1609 kg
xxx. 1741 litres water sampled or filtered
xxxi. 33 CTDs taken
xxxii. 1 brittle star recovered
xxxiii. 322 km seismic
xxxiv. 48,683 km^2 multibeam in survey area
xxxv. 11.268 km out of 36 km proposed.
xxxvi. 13 seismic shutdowns in total.
xxxvii. 7 low power and 1 line aborted due to bad weather.

STATION LOG

A total of 85 stations were occupied. They are designated A001-A042 for Area A and C001-C043 for Area C (see Table 1). The distribution of stations is shown in Figure 2. The Voyage Manager's daily situation reports are provided in Appendix 2.

Table 1. Station numbers, locations and samples.

Station	Longitude	Latitude	Piston core	Multi core	Kasten core	CTD	Plankton net	Camera tow
A01	115.647	-64.626				CTD01		
A02	115.284	-64.683					PN01	
A03	114.11	-64.951				CTD02		
A04	114.2442	-64.7751						CAM01
A05	115.623	-64.471	PC01	MC01	KC02	CTD03	PN02	
A06	115.043	-64.463	PC03	MC02	KC03			
A07	116.61	-64.554				CTD05		
A08	114.623	-64.5922						CAM02
A09	114.916	-64.318				CTD06		
A042	116.6403	-64.5387			KC14			
C10	119.4302	-64.9503				CTD07		
C11	120.4567	-65.0117				CTD08	PN03	
C12	119.3012	-64.675	PC05	MC03	KC04	CTD09	PN04	
C13	119.0183	-64.6538		MC04	KC05	CTD10		
C14	120.5433	-65.4283				CTD11, CTD12		
C15	118.696	-64.729		MC05	KC06	CTD16		
C16	118.382	-64.432				CTD18	PN05	
C17	118.07	-64.682				CTD17		
C18	118.498	-64.401			KC07			
C19	120.143	-64.819	PC06					
C20	119.739	-64.794			KC08			
C21	120.383	-64.74			KC09, KC10			
C22	120.049	-65.1313	PC07		KC11			
C23	120.7888	-65.4675				CTD20		
C24	120.0448	-65.4675				CTD21		
C25	120.8635	-64.9538	PC08		KC12	CTD22	PN06	
C26	120.385	-65.5615						CAM03
C27	120.4068	-65.5378				CTD23		
C28	119.914	-65.4963						CAM05
C29	120.383	-65.588				CTD24		
C30	120.372	-65.6845				CTD25		
C31	119.54	-65.5265				CTD26		
C32	119.240	-65.9426						CAM06
C33	119.5635	-65.404				CTD27		
C34	120.3543	-64.3908				CTD28		
C35	119.5844	-65.3052				CTD29		
C36	119.5426	-65.4435						CAM07
C38	119.1035	-64.4828			KC13		PN07	
C39	119.0548	-64.4796				CTD30		
C40	118.9361	-65.0865				CTD31		
C41	118.5231	-64.982				CTD32		
C43	122.8743	-65.3813				CTD33		

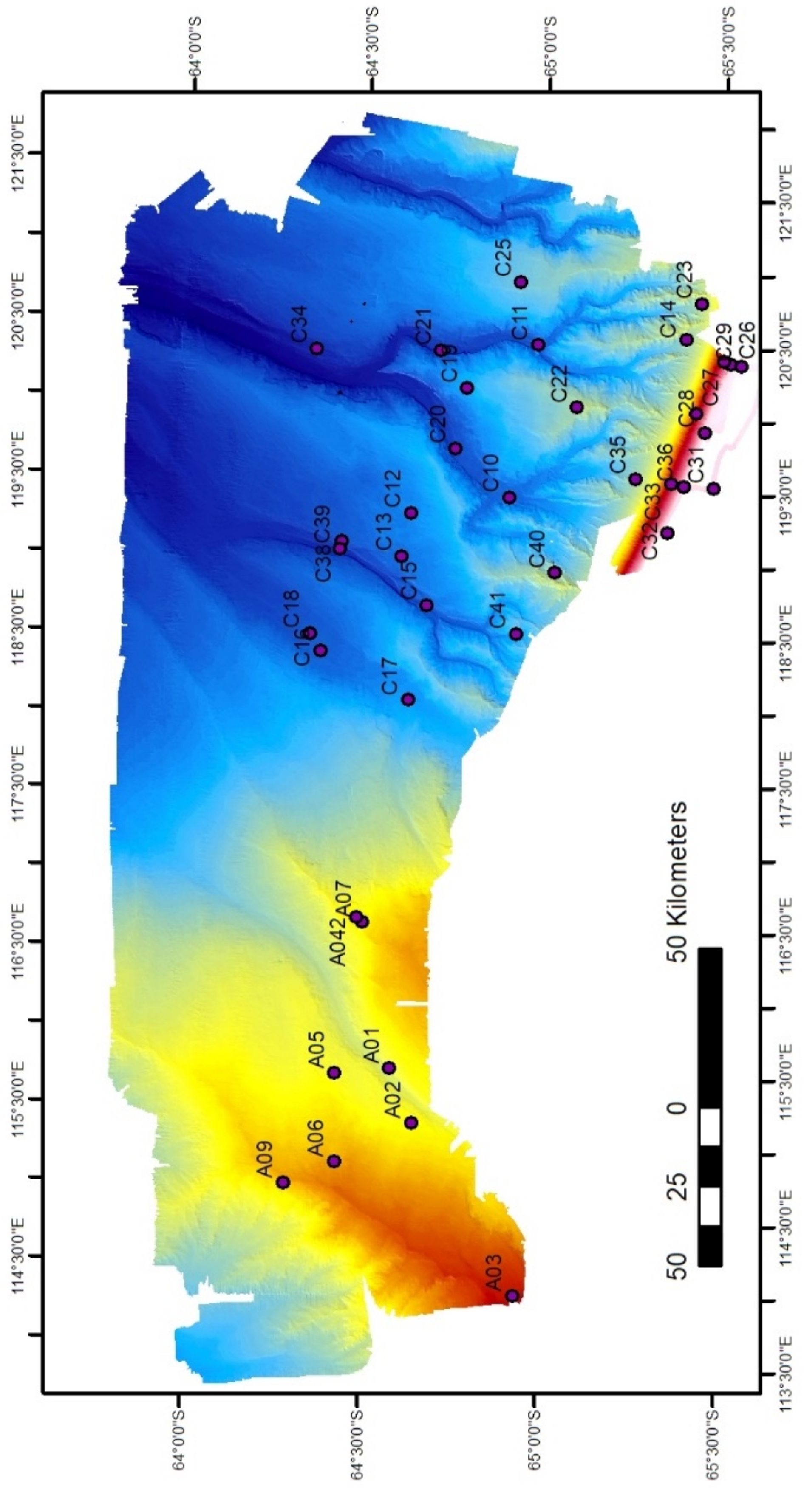

Figure 2. Station locations, Sabrina Sea Floor Survey.

SECTION 2. Scientific Surveying and Preliminary Results

Multibeam swath bathymetry

Methods

Bathymetry was acquired using two multibeam echosounders, a Kongsberg EM122 and an EM710. The EM122 is a 12 kHz full ocean depth multibeam echosounder and was operated at all depth ranges on the Sabrina Seafloor Survey. The EM710 is a high resolution 14-100KHz sounder used for mapping on the continental shelf and upper slope to depths of up to 2000 m. Sound velocity corrections were undertaken using observed data from CTDs and XBTs as required. Observations of sea surface temperature were also used to construct profiles within SVP builder.

Multibeam data were logged in Kongsberg's proprietary "*.all" format and were converted and processed within Caris HIPS and SIPS version 9.1.9. Raw files were generally converted into the HIPS and SIPS format using the batch processor, which after conversion loaded a zero-tide, computed Total Propagated Uncertainty (TPU) and merged the lines. A bathymetry filter was set up to reject beams outside a 65° angle from nadir. The data was then gridded at the highest resolution possible and further inspected for outliers and cleaned within the subset editor.

Students routinely undertook multibeam processing and assisted GSM staff during their watches. A swath angle surface at 50 m resolution was used as the 'working surface'. Upon departure from the survey area processing and QC of the data was undertaken by GSM staff. CUBE (Combined Uncertainty and Bathymetry Estimator) surfaces were generated at an appropriate resolution for the depth, the generated and alternative hypotheses being examined; surface filters were then used extensively to automate noise reduction and outliers that remained present on the surface. The final surface was gridded at a resolution of 200 m, with the EM710 data on the shelf and upper slope gridded to 10 m.

The output surfaces were exported as ASCII and geotif files, with the processed sonar data saved as ".xtf" and the Caris project also made available. The final map is shown in *Figure* 3.

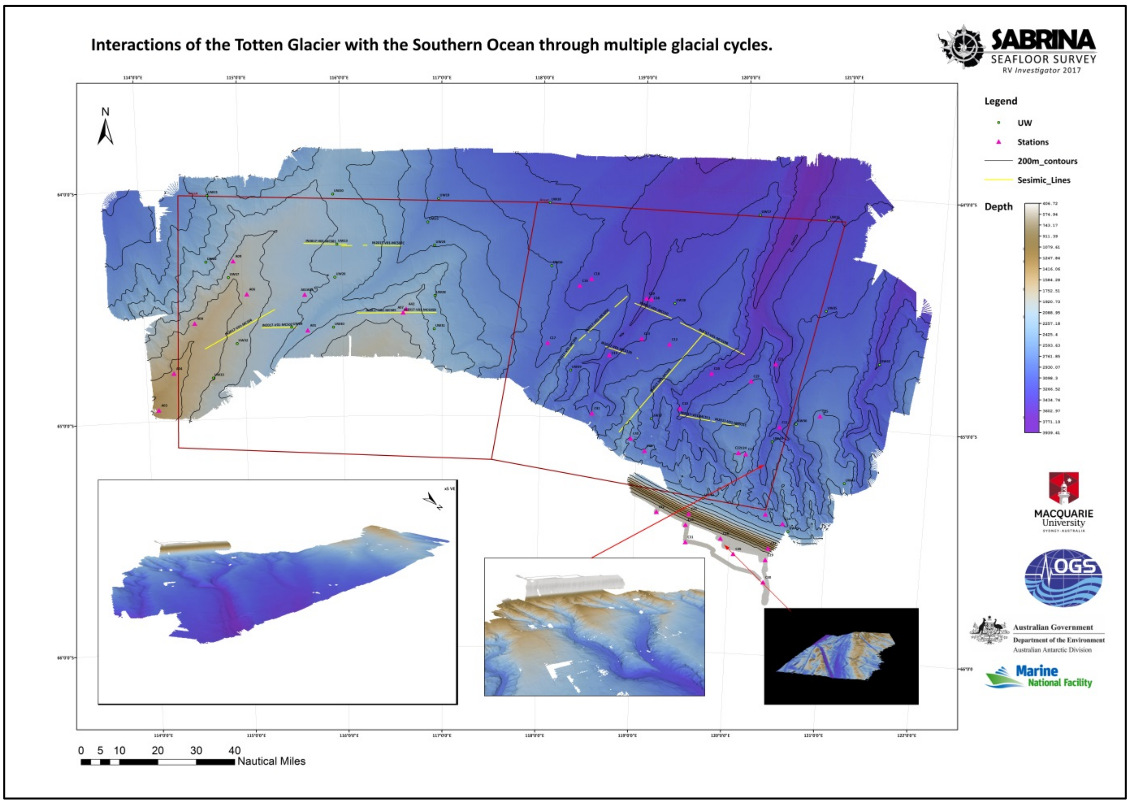

Figure 3. Bathymetry map for the survey area, with insets showing 3D views. *Additional ArcGIS layers also shown.*

Interpretation for survey area
Area A is dominated by two large NE-SW trending ridges, separated by a low sinuosity narrow submarine canyon flanked with terraces. The head of this canyon was not surveyed. The ridges have relatively smooth seafloor on their eastern facing slopes, with significant evidence of mass movement, such as well-defined slump scars and debris runout fields. The westward facing slopes have a more gullied terrain, with small dendritic gullies. The eastern ridge has lower slope than the western ridge, and is dominated by slump scars.

Area C is dominated by dendritic canyons, with meandering and sharp bends in their upper part, before joining onto less sinuous main channels. The floors of the channels contain terraces and closed depressions. The main channels are separated by asymmetric ridges, with thickest sediments on their eastern sides. Areas A and C are separated by a low sinuosity, low profile, broad depression, that links to one of the more dendritic canyons towards the lower slope. The upper slope consists of a smooth to gullied apron, with the heads of the canyons initiating just down slope of this upper slope apron. The gullies have a maximum depth range of up to 15 m, are closely spaced and symmetrical in cross section. The shelf break occurs at depths of 480 - 510 m.

Interpretation for transit
The outbound transit from Hobart, Tasmania to the north-eastern corner of Survey Area C was conducted along a compass bearing of 215 degrees (°) and covered a distance of 1,450 nautical miles (NM) in just over six (6) days. During this transit, a bathymetric survey was conducted using the RV *Investigator's* Kongsberg EM-122 multibeam echo-sounder that operates at a nominal frequency of 12 kilohertz (kHz). A beam angle of 75° was used during the outbound and inbound transit surveys. The swath width of the multibeam survey is determined by the depth to the ocean floor therefore during the outbound transit a swath width of between 15 to 20 km was produced.

Topography of the South Tasman Rise (STR) and the deep ocean floor of the Indo-Australian and Antarctic plates were imaged by the transit bathymetry, while also providing an indication of the structure of the underlying geology (Pollock, 2002). The geological structures that were identified within the oceanic crust included seaknolls, seamounts, transverse faulting and the ridges associated with rifting throughout the Tasman Basin, which has occurred as a consequence of the northwest to southeast Tasmanian-Antarctic Shear Zone (
Figure 4, Pollock, 2002).

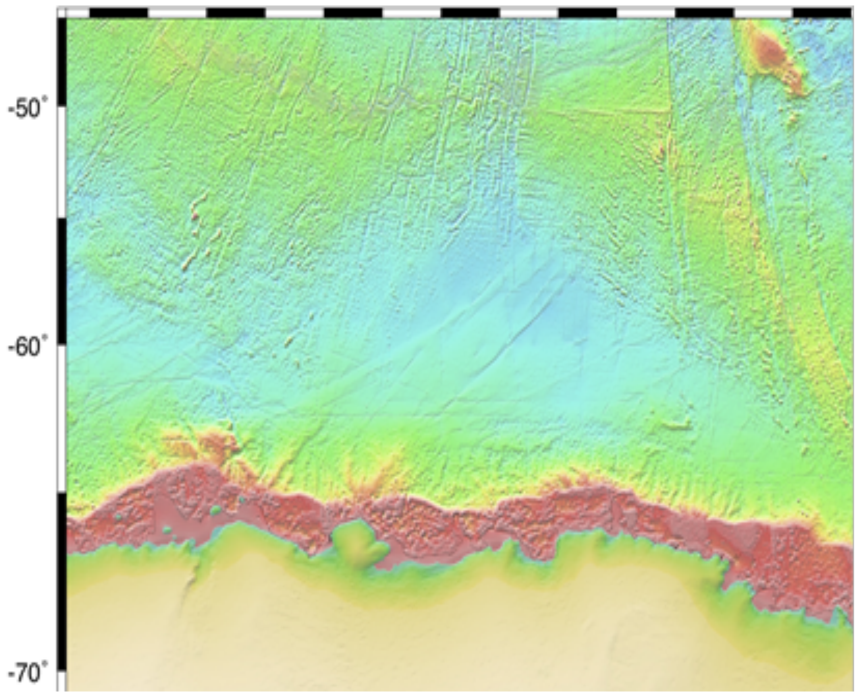

Figure 4. The northwest to southeast Tasmanian-Antarctic Shear Zone.

An area of interest, which was surveyed between 42°57.25 S, 143°18.13 E and 57°36.76 S, 133°10.64 E, over a distance of 694 NM, indicated the occurrence of significant activity that is associated with the northwest to southeast Tasmanian-Antarctic Shear Zone. There are four (4) distinct north-south trending transform faults that dominate the northern and central aspects of the area and these faults appear to correspond with the north-south trending shear zone faults that extend across the Tasman Basin. Directly associated with these fault zones are the north-south ridges on the eastern and western margins of the faults, and these ridges exhibit an angular discontinuity with the east-west trending ridges that are present in the surrounding ocean floor basins (**A** **B**

Figure 5A). While the centre of these basins were populated with northwest-southeast trending ridges, which also exhibit an angular discontinuity with the east-west trending ridges, they appear to have a significant association with the seamounts and seaknolls that occur predominately in the northern and the southern aspects of the area surveyed.

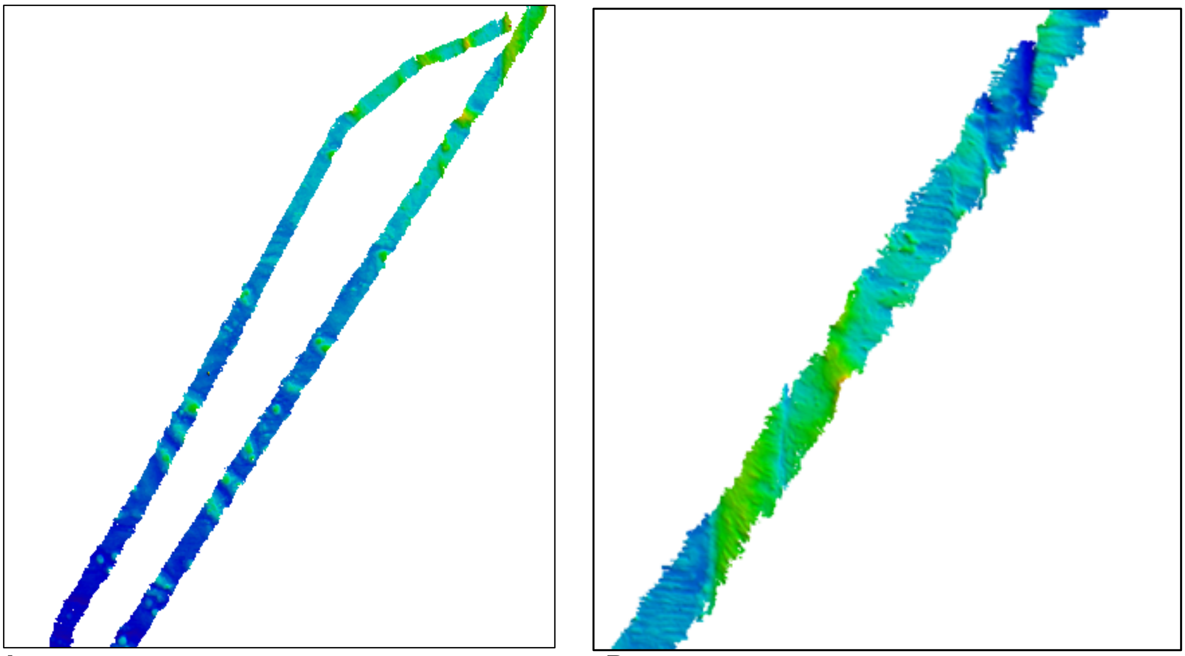

A **B**

Figure 5. Swath surveys. *A) Transform faulting in the outbound bathymetry; B) The inbound and outbound bathymetry surveys.*

The east-west trending ridges throughout the ocean floor basins indicate that the rifting centres of the basins were once positioned in an approximate east-west orientation for an extended time period. An abrupt orientation change of the rifting centres, which has possibly been influenced through the faulting of the Tasmanian-Antarctic Shear Zone, has repositioned the ridges at the near centre of the basins in an approximately northwest-southeast orientation. While the significant influence of the continued faulting throughout the shear zone appears to have possibly caused a cessation to the rifting events within these basins. However, the association of the northwest-southeast trending ridges with the occurrence of seamounts and sea knolls in the northern and the southern aspects of the survey area suggests that the transform faulting may have created a thinning of the oceanic crust near the centre of the rifting basins, which are positioned further away from the axis of the fault zone. Therefore, the thinning of the crust may have allowed for the intrusion of volcanics which have created the seamounts and sea knolls, and the northwest-southeast trending volcanic ridges in the southern aspect of the survey area.

The inbound transit course from the south-eastern corner of Survey Area C to Hobart, Tasmania was plotted to commence a parallel bathymetry survey at 57°03.32 S, 132°39.66 E, approximately 30 NM north-west of the outbound transit survey, along a compass bearing of 35°. At approximately 29 NM along the inbound survey transit the master of the vessel made a

decision to alter the transit bearing to 300° due to gale-force winds and extremely rough sea conditions, and the inbound transit survey course had to be abandoned.
The bathymetry survey conducted between 57°03.32 S, 132°39.66 E and 52°04.15 S, 139°23.11 E indicates that the geological structures are correlated between the two transit lines (Figure 5B).There are east-west trending ridges throughout the ocean floor basins of the inbound transit survey and these ridges appear to continue to exhibit an angular discontinuity with the north-south trending ridges of the shear zone transform faults and the northwest-southeast trending volcanic ridges in the southern aspect of the transit. Fewer seamounts, seaknolls and volcanic ridges are observed near the mid-ocean ridge.

The outbound and inbound bathymetry surveys identified that this segment of Tasmanian-Antarctic Shear Zone exists at a higher elevation than the surrounding ocean floor basins. While the shears zone contains four prominent north-south trending faults within a significantly higher oceanic crust.

SUB-BOTTOM PROFILING

Sub-bottom profile data was acquired as part of the gondola mounted array with a Kongsberg SPB120. On this voyage the system source was a linear chirp up with a sweep of 2.5-6.5 kHz. The pulse length was 6 milliseconds and up to 12 milliseconds on transit through deep water. In the survey areas the system operated in single ping mode but with burst during transit in deep water. A gain of 6 dB was applied to the data followed by gain correction, matched filter, instant amplitude processing and a time variable gain to enhance sub-bottom reflections. The sub-bottom profiler data was recorded and presented as two-way time sections. The Sub-bottom profiles were saved as segy (Society of Exploration Geophysics Y format) and Konsberg proprietary ".raw" files. Segy files were viewed in Seisee which allows adjustment of axes. The files were then exported as bmp files with the day and time along the horizontal axis and the two-way time along the vertical axis. All lines were numbered sequentially from the start to the end of the voyage with files being between 15-25 MB. All sub-bottom profiles were printed and ordered chronologically in folders for reference.
The profiles were used to identify coring locations and evaluate stratigraphy. Imagery of the sub-bottom profiles are presented in Section 4.

Recommendations: The benefit of Seisee is that it is a free program, so anyone can download it. However, it has various bugs and crashes frequently. It is also not possible to print directly from Seisee. A work-around solution of exporting files to bmp files, then inserting into PowerPoint was used. In some cases, screenshots of the seismic trace were taken using the Snipping Tool program, then pasted into PowerPoint. This process produced usable results, but was time consuming and rather tedious. We would recommend that for geoscience voyages, an alternative solution should be explored, such as obtaining a copy of the program Kingdom, SonarWiz or DUG Insight which are programs that allow for easier processing and spatial presentation of segy files.

BACKSCATTER

Backscatter refers to the strength of sea floor reflection in multibeam sonar data. Backscatter mosaics at 20 m resolution for the EM122 and 5 m resolution for the EM710 sonar was constructed within the Fledermaus Geocoder Toolbox (FMGT) (
Figure 6). FMGT allows the visualisation and analysis of multibeam backscatter data and allows the processing of the sonar files into mosaics. FMGT processing was largely automated in this case however the steps the software took to construct the mosaic are outlined below:

1. Adjust and extract the backscatter data and perform transmission loss corrections based on sonar type and bottom topography.
2. Filtering, angle varying gain (AVG) adjustments, and anti-aliasing of the backscatter data.
3. Creation of the mosaic at resolution pre-computed by FMGT.

Angle vs Range Analysis (ARA) was conducted to provide seafloor characterisation of the survey area. ARA is a method of seafloor characterisation which compares the actual backscatter response to expected acoustic response curves for a wide range of seafloor types, based within the Jackson mathematical model. Further analysis will be undertaken to determine how well this characterisation relates to the properties of the seafloor sediment samples.

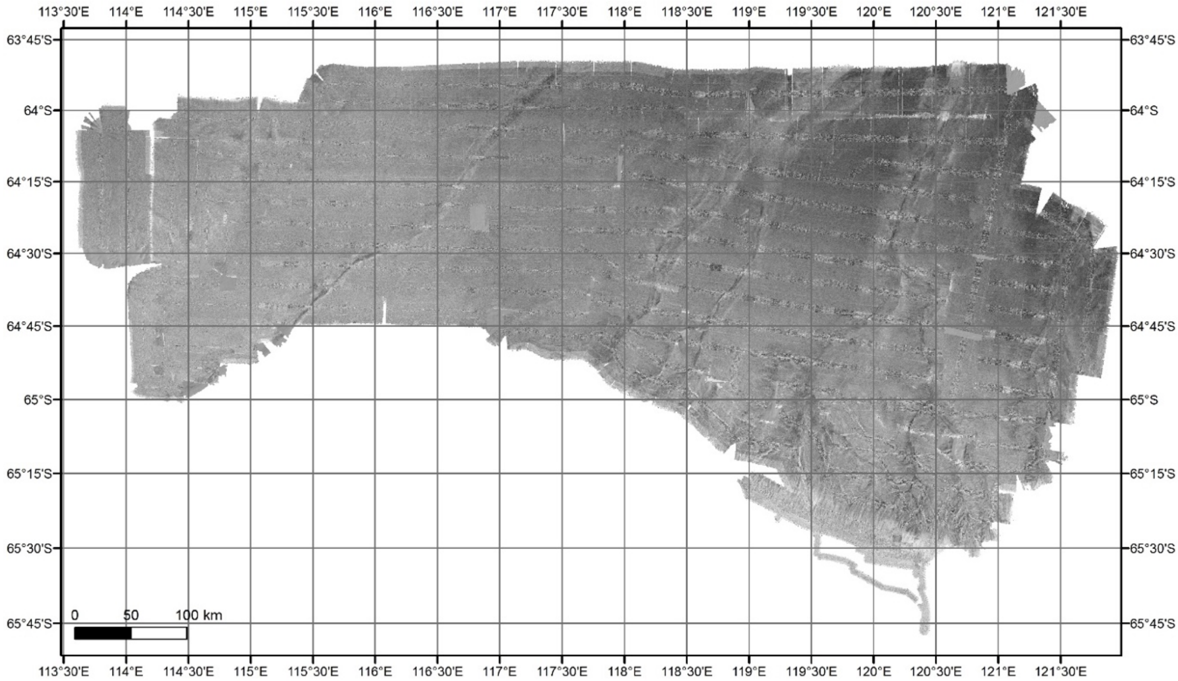

Figure 6. Backscatter mosaic processed in Fledermaus.

MAPPING IN GIS SYSTEMS

Mapping was undertaken using a combination of QGIS and ArcGIS. Data was projected using a Universal Transverse Mercator projection of Zone 50S. GIS was used to generate bathymetric contours at 200 m intervals and to derive a hillshade for display of the bathymetry grid. CSV files were generated for location data for each sample type and imported into QGIS and ArcGIS. A list of layers used is shown in Table 2.

Table 2 Layers generated for GIS maps

Filename	Type
200m contours	.shp
Area A	.shp
Area C	.shp
CTD	.shp
Deep_tow_camera_lines	.shp
Kastencore	.shp
MOA_Antarctica	.shp
Multicore	.shp
Pistoncore	.shp
PN	.shp
Seismic Lines	.shp
Southern_Right_Whale	.shp
Sperm_Whale	.shp
Stations	.shp
UW	.shp
EM122_Cube_200m_Interp	.asc
EM122_Cube_200m_Interp	.tiff

Proposed Canyon Names
Description and discussion of major features in the survey area is made easier by having unique place names. No such names existed in the International Hydrographic Organisation Gazetteer of undersea feature names nor in the SCAR Gazetteer of Antarctic place names.

After discussion amongst the science party, we approached the Southwest Land and Sea Council who represent the indigenous community living in SW Western Australia to see if they would be interested in providing place names. They responded with a list of words from the Noongah language from which canyon names have been selected. Their meaning is as follows (Figure 7):

1. **Boongorang Canyon** -Blowing in the wind – the area was visited because bad weather prevented other activities.
2. **Manang Canyon** -Pool of Water Canyon – after scour pools along the bottom of the canyon
3. **Maadjit Canyon** -Water Serpent Canyon – based on unusual curved part of its western branch.
4. **Jeffrey Canyon** - after the late Dr Shirley Jeffrey, an Australian scientist who pioneered the use of biochemistry in phytoplankton research. A kasten core (KC06) sampled the bed of the canyon and recovered thick diatom mats.
5. **Morka Valley** -Winter Valley – probably only active during very cold parts of the climate cycle
6. **Minang-a Canyon** -Whale Canyon- All the canyons could have been called this because there were whales everywhere, but we chose this one.

These feature names will be submitted to the Standing Committee for Undersea Feature Names.

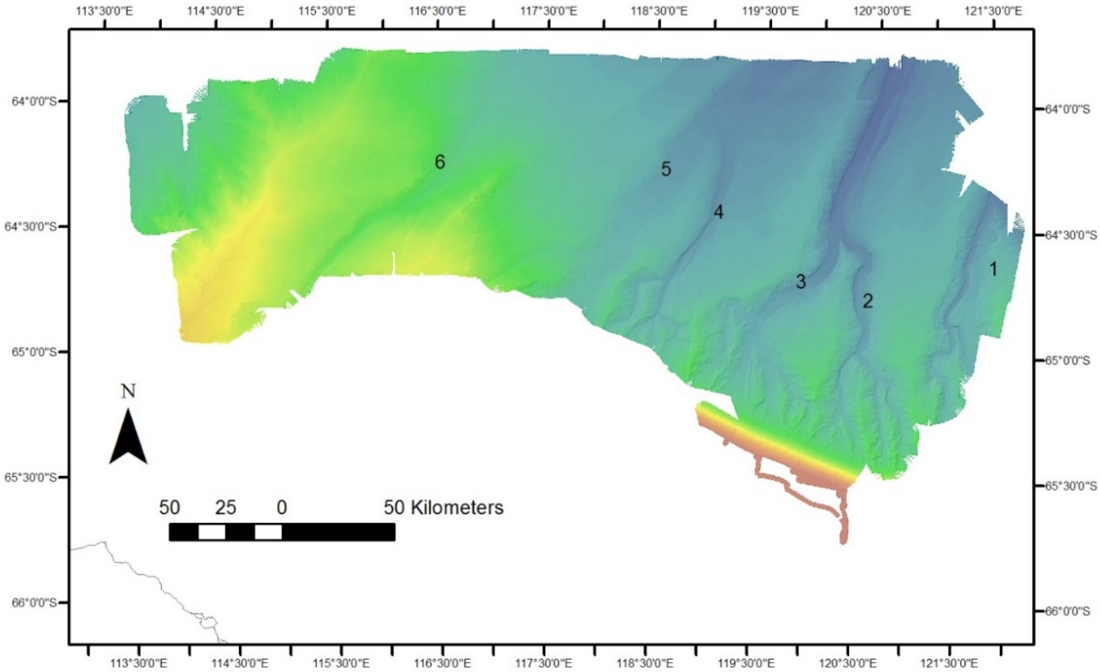

***Figure 7. Proposed canyon names. 1** Boongorang Canyon, **2** Manang Canyon, **3** Maadjit Canyon, **4** Jeffrey Canyon, **5** Morka Canyon, and **6** Minang-a Canyon.*

ECHOSOUNDER OBSERVATIONS

Two bioacoustics echosounders, an EK60 and ME70, were operational during the voyage. The EK60 is a narrow-beam, split frequency water-column sonar, which on RV *Investigator* operates with six frequencies. The ME70 is a multibeam scientific echosounder, which operates a sweep of frequencies across a fan-shaped acoustic array.

Table 3 Summary of frequencies in the bioacoustics.

Instrument	Frequencies (kHz)					
EK60	18	30	70	120	200	333
ME70	70-100	(frequencies vary across the beam)				

Both bioacoustic instruments recorded data throughout the voyage. The EK60 recorded to a constant 1500 m water depth and the ME70 to 200 m. The ME70 recorded with a 21-beam, inverse-V frequency array. Interference can be seen in the EK60 and ME70 data from shipboard ADCP instruments, which were left running as a priority to obtain high-quality oceanographic data.

Much of the data recorded is featureless, due to the sparse distribution of krill in the survey area. However, above several channels in the survey area, high-intensity acoustic returns were seen on masses of what is presumed biota, in the 50-70 m water depth (Fig. 8). Our interest in these features is based on observations of Quilty et al. (1985) from the Prydz Bay shelf slope break, where dense blooms of the diatom *Thalassiothrix* mats caused false bottom returns on their echosounder.

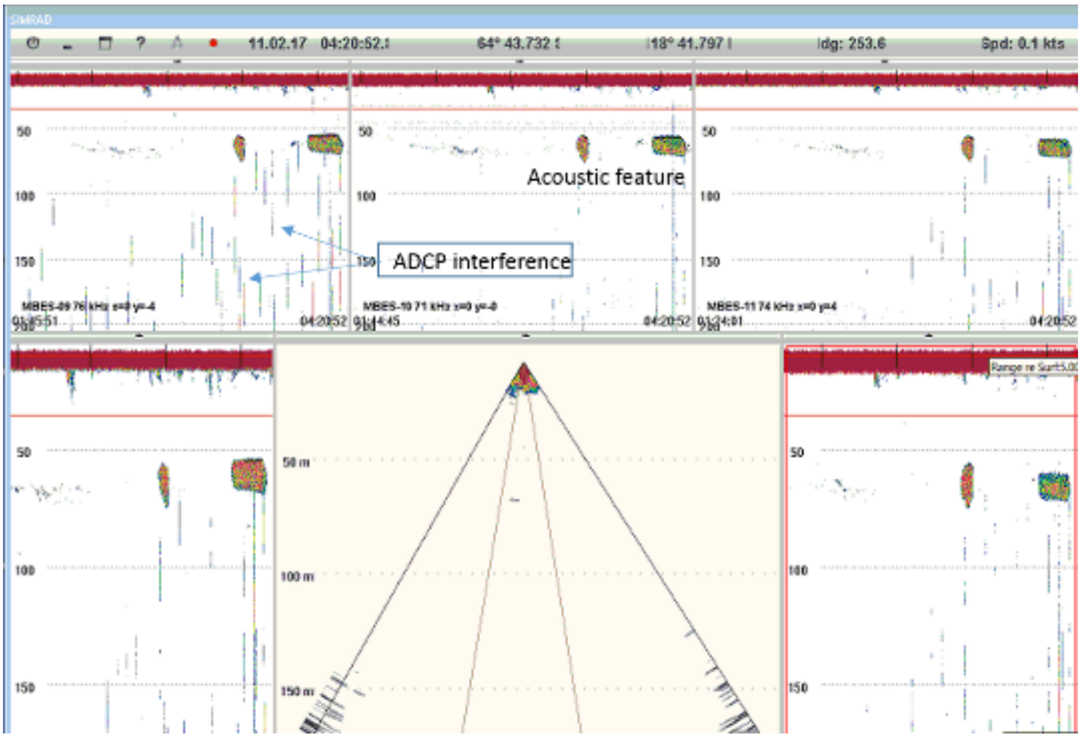

Figure 8. Screenshot of ME70 data showing high-energy acoustic return at 60-70 m water depth.

GRAVIMETRY

Acquisition Method

Gravitational acceleration was sampled at 1 Hz with an on board Micro-g Lacoste Air-Sea System II Marine Gravity Meter for the full extent of the voyage. The output is in the form of daily (UTC) produced plaintext *.DAT extension files, a generic data file type. Functionally the output file is a tabulated comma-separated values (csv) file.

The output contains 20 comma-separated columns. Column 1: File Type 2: Date (YYYY/MM/DD) 3: Time (HH:MM:SS.SS) 4: Julian Day 5: Gravity (Counter Units) 6: Spring Tension (Counter Units) 7: Beam position (Volts x 750,000) 8: VCC 9: AL 10: AX 11: VE 12: AX2 13: XACC2 14: LACC2 15: Cross Acceleration (Gal) 16: Long Acceleration (Gal) 17: Eotvos Correction (mGal) 18: Longitude 19: Latitude 20: Speed (Knots/hour) 21: Course

Preliminary results for survey area

On board preliminary work involved 1) Generation of free air gravity 2) Gridding of the data for the survey area

1) Free air gravity was produced using Python by:
    - Resampling the data to 0.0167 Hz
    - Conversion of gravitational acceleration (counter units) to gravitational acceleration (mGal) through a pre-defined calibration co-efficient
    - Application of the Eotvos correction through the addition of Eotvos (mGal) and gravitational acceleration (mGal)
    - Reading greater than two standard deviations for the resampled dataset were removed to avoid false signal related to erroneous readings which were a feature of the dataset. It should be noted that this is a poor method for removing erroneous data points. Figure 9 shows that removal of two standard deviations from the mean also removes real readings from the fringes of the dataset
    - Latitude correction was applied however it is of limited significance given the regional extent of the survey
2) Gridding of the data:
    - xyz file (longitude, latitude, free air gravity) were gridded in Surfer 10 using a variety of interpolation methods.
    - The resulting grids were plotted using both contour and scatter graphs (Figs. 10 and 11).

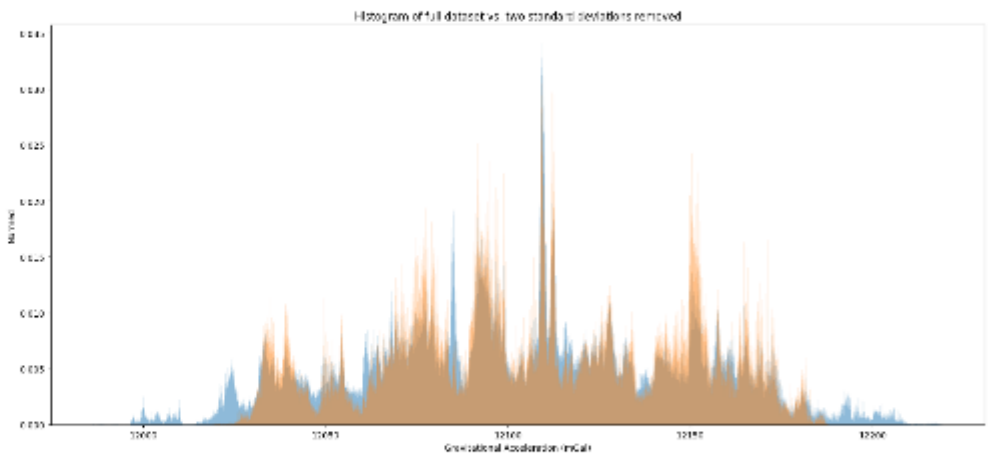

Figure 9. Gravimetry data. *In orange is the normal distribution of the regional dataset. In blue is the normal distribution of the regional dataset with readings above and below two standard deviations from the mean removed.*

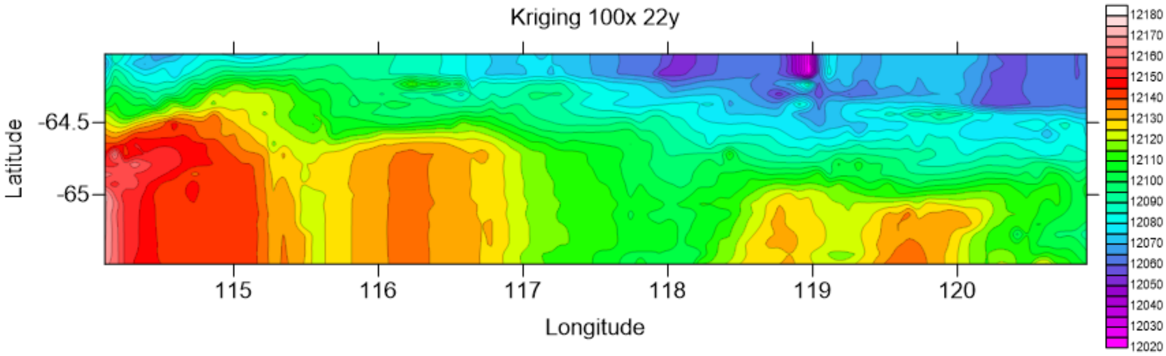

Figure 10. Contour plot of the processed gravity data (description above) for the survey area. *A kriging interpolation method was used with 100 columns and 22 rows. A scatter plot of the data for this plot is shown in Figure 11.*

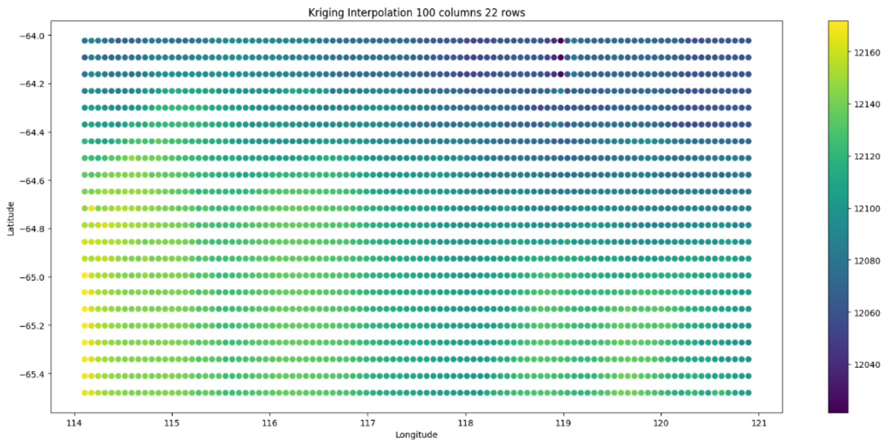

Figure 11. Scatter plot with the colour bar denoting gravitational acceleration (mGal). *The data display the result of a kriging interpolation with 100 columns and 22 rows for our processed regional dataset.*

Figure 10 will be the basis for discussion about preliminary findings. The most apparent signal in Figure 10 is the four large north-south trending high gravity anomalies. These four anomalies correspond to four areas of bathymetric highs where there is believed to be preferential delivery of sediment between channels. These features are approximately orthogonal to the continental shelf and hence reflect movement of sediment away from the shelf.

There is a north-south trending down step in gravitational acceleration north of -64.5°. This will be in some part the result of decreased quantities of sediment delivered further from the shelf and continent source. Some component of this signal may be related to the increased and highly heterogeneous thinning of the continental crust as a transition is approached between continental and oceanic crust. Previous seismic lines, such as GA 228/20, have shown the region is a non-volcanic rifted margin which features highly thinned and faulted continental crust which transitions north to oceanic crust.

Figure 10 shows that there are more expansive gravity highs in the west. Comparison to the bathymetry reveals there is preferential sediment delivery to the west. However, further north, particularly in the east, there is a lack of bathymetric features which can explain heterogeneities seen between 118 to 120° and -64° to -65°. There are large north-south trending channels in the bathymetry of the east which are not clearly represented in gridded gravity data. Instead there are limited north-south trending features however this may be related to the gridding method and its low resolution.

East-west comparison of bathymetry would also suggest that the signal from the sediment in the east is uncharacteristically high. In the east the two gravity highs, interpreted as sediment piles, are close in character to the gravity highs in the west. Comparison with bathymetry shows that sediment in the east lacks the topography or lateral extent to fully account for the resulting gravity signal. This, it should be noted, is only a preliminary hypothesis which should be further investigated.

With better data processing, improved and optimised interpolation as well as a series of new data products such as gridded data with bathymetry signals removed and inversions for crustal depth, hypothesis about the survey area can be properly studied. Further inspection of individual lines through the area where we have real reading would add further evidence to conclusions. The above study will be invaluable to revealing the true structure and nature of this newly mapped area and will likely disprove initial observations presented here.

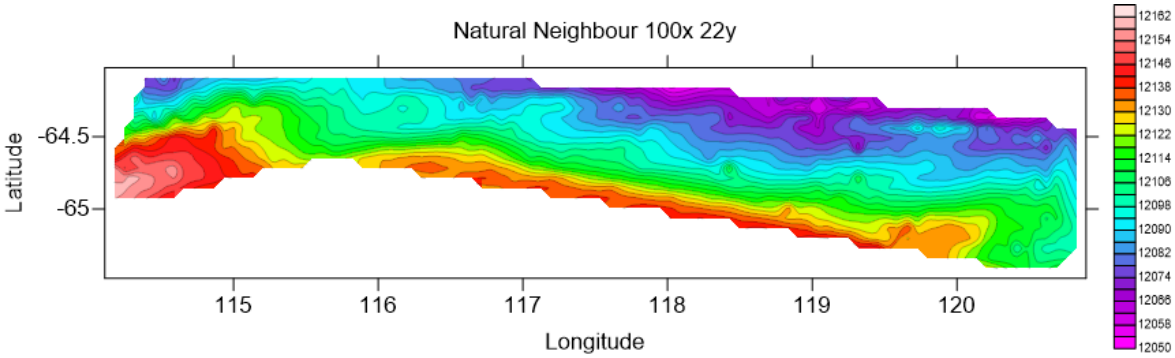

Figure 12. Contour plot of processed gravity data (description above) for the survey area. *A natural neighbour interpolation method was used with 100 columns and 22 rows.*

It can be seen through comparison between *Figure* 10 and *Fig*ure 12 the difference gridding decisions can have on the morphology or signals. Future work should take extra care to ensure accurate gridding and plotting are employed to ensure the interpreted figures are physically legitimate.

It should also be noted that for the initial processing presented here no drift correction is applied. This will be followed up upon return so as an appropriate correction can be made.

Preliminary results for transit

Eotvos and latitude-corrected gravimetry data for the outbound transit survey was plotted in Microsoft Excel to present the measured gravity in milligals (mGal) for the corresponding latitude position on the outbound transit (
Figure 13). A possible error in the latitude correction has created a plot that appears to increase linearly as the latitude increases during the progress of the transit southward. However, there is an increase in the gravity measurements which correspond to the latitude position of the Tasmanian-Antarctic Shear Zone and the two (2) prominent seamounts that are associated with the shear zone, as well as the intrusion of the seamounts across the ocean floor basins. These oceanic crust features were identified from the topography of the outbound bathymetry survey and are presented in preceding section.

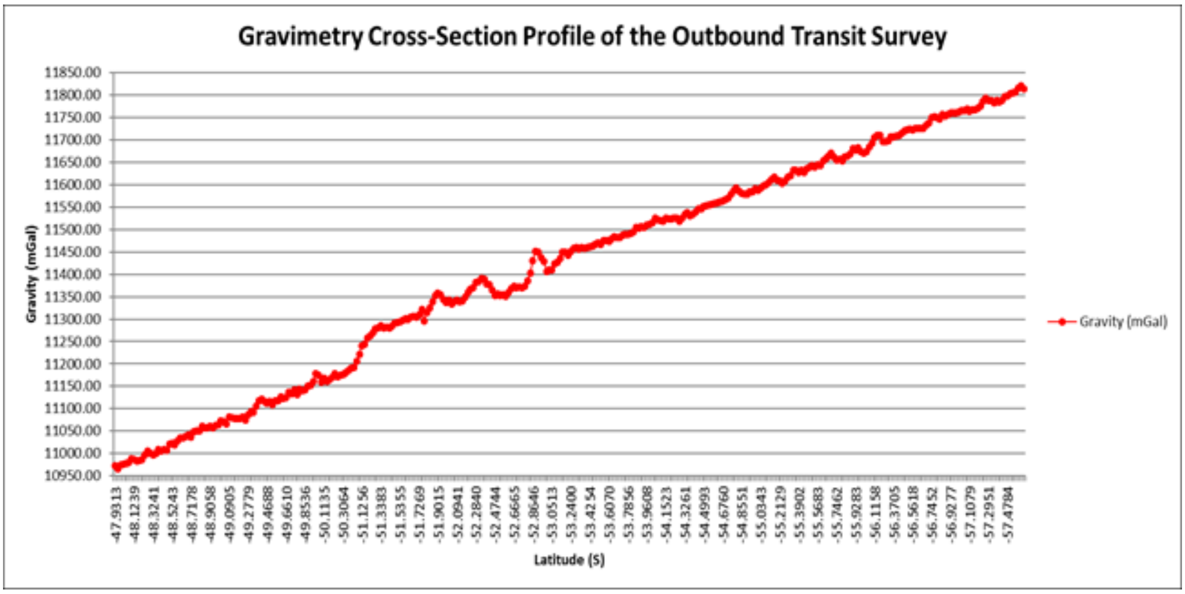

Figure 13. The gravimetry cross-section profile of the outbound transit survey.

A relatively constant gravity measurement is displayed for the ocean floor basin from 47°55.88 S to 50°26.94 S, with a decrease in the gravity at 49°15.04 S which corresponds to a subtle depression within the basin. There are also gravity measurement increases at 49°23.23 S and 49°56.23 S which correlate to the latitude position of the seamounts that are intruding into the ocean floor basin. This indicates that the volcanism associated with the seamounts have higher measured gravity in comparison to the surrounding basin.

The significant gravity increase between 50°26.94 S and 52°28.46 S corresponds to the position of the Tasmanian-Antarctic Shear Zone, and the two prominent increases in gravity within the shear zone correspond to the position of the seamount at 51°52.45 S and the north-south trending volcanic ridge at 52°20.29 S. While the decrease in the gravity at 52°28.46 S indicates the transition from the shear zone to the ocean floor basin and the increase in gravity at 52°53.48 S corresponds to the position of a seamount within this basin. The series of gravity increases between 54°42.08 S and 57°36.76 S correlate to the position of the seamounts or the larger sea knolls that are intruding the crust throughout the southern aspect of the transit survey. These increases in gravity measurements within the shear zone and across the basin also indicate that the associated volcanics provide an increased gravity measurement in comparison to the surrounding ocean floor basin.

Operations Summary

Mobilisation for the gravity meter included a drift (stable) gravity readings undertaken prior to departure, and wharf tie measurements relative to the absolute gravity site on the CSIRO wharf in Hobart.

The gravity meter recorded for the entire voyage, save for a period of several hours on the 20th of January, caused by the gravity meter unbalancing and requiring a period of re-equilibration. 1 Hz gravitational acceleration was recorded for the extent of the voyage. In the survey area, initial processing reveals bathymetry composes a high degree of the signal. Future work will attempt to reveal physically legitimate underlying structures.

SECTION 3. High resolution seismic reflection surveying

TYTAN PROJECT

Seismic reflection profiling activities were supported by the TYTAN (Totten Glacier dynamics and Southern Ocean circulation impact on depositional processes since the mid-late Cenozoic) Project of the Italian Programa Nazionale Di Richerche in Antartide (PNRA).
The TYTAN project is embedded into the Australian project that aims to understand the interaction of the Totten Glacier and its ice drainage basin with the Southern Ocean, during periods of warming and ice sheet retreat, in order to increase knowledge of present-day glacial retreat and to provide inputs for climate change modelling. The main objective of the TYTAN project is to provide insights for reconstructing the depositional environment of the continental margin off the Totten Glacier starting from the Miocene, when temperatures and CO_2 levels were more similar to those predicted for the next century.

Integrated analysis of the available SDLS (Seismic Data Library System) data and of the new geophysical dataset will allow identification of key acoustic features indicative of advances (e.g. massive debris flow deposits and erosional surfaces) and retreats (turbiditic and pelagic layered deposits) of the ice sheet, and of sediment reworking by along slope and downslope bottom currents (e.g. sediment drifts, moats, sediment waves, etc.). This analysis will lead to a better understanding of the mechanisms of sediment transfer from coastal areas to the continental slope and beyond, and to the detection of changes in the depositional setting related to: 1) the transition from highly dynamic temperate to more stable polar regime, 2) outburst ice sheet episodes, 3) the development of the Circum Antarctic current, and 4) shifts of along slope and downslope bottom current pathways, that may have occurred during warm intervals, characterized by reduced continental and sea ice. All this information will lead to the reconstruction of depositional processes that affected the continental slope margin off the Totten Glacier since the mid-late Cenozoic.

The TYTAN seismic grid will also provide the site survey for the IODP proposal that is in preparation by the international team involved into the Australian project. Comprehensive analysis of the seismic dataset will be crucial to prioritize areas of interest for IODP deep drilling, by identifying expanded and well preserved sedimentary successions (potentially preserving good paleoclimatic and paleoceanographic records), characterized by depositional process that appear to be acting continuously over the same site for long time spans (e.g. sediment waves and drifts) and/or when major changes that can be related to regional or global events rather than local causes, clearly occurred.Selected lines will also be analysed to detect seawater column reflectivity by means of seismic oceanography to understand the relationship between bottom water circulation and sea bed morphology.

To achieve the scientific objectives of this research, 3 areas were identified for geophysical and oceanographic exploration, 2 on the continental slope and rise off Sabrina Coast (areas A and C) and one on the continental shelf (area C). Because the area B was permanently covered by sea ice, only areas A and C were investigated.
Acquisition planned of multichannel seismic data was driven by:

1. As described previously: identification of expanded and well preserved sedimentary successions (potentially preserving good paleoclimate and paleoceanographic record), characterized by depositional process that appear to be continuously acting over the same site for long time span (e.g. sediment waves and drifts) and/or where major changes that can be related to regional or global rather than local causes, clearly occurred in selected areas identified on the basis of existing profiles and of the findings of previous studies which have already revealed the occurrence of suitable features for coring (Cook et al., 2013).
2. In order to correlate seismic units within our study region, to those identified in previously acquired data sets that cover a larger and more extended area, we selected lines to cross previous seismic profiles acquired in this area and available through the SDLS.
3. XBTs were launched at selected sites and along selected seismic lines. These will be analysed to detect seawater column reflectivity by means of seismic oceanography to understand the relationship between bottom water circulation and sea bed morphology.

IN2017-V01 MULTICHANNEL SEISMIC SYSTEM

Navigation

Navigation was managed by the RV *Investigator* Surveyors team using QINSy software (Quality Integrated Navigation System). The trigger has been managed by using the Teledyne Reson - PDS2000 software, configured to send the fire commands (fix) at 18.75 m shot point distance to trigger the Gun Controller. The Gun controller is set to NOT to send the trigger in case of misfire, to avoid different numbering for the fix and the record number. A comprehensive description of the navigation system and its interfaces to the seismic equipment is provided in Appendix 3.**Error! Reference source not found.**

Table 4 Geodetic parameters.

Acquisition Datum	WGS84	
	Spheroid	WGS84
	Semiaxis Major	6378137
	Inverse Flattening	298.25722356
Target Datum	WGS84	
	Spheroid	cs
	Semiaxis Major	cs
	Inverse Flattening	cs
Datum Transformation	Null	
Projection	Universal Transverse Mercator (UTM)	
	Zone	-50 (114' E - 120' E - Southern Hemisphere)
	Origin Latitude	00°00'00" N - Equator
	Central Meridian	117°00'00" E
	False Northing	1000000 m
	False Easting	500000 m
	Scale Factor	0.999600

Acquisition parameters

The choice of the acquisition parameters was driven by the need to compromise among resolving power, full discrimination of the shallower reflectors, and penetration to reach the target depth.

Seismic Source

For the High Resolution profiles, two GI guns in Harmonic mode were used. The total volume is 420 cu.in. For detailed description of the GI guns see Appendix 3. The GI guns (2 new and 2 used) are owned by the CSIRO-MNF.

The shot point distance was set to 18.75 m, corresponding to a time interval of about 9.375 seconds at a 3.5 knots speed. The record length was set to 5-6 seconds, long enough to reach the target depth and to allow the acquisition system to re-arm.
The array was towed to a depth of 4 m to have a 182 Hz upper limit. According to the λ/4 Rayleigh criterion, for speed of sound ranging from 1455 m/s to 3000 m/s, a resolving power from about 1 m for the shallower events to 2 m for the deepest ones can be expected.

Receivers

The data were collected by a 96 channel, 300 m long digital streamer, with a channel distance of 3.125 m corresponding to an effective horizontal sampling of 1.562 in the stacked section. The streamer was towed to a variable depth, dependent on the sea state, between 2 and 4 m below the sea surface. With an 18.75 m shot point interval, the fold coverage attainable was 8 traces/CDP.

The distance between the source and the first channel (near offset) was kept as short as possible, that is, in the same order of the minimum water depth but large enough to prevent saturation (data clipping) in the shallower part of the records. The near offset was set to 25 m. To keep the streamer at the target depth 4 levellers (DigiBIRDS) controlled by a TAP bird system have been used. For the streamer configuration see *Figure 14*. The TAP controller receives from the bird the information relative to the towing depth, and sends the commands to the wing to keep the bird at the "target depth".

The acquisition parameters are summarized in

Table 5, *Figure 15.* and *Figure* 16. A more detailed description of the seismic equipment can be found in Appendix 3. The SEGD format recorded data were logged on the acquisition computer and on an external Hard Disk at the same time. At the end of the day back-up copies were stored on an External Hard Disks.

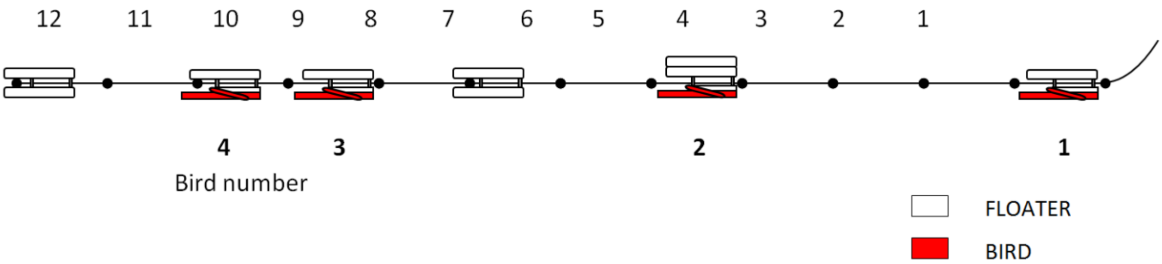

Figure 14. Streamer and bird configuration.

Table 5. Summary of acquisition parameters.

ACQUISTION PARAMETERS					
SOURCE		STREAMER		RECORDING	
Model	GI-GUN Sercel	Model	GeoEel	Model	Geometrics CNT-1
Array	2 x 210 cu.in. (3.44 l)	Length	300 m	Samp. rate	1.0 ms
Gun mode (HR)	105G+105I Harmonic	Ch. No.	96	Rec. length	5-7sec
Shot Interval	18.75 m	Ch. Dist.	3.125 m	LC filters	3 Hz (LC);
Depth	4 m ± 0.5 m	Depth	2 m ± 0.5 m	HC filters	Antialias
Pressure	140 atm.	Offset	12.5 m	Aux chan.	Ch.2
SYNCHRONIZATION					
Controller	RTS Sure Shot				
Aim Point	50 ms delay				

Table 6. Vessel's offsets.

	X [m]	Y [m]	Z [m]
Centre of vessel	0.00	0.00	-
GPS = MRU	+2.03	+9.30	-
Stern	0.00	-56.25	-
Seismic source	+8.86	-71.95	-4.00
Streamer CH1	-1.14	-96.95	-2.00/-3.00

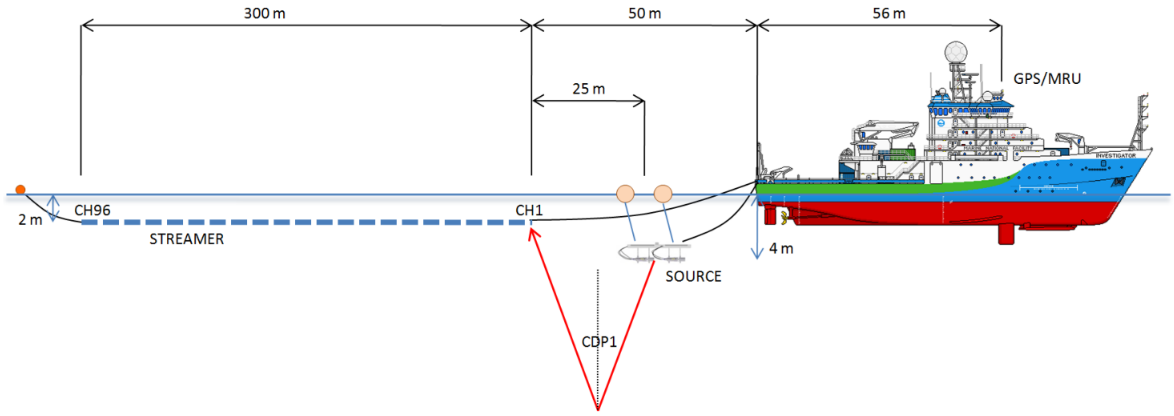

Figure 15. Acquisition geometry lateral view.

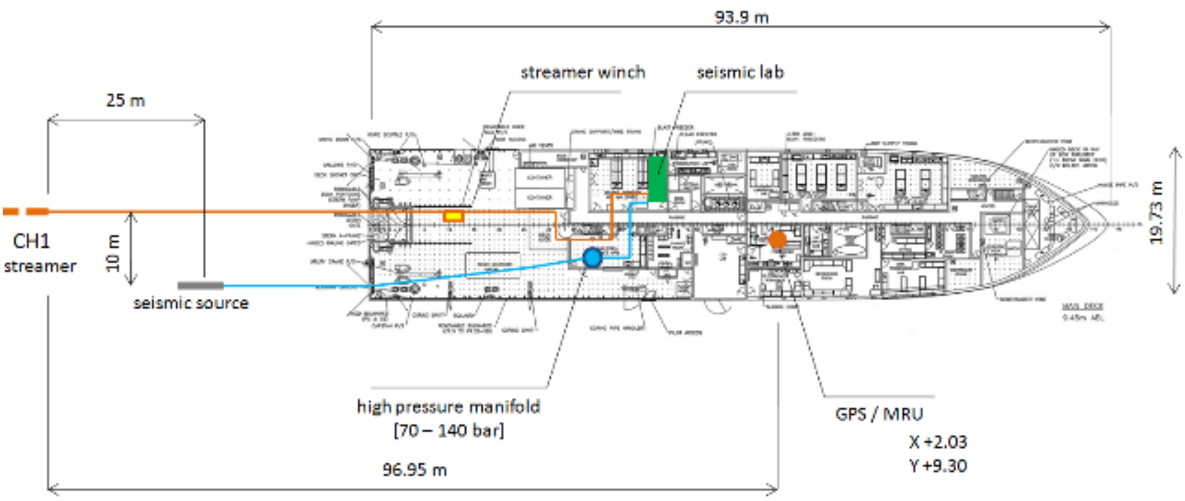

Figure 16. Acquisition geometry top view.

QUALITY CONTROL (QC) AND SHIPBOARD PROCESSING

The data were first transferred from the external backup HD to the processing laptop. The raw data were then loaded and reformatted from SEG-D to GEDCO Vista Seisimage processing package. Before proceeding with the scheduled processing, an overall check of the incoming data was conducted; thus QC was focused on:

- choice of the acquisition parameters, and specifically:
    1. to verify the energy (penetration) of the chosen sources, and,
    2. to verify that the energy presents on near offset traces does not saturate the digitizer;
- verification of the overall quality of the data by single shot and near trace screen display;
- identification of possible noise affecting the data and possibly its source (if environmental, electric, mechanic, etc.), its nature (if random or coherent) and its characteristics (such as dominant frequency, apparent velocity and wavelength, etc.) and suggesting a strategy to reduce its effects;
- depth of the source and the streamer by investigating the data amplitude spectrum.

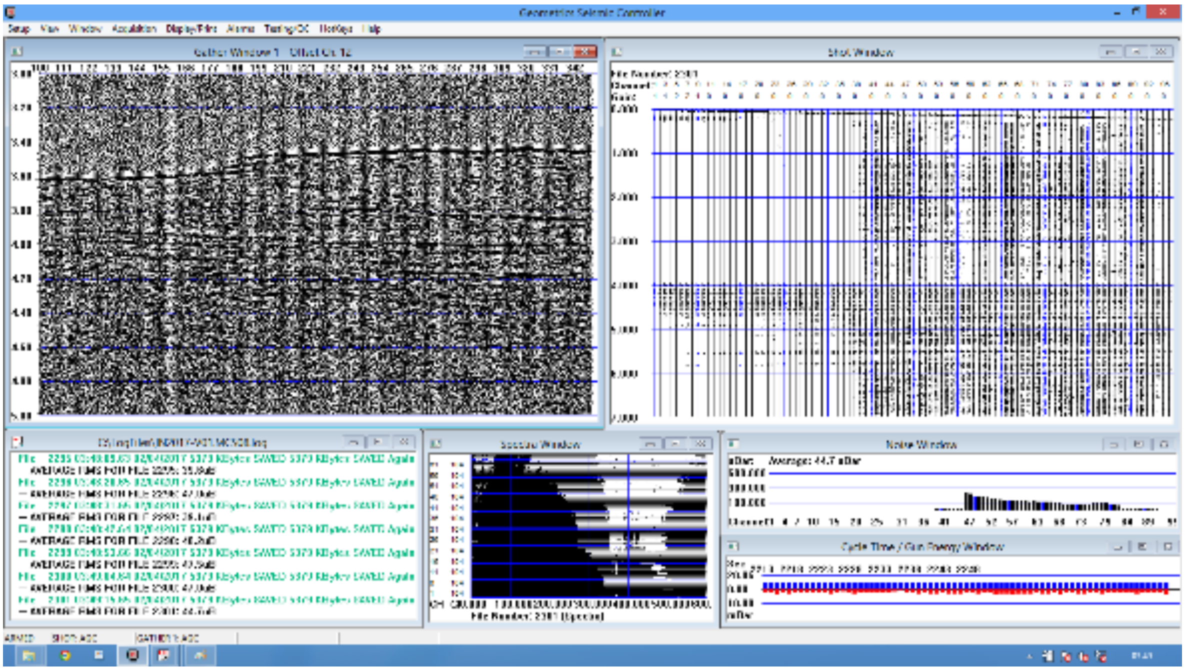

Figure 17. CNT 2 Marine Controller software display. *After the QC, a conventional processing sequence (Figure 18) was applied to the data in order to produce a preliminary stacked version of most of the profiles acquired (QC is here included as part of the sequence).*

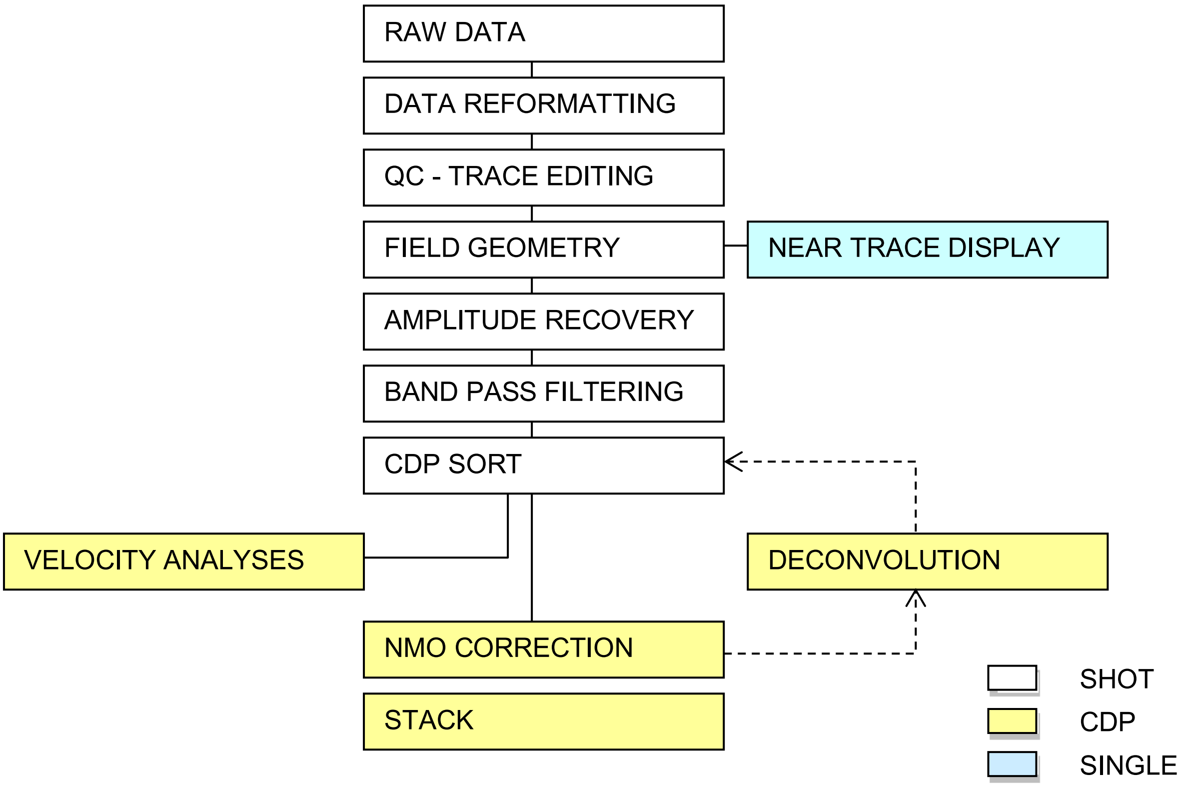

Figure 18. Basic processing sequence.

Field geometry assignment
Once the QC was accomplished, field geometry was incorporated within the seismic data. Based on surveying information, coordinates of shot and receiver locations for all the traces were stored within the correspondent headers.

Amplitude recovery
A gain recovery was applied to the data in the shot domain to correct for the amplitude effects of wavefront (spherical) divergence and absorption. At this stage of processing, a time dependent amplitude recovery function in an exponential time power form (Tn, being T = TWT and with n = 1.6) was chosen.

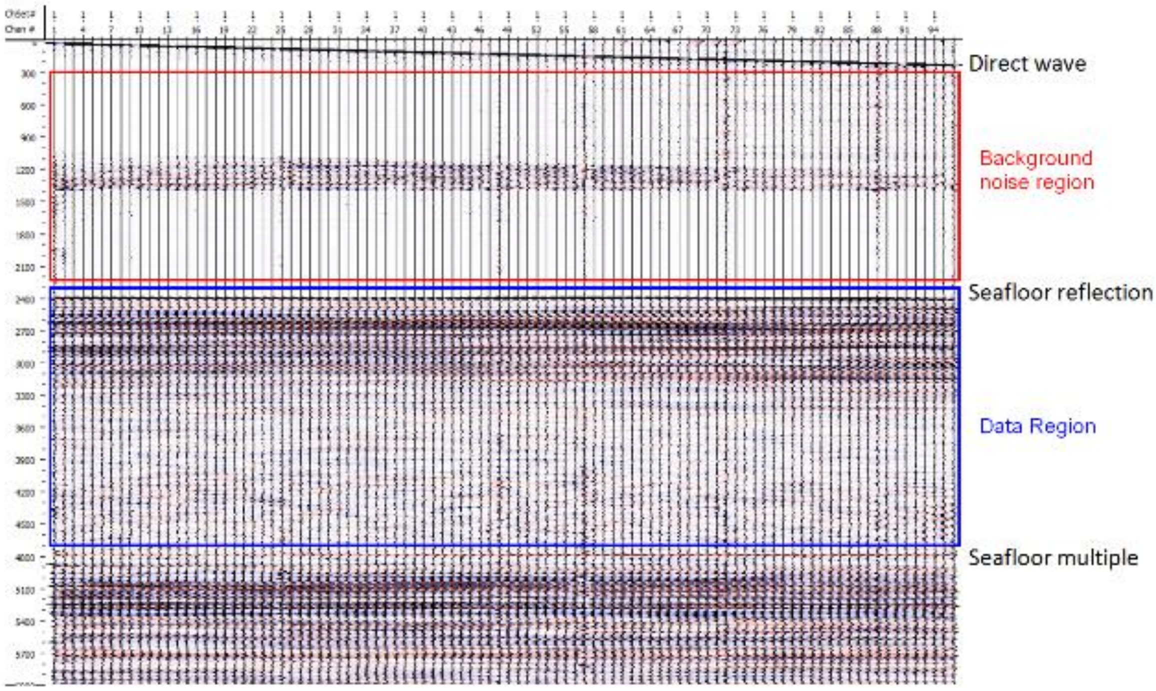

Figure 19. Raw data record example (SEGD). *The main events are highlighted at the right side.*

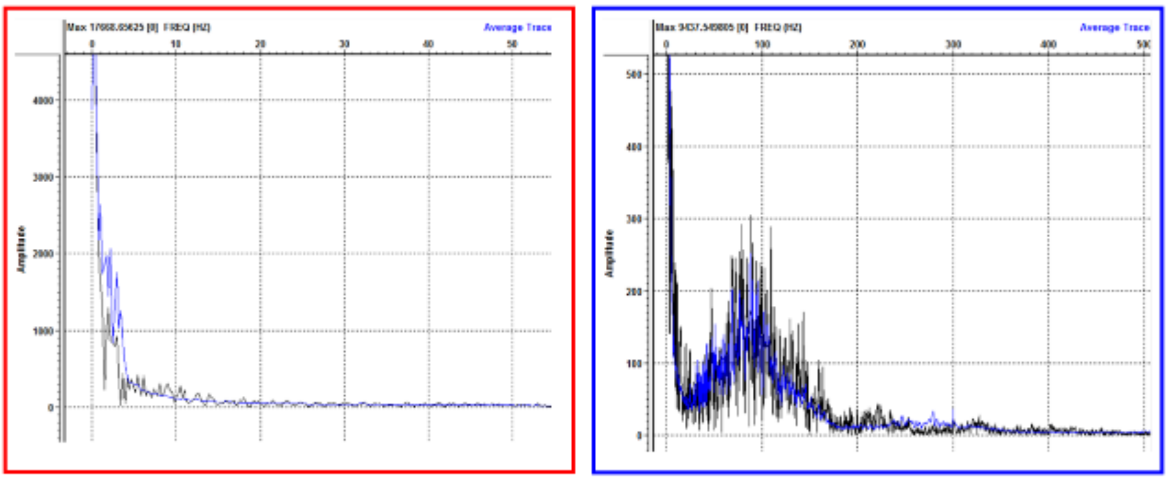

Figure 20. The reflected data spectrum. *Left: background noise region; Right: data region).*

Bandpass filtering
On the basis of the QC outcomes, a wide band-pass filter (Butterworth Low cut 12/24 – High cut 150/250) was applied so as to remove (or at least reduce) the unwanted low and very high frequency noise from the data. Prior to the gain and filter application, the record appears to be dominated by a very low frequency, high amplitude noise component (<10 Hz) affecting the near offset channels. This monochromatic noise is probably generated by the engines or the propeller of the boat; moreover, some traces seem to be offset by a direct current (DC) component. After the filter application, these noise result were totally removed.

CDP sort
Prior to the velocity analyses, the data were CDP sorted, which involved a co-ordinate transformation from shot-receiver to midpoint-offset. The groups of traces arranged in this way are called common depth point (or CDP) gathers, each of them containing the seismic signals recorded from rays incident at different angles upon a particular subsurface.

Velocity analyses
Velocity analysis were performed on selected CDP gathers, the output from this operation representing some measures of signal coherency along the hyperbolic trajectories governed by velocity, offset, and travel time.
Velocity spectra analyses were used together with the CVS method (data are stacked with a range of constant velocities, and the constant-velocity stacks themselves are used in picking velocities) and super-gather normal move out correction (a super-gather is formed by two or three adjacent CDPs).
Velocity analyses eventually provided a velocity field that was used in normal moveout (NMO) correction of CDP gathers. As a result of moveout correction, traces were stretched in a time-varying manner, causing their frequency content to shift toward the low end of the spectrum. Frequency distortion increases at shallow times and large offsets. To prevent this from happening, a mute function was applied that removed the upper part of the far offset record.

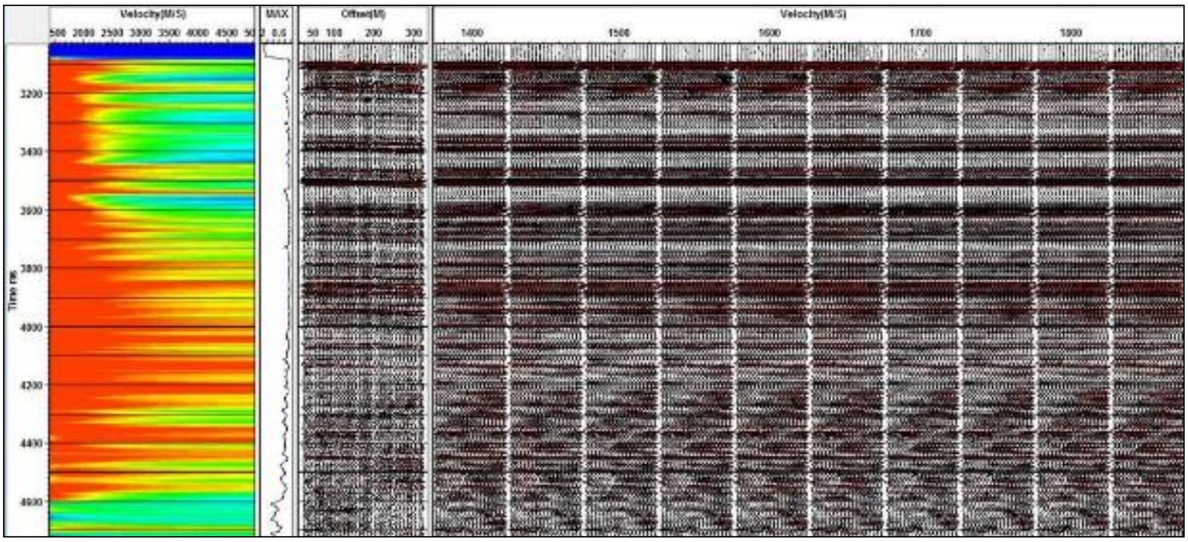

Figure 21. Velocity analysis session: Semblance, Supergather and CVS panels.

The brute stack sections of all the seismic profile acquired are shown in Appendix 3.

Normal Move Out corrections and Stack
After the velocity analyses, a Normal Move Out (NMO) correction was applied to the CDP traces. Successively, the single CDP traces were combined to improve the signal-to-noise ratio. This process, involving the sum the single traces of a CDP gather after the reflected signals has been aligned by the NMO correction, which is known as a stack.

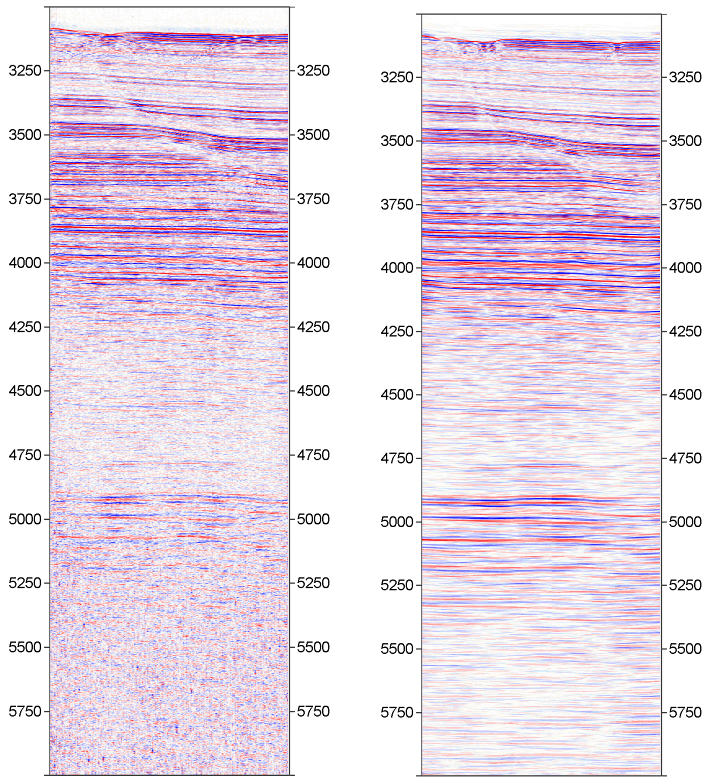

Figure 22. IN2017-V01-MCS07B - *Example of Brute stack (left) and Migration (right).*

SEISMIC OPERATIONS AND OBSERVATIONS

The seismic acquisition started on January 22nd and ended on February 24th. At the end of the survey, 10 seismic profiles, for a total length of 322 km, were recorded (see also cruise diary). The seismic acquisition was limited to day light time (basically from 8.00 to 18.00 hrs local time) due to safety reason and crew availability for deployment and recovery of the seismic gear. Refer to map in

Figure 23 for further details on the location of the profiles. In Appendix 3 the general statistics are summarized.

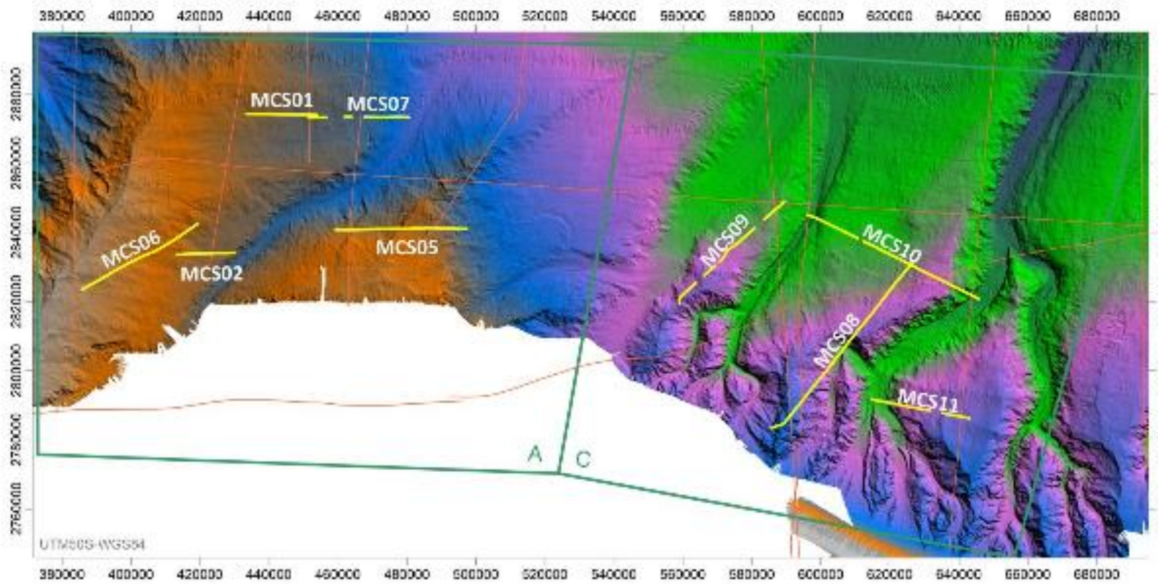

***Figure 23. Location of IN2017-V01 seismic lines**. Existing seismic lines acquired previously in the area and stored at the Seismic Data Library System (SDLS) are also shown (orange).*

Profile IN2017-V01-MCS01

The profile started on January 22nd at 00.24, after the soft start (ramp up) procedure. At 00.40 we increased the shot interval from 12.5 to 15.625 m due to a delay between acquisition and recording systems; at 00.43, for the same reason, the shot interval was changed to 18.75 m. At 01.36 (shot 649) Gun 1 was shut down due to a problem in the signal, and the acquisition proceeded with Gun 2 only. At 03.20 (shot 1292) the acquisition stopped for whales within the shutdown area. Due to the persistent presence of marine mammals in the area, it corresponds to the E.O.L.

Profile IN2017-V01-MCS05 and MCS05B

The profile started on January 23rd at 22.21, after the soft start procedure. At 01.48 one gun was stopped and the pressure reduced to 70 bar (low-pressure mode) for the presence of whales in the low –power area. At 01.55, acquisition was stopped due to the presence of whales in the shut-down area. The acquisition re-started at 03.12, after a loop to fill the gap, renamed as IN2017-V01-MCS05B, and proceeded regularly until the E.O.L. on January 24th at 05.41.

Profile IN2017-V01-MCS02

The profile started on January 24th at 22.03, after the soft start procedure. At 00.38 (25th January), due to the presence of rubble sea ice in the area, it was decided to recover the seismic gear in order to avoid damaging it and to stop the acquisition, E.O.L.

Profile IN2017-V01-MCS06
The profile started on January 27th at 04.12. From this line onward, due to the limited time available, we decided to start recording data at the soft start: timing and details about increasing pressure in the guns are in the cruise diary. Due to the favourable sea surface conditions, we moved the streamer up to 2 meters below sea surface from this profile onward. The acquisition proceeded regularly to the E.O.L. at 10.10.

Profile IN2017-V01-MCS07, IN2017-V01-MCS07B and IN2017-V01-MCS07C
The profile started on January 29th at 04.11, together with soft-start. At 04.58 we shut down the acquisition due to the presence of whales in shut-down area. From this line onward, if not strictly necessary, we decided to avoid the loop and save time in order to reach the planned end of the lines. At 05.59 we re-started the acquisition, named IN2017-V01-MCS07B. At 06.15 we shut down again for whales in the area, and E.O.L. 07B. At 06.55 re-start the acquisition, with line IN2017-V01-MCS07C, which proceeded regularly up to the E.O.L. at 08.55.

Profile IN2017-V01-MCS08
The profile started on February 3rd at 21.14. Starting from this line we moved to Area C, characterised generally by deeper water depth, and increased the record length to 7 sec. Acquisition took place at low-pressure (1 gun at 70 bar) due to mammals in low-pressure zone, from 23.03 until 23.17, and on February 24th from 02.23 until 02.50. The profile ended at 07.01.

Profile IN2017-V01-MCS09, MCS09B, MCS09C and MCS09D
The seismic line started on February 6th at 04.02. At 05.16 pressure reduced to 70 bar on 1 gun for whales in low-pressure zone. At 05.20 whales in shit-down area, stopped acquisition. At 05057 we re-started the acquisition (line IN2017-V01_MCS09B): at 06.32 low-pressure mode acquisition, and at 06.36, due to whales within the shut-down area, stopped acquisition. We re-started the acquisition (line MCS09C) at 06.56. At 08.18 acquisition took place in low-power mode, and at 09.06 acquisition was shut-down due to the presence of whales in restricted area. At 09.41 acquisition was re-started with line MCS09D, and ended at 10.54 (E.O.L.)

Profile IN2017-V01-MCS10 and MCS10B
Line MCS10 started on February 13th at 23.48. From 01.19 until 02.07 (on February 14th), acquisition was at 70 bar with 1 gun due to the presence of mammals in the low-power zone. At 02.21, mammals in shut-down zone caused a stop to data acquisition.
Acquisition was re-started at 02.39 with line MCS10B, and ended at 08.26 (E.O.L.).

Profile IN2017-V01-MCS11, MCS11B and MCS11C
Acquisition of line MCS11 started on February 17th at 21.38. Due to rough sea conditions, the streamer was moved down to 3 meters. At 23.57, acquisition was stopped due to the mammals in the shut-down zone. On February 18th at 00.04, we re-started line MCS11B, and at 00.19 stopped again for mammals in the shut-down zone. We re-started at 00.51 (line MCS11C), and proceeded regularly until the E.O.L. at 02.07.

Profile IN2017-V01-MCS12, MCS12B and MCS12C
On February 24th, before starting the acquisition, running streamer signal transmission and buoyancy tests, only the first 2 sections of the streamer could be seen by recording system. After recovering the streamer, we removed the 3rd section and acquired data on 88 channels on 11 sections. At 04.31 we started the line MCS12, but at 04.36 we had to stop the acquisition due to whales in shut-down zone. At 05.52 we re-started the acquisition (line MCS12B). At 07.33 stopped the acquisition due to whale in shut-down zone; at 09.16 we re-started the acquisition (line MCS12C), but we had to stop again due to whale (the same one observed previously) in shut-down zone (playing around the streamer!) and decide to end the acquisition (E.O.L.).

SEISMIC PRELIMINARY RESULTS

The area is generally characterised by sediment mounds and overbanking deposits cut by deep-sea channels/canyons.
The very preliminary results based on looking at the Brute Stack processed seismic profiles are essentially that:

- The sediment mounds on the continental rise are characterised in their upper part by a thick (up to 0.9 TWT sec) unit characterised by continuous parallel to sub-parallel reflectors, almost draping the underlying surfaces (Figure 24).

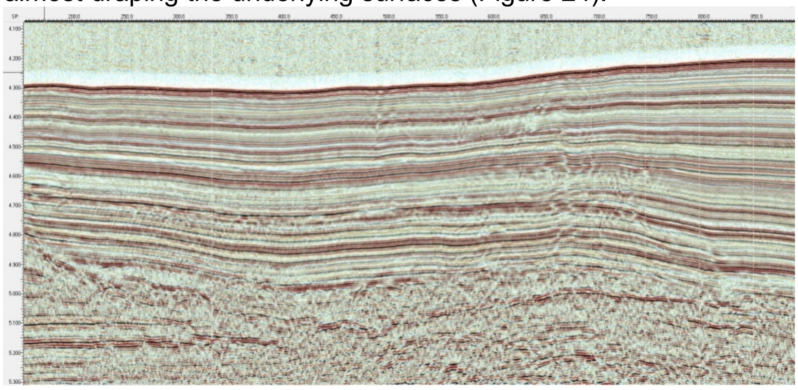

Figure 24. Example of the thick and continuous sedimentary sequence shown on line IN2017-V0.1-MCS10.

- On the ridges located in the western part (Area A), this stratigraphic unit is characterised by a more superficial part where the reflectors show lower amplitudes with respect to the underlying unit, where continuous reflectors with higher amplitudes occur (*Figure* 25).

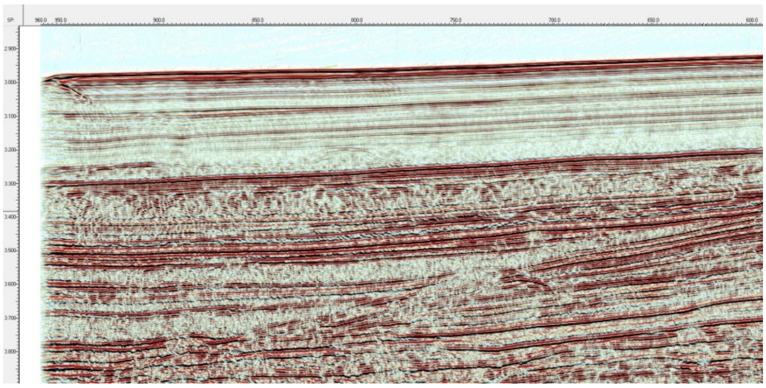

Figure 25. Lower amplitude continuous reflectors in the upper part of the stratigraphic sequence observed on line IN2017-V01-MCS02.

- Below these units, in the proximal part of the area, the occurrence of gravity flows/mass wasting deposits can be inferred by the occurrence of chaotic deposition and discontinuous reflectors, whereas in the distal part, the occurrence of sediment waves indicates a major influence of bottom current activity in the sediments transport and deposition (*Figure* 26).

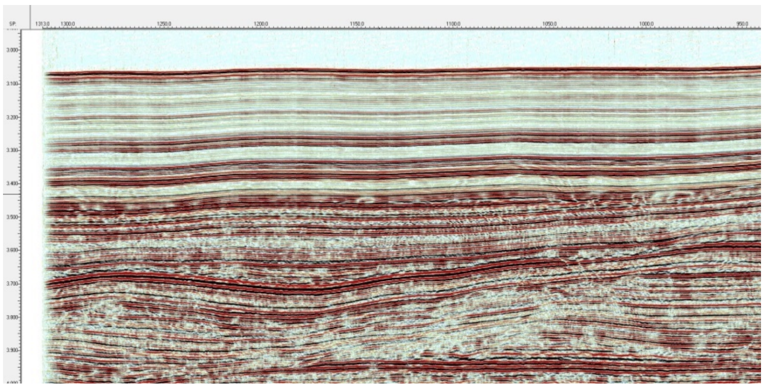

Figure 26. occurrence of sediment waves observed along the line IN2017-V01-MCS01

MARINE MAMMAL OBSERVATIONS (FOR SEISMIC PURPOSES)

All seismic survey vessels operating in Australian waters must undertake the following basic procedures during surveys irrespective of location and time of year of survey (Environmental Protection and Biodiversity Conservation Act EPBC Policy Statement 2.1, Australian Government, Department of the Environment, Water, Heritage and the Arts, September 2008). These requirements were supervised by a Marine Mammal Observer. The procedures comprised: (1) Pre start-up visual observation, (2) Soft start, (3) Start-up delay, (4) Operations, (5) Power- down and (6) Stop work. These procedures are described in detail in the section on Marine Biology. The primary results were that seismic operations could only be carried out during day light hours and that the presence of whales could result in delayed line starts, reduced power or shut down of the guns. Whales were abundant in the area so only 3 lines were completed without interruption.

OPERATIONS EVALUATION

Operations on board were carried out without any problem. The deployment and recovery deck operations worked nicely, due also to the facility offered by the ship and the ability and efficiency of the crew involved in the operations. Considering it was the first time that seismic gear was used on board this ship, it has been successfully accomplished.

During acquisition of line IN2017-V01-MCS01O on 22nd January, we encountered a problem with the hydrophone at gun 1. The hydrophones supplied by the manufacturer (Sercel) together with the CSIRO GI guns were the wrong type (near field for G Gun), so we used our hydrophones (OGS owner) on the G Gun support. Afterward, the hydrophone on the 1st Gun became detached and was floating beneath the GI Gun. Since the signal at the acquisition system was poor, we decided to acquire data with only the second GI gun. After recovering the equipment, we discovered the problem and fixed the bolt with stainless wire on both the hydrophones to the GI guns. This problem did not occur again during the rest of the survey.

On 24th January during acquisition of line IN2017-V01-MCS05 the DigiBIRd number 3 was not responding. The depth of the streamer wasn`t affected that much, since the other 3 DigiBIRDS were working correctly. After the recovery of the streamer, the batteries inside the DigiBird number 3 were changed and the BIRD worked well.

On February 24th, before starting the acquisition of line IN2017-V01-MCS12, while running streamer signal transmission and buoyancy tests, only the first 2 sections of the streamer could be seen by recording system. After recovering the streamer, we removed the 3rd section and acquired data on 88 channels on 11 sections. Since this was the last seismic acquisition of the cruise, after the recovery of the streamer at the end of the line, we put the damaged section at the end of the streamer to repair it back at our Institute.

The seismic data acquisition and recording location (workstation) was set up in the wet lab (dirty) close to the manifold to check the air pressure in the guns. In the future, we suggest that the acquisition and recording location be switched to the operations room and to utilize a remote control from the operations room to the air pressure system.

SUMMARY

The mission IN2017-V01 onboard of *RV Investigator*, otherwise known as the Sabrina Seafloor Survey mission, departed from the CSIRO Hobart wharf on the 14th January and ended on the 5th March 2017 (see time chart in Figure 27).

The Mobilization started on Thursday January 12th in Hobart Harbour, and involved the seismic equipment installation, PDS2000 configuration, Sureshot gun controller and TAP bird controller configuration. The first acquisition (seismic profile IN2017-V01-MCS01) started on January 22nd, after performing dry and wet test for the equipment, whereas the last acquisition (seismic line IN2017-V01-MCS12) has been carried out on February 24th.

As a whole, 322 km of multichannel seismic were recorded on 10 seismic profiles. All the data have been processed on board to Brute Stacks, and the data show good quality and good signal throughout the entire acquisition`s windows. Some of the seismic profiles show some gaps due to interruptions of the acquisition related to the presence of whales in restricted area.

If not strictly necessary, we decided to avoid the loop after the interruptions and save time in order to reach the planned end of the lines, due to the time limitations to complete the seismic operations (deployment, acquisition and recovery) which were restricted to daily light hours (generally 8.00 a.m. to 6.00 p.m.).

Only 3 seismic profiles were run continuously, without any stop: IN2017-V01_MCS01, MCS02 and MCS08. The longest continuous seismic record was achieved on profile IN2017-V01-MCS08 (64.207 km), whereas the more interrupted profile was the last one (IN2017-V01-MCS12), with 11.268 km acquired over almost 36 km planned (30% data acquisition). In contrast, only one planned seismic line was aborted due to bad weather conditions, on February 8th (sea state 5). Sub bottom profiles and multibeam were simultaneously acquired during multichannel seismic acquisition. The coordinates and the length of each profile is given in Appendix 3.

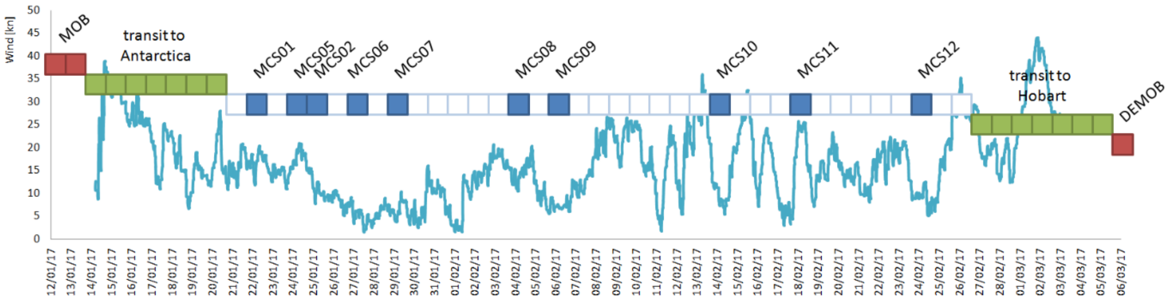

Figure 27. Time chart of the voyage

SECTION 4. Marine Geology

SUB-BOTTOM PROFILING

The sub-bottom profiles collected throughout the voyage were instrumental in identifying coring locations and understanding basic geomorphic and sedimentary features of the survey site. Upon review of all profiles, three main recurring features were identified:

- The submarine canyons – termed turbidite channels
- The plateau sediments – termed distal levee deposits
- Slump and mass movement features – often associated with the submarine canyons

The turbidite channels are thought to be the drivers of sedimentation in the area with course material funnelled from the shelf through the canyons and down to deeper regions. The fine fraction from the flow gets lifted and pushed to the sides forming the levee deposits that we see forming the ridges and plateaus parallel to the channels. As seen on the sub bottom profiles, these distal levees form well stratified, expanded packages of fine muddy sediment (*Figure* 28 and *Figure*). In area A, we see one straight channel that bisects two large shallow sediment packages. Most of the accretion is seen to occur on the western side of the channel for these north trending features. The thickest sediment package occurs proximally to the channel which then thins towards the ridge crest, exposing underlying stratigraphy at the top of the western ridge in area A (*Figure* 28A). This draping of stratigraphy on the larger western sediment package is not as prominent on the smaller eastern sediment package in area A which is has a flatter top and no pinch out towards the margins. On the western side of the ridge crest there is a change to a more erosional regime with multiple slump and mass movement features observed (*Figure* 28 and *Figure* 30).

In area C we see a network of dendritic channels stemming from the continental shelf. The structure of these channels changes rapidly with distance from the shelf. In the fluvial analogy, these could be thought of as due to the changes in the energy of the channels. The hard reflector surface seen consistently in the base of all the channels reflects the deposition of courser or denser material accumulating in the canyons (Figure 31). The crests of the plateaus are much more proximal to the channels in area C and again consistently occur along the western boundary of a given channel and gradually slope down to the west (Figure 32). These ridges, again thought to be formed as part of a levee deposit, are well stratified with expanded stratigraphy. The majority of the slumping and mass movement features seen occur along the western side of the canyon walls with some classic erosional and terrace features. When comparing the turbidite channels in areas A and C it was noticed that the singular channel in area A is not as well defined and not as incised as the channels in area C.

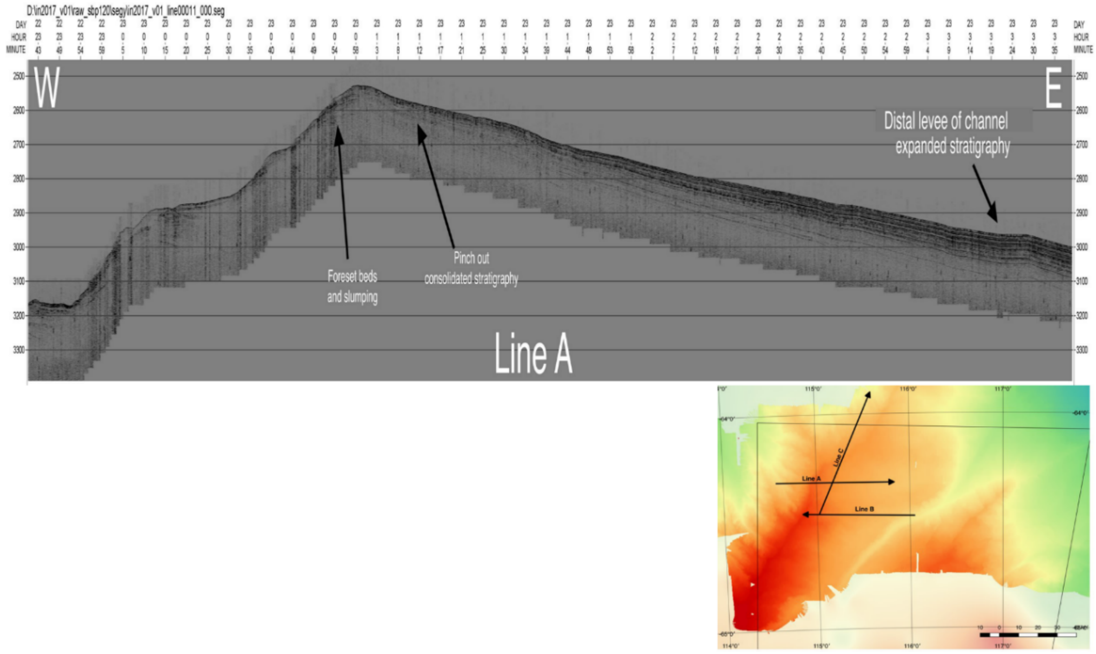

Figure 28. Sub bottom profile line A of ridge sediment in area A. *Inset is of bathymetric map of area A where arrows indicating direction of ship movement and extent of sub bottom line.*

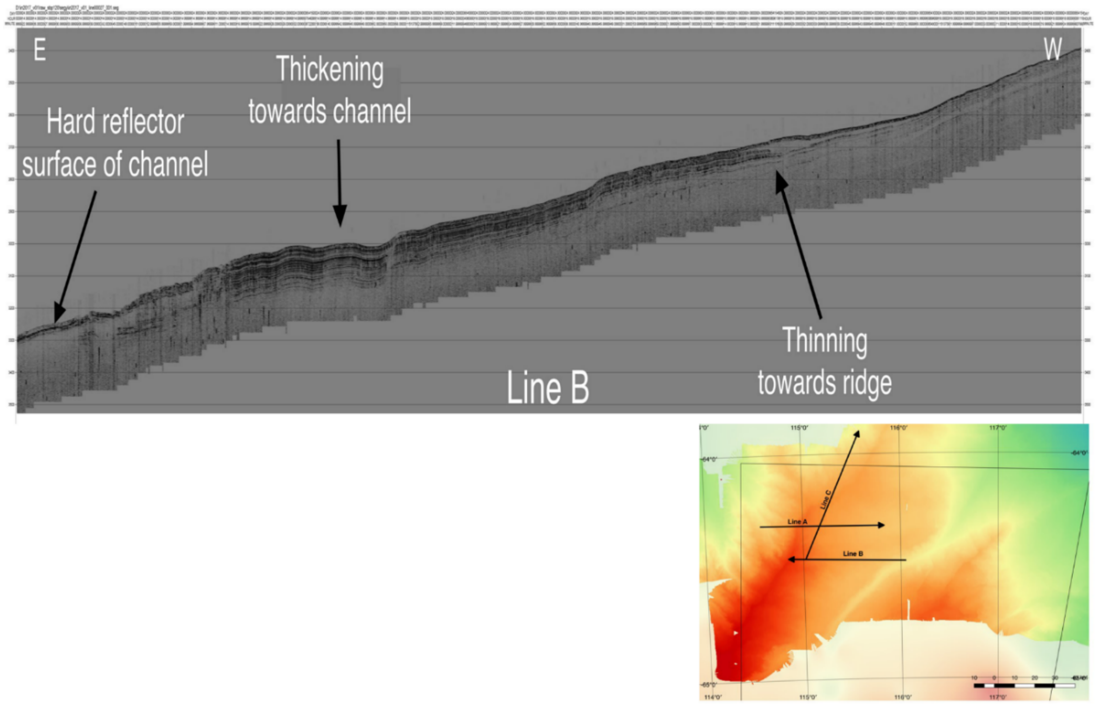

Figure 29. Sub bottom profile line B of ridge sediment in area A. *Inset is of bathymetric map of area A with arrows indicating direction of ship movement and extent of sub bottom line.*

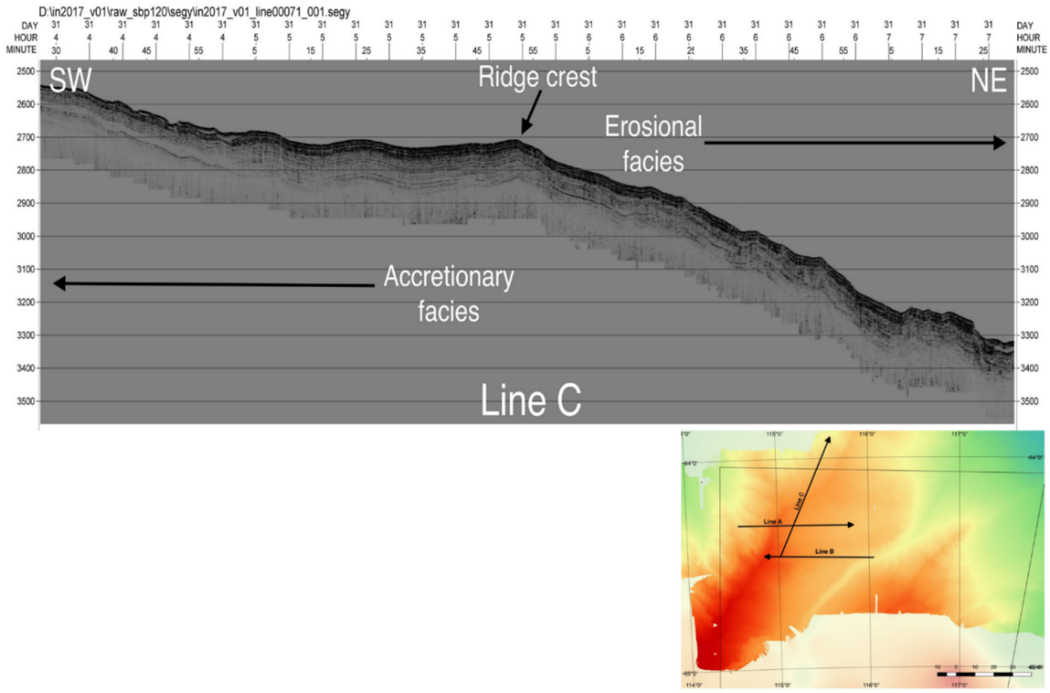

Figure 30. Sub bottom profile line C of ridge sediment in area A. *Inset is of bathymetric map of area A with arrows indicating direction of ship movement and extent of sub bottom line.*

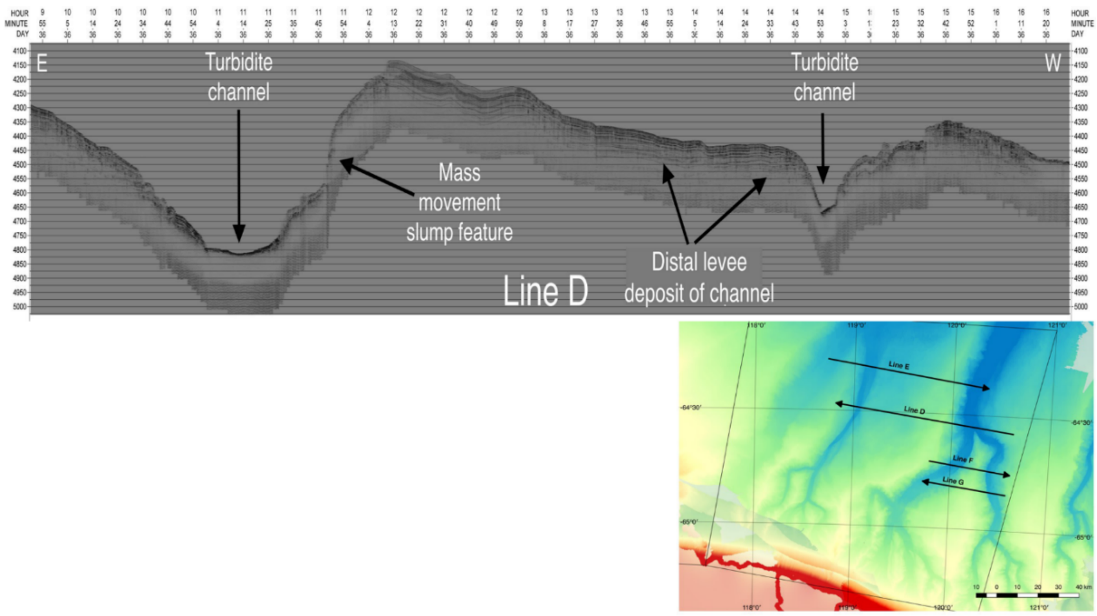

Figure 31. Sub bottom profile line D of channel and ridge morphology in area C. *Inset is of bathymetric map of area C with arrows indicating direction of ship movement and extent of sub bottom line.*

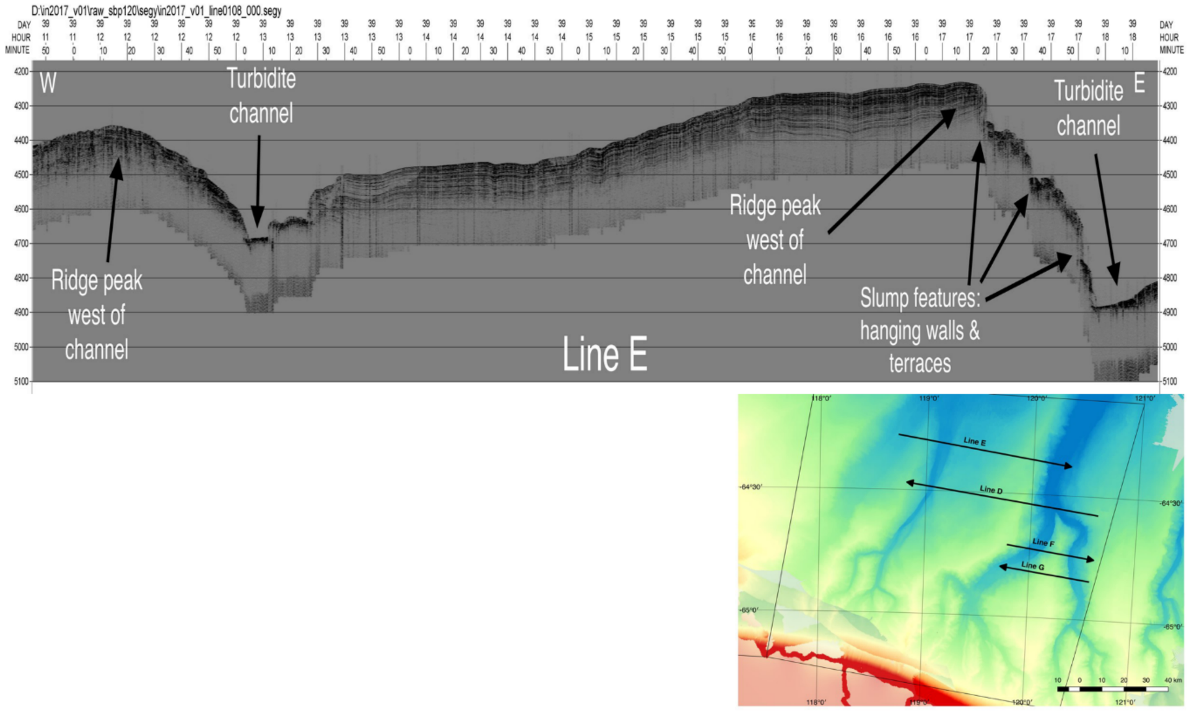

Figure 32. Sub bottom profile line E of channel and ridge morphology in area C. *Inset is of bathymetric map of area C with arrows indicating direction of ship movement and extent of sub bottom line.*

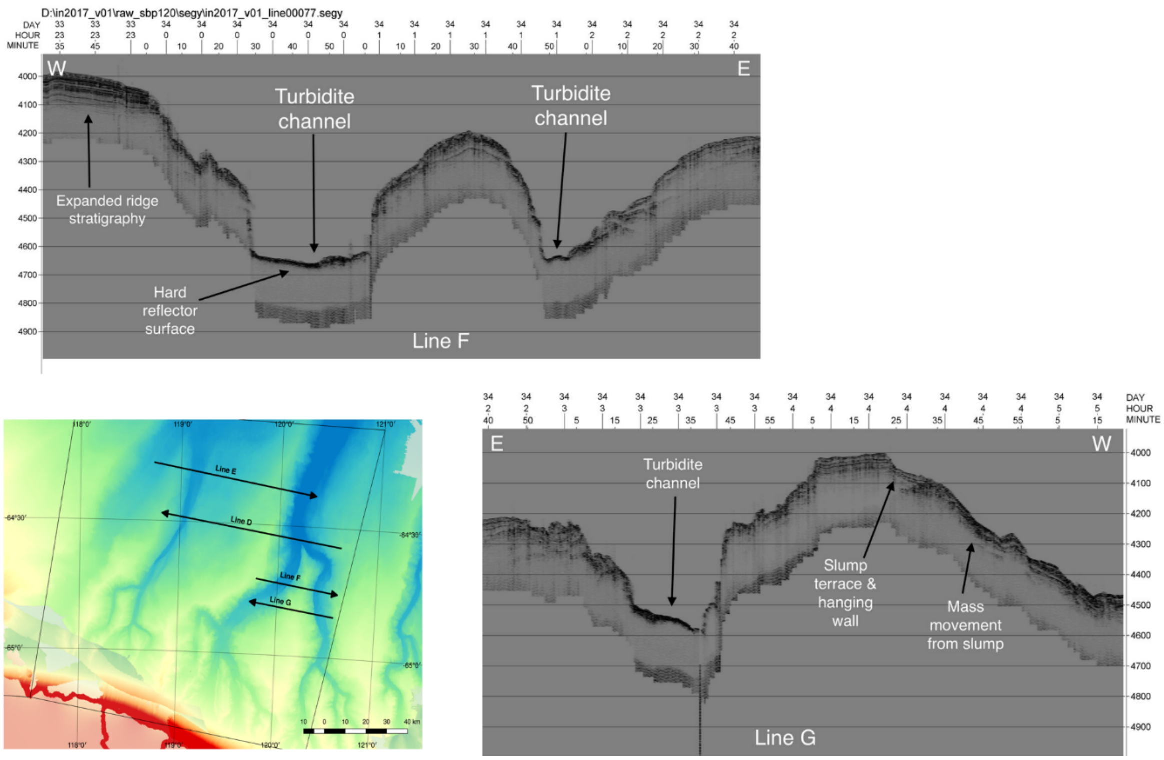

Figure 33. Sub bottom profile lines F and G of channel and ridge morphology in area C. *Inset is of bathymetric map of area C with arrows indicating direction of ship movement and extent of sub bottom line.*

VIDEO TOWS

A total of six camera tow transects were completed during survey IN2017-V01 using the MNF's Deep Tow Camera. This system collects downward facing still images and high definition video, with standard definition video from a forward-facing video. Several sensors are also attached to the towed body, allowing collection of CTD data, altimetry and location of the towed body on the seafloor.

Tows were conducted in waters shallower than 2000 m to maintain a winch load of less than 1.5 T. Two tows (CAM01 and CAM02) were targeted on a downslope transect from the top of a large deep ridge at the western edge of Area A. Four tows imaged transects from the shelf edge to the upper slope to the south of Area C (CAM03, CAM05, CAM06 and CAM07). Locations are shown on *Figure* .

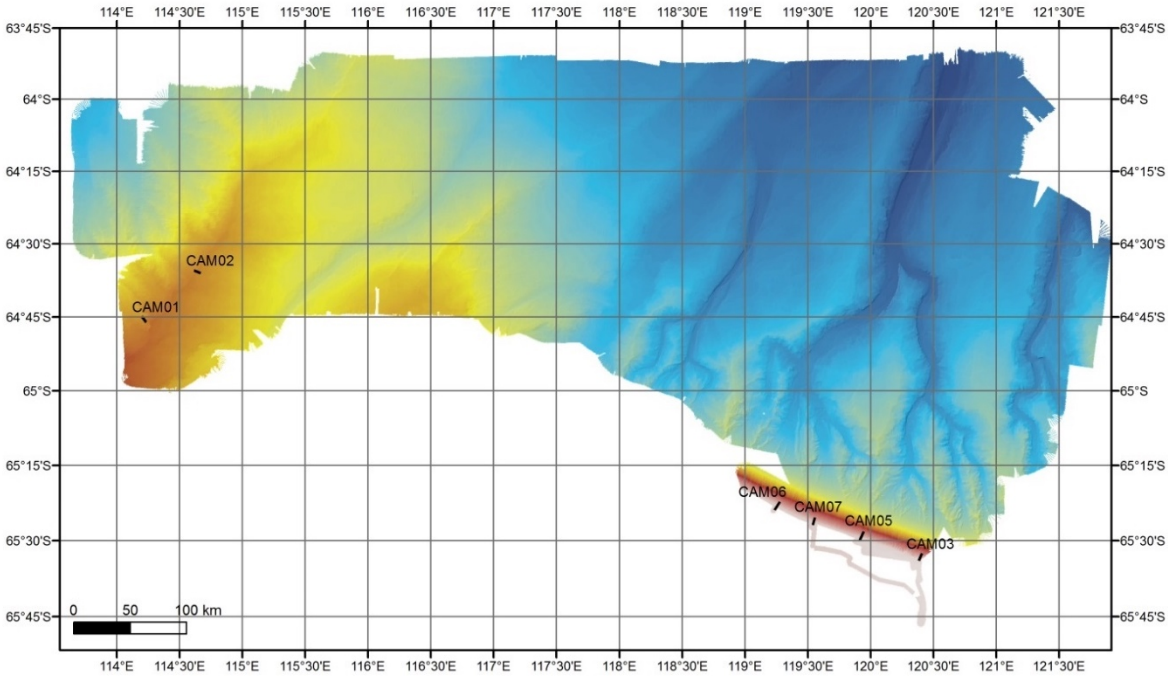

Figure 34. Location of camera tow sites.

Method

Camera tows targeted seafloor depths between 480 and 1680 m. Tows were designed to run down slope to reduce potential for colliding with the bottom. All tows were run with a ship speed over the ground of approximately 2 kt. Specifications for the Deep Tow Camera are shown in *Table 7*, with the sensors and camera systems illustrated in *Figure* 35.

An Excel spreadsheet was used to calculate the deployment position for the camera tow based on the water depth at the target, the vessel speed during deployment and wire deployment speed (Table 8). This spreadsheet allowed a deployment distance back from the target to be calculated, and Qinsy was used to define the latitude and longitude of this deployment position. An initial deployment speed of 4 kt was used to ensure that the camera dragged quickly clear of the vessel, with vessel speed reduced to 2 kt once the camera reached ~100 m depth. The position of the towed body was monitored via the beacon, and vessel and wire speed adjusted to ensure that the camera system reached the seafloor at or before the target. During CAM02 communication with the beacon was lost, so the wire out to depth ratio was used to monitor the position relative to the target. A layback correction was applied after completing the tow to determine the approximate tow location.

Table 7. Specifications of the Deep Tow Camera system.

EQUIPMENT	SPECIFICATIONS				
	Model	Depth rating	Software interface	Format	Other
CAMERAS					
Primary Stills Image Camera	Canon – 1DX	3000 m	EOS Utility	JPEG	
Primary Video Image Camera	Canon – C300	3000 m	Blackmagic Media Express	HD1080i50	
Secondary Video Image Camera – look ahead	Hitachi – HV-D30P	3000 m	VLC Media Player	PAL	
SENSORS					
CTD	SBE 37	7000 m	Labview		
Altimeter	Kongsberg Mesotech – 1007D	6000 m	Labview		Range: 0-500 m
Pressure sensor	Druck PMP 5074	6000 m	Labview		
LIGHTS AND LASERS					
Lights	DSP&L 3150 High Output SeaLite Sphere	6000 m	Labview		Quantity: 4
Lasers	DSP&L 3150 MicroSeaLaser	6000 m	Labview		Quantity: 2
BEACONS	Sonardynne WMT 8190	5000 m	Ranger 2 USBL		Quantity 2

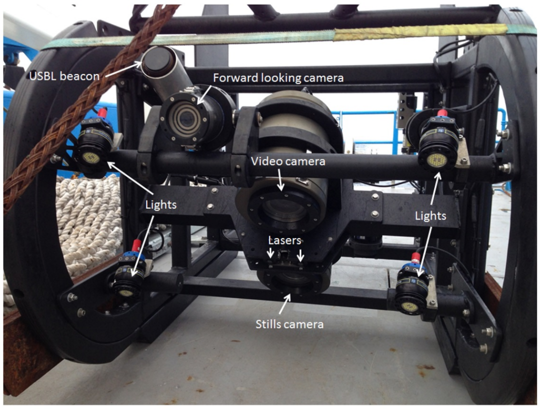

FRONT VIEW

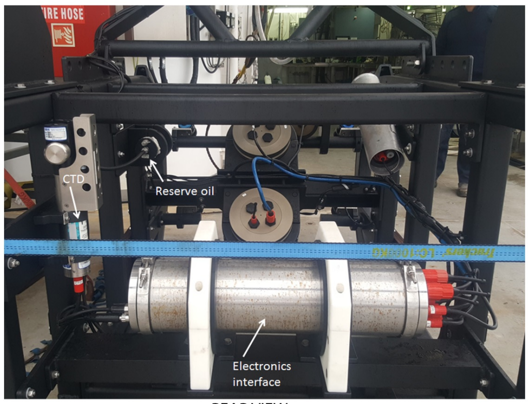

REAR VIEW

Figure 35. Set up and components of the Deep Tow Camera from the front (left) and rear view (right).

Table 8. Calculation of deployment distance from target

Target depth (m)	1615
Wire to depth ratio	1.6
Vessel speed over ground (kt)	2
Wire payout speed (m min-1)	60
Predicted wire out (m)	2584
Estimated layback (m)	2017
Time to pay out wire (min)	43
Vessel speed (m min-1)	60
Vessel transit distance during deployment (m)	2584
Ship distance from target at deployment (m)	567
Distance to allow for 10 minutes deck ops (m) at 4 kt	1200
Total distance from target (m)	1767

During the tows a live feed provided footage from the forward and downward looking video and still cameras. The forward-looking camera was used by the winch driver to navigate up and over rocks and ridges. Where possible, a height of 2 m off the seafloor was maintained throughout the tow. Still images were set to record every 5 seconds. All video and still images were recorded directly to the computer. A change in software meant that stills were not recorded automatically for the first tow, and therefore only 2 stills were recorded. Details of tows are provided in

Table 9.

Table 9. Details of camera tow transects. Positions and depths are shown for the towed body. SOL = Start of Line, EOL = End of Line.

Site	Event	Ship latitude	Ship longitude	Ship depth (m)	Camera latitude	Camera longitude	Camera depth (m)	Stills count	Duration (mins)
A004CAM01	SOL	-64.7643	114.2258	1658	-64.7751	114.2442	1609	2	32
A004CAM01	EOL	-64.7513	114.2017	1719	64.7677	114.2305	1628		
A008CAM02	SOL	-64.6160	114.6519	1687	-64.5922	114.6238	n/a	315	29
A008CAM02	EOL	-64.6237	114.6835	1678	-64.5991	114.6548	n/a		
C026CAM03	SOL	-65.5577	120.3903	535	-65.5615	120.3857	466	455	39
C026CAM03	EOL	-65.5390	120.4128	770	-65.5464	120.4028	780		
C028CAM04	SOL	n/a aborted due to beacon failure						n/a	n/a
C028CAM05	SOL	-65.4928	119.9192	489	-65.49636	119.9148	470	537	55
C028CAM05	EOL	-65.4643	119.9508	1059	-65.47392	119.9395	816		
C032CAM06	SOL	-65.3903	119.2464	490	-65.39426	119.24	485	552	47
C032CAM06	EOL	-65.3697	119.2812	775	-65.37519	119.2711	674		
C035CAM07	SOL	-65.4400	119.5462	505	-65.44359	119.5426	479	407	35
C035CAM07	EOL	-65.4208	119.5605	827	-65.42809	119.5537	701		

Processing
Still images were colour corrected in Adobe Photoshop to remove the blue bias. Selected images were also enhanced in Adobe Lightroom. Location information for each image was extracted from the USBL beacon and combined with other sensor data in a single spreadsheet.

Preliminary Results
CAM01 and CAM02 were located on the western most ridge in Area A. These transects revealed a predominantly muddy substrate, but with a large number of dropstones and patches of gravel. The fauna was relatively sparse along these transects, dominated by brittlestars, with holothurians, urchins and sea stars also common. Sponges were occasionally observed on dropstones, as were stalked crinoids. Siphons on the sediment surface indicated an abundant

infauna. One photograph revealed the presence of bones, most likely from a seal. Examples are shown in *Figure* and Figure 37.

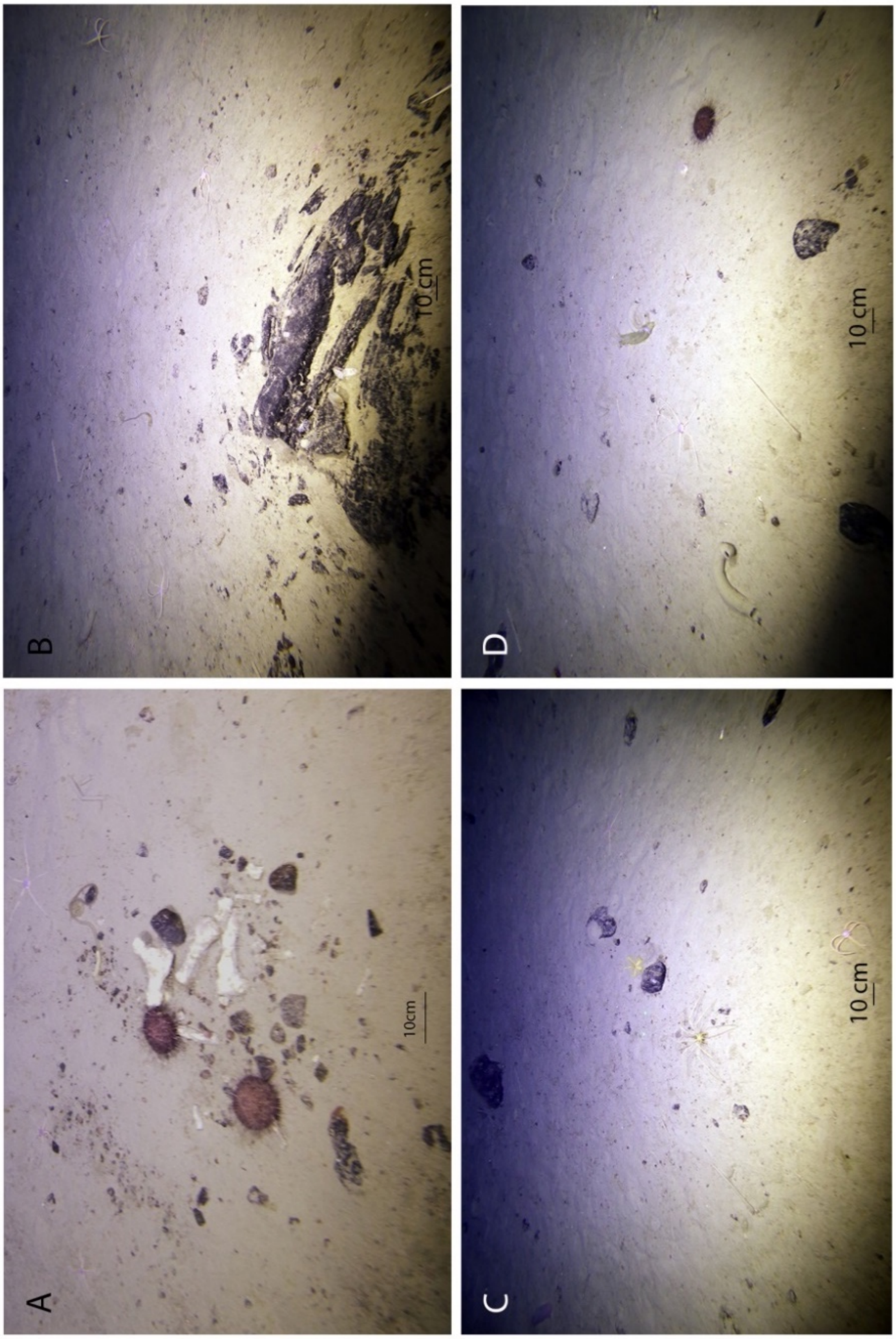

Figure 36. Examples of substrates and fauna encountered. *A) Seal bones with urchins, an acorn worm and brittle stars; B) Dropstones with sponges, a bryozoan and hydrocoral. An acorn worm and brittle stars are on the sediment; C) Stalked crinoid, sea spider, siphons and brittle stars; D) Holothurians, brittle stars, siphons, urchin and waste cast.*

Camera tows 03, 05, 06 and 07 were all located on the shelf break, with the transect starting on the edge of the shelf at 470-490 m and finishing on the upper slope at ~700-800 m depth. The shelf edge and upper slope consisted of heavily iceberg scoured seafloor forming rugged ridges. There were also abundant dropstones and gravel lags, which in some cases formed ribbons on the seafloor. Brittle stars were the most abundant taxa, with gorgonians, other soft corals and sponges also common on dropstones. Urchins were also relatively abundant, creating networks of feeding trails on both muddy and gravelly sediments. Fish, octopus and skates were also observed on each of the shelf edge transects. Camera tow 05 followed a shallow gully on the upper slope before climbing onto the adjacent ridge. The ridge contained a dense abundance of crinoids and brittle stars in contrast to the much sparser fauna, with an absence of crinoids, within the gully.

Operations evaluation (issues/solutions/improvements)
During cast 4 of the towed camera communications with the USBL beacon 2702 mounted on the camera could not be established. It was decided to abort the cast to determine the communications fault between the Ranger 2 software and the beacon. Once on deck, a quick test with the USBL iWand tester showed the beacon was not communicating so it was removed from the towed camera and a spare was installed in its place. The spare was re-configured with address 5201 and tested with the iWand tester and it showed to be communicating so the camera was re-deployed. On further investigation it was found beacon 2702 had 10 % battery left and had locked up for an unknown reason. The beacon was charged and washed and stored in the storeroom.

So, casts are not interrupted with problems or faults from the USBL beacon it is recommended a quick communications check on deck with the iWand is carried out 30 min prior to the cast time.

During the recent months prior to the voyage the Towed Camera was rebuilt and tested during the trials voyage prior to IN2017-V01. From the test results, minor adjustments to the lighting on the camera were required during the voyage. After the second cast of the Towed Camera the best angle for the 4 spot beam lights was determined and once on deck the lights were adjusted. Subsequent casts showed the lighting to be at the correct angles for picture quality. Also, minor Camera adjustments were carried out on the HDSDI camera as recommended from the trials voyage. These were; Focus set to Auto, ISO set to 12800, and shutter speed set to 1/150th. After these settings were made an analysis on the video feed and picture stills was carried out and it was determined to leave the settings as they are as they produced good video feeds and stills.

The Depth limitation of the Towed Body Camera was not determined on this voyage as casts beyond 2000 m were not undertaken. The depth limitation of the towed body camera is determined by the 1.5 tonne tension limit on the Towed Body cable/wire, this was not reached at the depths we cast the Towed Camera to on IN2017-V01. Further casts beyond 2000 m will have to be undertaken on future voyages to determine an approx. depth limit for the camera.

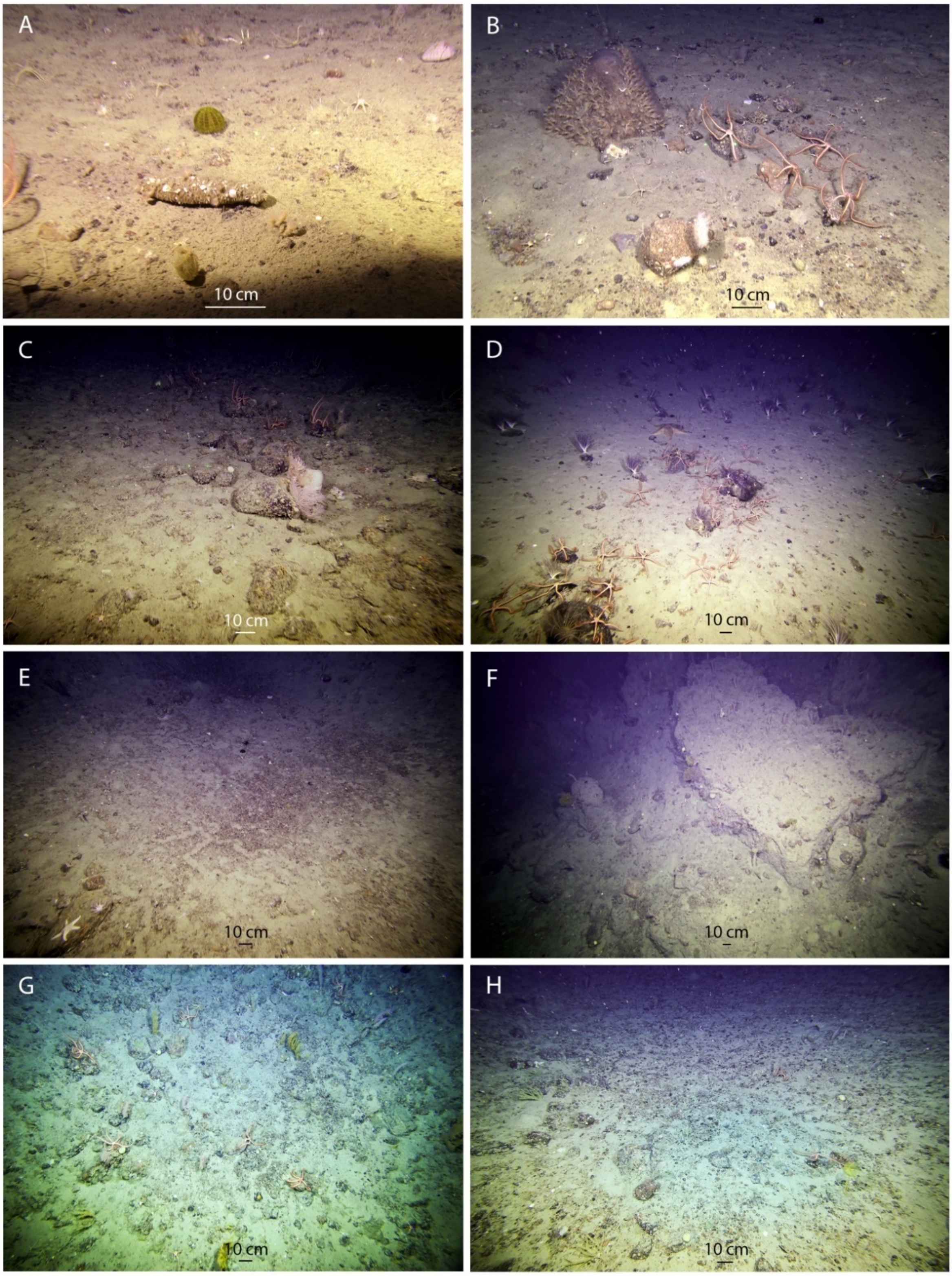

Figure 37. Examples of substrates and fauna encountered. *A) CAM03 – slightly gravelly muddy substrate with holothurians, urchin, brittle stars, a cup sponge and anemones. B) CAM03 – gravelly muddy substrate with dropstones covered in anemones, and brittle stars, sponges, gorgonians, polychaete tubes, solitary corals and bryozoa. C) CAM05 – abundant dropstones with slightly gravelly muddy sediments. Taxa include brittle stars, gorgonians, sponges, holothurians, crinoids and anemones. D) Slightly gravelly muddy substrate with pebbles and dropstones on ridge. Taxa include brittle stars, stalked and free-swimming crinoids, sea star, holothurians and urchins. E) Muddy gravel with dropstones with sea star, anemone, brittle stars, pencil urchin, heart urchin and solitary coral. F) Rugged topography due to →*

(Caption continued from previous page)…iceberg scouring with various gorgonians, brittle stars, anemones, sponges, holothurians, pencil urchin, bryozoa and solitary corals. G) rugged slope with cobbles and pebbles in a gravelly mud. Taxa include various gorgonians, brittle stars, sponges, anemones, solitary ascidians, bryozoa and a sea star. H) Dropstones with muddy gravelly substrate. Taxa include bryozoa, brittle stars, sponges, gorgonians, stalked crinoid, sea star, and anemones.

SECTION 5. Coring operations

KASTEN CORES

The Kasten corer was deployed at 14 locations, 3 in Area A and 11 in Area C (Fig. 38). The first deployment in Area A failed; most likely the Kasten core was not deployed all the way to the sea floor. Another further deployment in Area A was successful. Five deployments in Area C were successful, followed by two failed deployments that attempted to retrieve coarser sediments in the base of a canyon. Three more deployments in Area C and a final deployment in Area A were successful.

The first 12 deployments used the 3 m Kasten corer, while the last two deployments were with the 4 m core barrel. Deployments with the 3 m core barrel yielded between ~210 and 260 cm of sediment, and the 4 m deployments retrieved cores of ~340 cm length.

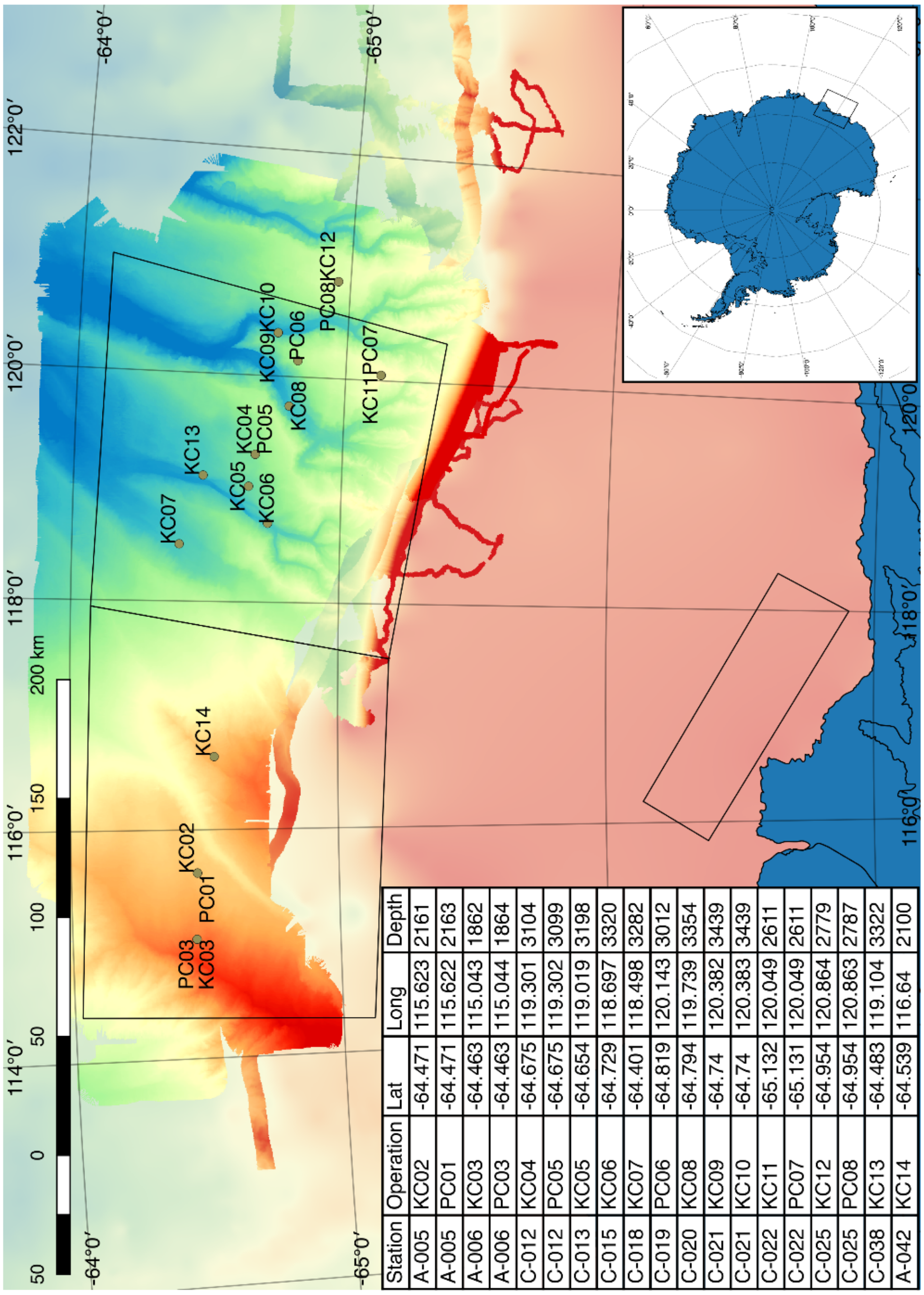

Station	Operation	Lat	Long	Depth
A-005	KC02	-64.471	115.623	2161
A-005	PC01	-64.471	115.622	2163
A-006	KC03	-64.463	115.043	1862
A-006	PC03	-64.463	115.044	1864
C-012	KC04	-64.675	119.301	3104
C-012	PC05	-64.675	119.302	3099
C-013	KC05	-64.654	119.019	3198
C-015	KC06	-64.729	118.697	3320
C-018	KC07	-64.401	118.498	3282
C-019	PC06	-64.819	120.143	3012
C-020	KC08	-64.794	119.739	3354
C-021	KC09	-64.74	120.382	3439
C-021	KC10	-64.74	120.383	3439
C-022	KC11	-65.132	120.049	2611
C-022	PC07	-65.131	120.049	2611
C-025	KC12	-64.954	120.864	2779
C-025	PC08	-64.954	120.863	2787
C-038	KC13	-64.483	119.104	3322
A-042	KC14	-64.539	116.64	2100

Figure 38. Piston and Kasten coring locations within survey areas A and C.

SUB-BOTTOM AT CORE SITES

A005_KC02/PC01

A005 was the first coring location and was taken into an overbank deposit on the upper western side of a turbidite channel (Fig. 39). The depth is 2161m. The location was chosen on the sub-bottom due to strong penetration and clear reflectors indicating a seafloor and upper stratigraphy composed of soft mud layers which are ideal for kasten and piston coring.

A006_KC03/PC03

Site A006 was chosen on the upper side of the same ridge as site A005 (Fig. 39). The setting is shallower at 1862m depth with a lower sedimentation rate and possible higher energy environment. The sub-bottom profile shows the upper stratigraphic section pinching out to reveal the underlying section. Hence the site was targeted for an older and more condensed coring location.

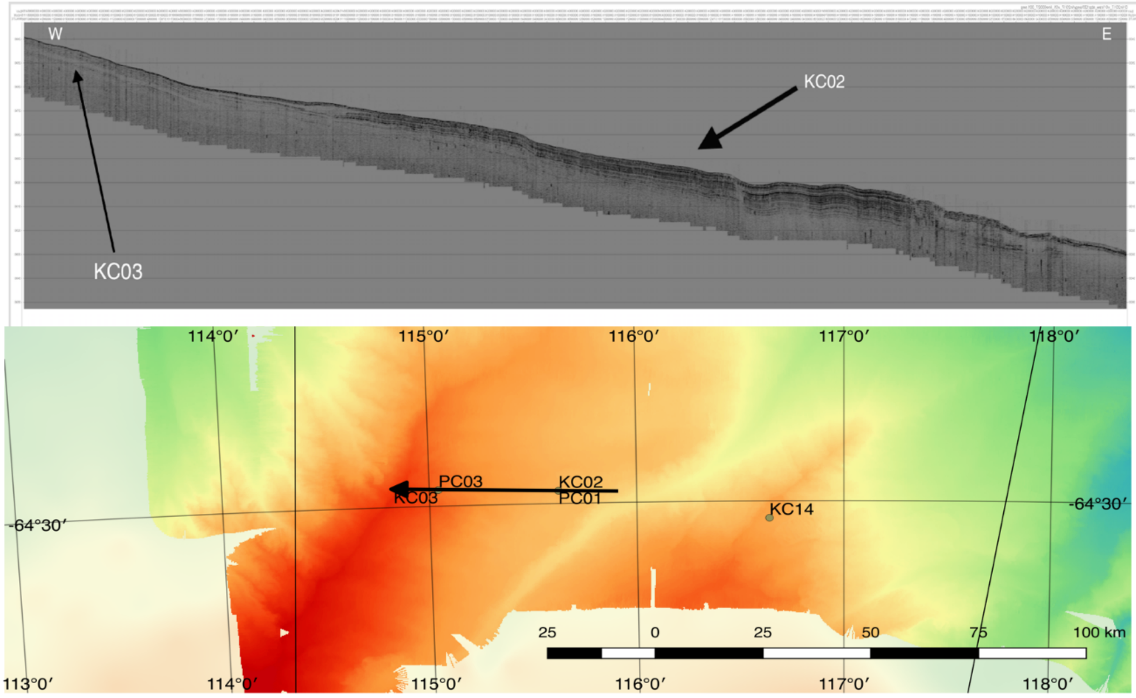

Figure 39. Area A coring locations A005 and A006 with sub-bottom profile along ship track. *Arrows on profile indicate coring location, arrow on map indicates ship movement direction and extent of line.*

C012_KC04/PC05
Site C012 was the first coring location in Area C and was taken in the middle of the ridge between two canyons (Fig. 40). The depositional environment was again thought to be an overbank deposit generated by the turbidite flows through the canyons allowing finer sediment to build up along to sides. The water depth at this site is 3104m and appears to have a high sedimentation rate in a low energy environment. The sub bottom profile shows good penetration into layered sediment indicating mud layers suitable for coring. This site was targeted again for a high resolution and younger age.

C013_KC05
Site C013 was chosen just to the west of site C012 on a lower section of the same overbank deposit (Fig. 40). The water depth at this site was 3198m and was thought to be again a low energy and high sedimentation rate site. The sub-bottom profile shows a perched lens of reflection poor material that is inconsistent with the surrounding stratigraphy and was thought to be a further expanded section. This core site was targeted as it was thought to be analogous to A005 in obtaining a very high resolution core that is also young in age.

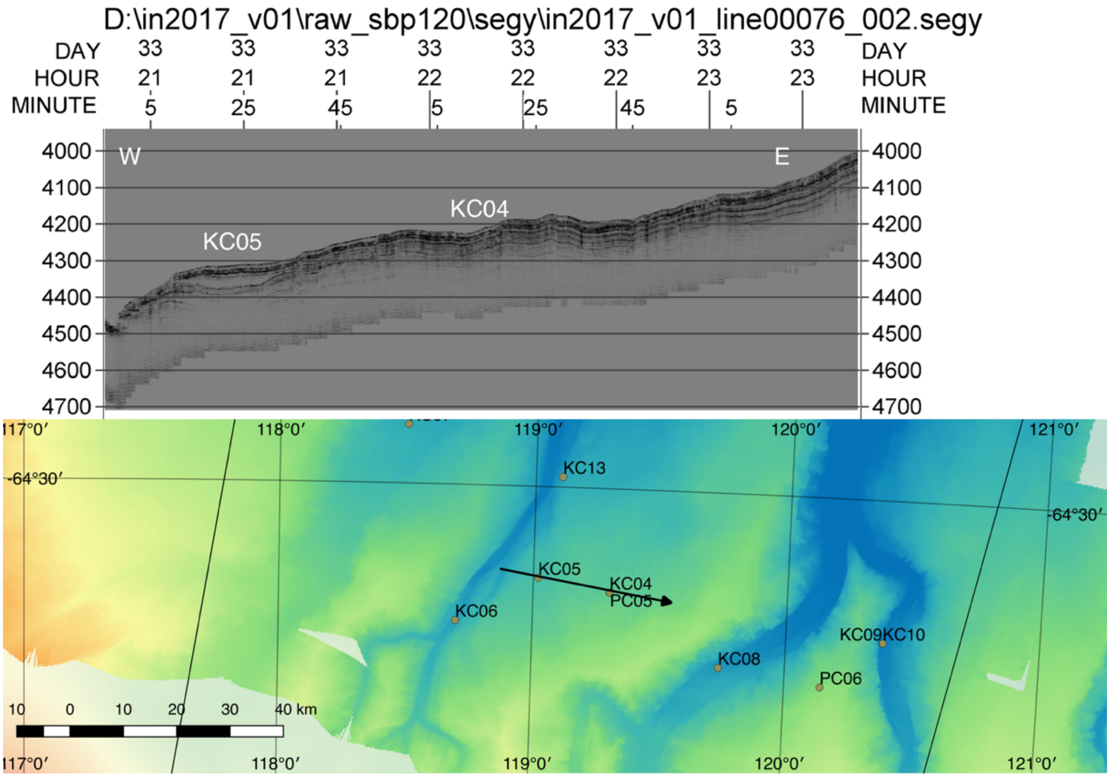

Figure 40. Area C coring locations with sub-bottom profile for sites C012 and C013. *Arrow on map indicates direction of ship movement and extent of line. Sub-bottom profile is annotated with kasten coring location and orientation.*

C015_KC06
Site C015 was taken in the channel of a narrow, submarine canyon thought to be formed by the incision of turbidites moving down the continental slope (Fig. 41). The site depth was 3320m and was thought to be high in energy. The sub-bottom profile shows a hard reflected surface on the seafloor and very little penetration beyond. This site was targeted in the hope of obtaining some of the course detrital material that is thought to be flowing through the canyon.

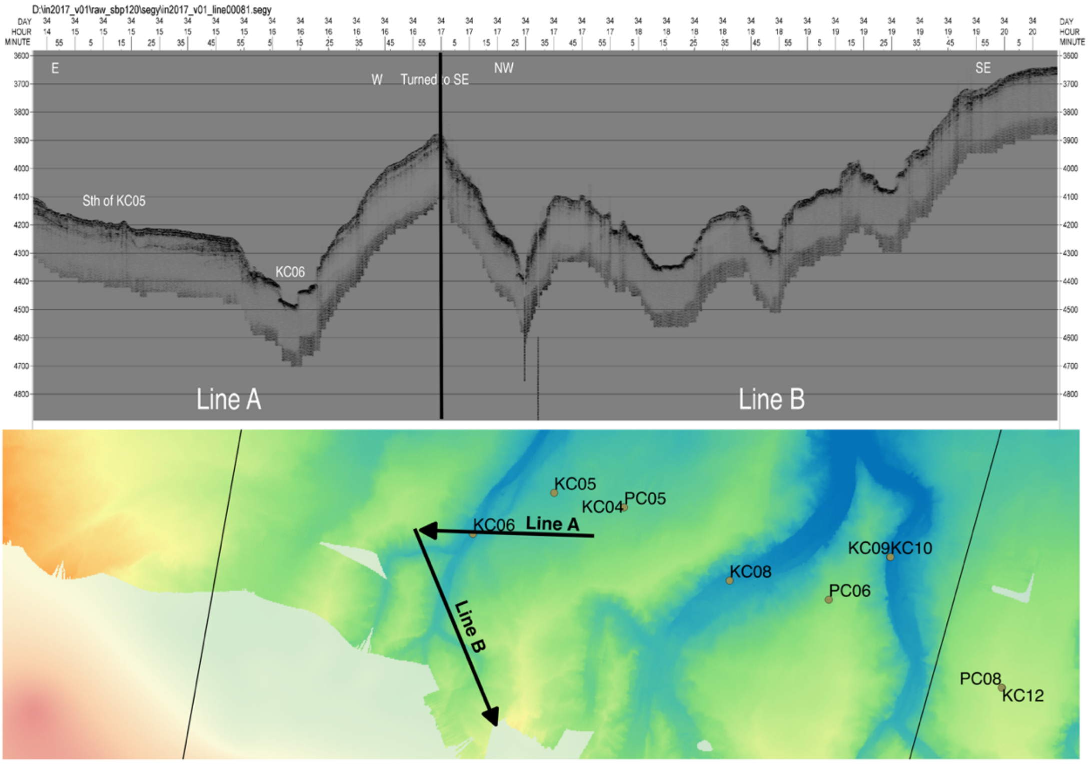

Figure 41. Area C coring locations with sub-bottom profile for C015. *Line A shows the ships track moving from east to west turning to the south east at the start of line B. Sub-bottom profile is annotated with coring location, orientation and line.*

C018_KC07
Site C018 was in the channel of a straight and narrow submarine canyon towards the western side of area C (Fig. 42). The depth of this site was 3282m. The larger width of this canyon indicates that it is not incising as rapidly as others to the east suggesting that it is lower in energy. The sub-bottom profile of the canyon again shows a hard seafloor and minimal penetration below. Considering the surprising results of KC06, this canyon was targeted as part of a scheme to sample each of the turbidite channels to see if they are consistent or have different depositional regimes.

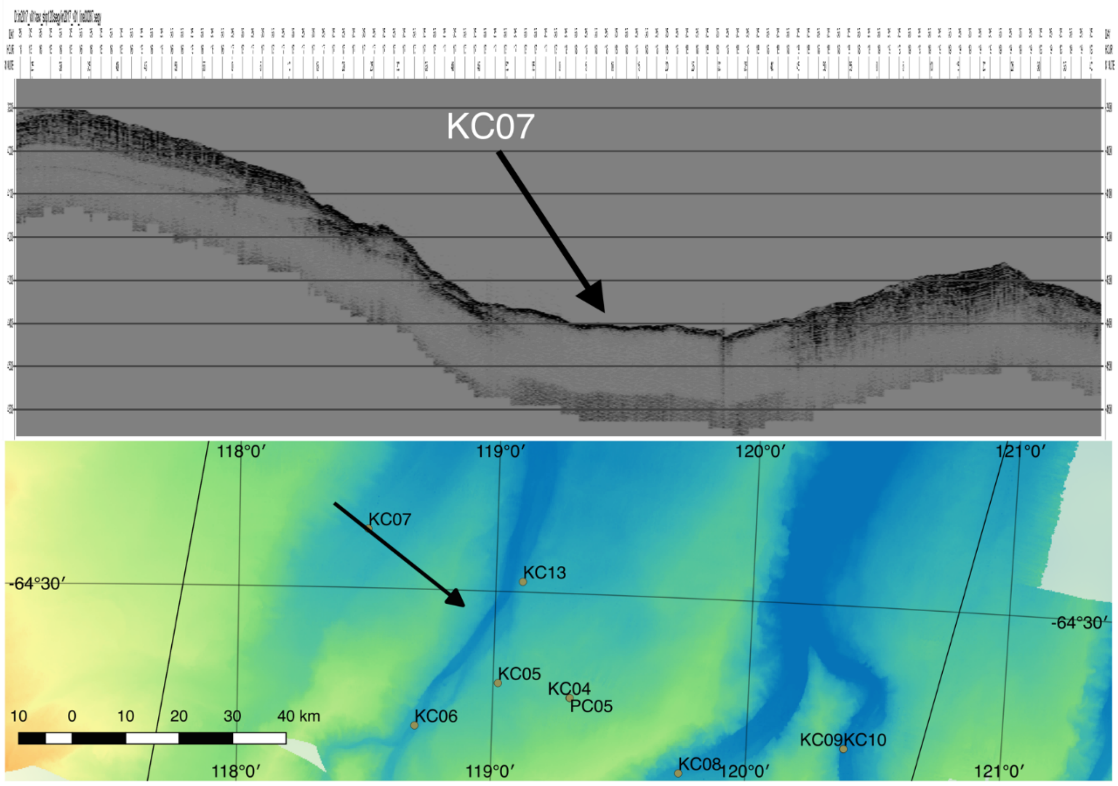

Figure 42. Area C coring locations with sub-bottom profile for site C018. *Sub-bottom profile is annotated with coring location, orientation and line.*

C019_PC06

Site C019 (PC06) is located on a terrace on the western side of a ridge separating two meandering submarine canyons (Fig. 40). The stratigraphy on the top of the ridge is again thought to be an overbank deposit formed by the adjacent turbidite channels. The water depth at the site is 3012m. The sub-bottom profile shows that the terrace has exposed a lower section of the ridge that is uncovered. The terrace appears to be part of the hanging section of an old slump formation due to the discontinuous layers of the upper section showing where the section has faulted. This was chosen for a piston core location to target older age sediments.

C021_KC09/10

Site C021 was in the channel of another submarine canyon system as part of the systematic sampling of all of the turbidite channels (Fig. 43). The sub-bottom profile shows a hard reflector surface with minimal penetration into the subsurface. After two attempted kasten cores at this location, both failed to retrieve any substrate. This indicates that either the material in this channel was either too coarse to be retained in the core barrel or the core was unable to penetrate material similar to that found at site C015.

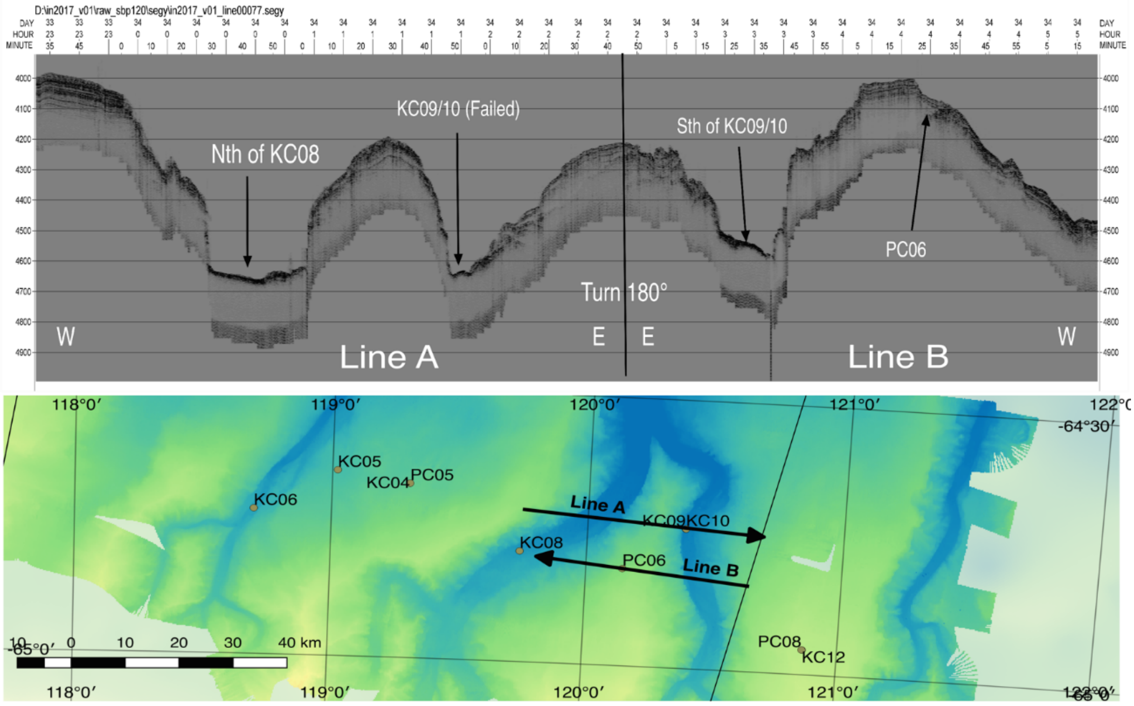

Figure 43. Area C coring locations with sub-bottom profile for sites C019 and C021. *Line A shows the ship track from west to east upon which the ship turned briefly to the south before beginning line B running east to west. Sub-bottom profile is annotated with coring location, orientation and line.*

C020_KC08
Site C020 was located on the western edge of the channel of a narrow, meandering submarine canyon (Fig. 44). The site depth was 3354m. The sub-bottom profile for this location shows a dark reflector indicating a hard seafloor, however there is some penetration into the subsurface which potentially shows highly consolidated layers. This site was targeted again to try and sample some of the detrital material coming through the canyons and at the same time test if the depositional regime is consistent in all the turbidite channels of area C.

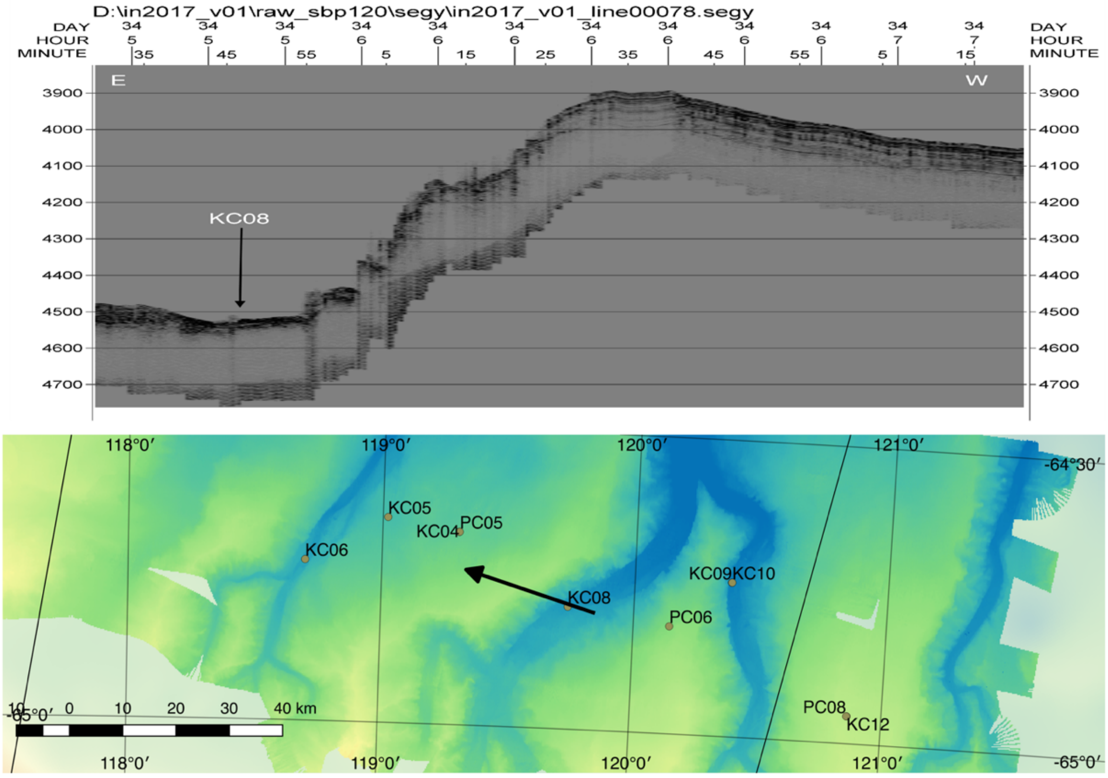

Figure 44. Area C coring locations with sub-bottom profile for site C020. *The arrow on the map indicates the direction of ship movement and extent of the line. Sub-bottom profile is annotated with coring location and orientation.*

C022_KC11/PC07

Site C022 was located at the top of a ridge between two braided submarine canyon systems and was the most southerly coring location for the voyage (Fig. 45). The water depth at this location was 2611. The sub-bottom profile shows good penetration into the sub surface and expanded stratigraphic layers. This location was targeted primarily for its shallower water depth in the hope of sampling a higher fraction of microfossils, particularly foraminifers. The expanded layering does however provide a good location for another high resolution, younger core that could be analogous to site A005.

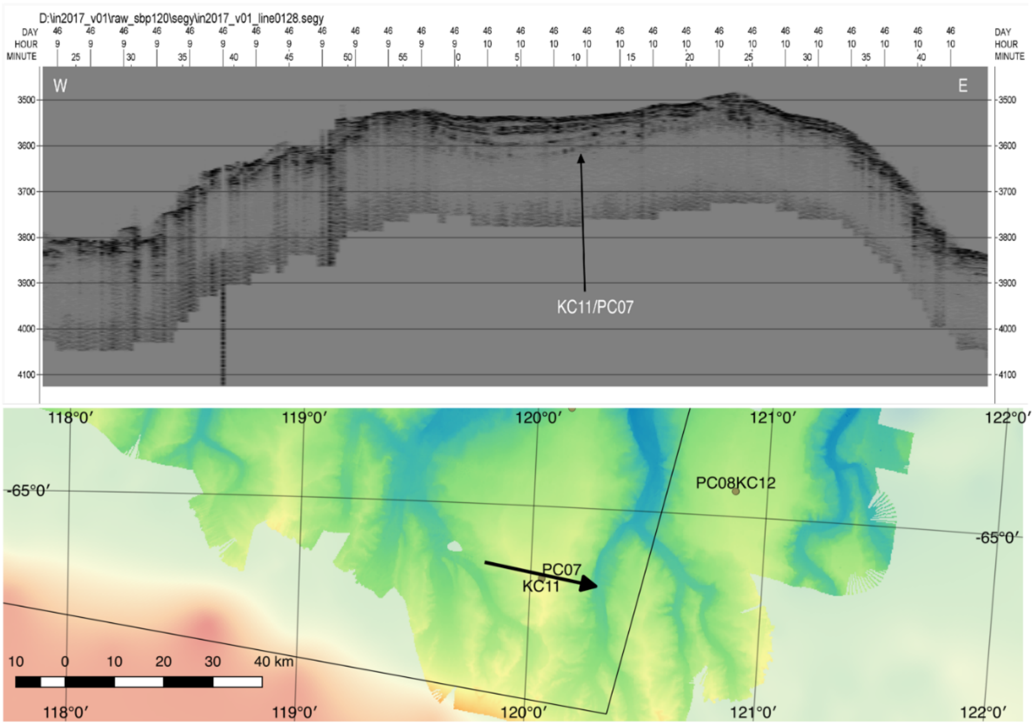

Figure 45. Area C coring locations with sub-bottom profile for site C022. *The arrow on the map indicates the direction of ship movement and extent of the line. Sub-bottom profile is annotated with coring location and orientation.*

C025_KC12/PC08

Site C025 is located outside the boundary of area C and is the western most core location of the survey (Fig. 46). The site is another ridge between two submarine canyon systems that has accumulated as an overbank deposit from the turbidite channels. The sub-bottom profile of the site shows excellent penetration into the subsurface and well defined stratigraphic layers that appear to be slightly pinching out towards the west. This location was targeted for its unconsolidated units as well as for the systematic sampling of the overbank deposits in the area. It was thought that this location would be another high resolution, younger age core.

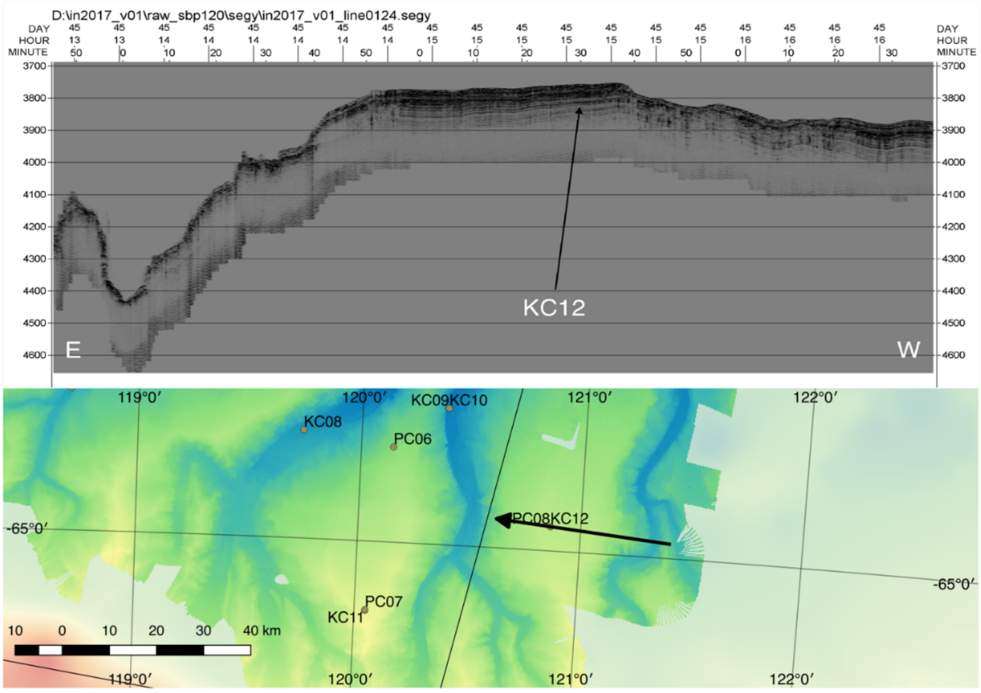

Figure 46. Area C coring locations with sub bottom profile for C025. *The arrow on the map indicates the direction of ship movement and extent of the line. Sub-bottom profile is annotated with coring location and orientation.*

C038_KC13
Site C038 is located on the upper lip of the same submarine canyon that was the location for site C015_KC06 (Fig. 47). The site is another overbank deposit created from the turbidite channel and is the same sediment package that was cored at site C013_KC05. The water depth at this site is 3322m. The sub-bottom profile for this site shows that there is outcrop of underlying stratigraphy that could be near the surface of the sea floor on the upper slope of the canyon. This location was hence targeted to obtain an older reaching sedimentary record that could be potentially used in conjunction with site C013.

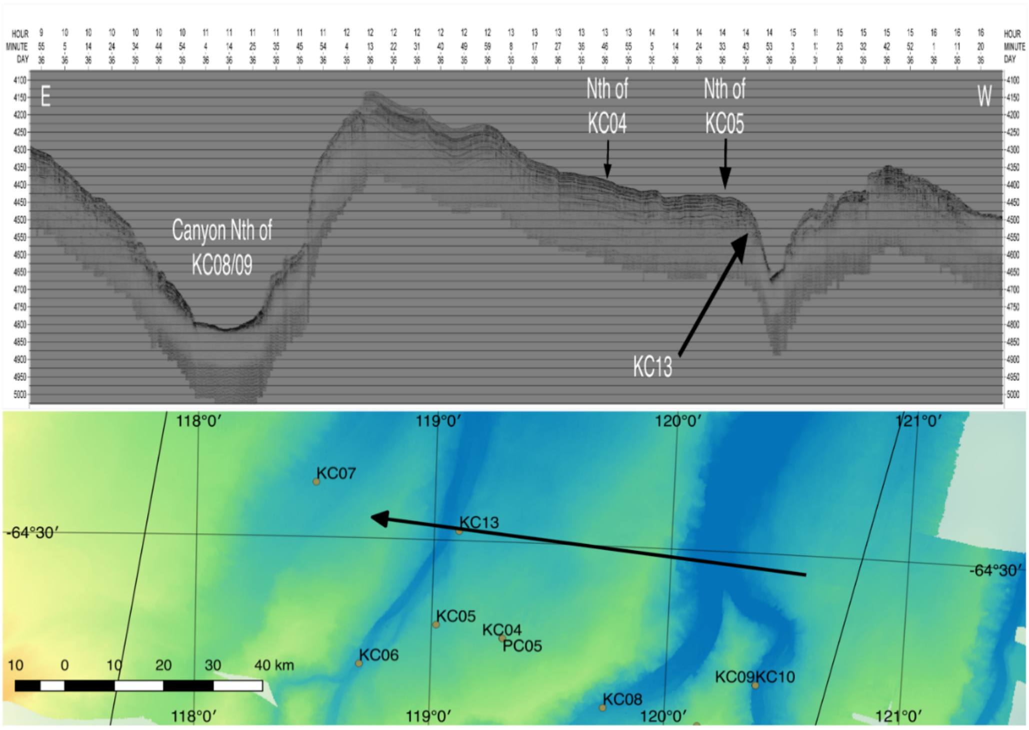

Figure 47. Area C coring locations with sub bottom profile for C038. *The arrow on the map indicates the direction of ship movement and extent of the line. Sub-bottom profile is annotated with coring location and orientation.*

A042_KC14
Site A042 was the final coring location for the survey, situated on top of the second smaller ridge in area A (Fig. 48). Unlike the other ridge to the west, this ridge is more tabular in shape with gentler slopes and a flatter upper section. The sub-bottom profiles for this location show build up of expanded and well stratified sediments to the east of the ridge crest. On the western side of the ridge crest, slump features are again noticeable. The water depth at this core site is 2100m. This site was targeted specifically for its relatively shallow water depth which is conducive to the preservation of foraminifers. The site is also very well stratified and would provide another high resolution, younger timescale sequence.

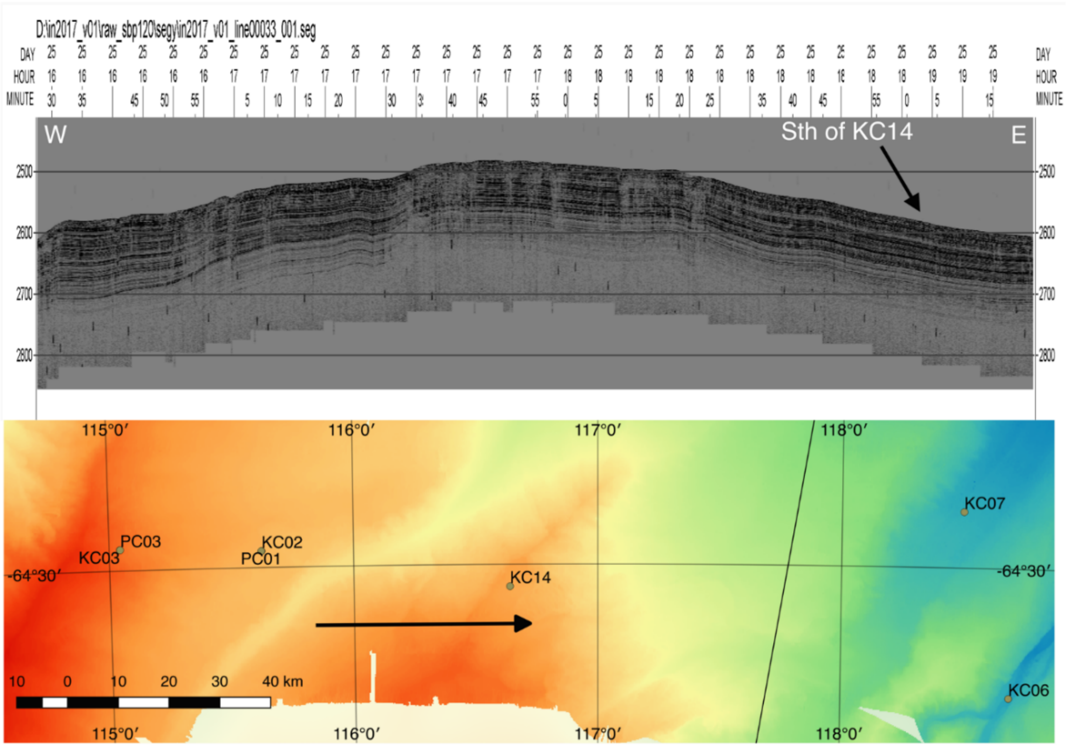

Figure 48. Area A coring locations with nearby sub bottom profile for site A042. *Exact core location could not be generated due to disruptions in sub bottom recording. The arrow on the map indicates the direction of ship movement and extent of the line. Sub-bottom profile is annotated with coring location ad orientation.*

Description and sampling methods
Upon retrieval, Kasten cores were brought in to the dirty wet (mud) lab, and were secured to the roller rack. The cutter nose was removed and the sediment within bagged and labelled. The top plates of the core barrel were removed sequentially from top to bottom. In many cases, some sediment would stick to the top plate. In most cases, this sediment was not replaced due to concerns about contamination. In instances where significant amounts of sediment were stuck to the top plate, it was carefully scraped off and replaced within the main core barrel.
Prior to sampling, the Kasten core surface was scraped from one side to the other using metal spatulas. The metal spatulas were cleaned with bleach solution and ethanol between each scrape.

A tape measure was placed alongside the core for reference. The core was photographed using a tripod and flash lights, which were held on either side of the camera. The core was photographed at ~20 cm intervals, with greater than 50 % overlap between photographs to aid with the subsequent photo stitching. In some cores, we were concerned about losing structural features due to scraping, so the cores were photographed both before and after scraping.
Preliminary lithologic description of the sediment was done following a template (

Table 10), where visible features were noted including; lithology, grain size, colour (as per the Munsell Color Chart) and the nature of any contacts (sharp, gradational) between colour or lithology types. Structural features such as laminations and burrows were noted, as was the presence of fossils, ice rafted debris, and mud clots. The core descriptions and logs can be found in Appendix 4, descriptions of sediment sample coarse fractions in Appendix 5 and samples taken are listed in Appendices 1.1, 1.2 and 1.3.

Table 10. Kasten core sampling procedure

Step	Procedure
1.	Scrape/clean the core using metal spatulas; clean using bleach solution and ethanol between each scrape.
2.	Photograph each section using tripod making sure the tape measure is along-side.
3.	Describe core using template and make appropriate smear slides.
4.	Preserve core catcher by either sampling with u-channel or bags depending on integrity.
5.	Linda's samples – DNA, GDDT's, HBI.
6.	Amaranta's samples for single cell genomics.
7.	Alix's sample of core top.
8.	Radiocarbon samples into glass jars and sample any macrofauna for ^{14}C.
9.	Taryn's sample of small u-channel is put in 1m or less sections along the core.
10.	Phil/Alix's sample for ASD mineralogy and grain size.
11.	Amy's samples – every 10 cm.
12.	Physical properties samples in pre-weighed vials.
13.	Brad's samples – 20cc as possible every 20 cm – to be sieved immediately.
14.	Dimitri/Adrian's samples – 20 cc every 20 cm.
15.	Dr Pant's samples for sand fraction.
16.	Taryn's samples for IRD (2 cm intervals).
17.	Large U-channel sample for archive.
18.	Run magnetic susceptibility on both archive u-channels.

The order of the sampling scheme was decided based on the need for uncontaminated biological sampling. The biological samples also need to be collected quickly in order to preserve their integrity. These samples included ancient DNA, GDGT, HBIs, and genomics. In general, these samples were taken at the following intervals; every 2 cm from 0–10 cm, every 10 cm from 10–100 cm, and every 20 cm from beyond 100 cm. Samples for single celled genomics were taken at 0 cm and 10 cm. The biological sampling was restricted to one half of the core, leaving the other half for placement of the small 25 x 25 mm u-channel. See 0. for the detailed u-channel sampling procedure.

After the biological samples were taken and the small u-channel was in place, the other samples were taken, with intervals selected to maximise the use of the sediment. Diatom samples (~5 cc) were taken at 5 cm intervals. Permanent smear slides were made every 10 cm or 20 cm from these samples; these slides are curated with chief scientist Assoc. Prof. Leanne Armand.

Samples of ~30 cc size were taken for foraminifera analysis. Sample intervals were dependent on foraminiferal content, as evaluated based on the appearance of the sediment and quick sieving of a few samples of the core. The samples were generally taken at 5 or 10 cm intervals in the upper biologically rich Holocene sediment, and then every 10 or 20 cm beyond that in the less biogenic older sediment. Post-sampling, these samples were washed with fresh water through a 63 μm sieve to retain the coarse fraction. For IN2017-A005 -KC02, IN2017-A006-KC03 and the upper 1 m of IN2017-C012-KC04, the entire sample set was sieved and air-dried, and the residue was put in plastic vials. For the remaining cores, only a sub-sample of ~5 cc (this amount was variable) was sieved and the remainder of the sample retained in case further quantitative analysis is required.

Radiolarian samples were taken at more closely spaced intervals (at 5 cm intervals) in the upper biogenic sediment, and then every 10 or 20 cm beyond that in the older sediment. Surface sediment samples for physical properties were taken in the upper 2 cm. Physical properties samples were also taken at 5 cm intervals, in pre–weighed vials. The vials were taped shut with electrical tape, to prohibit water loss before drying. Samples will be weighed both wet, and after drying for calculation of water content. Other analytical work that can be done on these samples include grain size analysis, total organic carbon and nitrogen content, and the $\delta^{13}C$ and $\delta^{15}N$. XRD and ASD samples were taken at every ~20 cm. Samples for sand fraction analysis were also taken at intervals of 20–40 cm.

Three to five samples were taken from each core for radiocarbon dating. These were collected in 60 ml glass snap-cap jars. The intervals selected were generally at the surface, and within and at the base of the biologically rich section brownish-green mud. However, after diatom smear slides were examined it became apparent that diatoms remained abundant even below the upper brownish-green mud; diatoms continued to contribute to the sediment within the uppermost gray silty clay sections. We were able to take samples at the base of the diatomaceous sediments based on the samples previously taken in 2 cm increments through the kasten cores. All sediments were dried on board at <40 °C. All sample intervals are recorded in the core sample logs (Appendix 1.1, 1.2).

After these samples were collected, the surface of the core was re-scraped, and sometimes re-photographed. One metre lengths of the large 100 x 100 mm u-channel was put in place on one side (Appendix 1.3). The remaining sediment was removed and bagged at 2 cm increments for later analytical work on ice rafted debris, etc. Any dropstones found within the sediment were retained and labelled according to the depth at which they were found.

Finally, any remaining sediment was removed and the core barrel was hosed clean on deck, and rebuilt for the next deployment.

Detailed method for u-channel sampling

Two sizes of u-channel are available in 4 m sections: 25 x 25 mm and 100 x 100 mm. The larger channel is to section the ‘working’ half of the core, for later sampling off shore. The smaller size is an ‘archive’ section that will be used for scanning XRF analysis.

- Measure the core length and cut the u-channels into the appropriate size, allowing for 3 cm extra for the end channel.
- After sediment scraping and documenting, and any other critical discrete sampling (e.g. DNA) place the small 25x25 mm u-channel on the surface of the core and cut around the outside. This provides a groove/space for the channel to slide into easily without deforming the mud. Do not sample the outer centimetre of the Kasten core.
- Remove the sediment around the side of the small u-channel before trying to pull it out. Depending on the consistency of the mud, use a one meter long rule and slide it underneath the small u-channel from the exposed side, and use it to hold the sediment inside the channel as you lift it out.
- U-channel is labelled with core ID, arrow indicating top of core and section measurements.
- For the large u-channel: Place it on top after all sampling has been completed. Level out the surface before placing the channel in and cutting around the outside and pushing it the mud.
- Draw arrows pointing to the top of the core and label the depths at each end before the next step.
- Remove the surrounding mud from around the sides of the channel and tip the frame of the Kasten core onto its side.
- Use fishing wire and cut under the length of the core, using the wire to pull the core out from the Kasten core.
- Clean up by wiping the sides of the u-channel. Stabilising the ends with dense foam where appropriate and tape to secure, and prevent the mud from falling out.
- Wrap plastic wrap across the surface of the core, tucking it into the sides of the mud.
- Clip the lid on. Wrap the ends of each core in plastic bags and secure with tape.

- Label each core section with an ID number, arrow indicating the top of the core and the section measurements.

Consumables needed:
- 25 mm x 25 mm u-channel
- 100 mm x 100 mm u-channel
- Foam to secure the ends
- Plastic wrap
- Large paint scraper to scrape the surface of the core
- Hand saw with spare blades
- Plastic bags that fit around the 25 mm^2 and 100 mm^2 u-channels tops and bottoms
- Tape (office size for small u-channel and packing size for large u-channel)
- Marker pens to record depths
  20 L buckets with lids to collect any left-over mud.

Table 11. List of sampling requirements for Kasten core samples.

Sample	**Receptacle**	**Size**	**Quantity**
small archive u-channel	electrical ducting	25 mm	4 m sections
large archive u-channel	electrical ducting	100 mm	4 m sections
Ancient DNA			
GDGT			
HBI			
HBI-Spectroscopy			
Single Cell Gen.			
Diatoms	Write-on Whirl-pak bag	2 oz	Up to 80 per 4m core
Forams	Bags Vials for sieved sediment	4 oz or larger, 7 dram vials	Up to 30 per 4m core
IRD	Bags	4 oz	
XRD	Bags	Small–medium	
ASD			
Surface phys prop	Bags		
Sand Fraction	Bags	Small–medium	
Physical Properties	Polystyrene snap cap vials	7 dram	Up to 80 per 4m core
Radiocarbon	Glass jars with snap-cap lids	60 ml	Up to 4-5 per 4 m core
Smear slides			
Rocks	Write-on Whirl-pak bag	2 oz, 4 oz	20/core max

Recommendations
- All bags should have white write-on sections to avoid issues with marker pen labels being rubbed off plastic bags.
- Have extra bags in case people underestimate how many they will use.

- Have a range of sizes of bags, as trying to fit large samples in small bags can be messy.
- MANY sponges (large and small), chux wipes would be useful.
- More of larger sampling spatulas would be useful.
- More finer point marker pens would be useful.
- Sieved samples should be stored in small glass vials rather than the polystyrene used, to reduce problems with static.

Photography

The technique for photographing the Kasten cores was refined as the voyage progressed, arriving at an acceptable solution by core number four (C012-KC04). There was always a buzz around the arrival of a core, with pressure to photograph quickly and allow sampling to commence. Without a firm protocol in place for core photography, this led to inconsistencies in technique, and ultimately variations in the quality of images from core to core.

The majority of the cores were photographed using a Canon 5D mark III fitted with a Canon EF 24-105 mm f/4L IS USM lens set to 50 mm, recorded as a RAW file (.CR2) with dimensions 5760 x 3840 pixels. The camera was set up on a Manfrotto 055XPROB tripod with a pivoting centre column that allowed the camera to be placed directly over the core, thereby maintaining a constant height from the core surface. The entire core was incrementally moved under this set-up, with photos taken every 10-15 cm, centre to centre. Our best lighting set-up used two 24 LED portable work lights held either side of the camera in line with the core, at a ~45-degree angle. The placement and angle of these lights varied from core to core, as different people were involved nearly every time, with subtle variations in lighting apparent in each set of photographs.

Cores were photographed on opening if there were interesting textural or structural features observed. All cores were photographed after the surface that had been in contact with the core liner was scraped away. Some cores were photographed after initial sampling, and prior to archiving.

In post-processing the images, white balance was set using the white block on a Kodak Color Control Patch in Adobe Lightroom CC (2015). Geometric corrections were applied to all images in Lightroom, using the Adobe lens correction profile for the Canon 24-105 mm lens (when used), and horizontal and rotational transforms if required. The latter were applied when the camera was not at right angles or directly in line with the core, to remove parallax and rotational issues encountered before “stitching” the photos together.

RAW images were exported from Lightroom as full resolution JPEG files (Quality 100, Colour Space sRBG). These files were manually “stitched” together in Photoshop CC by importing each image as a separate layer, visually aligning adjacent images, and by using a layer mask and a feathered “brush”, painting out overlapping sections to achieve a smooth, blended join between the two.

Table 12. Summary of Kasten core photography

Core No. Date Photos taken	Camera	Light Source	Photographer	Comments
A005-KC02 2017-01-28 scraped (5) scraped (7) pre-archive (14)	Canon EOS 7D, EF-S18-55 mm f3.5-5.6 IS @ f3.5, 20 mm ISO 320; f4, 18 mm ISO 2000. Apple iPhone 6, 4.2 mm f2.2 ISO 80	Ambient lab lights.	A. Post & A. Leventer	Three attempts at photography, including pre-archive shots by A. Leventer on iPhone6
A006-KC03 2017-01-30 scraped (16)	Canon EOS 5D mk III, EF f4 L IS 24-105 mm @ f6.3, 55 mm. ISO 400, 1/200 sec.	Canon 550EX Speedlight with some ambient lighting from lab.	D. Thost	Photos of core “scraped” prior to sampling. Reflections from flash light source in centre of images.
C012-KC04 (photo set 1) 2017-02-03 scraped (17)	Panasonic DMC-GH4, Olympus M.25 mm f 1.8 @ f11. ISO 400, 1/125 sec.	Canon 550EX Speedlight with diffuser, with some ambient lighting from lab.	D. Thost	Photos of core “scraped” prior to sampling. Strong reflections from light source.
C012-KC04 (photo set 2) 2017-02-04 pre-archive (25)	Canon EOS 5D mk III, EF f4 L IS 24-105 mm @ f10, 35 mm. ISO 1000, 1/125 sec	2 x “Power Light” 24 bright LED lights; colour temperature ~5850 K	D. Thost	Photos of core after initial sampling, prior to archive. Good even lighting
C013-KC05 2017-02-07 scraped (22)	Canon EOS 5D mk III, EF f4 L IS 24-105 mm @ f8, 50 mm. ISO 400 (Aperture Priority: shutter 1/30 to 1/50 sec)	2 x “Power Light” 24 bright LED lights; colour temperature ~5850 K	D. Thost	Photos of core “scraped” prior to sampling. Good even lighting. Minor variation in exposure due shutter speed.
C015-KC06 2017-02-11 scraped (25)	Canon EOS 5D mk III, EF f4 L IS 24-105 mm @ f5.6, 50 mm. ISO 400, 1/80 sec.	2 x “Power Light” 24 bright LED lights; colour temperature ~5850 K	D. Thost	Photos of core “scraped” prior to sampling. Good even lighting. Variation in exposure in top two shots: f6.3.

Core No. Date Photos taken	Camera	Light Source	Photographer	Comments
C018-KC07 2017-02-12 scraped (27)	Canon EOS 5D mk III, EF f4 L IS 24-105 mm @ f8, 50 mm. ISO 1000, 1/80 sec.	2 x “Power Light” 24 bright LED lights; colour temperature ~5850 K	D. Thost	Photos of core “scraped” prior to sampling. Good even lighting.
C020-KC08 (photo set 1) 2017-02-15 on opening (12)	Canon EOS 5D mk III, EF f4 L IS 24-105 mm @ f8, 50 mm. ISO 1000, 1/80 sec.	2 x “Power Light” 24 bright LED lights; colour temperature ~5850 K	D. Thost	Photos taken prior to “scraping” to capture detail of clasts in upper section.
C020-KC08 (photo set 2) 2017-02-15 scraped (20)	Canon EOS 5D mk III, EF f4 L IS 24-105 mm @ f8, 50 mm. ISO 1000, 1/160 sec.	2 x “Power Light” 24 bright LED lights; colour temperature ~5850 K	D. Thost	Photos of core “scraped” prior to sampling. Good even lighting.
C022-KC11 (photo set 1) 2017-02-17 on opening (12)	Canon EOS 5D mk III, EF f4 L IS 24-105 mm @ f8, 50 mm. ISO 1000 (Aperture Priority: shutter 1/160 to 1/320 sec)	2 x “Power Light” 24 bright LED lights; colour temperature ~5850 K	D. Thost	Photos taken prior to “scraping” to capture detail of clasts in upper section. Minor variation in exposure due shutter speed.
C022-KC11 (photo set 2) 2017-02-17 scraped (26)	Canon EOS 5D mk III, EF f4 L IS 24-105 mm @ f9, 50 mm. ISO 1000, 1/125 sec.	2 x “Power Light” 24 bright LED lights; colour temperature ~5850 K	D. Thost	Photos of core “scraped” prior to sampling. Light flare on left hand side of image particularly noticeable in lower section of core.
C025-KC12 (photo set 1) 2017-02-19 on opening (25)	Canon EOS 5D mk III, EF f4 L IS 24-105 mm @ f11, 50 mm. ISO 1000, 1/200 sec.	2 x “Power Light” 24 bright LED lights; colour temperature ~5850 K	D. Thost	Photos taken prior to “scraping” to capture detail throughout core including clasts, and fine laminations at base.
C025-KC12 (photo set 2) 2017-02-19 scraped (26)	Canon EOS 5D mk III, EF f4 L IS 24-105 mm @ f9, 50 mm. ISO 1000, 1/200 sec.	2 x “Power Light” 24 bright LED lights; colour temperature ~5850 K	D. Thost	Photos of core “scraped” prior to major sampling, but after minor “mini cores” for DNA.

Core No. Date Photos taken	Camera	Light Source	Photographer	Comments
C038-KC13 (photo set 1) 2017-02-23 on opening (34)	Canon EOS 5D mk III, EF f4 L IS 24-105 mm @ f10, 50 mm. ISO 1000, 1/100 sec.	1 x “Power Light” 24 bright LED light; 2 smaller hand held LED lights; ~5700 K	D. Thost	Photos taken prior to “scraping”. Rough core on opening with many sections sticking to core wall. Lighting compromised due to loss of one large LED light.
C038-KC13 (photo set 2) 2017-02-23 scraped (34)	Canon EOS 5D mk III, EF f4 L IS 24-105 mm @ f9, 50 mm. ISO 1000, 1/100sec.	1 x “Power Light” 24 bright LED light; 2 smaller hand held LED lights; ~5700 K	D. Thost	Photos taken after “scraping”. Lighting compromised due to loss of one large LED light.
A042-KC14 2017-02-25 scraped (35)	Canon EOS 5D mk III, EF f4 L IS 24-105mm @ f10, 50mm. ISO 1000, 1/125sec.	2 x “Power Light” 24 bright LED lights; colour temperature ~5650K	D. Thost	Photos taken after “scraping”. Slight flare on Left Hand Side of images. Centre good.

Magnetic susceptibility acquisition methods for Kasten Cores
BARTSOFT software (v.1.7.1) and a USB Magnetic Susceptibility Meter MS3 were used to acquire magnetic susceptibility data at 2 cm intervals, for both big and small u-channels, from all Kasten cores.

The big u-channels were scanned using the MS2EI high-resolution surface scanning point sensor (Serial No. 088). For the small u-channels, the MS2C Core Logging loop sensor of 45 mm internal diameter (Serial No. 298) was used. Both sensors (point and loop) were attached to the MS3 meter and connected via USB to the host PC. Before the start of the scanning, zeroing of the sensor was performed. Measurements were recorded in 10x-5 SI units. Data were saved and exported via BARTSOFT software as text files and were plotted using Microsoft Excel. Additional graphical editing was performed using the Adobe Illustrator CC A2015.3.

Operations evaluation (issues/solutions/improvements)
The Kasten corer was a very reliable tool after the first abortive attempt. It was easy to deploy and recover and provided large sample volumes. The usual disadvantage of Kasten cores in not providing archive samples was overcome by the use of electrical conduit with square cross sections. Three deployments failed to recover sediment. The first may not have hit the bottom whereas cores KC09 and KC10 were intended to recover sand from a canyon floor. The core barrel was polished and scratched on recovery so it is likely it penetrated the sediment but the sand was not retained in the barrel. The main improvement would be changing the access to the lab to allow for longer barrels.

Preliminary results
The Kasten cores provided excellent samples of the upper meters of the stratigraphy (Fig. 49 and Appendix 4). The typical sequence in cores taken between canyons comprises diatom rich-clays presumed to represent deglacation to Holocene sedimentation overlying grey diatom poor clays probably deposited during the Last Glacial Maximum. Exceptions to this are two cores from the floor of canyons, KC06 and KC08 which recovered intervals of laminated to clotted diatom ooze below the upper diatom rich clay.

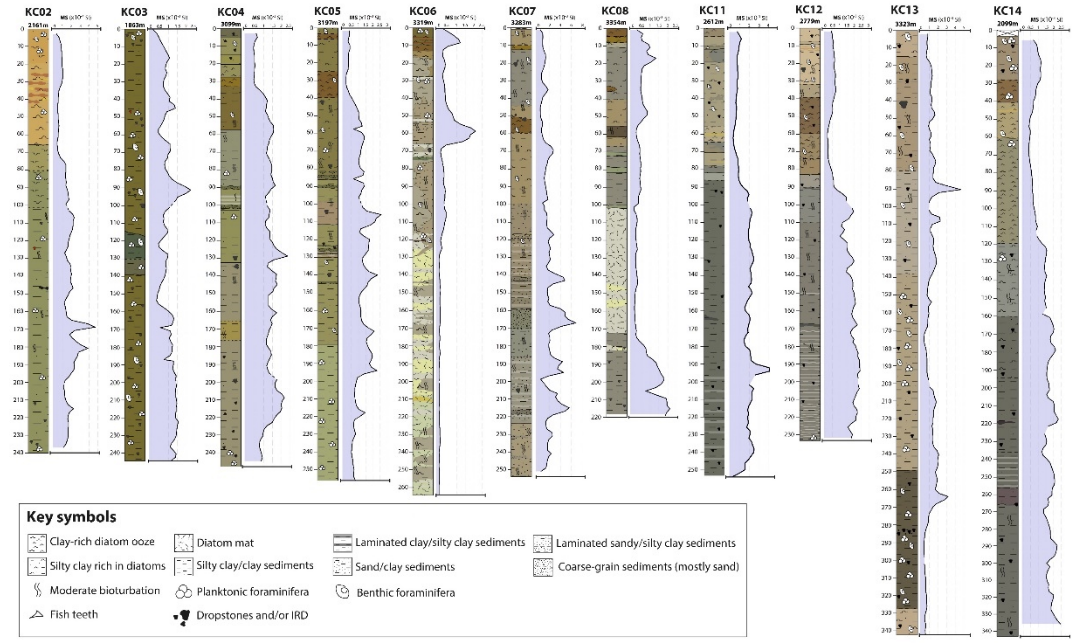

Figure 49. Summary logs of Kasten cores collected by the Sabrina Seafloor Survey.

PISTON CORES

Six piston cores were successfully recovered out of 10 attempts (Fig. 50). The longest core was 16.28 m in an 18 m barrel. Of the failed attempts, 3 were caused by mechanical problems on which the MNF is working on rectifying. The final attempt (PC11) probably hit a boulder, which caused the barrel and liner to break. Cores were not split and sampled on board but processing is described below.

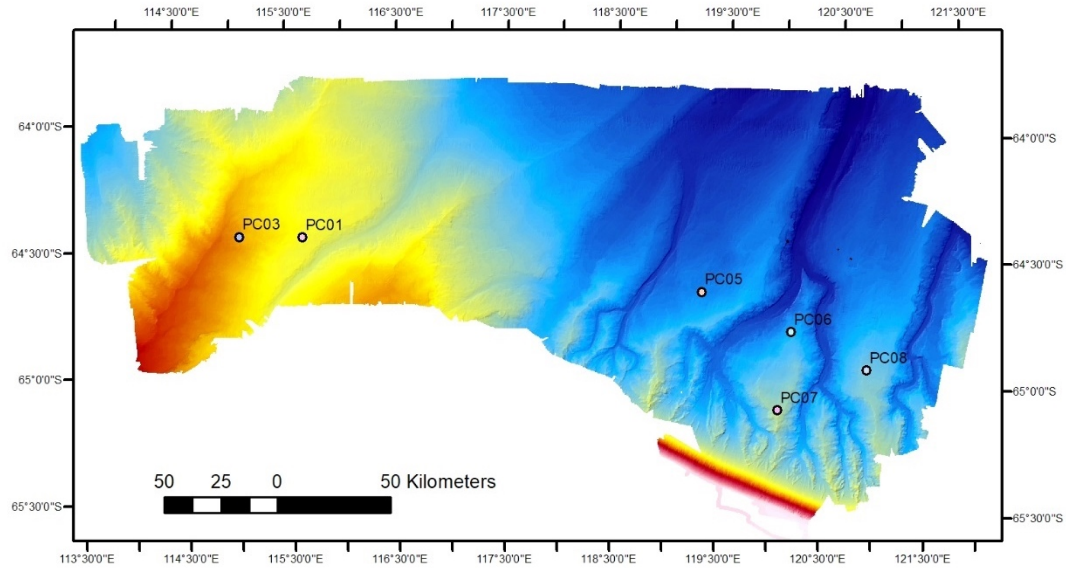

Figure 50. Location of piston cores.

Description and sampling methods
When the piston core was recovered and secure, mud that was recovered on the piston core 'bomb' was sampled with a clean spatula and put into a bag and labelled as "mud on bomb." The trigger core was marked with an up arrow. The cutter nose and core catcher were removed on deck and brought into the dirty wet lab, where the mud was removed and placed in a labelled bag. On deck, if the bottom of the sediment was not at the bottom of the core liner, 1 cm foam plugs were inserted in order to be level with the bottom of the liner. The liner was capped and taped, removed from the trigger core bomb, and brought into the lab where it was secured. The upper surface of the core was then plugged with ~1 cm thick foam plugs, and excess core liner cut off using a hacksaw. The upper part of the core was then capped and taped. The core was dried and labelled. The number of foam plugs on each end was recorded, as was the core length and weight.

On the piston core, the cutter nose and core catcher were removed from the piston core barrel and brought into the lab. The mud was removed, and bagged and labelled. These were bagged separately if both were filled with mud.

Following removal of the cutter nose and core catcher, the PVC liners were sequentially removed. The lowermost outer metal core barrel section was unscrewed and removed to reveal the lowermost PVC core liner. The first 3 m interval was marked with an up arrow and measured. The top of the section also was marked with a 'T' and the bottom with a 'B'. The first section was labelled with the Roman numeral 'I'; subsequent sections were labelled sequentially as II, III, IV etc. (See Fig. 51).

Each section was cut at the 3-m mark with a PVC pipe cutter, then the sediment was cut using a large trowel. The two ends of the 3-m section were plugged with foam, if necessary, with the number of foam plugs used at each end recorded. The bottom end was capped; note that the caps are easier to handle when kept warm until used. A trowel was held firmly against the end of the next core section to stop sediment loss from the exposed end, before this end was also plugged with foam.

The core was pulled out further (or the next core barrel section removed if the core liner did not pull out easily) to cut the next 3 m section, which was labelled as per the first section, but with a Roman numeral II. The same procedure was followed till the last section of core carrying sediment was retrieved, each section being labelled with the sequential Roman numeral.

Each 3-m section was carried into the sheltered workshop where the end caps were secured with duct tape. They were sprayed clean with water and dried with a tea-towel. The 3 m section was marked at 1 m intervals and each 1 m section labelled with:
'IN2017_V01_station number####_Piston core number PC##' (i.e. IN2017_V01_A005_PC02). An arrow pointing towards the top of the core was drawn on each 1 m section, and each section labelled with 'T' at the top and 'B' at the bottom. Each 1 m section was labelled twice (on each side of the core).

The first metre of core (the bottom-most metre of sediment) was labelled '1', the next meter up labelled '2', and the next '3' and so on till all 1 meter sections were allocated a number. The last 1 meter section of core retrieved (the top-most sediment) was given the letter 'A', written next to its allocated number. The next metre section down-core is given 'B', and the next is given 'C', continuing all the way down-core.

The 3 m liners were then brought into the dirty wet lab where they were cut into 1 m sections. While this was done, a pea sized sample for making smear slides was taken at each cut surface using a toothpick. The smear slide samples were bagged in 2 oz whirlpak bags) and labelled according to its location in the core (e.g. top of 3H). The exposed ends of the core were capped and duct-taped. Each core section was measured and weighed, and then carried to the refrigerated room for storage. Finally, each section was later analysed on the Geotek core logger on board, after being brought out of the refrigerated room and allowed to come to room temperature.

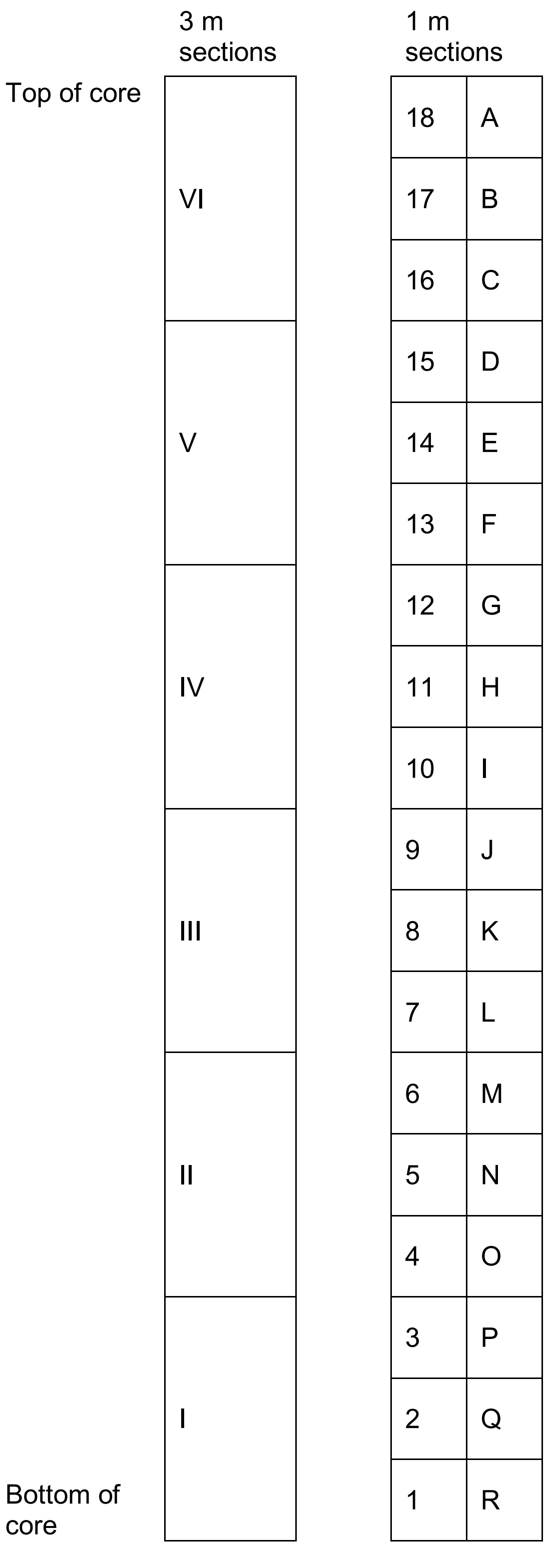

All sections were labelled with:
- an arrow pointing to the top of the core
- T, and B indicating the top and bottom of the section
- voyage ID
- Station ID
- Piston core ID
- metre section number and letter

Figure 51. Schematic showing labelling system for Piston Core sections.

GEOTEK core logger methods
GEOTEK Multi-Sensor Core Logger (MSCL) was used for surface measurements on whole round piston cores. Individual core sections were moved by core pusher through each sensor. Four sensors have been integrated into the system:

- P-wave Velocity
- Electrical Resistivity
- Magnetic Susceptibility
- Natural Gamma

P-wave velocity transducer was mounted on the vertical slide which is raised or lowered by the Z motor, whereas non-contact sensors, such as resistivity, magnetic susceptibility and natural gamma are mounted along the track.

Calibration
Calibration was performed approximately 12 hours before the logging, due to the time that Natural Gamma requires for acquiring the background. *Utilities* software was used to test each individual sensor before every core logging. Specific values were recorded for each sensor to use for later processing.

P-wave velocity
A 30 cm core liner was cut, capped, taped and filled with distilled water. This short liner was placed between the P-wave transducers for the calibration of the sensor. Temperature and total travel time was recorded using test panel in *Utilities* software and together with total thickness and total liner thickness were saved in the calibration excel file for calculating the P-wave Travel Time Offset, which was used during the processing of the raw data.

Electrical Resistivity
A series of saline solutions at different concentrations (see below) were used to record sensor response (mV). The latter values together with temperature were then saved in the calibration excel file and used during processing of the raw data.

- 17.5 g/l
- 8.75 g/l
- 3.5 g/l
- 1.75 g/l
- 0.35 g/l

Magnetic Susceptibility
A standard calibration sample (Serial No.347) provided by the manufacturer (Bartington Instruments Ltd) was used to check for the consistency of the calibration.

Natural Gamma
Three energy calibration standards obtained from the International Atomic Energy Agency (IAEA) in Austria were used for the calibration of Natural gamma sensors:
Potasium Sulfate (IAEA-RGK-1), Thorium Ore (IAEA-RGTh-1) and Uranium-Ore(IAEA-RGU-1). Each standard sample was placed in the Natural Gamma lead cube for 10 minutes to acquire a spectrum using bMCA interface in MSCL Utilities software. WINTMC software was used then to open the acquired spectrums and detect the peak for each element (K, Th and U). Peaks were selected and fitted to standard energy values (see list below).

- Potasium: 1460.75 keV
- Thorium: 2615 keV
- Uranium: 609 keV

Once calibration was done, energy values were saved and loaded for each detector.
Before core logging, background measurements were being collected over night for about 12 hours.

Data Acquisition
MSCL 7.9 operating software controls the data acquisition process, stores data and is used to process raw data. All piston cores were scanned at 5 cm sampling intervals. In addition, the trigger cores from each piston core were logged at 1 cm sampling interval. Trigger core A005 PC01 and A006 PC03 were scanned only for Magnetic susceptibility, whereas trigger cores

from piston cores, PC05, PC06, PC07, PC08 and PC11 were scanned every 1 cm for both magnetic susceptibility and natural gamma. When all sections of a core are finished, raw data were exported in asci files and were processed using the calibration values saved in the calibration excel file, for each sensor respectively. Processed data were imported and plotted to Strater software v.3, and then additional graphical editing were performed using Corel Draw X7.

Operations evaluation (issues/solutions/improvements)
The deployment of the piston corer provided significant problems for the technicians and crew. which are the subject of extensive reports elsewhere. Our survey was fortunate in have benign sea states during all deployments. This combined with the persistence and ingenuity of the staff allowed is to be successful. The system does produce excellent penetration once deployed.

Results
On-board results from piston coring are restricted to observations of MSCL data and some biostratigraphic samples. The Magnetic Susceptibility (MS) and Natural Gamma ray data show similar down-core changes suggesting that they primarily reflect siliciclastic vs biogenic content of the cores with low MS and low Gamma corresponding to sediment rich in biogenic silica and high MS, high Gamma sediment being rich in potassium-bearing detrital minerals such as clays and feldspars. Five cores show MS and Gamma changes that resemble δ18O curves (Fig. 52) strongly suggesting that sediment properties vary with glacial-interglacial cycles (cf. Presti et al., 2011). These cycles combined with the very early biostratigraphy suggest that cores reach back to Marine Isotope Stage 10. The exception is PC03 which does not exhibit such clear cyclicity. It targeted a condensed sedimentary sequence in order to access older sediments.

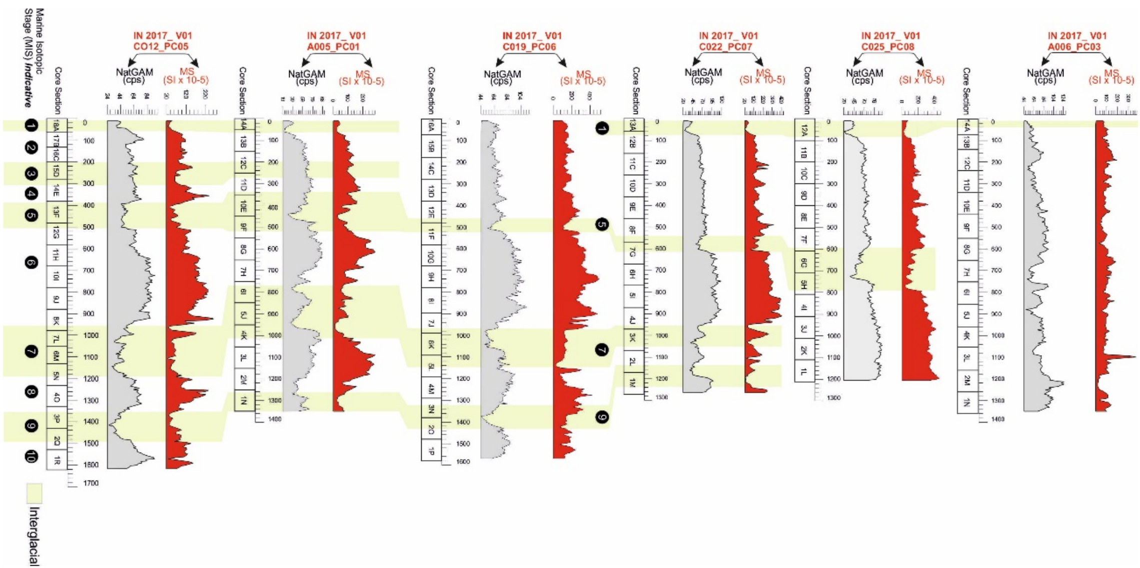

Figure 52. Core sections, Natural Gamma and Magnetic Susceptibility logs for all piston cores. *Suggested correlation of Marine Isotope Stages between cores also shown based solely on log data.*

MULTICORES

Multicores were successfully retrieved at five sites, with two in area A and three in area C. Each time, six tubes were collected. Additional attempts were made at two more sites in Area C, but no samples were obtained (Fig. 53). Failure at these last two sites was most likely due to triggering of the core in the water column because of pressure on the wire caused by the swell, and on one occasion due to a sudden halt of the wire. A niskin bottle was used to collect water at the seafloor during each deployment.

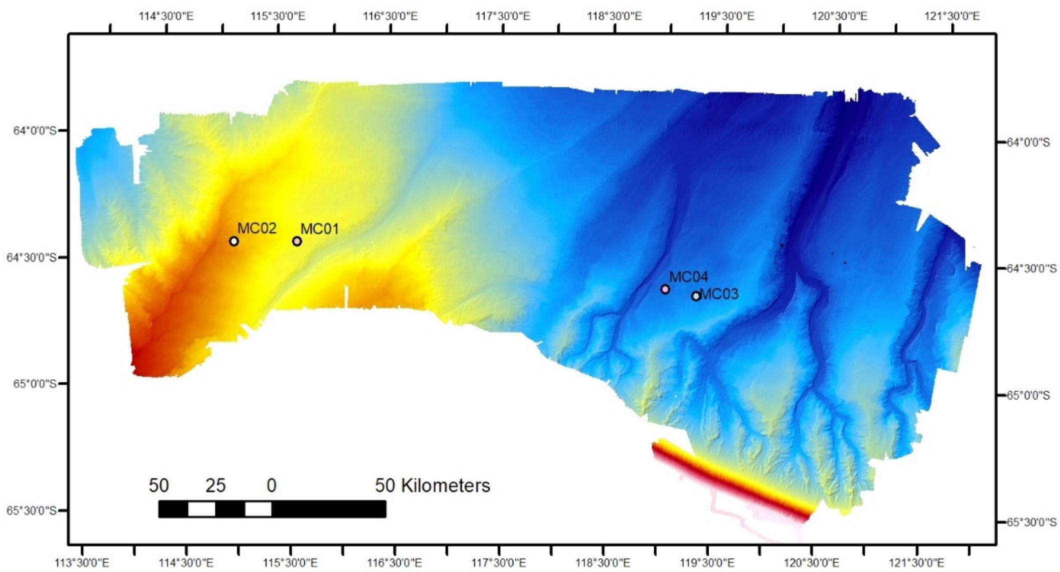

Figure 53. Location of Multicore sites.

Description and sampling methods

On deck, cores were immediately capped, with a plastic insert placed in the base of each tube and the caps secured with tie down straps as shown on *Fig*ure 54A. A neoprene cap was used at the top over glad wrap to ensure no leakage. Each tube was then stored in holders on the wall of the cool store until we were ready to sample.

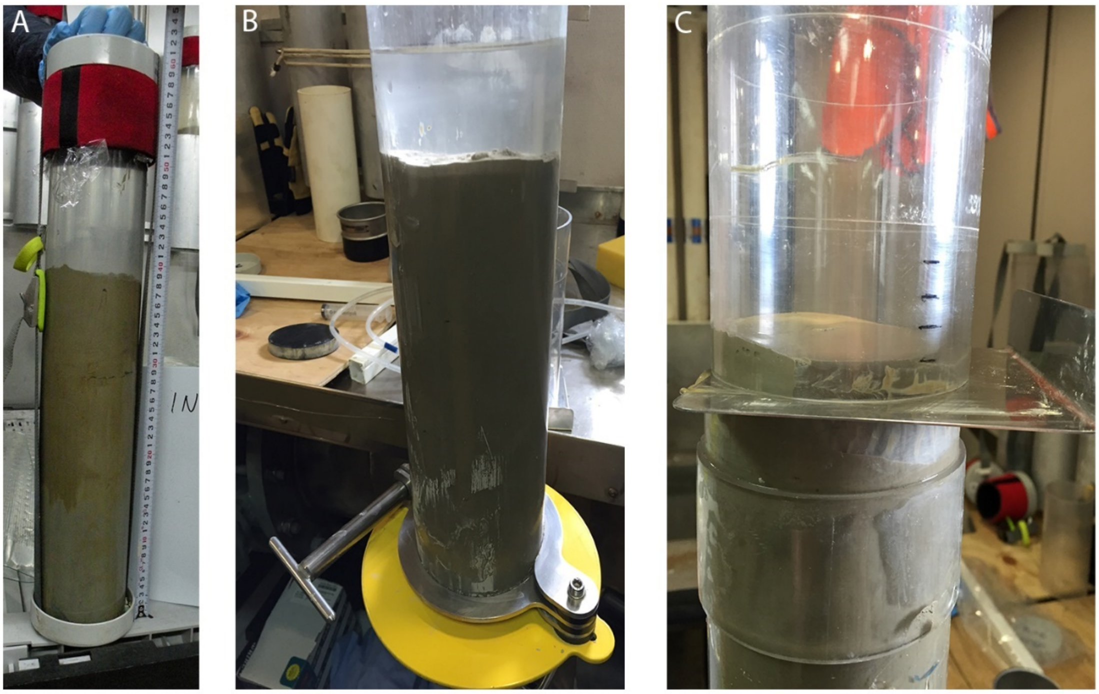

Figure 54. Multicore collection and processing stages. *A) Core caps were strapped to each tube, with neoprene liners and glad wrap on the top cap to prevent leakage. B) Cores were extruded through the top of the tube. C) A tube was placed on top to measure the sample interval for each slice.*

Before extruding the cores, the water was sampled from the top of the cores and the niskin bottle was also sampled and filtered. The small amount of water remaining in each core tube was then allowed to settle before siphoning off with a syringe and plastic tubing. The sediment

from each tube was sampled by extruding each tube out the top. A plastic liner with centimetre markings was used to sub-sample at defined intervals. A tube from each multicore was extracted into a PVC liner and retained as an archive. Samples and sample depths extracted from each tube and the niskin bottle are summarised in
Table .

Table 13. Processing methods for Multicore samples.

Sample set	**Sampling scheme (cm)**
Macrofauna	0 – 5 cm. Sieved >500um. Living fauna preserved in ethanol.
Diatoms	Every 1 cm for the top 20 cm, then every 2 cm.
Forams	Every 1 cm for the top 20 cm, then every 2 cm.
Geochemistry	Every 1 cm for the top 20 cm.
aDNA, GDGT, HBI, HBI spectroscopy	Every 1 cm for the top 5-6 cm, then every 5 cm.
REE, Nd isotopes, 230Th	Every 1 cm.
Fluff	Upper surface scrape where present.
Bottom water DNA	Pooled water from all tubes (2 L DNA Sterivex).
Bottom water plankton	Pooled water from all tubes (200 mL in Lugols).
Bottom water salts & nutrients	Pooled water from all tubes (~0.5 L, analysed on board).
Bottom water isotopes	Pooled water from all tubes (~5 L filtered).
Niskin Water	~0.5 L salts & nutrients, analysed on board.
Niskin Water	1 L DNA Sterivex.
Niskin Water	~4 L filtered.

Photography
Photos of each individual multicore were taken in the cold room after cleaning the PVC tube with a tea towel. A sign was held up next to the core with core and tube number. The amount of sediment was measured from the bottom as the distance between the bottom of the tube and the sediment-water interface.

GEOTEK core logger methods for Multicores
All archive Multi-cores were scanned in GEOTEK for only magnetic susceptibility at 1 cm intervals. For more details about calibration and data acquisition see chapter above.

Operations evaluation
Multicorer operations were reasonably successful. The coring system is inclined to trigger in the water column in response to ship movement so success was determined mostly by sea state. This resulted in only 5 multicore sites.

MICROPALAEONTOLOY

Foraminifers
Sampling was conducted for foraminifera microfossils at varying intervals for all kasten cores. Upon washing the wet samples through a 63 µm sieve the dry samples were examined under a microscope between 1.5-6x magnification and all samples containing both planktonic, benthic and agglutinated foraminiferal microfossils were documented.

Planktonic foraminifers were observed in the Kasten core samples at locations A005, A006, C012, C013, C038 and A042. All planktonic foraminifers were documented as

Neogloboquadrina pachyderma although individuals were not examined in great detail and there is a possibility of different morphological sub-species and potentially rare individuals from other *Globogerina* genera present. Individuals of *N. pachyderma* were initially examined for coiling direction although this approach was abandoned as an on-board exercise due to not having appropriate tools. From the individuals that were briefly examined however, in the first 5 cm of A005_KC02, 99 % of individuals were of sinistral orientation.

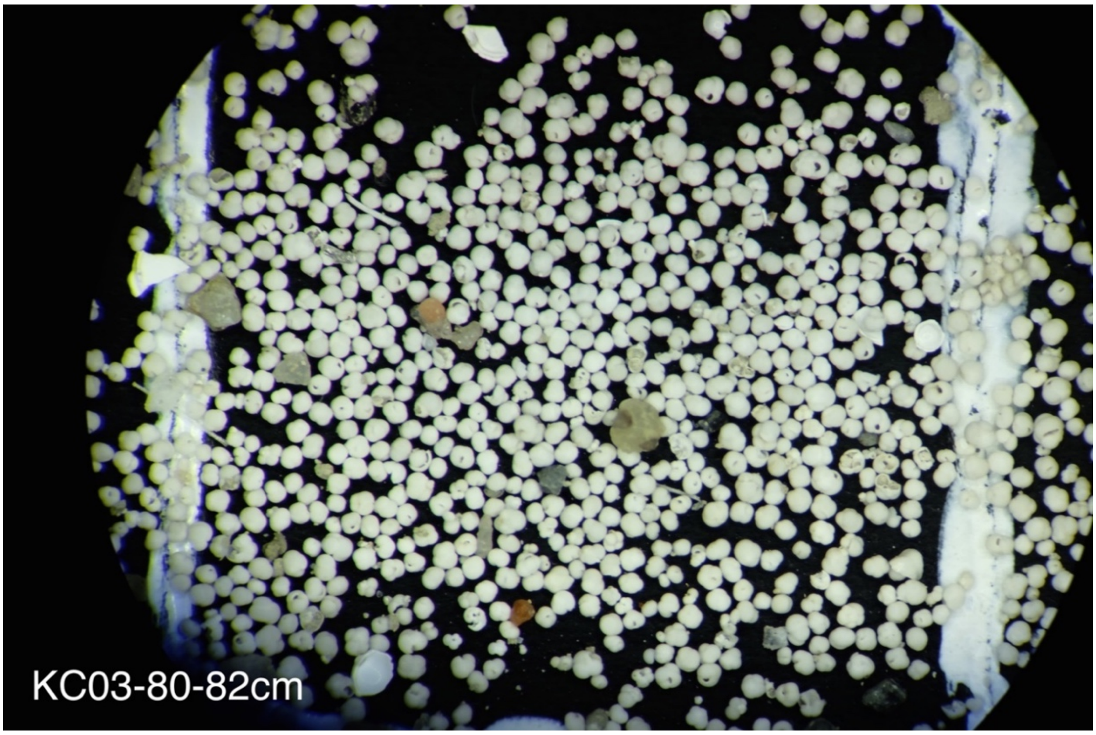

Figure 55. Sample coarse fraction photo of A006_KC03_80-82 cm, with abundant planktonic foraminifera predominated by N. pachyderma. *All samples were viewed within a 1 cm^2 box on a black background.*

In A005_KC02 planktonic foraminifers were found from the top of the core to a depth of 5 cm. They were then observed again at the bottom of the core in sample 238 cm to the end. These lower samples were particularly abundant in planktonic foraminifera comprising approximately 90 % of coarse fraction. At core location A006_KC03 the kasten core, which was targeting older, more condensed sediments, was particularly interesting because of the high abundance throughout in planktonic foraminifera. *Neogloboquadrina pachyderma* was found in abundance from the top to 7 cm, then again from 45 cm to the bottom (Fig. 55). In the section from 45 - 255 cm planktonic foraminifera were the primary constituent >63 µm with high percentage recovery from the sieved wet fraction. In A042_KC14, on the eastern sediment package, planktonic foraminifera were found in the upper 4 cm of the core and from then only rare individuals were observed at singular depths intervals.

In area C, rare planktonic foraminifera were observed in the first 2 cm of C012_KC04. They then reappeared at a depth of 240 cm and continued to the bottom in abundance. Some rare individuals were also found at depths of 50, 55, 85 and 95 cm. The nearby core of C013_KC05 showed a very similar distribution. Planktonics were observed in the very top 2 cm of the core and rapidly disappeared. Rare individuals then reappeared at a depth of 190 cm and continued into abundance from 215 cm to the end of the core. The core C038_KC13 which was taken from the same sediment package as the C012 and C013 also contained sections of abundant planktonic foraminifera. From 150 cm to 204 cm planktonic foraminifera, again *N. pachyderma*, were found in high abundance particularly between 170-190 cm. Individuals were then observed again in the interval of 280-304 cm but in much less abundance the further up the core. For the remaining kasten cores taken in Area C at locations C015, C018, C020, C022 and C025, only individuals were found in some depths with others containing no traces of planktonic foraminifera.

Also, sampled and recorded as part of the >63 μm analysis were any benthic and agglutinated foraminifera. No species identifications were made on board although the identity of some benthic samples is pending from land based investigators. Most of the benthic foraminiferas observed were stained yellow or brown in colour and are thought to be reworked or relict. Very few well preserved benthic foraminifera samples were observed in any of the Kasten core samples. The highest concentration of benthic foraminifera was found in KC13 from 310 cm to the bottom of the core (Fig. 56).

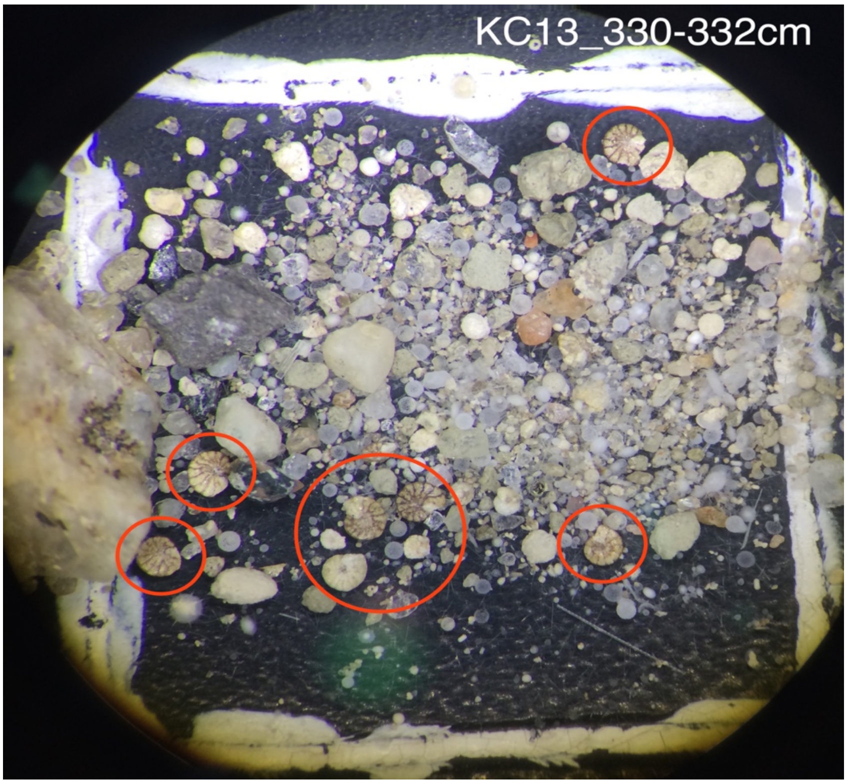

Figure. 56. Sample coarse fraction photo from C038_KC13_330-332 cm with multiple unidentified benthic foraminifera. *Individuals are seen to be stained brown and are termed as reworked.*

Further studies concerning the foraminiferal microfossils obtained on the voyage are to be conducted at the Australian National University. This will include the compilation of a stable oxygen isotope stack paired with Mg/Ca paleothermometer data on discrete intervals for one of the piston cores obtained in conjunction with its respective kasten core. It is hoped that this will give insights into the regional changes in temperature and salinity across multiple glacial-interglacial cycles.

Diatoms

Permanent smear slides were made from kasten cores (11) and piston cores (6) for preliminary analysis of fossil diatom assemblages. Cover slips were first cleaned with potato and Milli-Q. Small, non-quantitative samples of sediment were obtained with a toothpick and smeared onto coverslips. Once dry, coverslips were permanently adhered to a slide using Norland Optical Adhesive and dried under UV light.

In kasten cores, slides were made approximately every 10 cm with additional slides made at depths with higher apparent diatom content and laminae with distinct coloration. Slides were observed under 400x magnification on an Olympus BH-2 microscope and examined for approximate diatom abundance and preliminary assemblage observations. *Fragiliariopsis kerguelensis* dominates the Holocene sections in the upper part of each core and have high morphologic variability. The next most abundant diatom observed in all kasten cores is *Thalassiosira lentiginosa,* which also has some morphologic variability with valves ranging from nearly circular to more flattened. Other frequently observed diatoms include *Eucampia antarctica*, *Rhizosolenia*, *Thlassiothrix*, and centrics >20 μm. Notably, KC06 contained large *Thalassiothrix* diatom mats which gave the core a "cottony texture". In most of the core, diatoms are very abundant in the top ~100cm and decrease abruptly downcore, with the occurrence of more terrigenous sediments that were likely deposited during the last glacial period. In some of the kasten cores, diatom abundance increases again at the bottom of the core. Estimated diatom abundances from kasten cores are included in the kasten core graphic logs (Appendix 4). All preliminary observations can be found in Appendix 6.1.

Permanent smear slides also were made from the piston cores, at depths where the cores were cut into sections. These slides provide preliminary observations regarding biostratigraphic marker species, and abundance data for comparison with magnetic susceptibility records from the Geotek core logger. Slides were observed under oil at 1000x magnification on an Olympus BH-2 microscope. Biostratigraphic observations were made after a minimum of three transects. Initial observations show highly variable diatom abundances ranging from very rare to very abundant, with *F. kerguelensis* uniformly the dominant species. Biostratigraphic marker species *Rouxia leventerae* (last occurrence in upper MIS 6), *Rouxia constricta* (last occurrence in lower MIS 8) and *Hemidiscus karstenii* (last occurrence in lower MIS 6) are tentatively identified in the lower parts of most piston cores. PC03 varies notably from the other piston cores and contains more older species including some tentatively identified as Miocene and Pliocene. All preliminary observations can be found in Appendix 6.5.

Radiolarians

Sampling Methods

Kasten core, multi-core and vertical plankton tows provided sedimentary and seawater material from which a portion was allocated for radiolarian research. Samples were taken for two different uses – for further, onshore, analysis at the completion of the voyage and for photographic purposes both onboard and ashore.

Wet sediment samples were collected for future analysis from nine kasten core and two multi-core operations at regular depth intervals depending on the lithology of the core. The average sample size was approximately 40 grams and the samples were stored in whirlpak bags at a temperature of 4 °C. These samples are to be used for further analysis by Kelly-Anne Lawler, Leanne Armand and Giuseppe Cortese.

Wet sediment samples were also collected from six of the kasten cores for preliminary analysis onboard. A number of these samples were sieved, dried and used to make permanent slides while onboard the vessel. An inverted light microscope was used to view the slides, photographs were taken and sent ashore to Giuseppe Cortese in order to confirm the identities of some of the species present in the sediment core. Sediment samples which were not sieved and used for making slides onboard will be taken ashore for further photography using both inverted light microscope and scanning electron microscope (SEM).

Seawater samples were taken from three vertical plankton net sites for the sole purpose of sieving and creating slides for light microscope photography. A 100μm plankton net was deployed to a depth of 100 m with 500 ml of the resulting assigned to radiolarian microscopy. 250ml of the sample was sieved through 63 μm mesh and 250 ml sieved through 37 μm mesh. The remnants were dried and mounted on permanent slides for viewing and photography with an inverted light microscope.

Figure 57 and Table 14 show the locations at which kasten core, multi-core and plankton net samples we taken for radiolarian research. A list of all samples and their depths, and all slides are included in Appendix 1.1.

Table 14. Locations sampled for radiolarian research.

Operation Number	Latitude (°)	Longitude (°)
KC04	-64.68	119.30
KC05	-64.65	119.02
KC06	-64.73	118.70
KC07	-64.40	118.50
KC08	-64.79	119.74
KC11	-65.13	120.05
KC12	-64.95	120.86
KC13	-64.54	119.10
KC14	-64.48	116.64
MC01	-64.47	115.62
MC02	-64.46	115.04
PN06	-64.95	120.86
PN07	-64.48	119.11
PN08	-64.54	116.64

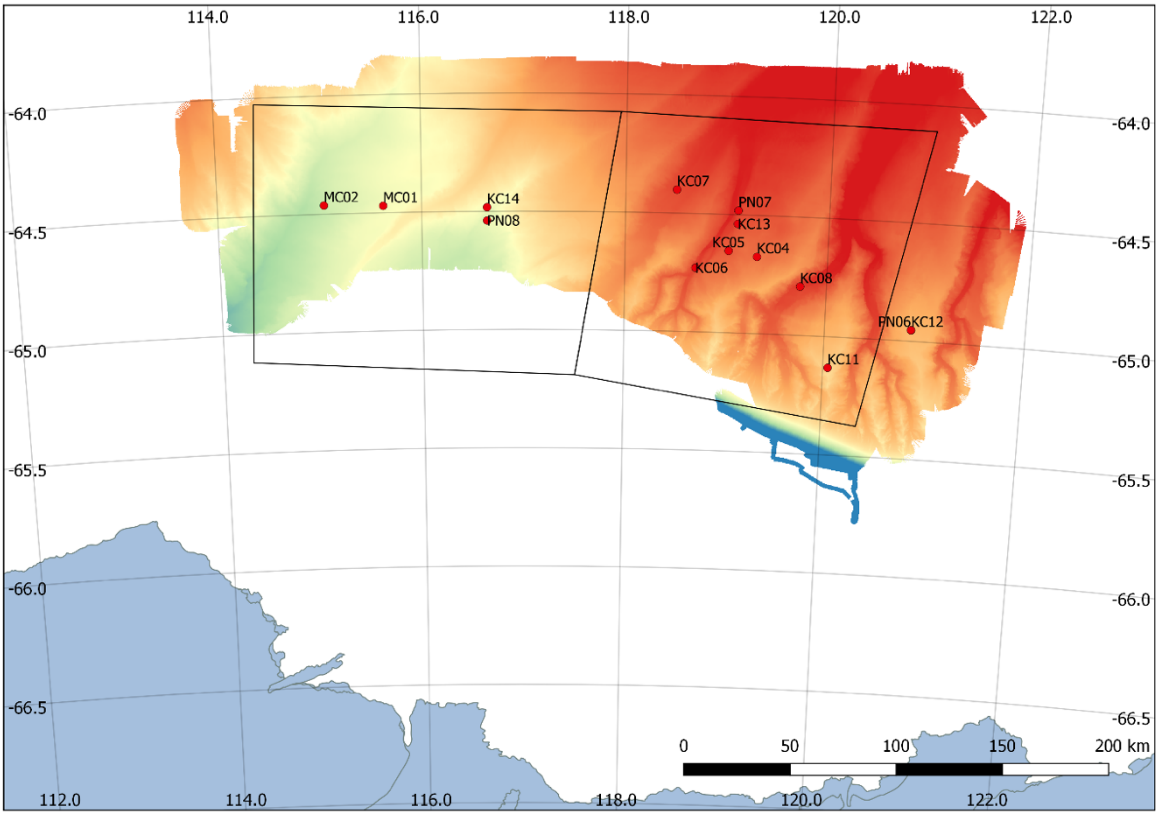

Figure 57. Map showing locations of kasten cores and vertical plankton nets sampled for radiolarian research. *Map created using QGIS by Kelly-Anne Lawler, March 2017.*

Preliminary Results

Kasten core samples

Most samples which were mounted on slides did include radiolarians. Three of these samples (KC07 – 8-10 cm depth, KC08 – 6-8 cm and KC13 – 150-152 cm) were photographed and many species identified thanks to the help of Giuseppe Cortese. A selection of these are contained in Appendix 6.6.

Vertical plankton net samples

Slides made using samples from plankton net operations PN06 and PN08 each contained only one radiolarian specimen. However, the slides made from the sample taken from PN07 contained more than twenty different radiolarian species – a selection of these are contained in Appendix 6.4.

Future research

Kasten core and multi-core samples will be used to identify and quantify radiolarian distributions in the Sabrina Coast region of East Antarctica over time in cores as part of a Master thesis at Macquarie University under the guidance of L. Armand and G. Cortese (GNS, New Zealand).

MICROBIOLOGY SAMPLING

Ancient DNA (aDNA)

Sampling for ancient DNA (aDNA) analyses from Kasten Cores was generally conducted per the following scheme: every second cm in the top 10 cm, then every 10 cm until 110 cm, and every 20 cm after. Interesting layers were sampled in addition. Sampling was done from the bottom to the top of the core.

Figure 58. aDNA sampling from Kasten Core using minicores.

aDNA samples were taken immediately after core photography was completed (~30 – 60 minutes after core opening). The outer 0.5 cm of core surface were scraped off perpendicular to the core, from core bottom to top, using metal scrapers that were cleaned with 10 % bleach and 70 % ethanol after each scrape. Each sampling depth was marked with a toothpick and duplicate 10 ml minicores were taken using sterile bottomless 15 mL FalconTM tubes (*Figure* 58). The minicores were transferred into sterile Whirl-Pak® bags, kept in liquid nitrogen for ~15 mins and in -80 °C thereafter. Liquid nitrogen was not available for core KC08 - KC14 and samples were placed directly into -80 °C.

Sampling for aDNA from multicores was conducted according to the following scheme: every cm in the top 6 cm, then every 5 cm (1 cm thick slices) until the bottom end of the core. Sampling was done using an extruder. A metal slicer was used to cut one multicore (tube 3), and the edges were removed using a metal spatula to avoid age-contamination. About ½ of the material as placed in a sterile Whirl-Pak® bag, frozen in liquid nitrogen for 15 minutes followed by storage at -80 °C.

All aDNA sediment samples (316 in total, for a complete list see Armbrecht quarantine report-aDNA) will be transported to MQ on dry ice where processing and analysis of aDNA samples will be completed by Dr L. Armbrecht. The aim will be to determine eukaryotic phytoplankton community changes and changes in the evolution and activity of RuBisCO Ribulose-1,5-Bisphosphate Carboxylase/Oxygenase (RuBisCO; critical for the initial step of carbon-fixation in phytoplankton) over the past 30,000 years. Complementary data for this study will be produced by GDGT (see section 3.4.3.1), 14C dating and δ13C analysis (past CO2), and microfossil analysis of the same sediments by Prof. A. Leventer and Ms M. Duffy, Colgate University, US (chapter 0). Additionally, modern phytoplankton/microbial and environmental data collected from the underway intake and CTD water sampling sites of IN2017-V01 by Dr. L. Armbrecht, A/Prof. L. Armand, Ms. A. Focardi, Dr A. Leventer, Ms M. Duffy and Dr P. Hughes will contribute to characterise planktonic communities in the Sabrina coast region (see chapter 0 Marine Biology).

Multicore water sampling

Two types of water were sampled from the multicorer: (i) water from a 5 L Niskin Bottle (OceanTest Equipment Inc. Florida) attached to the multicorer frame, which automatically shut when the multicorer hit the bottom (hereafter referred to as ‘multicore niskin water’); and (ii) water retained within all six multicorer tubes (‘bottom water’), which was siphoned off and pooled in a 10 L carboy (*Figure* 59).

Figure 59. Example of bottom water sampling from Multicore.

Subsamples from multicore and bottom water (12 in total) were collected separately for DNA (1 – 2 L, Sterivex), plankton abundance (200 mL, Lugol’s preservation, bottom water only due to limited volume of niskin water) alongside nutrient/salinity analysis (~ 500 mL, hydrochemistry, on board, Dr P. Hughes) and isotopes/rare earth elements (~4 L filtrations, Dr T. Noble). The fluff layer from two tubes (3 and 4) was collected and preserved with Lugol’s solution in separate amber glass bottles.

The aim of multicore water sampling is to determine planktonic communities and environmental conditions directly above the cored sediment. DNA and planktonic community composition will be determined by Dr. L. Armbrecht and Ms A. Focardi at MQ. Hydrochemical measurements will be undertaken on board by P. Hughes. Analysis for rare earth elements and Nd isotopes, and potentially Th isotopes, biogenic silica and trace metal geochemistry, will be undertaken by Dr T. Noble (UTAS).

Operations evaluation

When conducting the observations of microfossil assemblages in the >63 µm fraction a few improvements could have been made to the overall method and the tools used on board. In order to make the observations quantitative rather than qualitative it would have been ideal to weigh out equal amounts of dried bulk sample to be sieved to not only keep the analysis consistent but also to determine a recovery percentage of the dried course fraction.
Additional tools that would have been useful for the analysis include, a millimetre square picking tray and picking tools such as a fine paint brush. These tools would have been particularly useful for the coiling direction analysis; without a fine brush this became too arduous to pursue on board.
The sampling for aDNA is highly time-sensitive once the core is on board and opened. Sampling was conducted as soon as possible after opening and photography had taken place, however, 30-60 minutes passed until the material was sampled. Liquid nitrogen was unavailable for samplings KC08-KC14 and samples were directly transferred into -80 °C. The time-loss before sampling and slower freezing at -80 °C might impact aDNA data. Fast sampling and availability of liquid nitrogen for snap-freezing is recommended. Contamination of sediments from different age is considered unlikely due to rapid and thorough cleaning procedure applied between each sampling depth.

Summary

- Wet samples retrieved from the kasten cores were put through a >63 µm sieve, air dried and viewed under a microscope between 1.5-6x magnification. The presence of all planktonic, benthic and agglutinated forams was noted with the depths at which they occurred as well as their abundance.
- Well-preserved planktonic foraminiferal microfossils identified as *N. pachyderma* were found in seven out of the ten kasten cores. Reworked benthic forams, currently unidentified, were observed as singular individuals in nine out of the ten cores with all appearing stained brown.
- Due to the presence of foraminifera in sections of the kasten cores, their presence is likely in previous interglacial phases; this can be evaluated through future sampling and analysis of the piston core sediments. Foraminifera will picked from all samples for oxygen isotopic analysis to better understand regional changes in ocean temperature and salinity going back through multiple glacial-interglacial cycles.
- Smear slides document the presence of a diverse and abundant diatom assemblage in the upper part of the kasten cores, likely during the Holocene, with decreased abundance during glacial and deglacial intervals with much higher terrigenous input. Quantitative diatom abundance data will be generated to evaluate changes in paleoceanography, potentially as far back in time as MIS3.
- KC06, one of the “canyon cores” was anomalously diatomaceous, characterized by abundant *Thalassiothrix* mats. Study of this core will focus on the character of these laminations – factors controlling their initial production followed by their concentration in this limited area of the slope.
- Sediment samples were taken from kasten cores and multi-cores, and seawater was collected using a 100-m deep vertical plankton net for future research into radiolarian species found in the Sabrina Coast slope environment.
- More than 30 species of radiolarian were photographed during preliminary analysis of kasten core samples, while one plankton net sample (PN07) contained more than 20 species of radiolarian.
- Samples collected during IN2017_V01 will be used to identify and quantify radiolarian distributions in the region and over time as part of a Master’s thesis by K-A. Lawler at Macquarie University under the guidance of L. Armand and G. Cortese (GNS, New Zealand).
- A total of 361 aDNA samples were collected from Kasten and Multicores. The combination of aDNA and environmental data from Kasten and Multicore sediments (GDGT, 14C and δ13C) will provide new information on past eukaryotic phytoplankton community changes and the evolution in the carbon-fixation enzyme RuBisCO as a response to changes in ocean temperatures and CO_2 over the past 30,000 years. A total of 12 modern DNA and plankton abundance samples from multicore niskin and bottom water will provide a picture of modern communities just above the cored sites.

- Together, the multiple biological, geochemical and sedimentologic proxies will be used to develop a comprehensive understanding of glacial to interglacial conditions along the Sabrina Coast continental slope. Chronologic control will be based on radiocarbon dating of acid insoluble organic matter, with additional carbonate dates from foraminifera where possible.

GEOCHEMICAL SAMPLING

Glycerol dialkyl glycerol tetraether (GDGT)

Sampling intervals for glycerol dialkyl glycerol tetraether (GDGT, proxy for past SST) resembled aDNA sampling intervals for both Kasten and Multicores (see chapter 0). About 10 cc sediment were placed into precombusted aluminum foil squares (12 hrs at 400 °C) before placing them into sterile Whirl-Pak® bags and storing at -20 °C. Metal spatulas cleaned with water after each sampling interval were used to transfer the sediments into the aluminium foil.
All samples will be transported to MQ on dry ice where processing and analysis of GDGT samples (316 in total, see Armbrecht Quarantine report 'GDGT' for sample details) will be completed by Dr L. Armbrecht. The aim will be to determine rates of change in ocean warming over the past 30,000 years alongside changes in eukaryotic plankton community changes determined from aDNA analyses (see chapter 0).

Highly-branched isoprenoids (HBI)

Sampling intervals for highly-branched isoprenoids (HBIs, sea-ice proxy) resembled aDNA sampling intervals for Kasten and Multicores (see chapter 0). About 3 g of sediment were collected by transferring material with small water-cleaned metal spatulas into 2 mL cryovials (Corning) or 1.7 mL centrifugation (LabAdvantage, VWR) tubes. The samples were stored at -80 °C.

All samples (316 in total, see Armbrecht Quarantine report 'HBI-sediments' for sample details) will be transported to Plymouth University, UK, on dry ice where processing and analysis of HBI samples will be completed by Prof. S. Belt. The aim will be to determine concentrations of HBIs in sediments alongside measurements from the water column (see chapter 0
Marine Biology). The HBI data will be complemented by spectroscopy, and genomics data (see chapter 0
Spectroscopy and chapter 0
Marine Biology) and deliver a detailed picture of present and past HBI production by diatoms in the Sabrina Coast region.

Spectroscopy

Sampling intervals for spectroscopy resembled aDNA sampling intervals in Kasten and Multicores (see chapter 0). Duplicate samples of about 3 g of sediment were collected by transferring material with small water-cleaned metal spatulas into 2 mL cryovials or 1.7 mL centrifugation tubes. The samples were wrapped in aluminium foil and stored at -80 °C.
All samples (621 in total, see Armbrecht Quarantine 'Spectroscopy-sediments' for sample details) will be transported to Monash University, Australia, on dry ice where processing and analysis of HBI samples will be completed by Prof. P. Heraud. The aim will be to spectroscopically characterise HBIs in sediments complementing HBI, and genomics data (see chapter above (
Highly-branched isoprenoids (HB) and chapter 0
Marine Biology) to deliver a detailed picture of past HBI production by diatoms in the Sabrina Coast region

Operations evaluation

Although all samplings for GDGT's was conducted using metal to avoid any trace metal contamination, contact of sediments by plastic minicores might have contaminated the sampled sediments. Three unused minicores will be tested for contamination alongside GDGT measurements as a control. However, in future samplings, any contact with plastic should be avoided. The first multicore was sampled using metal equipment for REE's, which might impact on the results. All other multicores were sampled using plastic equipment only for REEs.

Summary
A total of 316 GDGT samples were collected from Kasten amd Multicores. The GDGT data (alongside 14C and δ13C) will provide the environmental context for changes in eukaryotic phytoplankton communities determined by aDNA analyses over the past 30,000 years (see chapter 7).

A total of 316 HBI (Sea-ice proxy) and 632 spectroscopy samples were collected from Kasten Cores. This data will be placed in context with HBI focused spectroscopy and genomic measurements of water samples collected during IN2017_V01 and reveal new information on HBI-producing diatoms and past sea-ice extent in the Antarctic Sabrina Coast region.

Radiocarbon
Radiocarbon dating will be carried out on selected Kasten cores (e.g. KC02, KC12, KC14). Where possible, radiocarbon analyses of planktic foraminifera will be carried out at ANU, and ideally paired with dating of the acid insoluble organic fraction (ANSTO). Where the bulk acid-insoluble organic fraction is much older than acceptable given the age of the surface waters in the Southern Ocean, a selection of samples will be analysed using the ramped pyrolysis method in association with Brad Rosenheim (USF). This method uses programmed temperature combustion and analysis to provide low and high temperature radiocarbon dates, which separates out the reworked organic carbon from the targeted fraction. About five dates result from this method so preliminary dating of the bulk acid-insoluble organic fraction is not wasted. Funds for this work will be provided by contributions from ANU (B. Opdyke), pending Australian Antarctic Science proposal (AAS4419; Noble) and a proposal will be submitted to ANSIE in the next round to further support costs.

Bulk Inorganic geochemistry
U-channels were taken of each Kasten core as 25mm x 25 mm and 100 mm x 100 mm channels, generally in 1 m sections. The 25 mm x 25 mm u-channel will undergo scanning X-ray fluorescence (XRF) analysis in June 2017 using the Itrax core scanner at the Australian Nuclear Science and Technology Organisation (ANSTO), Lucas Heights, NSW. This is a non-destructive technique that can provide high-resolution geochemical characterisation of the sediment core. In addition to geochemical analyses, the cores will be measured for magnetic susceptibility and x-rayed. Once the small u-channels have been analysed they will become the archive section of the Kasten cores. The larger 100 mm x 100 mm u-channels were taken for future targeted geochemical analyses and act as a working section of the Kasten cores.
All the u-channel sections will be analysed using the Itrax core scanner. The following geochemical measurements will be conducted on KC02, KC012 and KC14 to extract the proxies of past ocean dynamics and ice sheet behaviour since the last termination.

Tracing past water masses on the continental shelf will be conducted by chemical extraction of the seawater-derived phases (Fe-Mn oxides) in the bulk sediment, using a weak acid solution buffered to pH 4. The down core ice-ocean interaction and provenance study will require dissolution of the sediment using a microwave digestion procedure. Aliquots of the same sediment digestion can be used for multiple measurements e.g. Nd and Sr isotopes for provenance work, major, trace and redox metals for provenance, as well as Th and U isotopes for Th-normalisation.

Nd isotopes
Chemical extractions (water mass reconstruction) or detrital dissolution (sediment provenance) will be processed using two sets of column chromatography to separate the Nd isotopes. These processing steps will be carried out in a trace metal clean laboratory at the University of Tasmania. The analysis of 143Nd/144Nd ratios will be carried out on the Neptune Plus Multi-collector inductively coupled mass spectrometer at the ANU by T. Noble.

Sr isotopes
Sediment dissolutions will be processed to separate Sr from major cations and interfering isotopes. The 'waste' from the first set of Nd isotope column chromatography contains the Sr fraction of the sample. This fraction will be collected and passed through the Eichrom Sr SPEC resin to isolate the Sr isotopes for analysis of the 87Sr/86Sr ratio at the University of Tasmania.

The samples will be analysed at the ANU using the Triton Thermal Ionisation Mass Spectrometer.

Th and U isotopes
To calculate vertical fluxes of terrigenous and biogenic components of past conditions, isotopes of thorium (230, 232) and uranium (234, 235, 238) will be measured by isotopic dilution over 229Th and 236U respectively using an Aridus II desolvating nebuliser sample introduction system (Cetac) attached to an ELEMENT 2 sector field ICP-MS at UTAS Central Science Laboratory.

Rare Earth Elements (REE) and redox sensitive metals.
REE patterns will be determined from sediment digestions of the Kasten cores, and multicore MC01. In association with REE and Nd isotope data from the seawater samples collected on this voyage (Appendix 1.5), these data will help constrain the use of Nd isotopes in tracing past water masses in this region.

Redox metals will be measured in the Kasten cores as an additional tracer of bottom waters along the slope. Cold Antarctic sourced waters will have a high oxygen content compared to warmer and lower oxygen circumpolar deep waters. The Uranium (U) and Rhenium (Re) precipitated in the sediment under low oxygen levels, and Manganese (Mn) precipitated under high oxygen levels in bottom waters, will be measured by ICP-MS at UTAS.

Opal concentrations
The opal content of the sediment will be measured by spectrophotometry following alkaline leaching in 2 M Na2CO3.

Ice rafted debris (IRD) concentrations
The Kasten cores were sampled every 2 cm for KC02, KC04, KC07, KC08, KC11, KC12 and KC14; while KC03, KC05, KC06, and KC13 were sampled every 5cm or less. The sediment will be freeze-dried, and weight determined. The sediment is placed in a beaker of MilliQ water and disaggregated using a shaker. The sediment is sieved using a 63 micron mesh and the coarse 150 micron to 2 millimetre size fraction weighed. This fraction is split and at least 500 grains will be counted using a binocular microscope into biogenic and terrigenous components (e.g.quartz, feldspars, mafic minerals, lithic fragments, diatoms, benthic foraminifers, planktonic foraminifers, radiolarians) to determine the volume percent of IRD. The concentration of ice-rafted debris in mg/g is calculated using the weight of the 150um-2mm fraction.

Heavy minerals will be separated from sediment, mounted on doubled sided sticky tape and encased within 2.5cm round epoxy mounts. Polished and cleaned mounts will be carbon coated for scanning electron microscope (SEM), back scattered electron (BSE) and cathodoluminescence (CL) imaging to identify internal zonation and core-rim structures that can then be targeted for U-Pb isotope analysis. U-bearing minerals (zircon, monazite, rutile and titanite, where identified) will be analysed via Laser Ablation-Inductively Coupled Plasma Mass Spectrometer (LA-ICPMS). Pb isotope dating of feldspars will also be carried out.

Near-Infrared Mineral Analysis
Kasten core samples were subjected to an experimental mineralological analysis using near-infra red reflectance spectroscopy. This technique has been used extensively in mineral and petroleum exploration but has not been used on marine sediments. It can be used to derive a semiquatitative estimate of the major mineral phases within a sample, although not all mineral have a reflectance spectrum. For example, quartz and biogenic silica do not produce a spectrum. It was hoped the method would detect any changes in clay or micaaceous mineral composition. The advantage of the technique is that it produces rapid results with minimal sample preparation.

We used an ASD Terrascan field spectrometer. Initially, kasten cores were sampled at 20 cm depth increments though this was reduced to taking samples where significant colour changes were observed. Samples were dried in an oven at 40^{o}C. Sample spectra were then measured on the dried sample however, this produced inconsistent results so samples were pulverized by hand to fine sand to silt sized fragments and re-run. Spectra recorded by the Terrascan were loaded into The Spectral Geologist (TSG) software and a computer-based estimate of mineralogy produced. Spectra were then examined visually, both as raw curves and as Hull Corrected curves.

Results

Subdued spectra were produced by most samples which the software found difficult to produce a consistent estimate of mineralogy. The most consistent identification is for the sample to be dominated by montmorillonite. Visual inspection of the spectra suggests that the dominant mineral is mixed layer montmorillonite-illite although the number of aspectral samples and the subdued nature of many of the spectra suggest that biogenic silica in the form of diatoms is also important and sometimes dominant.

Summary

- Sea floor sampling activities were highly successful in delivering for the major project goals, helped by excellent sea conditions.
- The Kasten corer was relatively easy to deploy and effective, except in sandy sediment.
- The Piston corer had significant issues on deployment which are addressed by MNF reports but it was effective in recovering long records.
- The multicorer worked well in calm conditions.
- Kasten core access to the Wet Dirty Lab needs to be reviewed to allow longer barrels to be used.
- Kasten core archiving using electrical conduit for channel sampling was an excellent innovation.

SECTION 6. Physical Oceanography

CTD ROSETTE

Equipment/Method

Figure 60. CTD rosette with Niskin bottles.

An SBE911plus CTD (Seabird Electronics) fitted with fluorescence, oxygen, turbidity and altimeter sensors (Seabird Electronics) mounted on a rosette (SBE11) holding 24 twelve litre Niskin Bottles (OceanTest Equipment Inc. Florida) was used (Fig. 60). The CTD was allowed an ~3 min surface soak before lowering it to just above (~10 m) the seafloor, based on measurement from the mounted altimeter. While the CTD was lowered the profile of all parameters (primary and secondary fluorescence, temperature, photosynthetically active radiation, turbidity, oxygen) was observed and water samples were collected during the upward cast based on interesting water mass features. In general, sampling included the surface (between 2.5 – 4 m), the deep chlorophyll maximum (DCM), below the DCM, the temperature maximum and the deepest part of the water column. For the characterisation of the water masses samples for hydrochemistry analysis (oxygen, salinity and nutrients) were collected at each of the selected depths. Water for biological parameter assessment included samples for phytoplankton composition and abundance, chlorophyll a, DNA, flow cytometry and the Viriome. Grazing experiments were conducted based on surface or DCM water from selected CTD casts.

During CTD casts 01 and 02 we collected water for HBI analyses, however, much more material was acquired during vertical plankton net tows (see section 5.1 Plankton net) and thus used for HBI analyses instead of any further Niskin bottle water.

From CTD cast 07 we collected samples for RNA extraction from 2 depths, surface and DCM. For details on the different types of analyses from CTD Niskin water please refer to Section 4.4. Hydrochemistry and 5. Marine Biology.

Ten litres of seawater were collected for rare earth element concentrations and neodymium isotopic analysis from 13 stations (A005-CTD2, A005 CTD3, C018-CTD19, A007- CTD5, C010-CTD7, C011-CTD8, C012-CTD9, C015-CTD16, C024-CTD21, C027-CTD23, C030-CTD25, C034-CTD28, C043-CTD33). See the table in Appendices 7 and 1.5 for information on which casts were sampled and respective depth intervals. The seawater was collected into 10 L carboys with a 38 mm neck made of polypropylene. The bottles were cleaned by soaking in Decon (1 day), 50% reagent grade hydrochloric acid (2 days) and MilliQ water (1 day), and double wrapped in plastic bags. Seawater was drained by attaching a 12.7 mm LDPE tubing to the spout of the Niskin bottle and a 0.45 µm Millipore filter cartridge. Each sample took about 30 minutes for the seawater to filter through the cartridge. The bottles were carried into the clean dry lab and acidified in the laminar flow hood with distilled 6M HCl to pH 2 (2 mL/L seawater). Acidifying the seawater keeps the trace metals of interest in the dissolved phase, prior to pre-concentration and processing in the lab.

Casts and Profiles

A total of 32 CTD casts were deployed (Fig. 61, Table 15), seawater was collected for hydrochemistry analysis, isotope composition and biological samples (see sections on *Hydrochemistry* (pg 104) and *Marine Biology (Section7)* for more information and Appendices 7 and 1.5).

Cast 8 was aborted due to being in an incorrect geographic position, cast 11 and 12 were aborted due to sensor issues, and cast 24 was aborted due to no communication with the CTD. In addition, cast 13, 14 and 15 were deployed to resolve issues and test the new settings.

We collected water and observations from six CTD stations in Area A, and 15 stations in Area C and the shelf section of Area C. There is one CTD station (CTD 33) that is east of the Dalton ice tongue (see Fig 61).

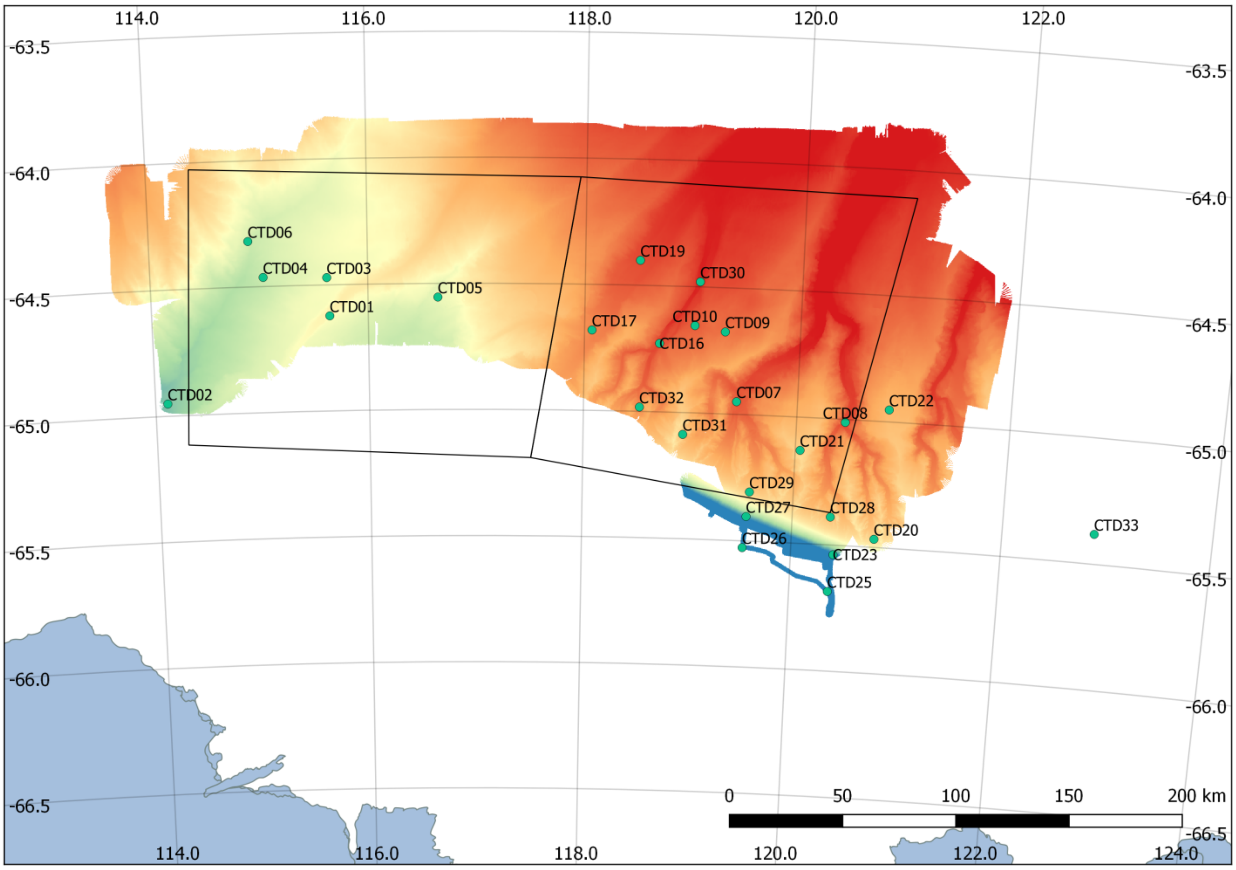

Figure 61. Map of the CTD casts. *Map created by Kelly-Ann Lawler, 2017.*

The first CTD (CTD01) was deployed in close proximity to an Iceberg (less then 2 miles); floating icebergs are thought to be localised hotspots for primary production (Smith et al. 2007) as freshwater input produces stratification and the release of different trace chemicals, such as iron into the surrounding ocean. When icebergs melt, they release trace elements that are usually at very low concentration in in the surrounding water.

Casts 3, 4, 9, 10, 16, 19, and 22 were deployed at Kasten, multi- or piston coring stations. Preliminary graphs of the unprocessed data derived from the CSIRO software used during deployment are shown in Figure 62.

Six casts (23,25,26,27,28,29) were deployed in the Dalton polynya area, along two N-S transects, with two CTDs on the shelf, two close to the shelf-slope break and two slightly to the north, in deeper waters of the slope.

Table 15: Summary of CTD casts sampled during IN2017-V01. *The information shown is for the bottom of each cast.*

Station ID	Cast ID	Date and time (UTC)	Latitude (°S)	Longitude (°E)	Depth of bottom bottle (m)
A001	CTD1	25/01/17 3:04	64 37.56	115 38.83	206
A003	CTD2	26/01/17 16:39	64 57.07	114 06.64	399.7
A005	CTD3	27/01/17 12:35	64 28.26	115 37.39	2177.8
A006	CTD4	27/01/17 16:48	64 27.78	115 02.58	1875.3
A007	CTD5	29/01/17 12:05	64 33.23	116 38.61	2106.4
A009	CTD6	30/01/17 5:34	64 19.05	114 54.88	1945.8
A010	CTD7	1/02/17 18:52	64 57.02	119 25.81	3232.8
C011	CTD8	2/02/17 4:41	65 00.7	120 27.4	3315.5
C012	CTD9	4/02/17 9:18	64 40.539	119 18.080	3135.7
C013	CTD10	5/02/17 1:18	64 39.23	119 01.0	3232.2
CO15	CTD16	11/02/17 9:24	64 43.71	118 41.77	3361.1
CO17	CTD17	11/02/17 13:16	64 40.89	118 04.17	3055.8
CO18	CTD19	11/02/17 18:37	64 23.98	118 29.99	3325.8
C023	CTD20	17/02/17 10:39	64 28.124	120 47.518	2558.9
C024	CTD21	17/02/17 17:34	65 07.9	120 03.01	2633.3
C025	CTD22	19/02/17 6:19	64 57.19	120 51.57	2806.6
C027	CTD23	20/02/17 10:59	65 32.27	120 24.38	941.9
C030	CTD25	20/02/17 10:59	65 41.07	120 22.32	429.3
C031	CTD26	21/02/17 4:22	65 31.59	119 32.40	483.7
C033	CTD27	21/02/17 9:01	65 24.24	119 33.81	1183.8
C034	CTD28	21/02/17 19:43	65 23.36	120 21.69	2721.5
C035	CTD29	22/02/17 1:21	65 18.31	119 35.08	2629.1
C039	CTD30	23/02/2017 5:46	64 28.78	119 03.29	3454
C040	CTD31	23/02/2017 12:40	64 05.19	118 56.16	2647
C041	CTD32	23/02/217 17:07	64 58.96	118 31.98	3013
C043	CTD33	25/02/217 22:26	65 22.77	122 53.22	2368

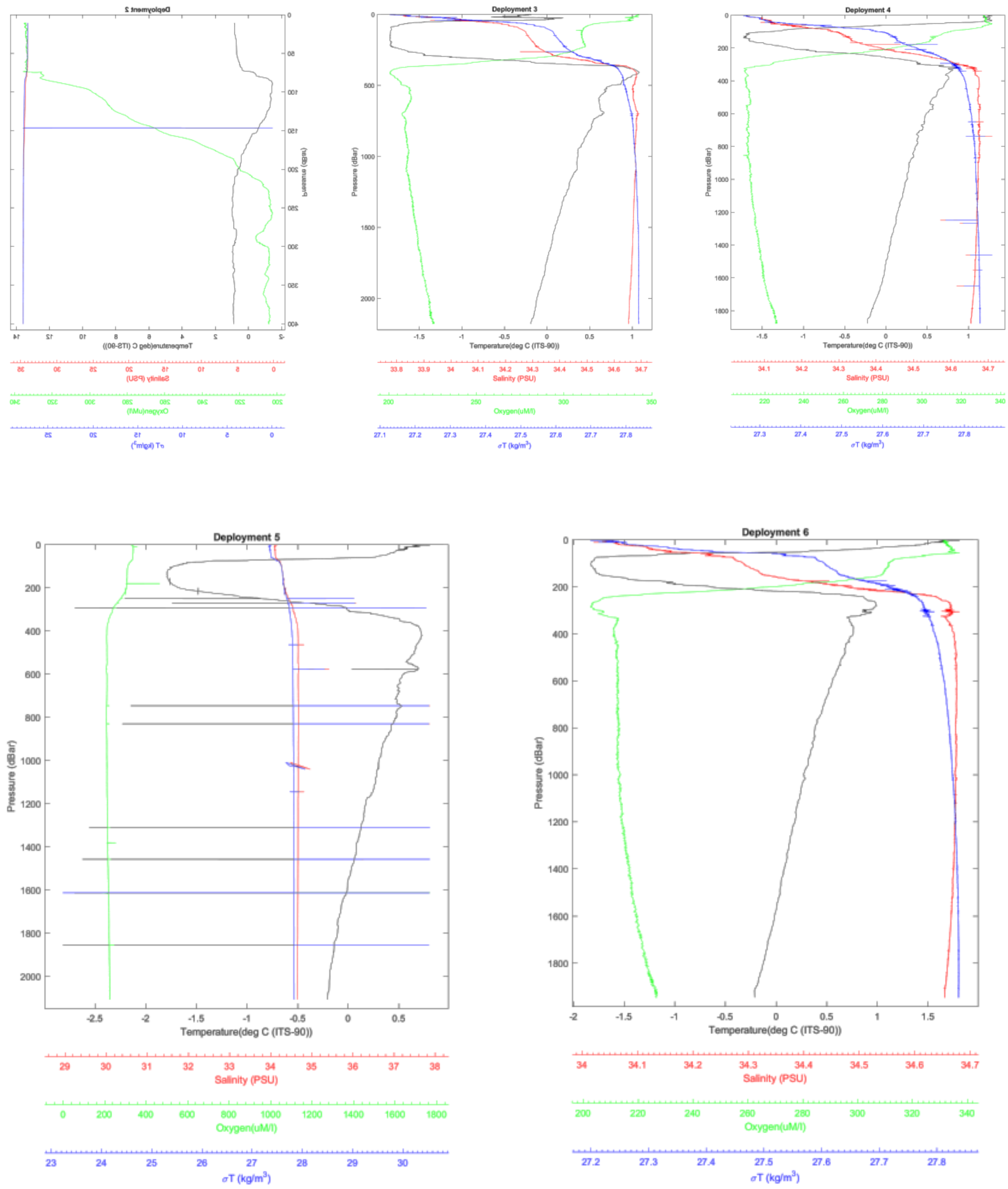

Figure 62: Preliminary downward cast of CTD (unprocessed data) cast deployed during IN2017-V01. *Deployment locations shown in Figure 61.*

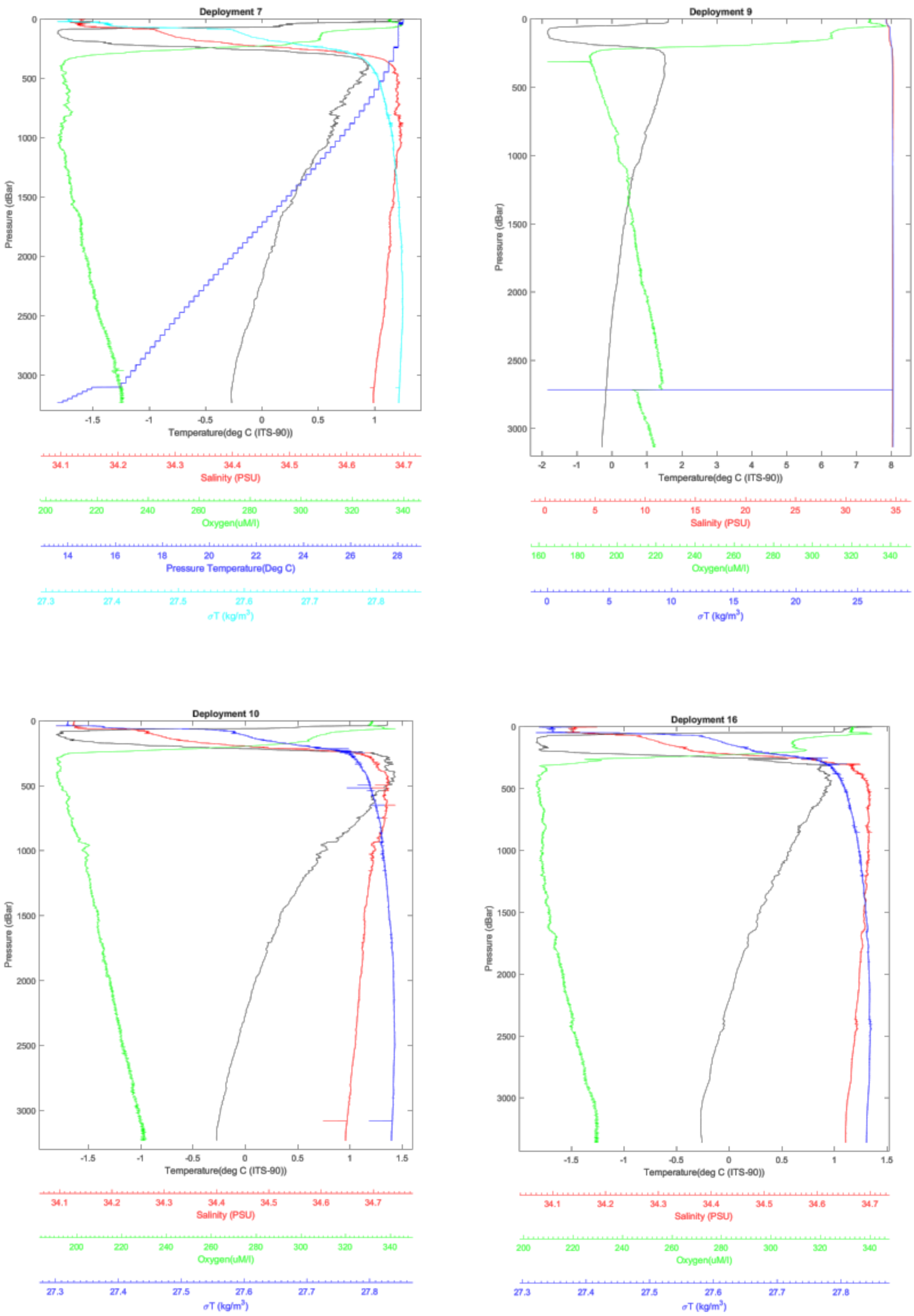

Figure 62 continued: Preliminary downward cast of CTD (unprocessed data) cast deployed during IN2017-V01. *Deployment locations shown in Figure 61.*

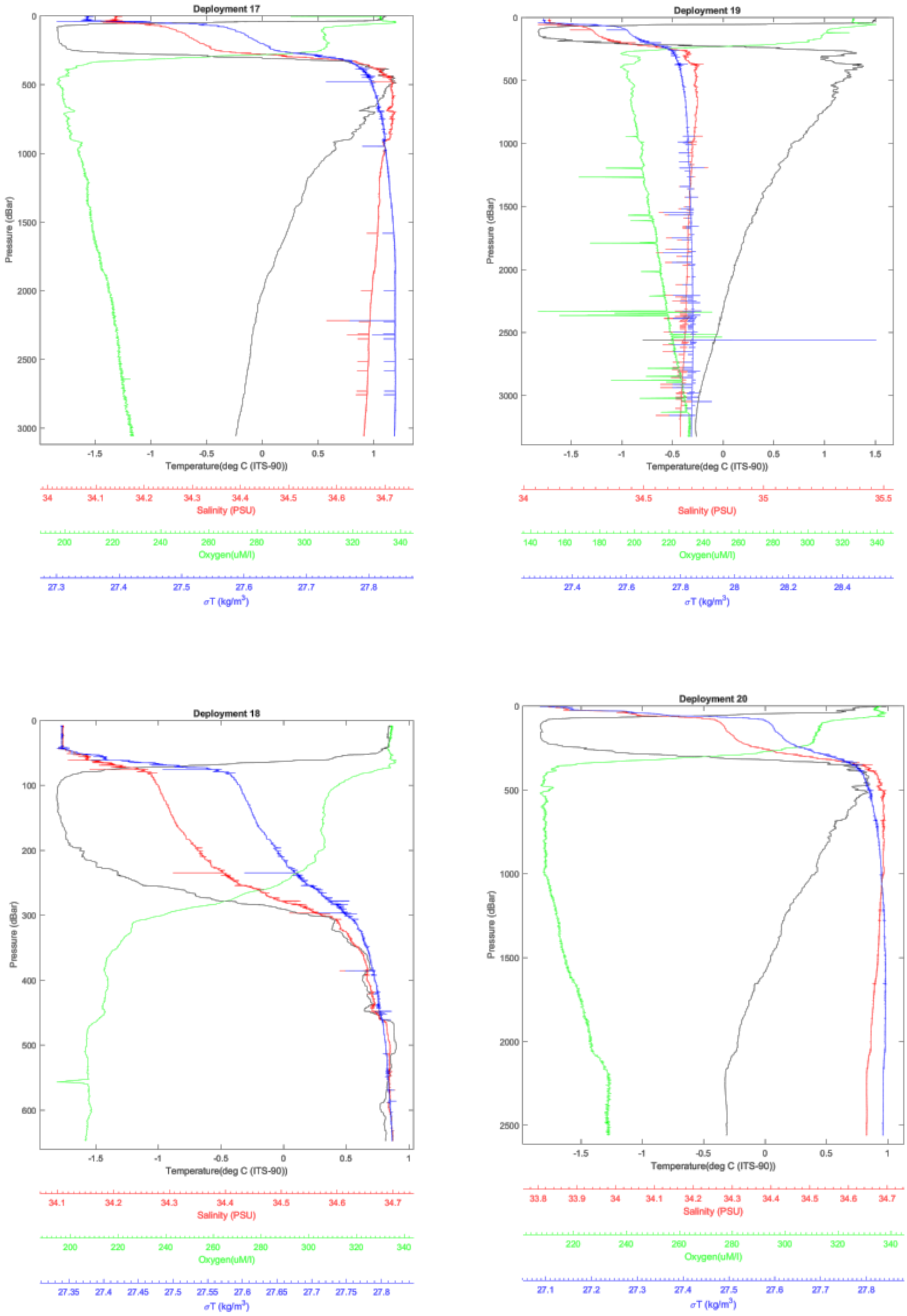

Figure 62 continued: Preliminary downward cast of CTD (unprocessed data) cast deployed during IN2017-V01. *Deployment locations shown in Figure 61.*

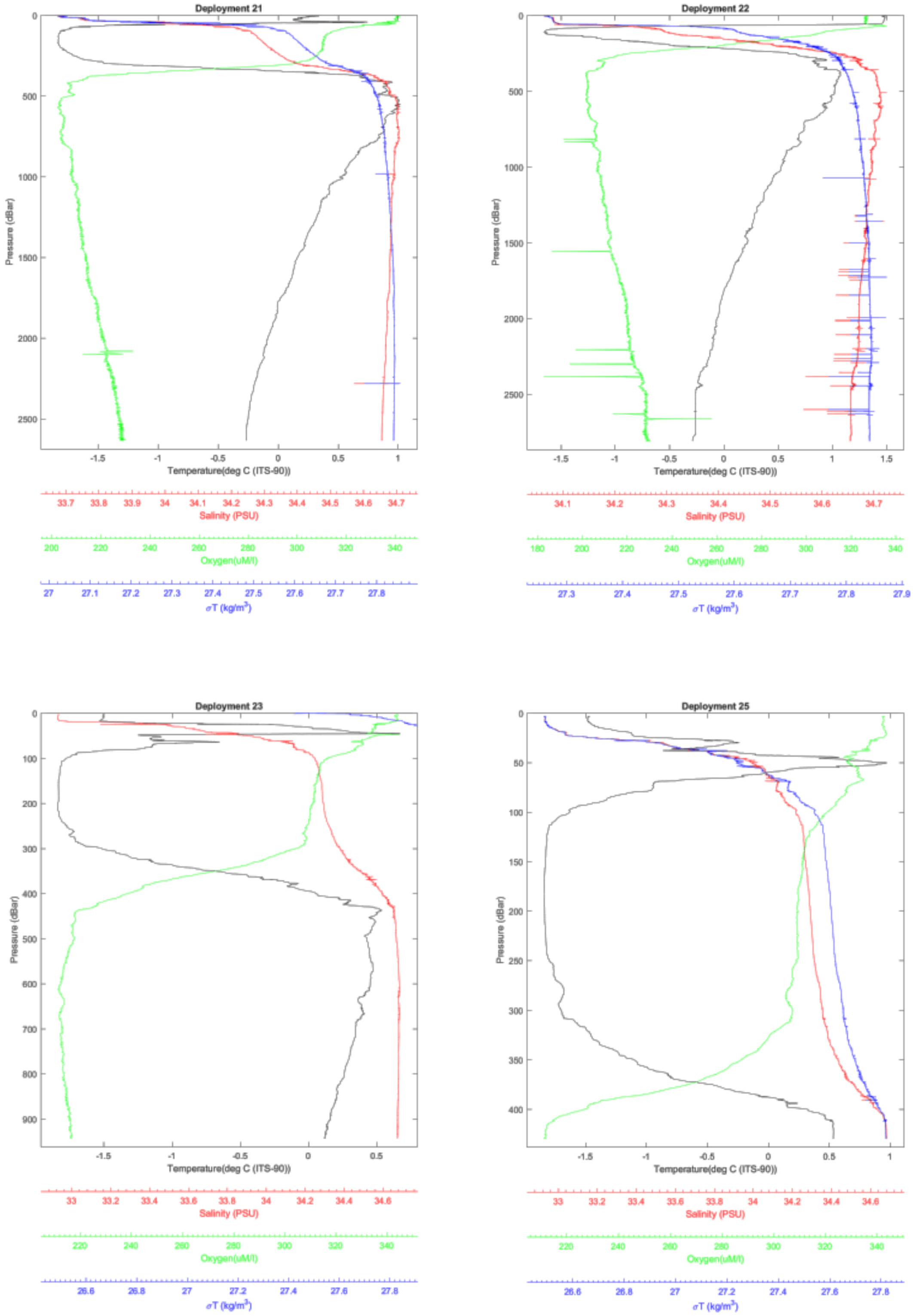

Figure 62 continued: Preliminary downward cast of CTD (unprocessed data) cast deployed during IN2017-V01. *Deployment locations shown in Figure 61.*

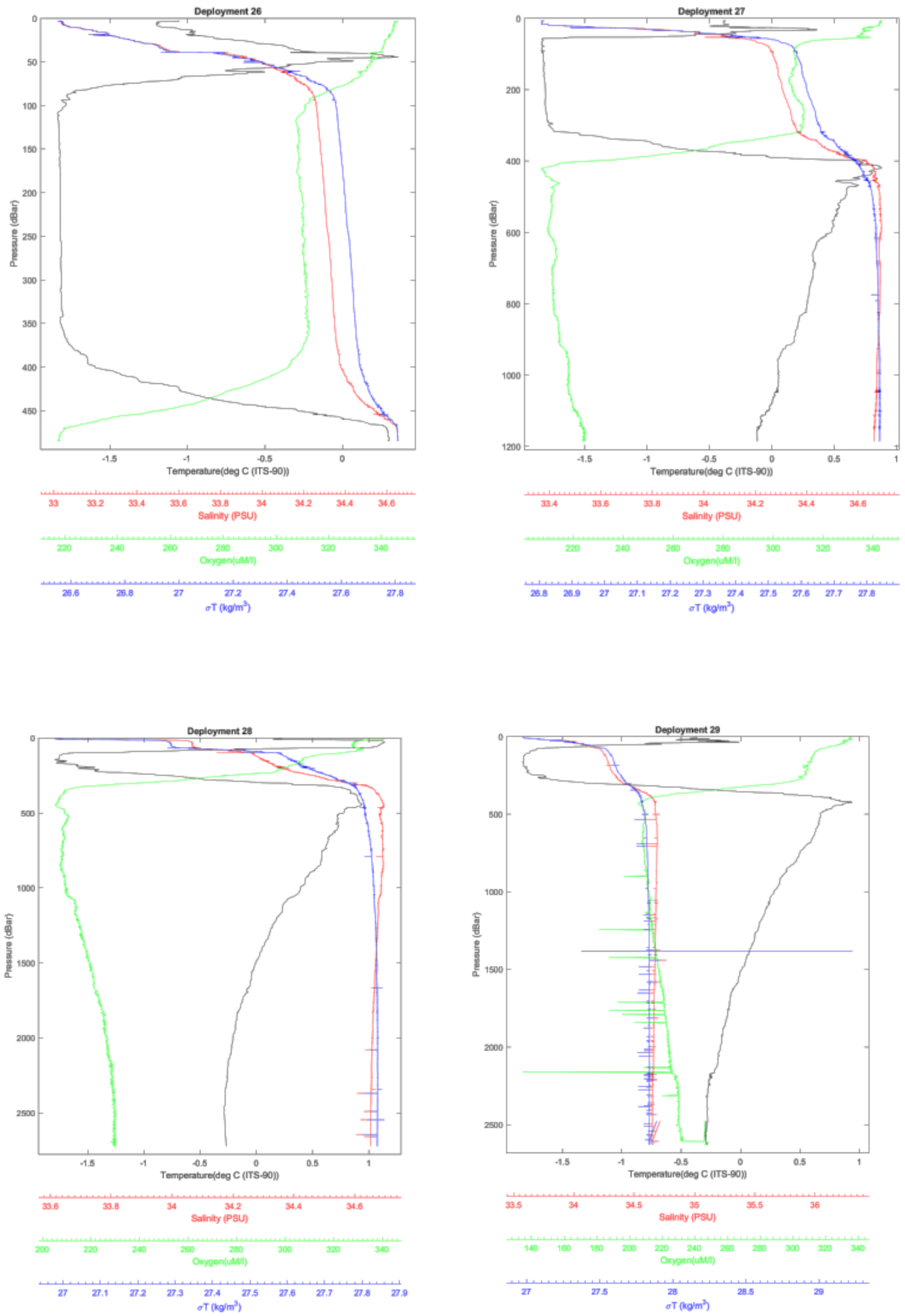

Figure 62 continued: Preliminary downward cast of CTD (unprocessed data) cast deployed during IN2017-V01. *Deployment locations shown in Figure 61.*

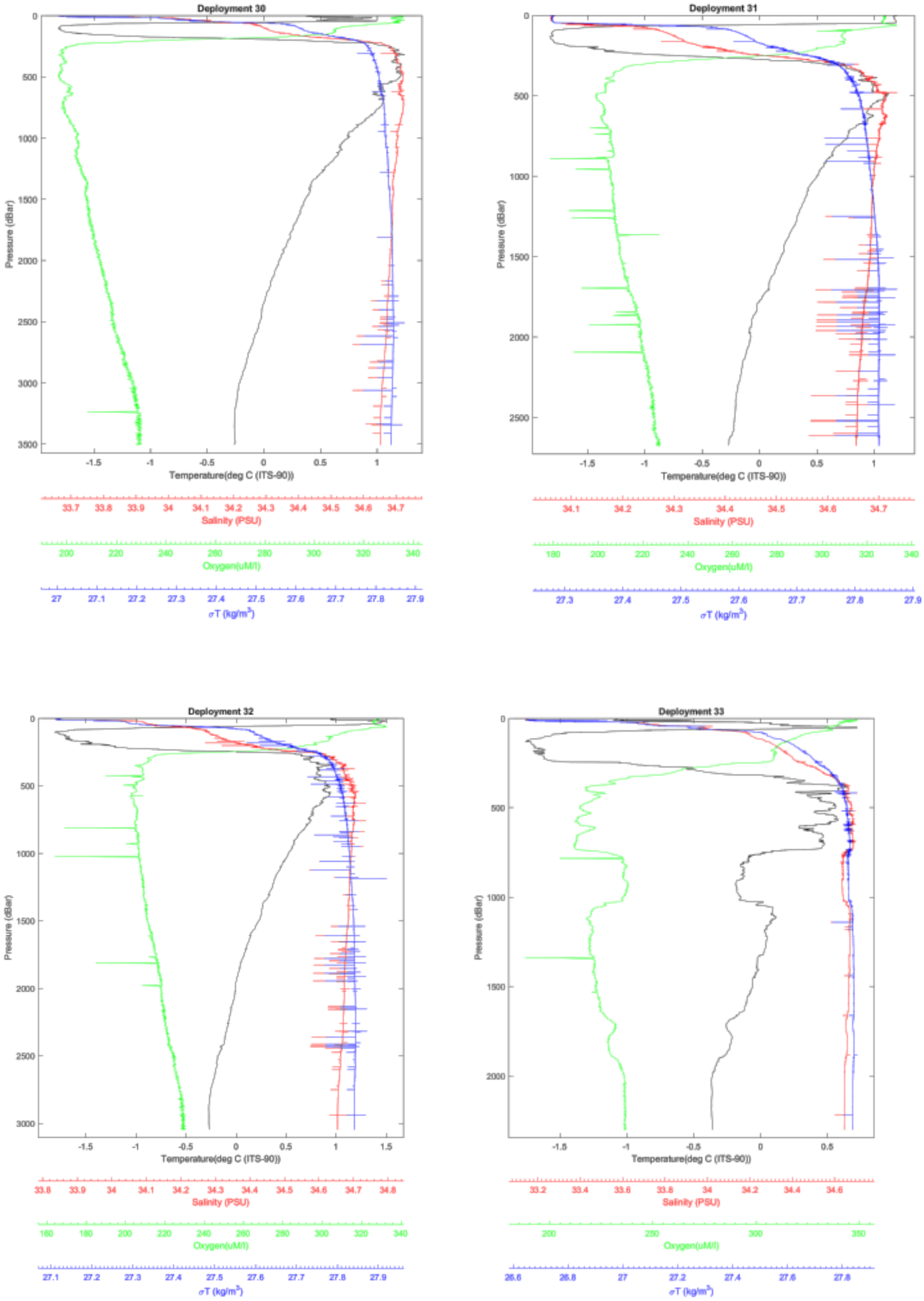

Figure 62 continued: Preliminary downward cast of CTD (unprocessed data) cast deployed during IN2017-V01. *Deployment locations shown in Figure 61.*

General Observations

In general, the upper water column shows warmer surface waters ~0.5 °C mixing with the coldest waters observed ~-1.4 °C in the upper 200 db. This lens of cold water has a lower conductivity than the waters lying above or below, therefore likely to result from Antarctic melt. Mixing between this cold fresh water and warmer mid-depth water mass general occurs around 400 db. In some CTD casts the signature of a slightly colder, more well ventilated water mass between 500 -700 db is present, after which the classical vertical structure is observed with temperatures decreasing down to 0.2 °C. The uncalibrated oxygen trend shows a slight increase with depth, while conductivity is largely constant (Fig. 63). The final CTD (CTD33) was our farthest east deployment, with the goal of assessing water mass characteristics to the east of the Dalton Ice Tongue. Sea-water temperatures for the Dalton polynya casts are plotted in Figure 64.

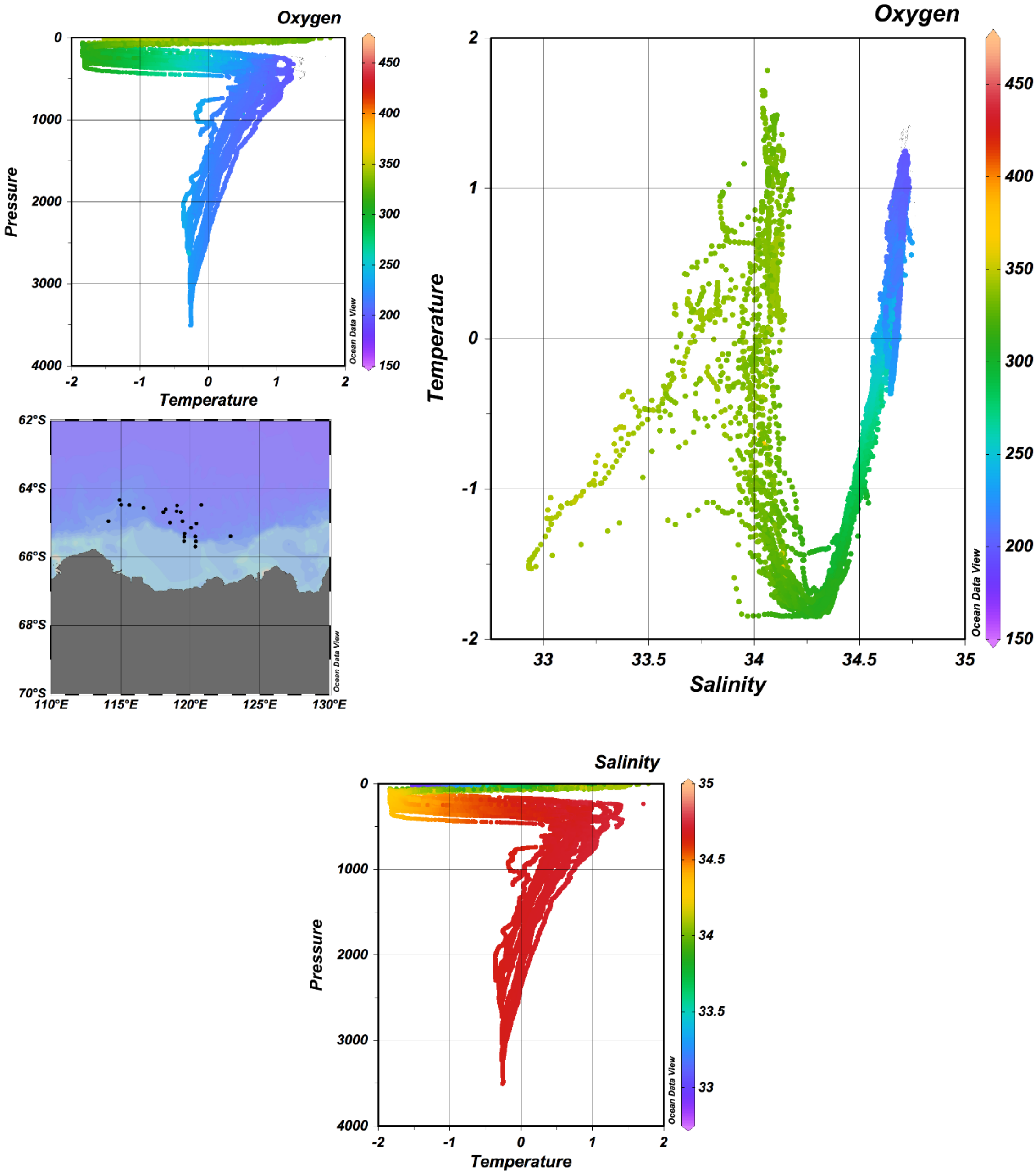

Figure 63. *From top left: Profile of temperature data from available CTD data and uncalibrated oxygen, cross-plot of temperature and salinity, map of the CTD sites, and temperature profile with salinity data.*

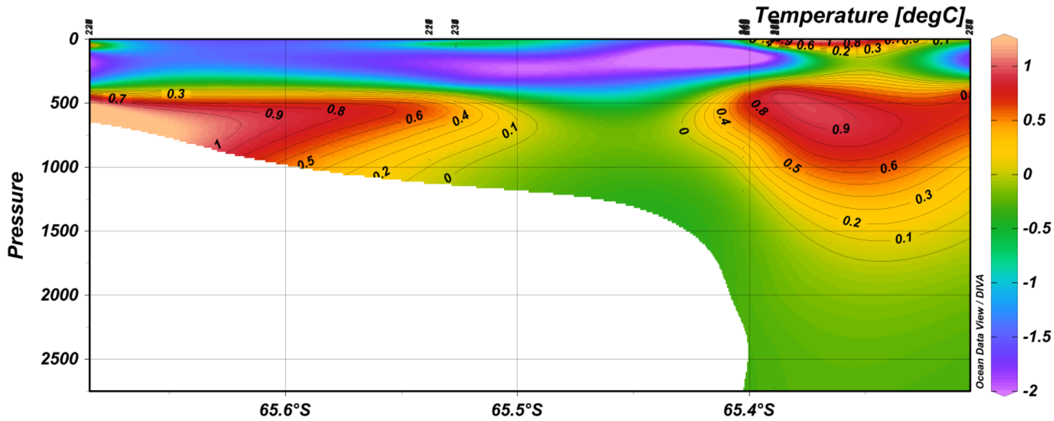

Figure 64. Cross section showing temperature change along a latitudinal gradient with depth (dbar) measured during the Dalton polynya casts.

Operations evaluation

Most CTD casts were successful, with data and seawater being acquired in the anticipated locations. There were a few technical issues, both concerning the CTD itself (e.g., instrument failure, frequently high numbers of spikes in sensor measurements, Fig. 65) and the door through which the CTD is operated. All issues were sufficiently resolved on board so that CTD casts could continue. Some CTD casts followed very quickly onto each other, which required very rapid water sample processing (filtrations) and setting up the CTD for the next cast.

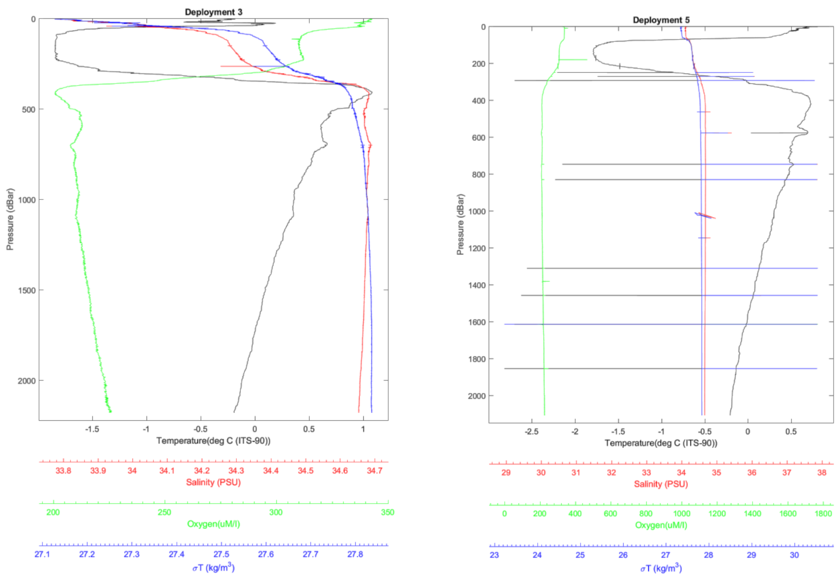

Figure 65. Deployment number 3 with minor spike and 5 with spikes during the entire deployment.

Summary

A total of 33 CTD casts were conducted during IN2017-V01, most of which were in 2000-3000 m depth or deeper. CTDs were primarily conducted at coring locations and along two cross-shelf / slope transects in the Dalton polynya to capture detailed changes in water masses with depth in this region. Downward real-time data from the water property sensors mounted on the CTD enabled the selection of adequate water sampling depths for hydro-chemical and biological purposes. Analyses to be conducted on the Niskin water will include detailed analyses of nutrients, dissolved oxygen, salinity, DNA, phytoplankton, chlorophyll *a*, flow cytometry and isotopes.

XBT

Equipment/Method

XBTs on the voyage were deployed using a Turo/QUOLL system. There were a total of 28 XBTs deployed during the course of the voyage: 24 Lockheed Martin Deep Blue XBTs, and 4 T5s. XBTs were deployed within the survey zone, frequently coinciding with seismic lines.

Table 16. Location of XBT deployments.

Date Time	Latitude (S)	Longitude (E)	XBT	Type	Type	Drop	Comment
20/01/2017 22:16	64 04.17	117 32.37	in2016_v06_002	Deep blue	1244598	OK	
20/01/2017 22:16	64 04.17	117 32.37	in2017_v06_001	Deep blue	1244597	OK	
21/01/2017 8:34	64 01.68	114 28	in2016_V06_003	Deep blue	1244565	OK	
23/01/2017 21:17	64 33.32	116 54.36	in2017_v01_001	Deep blue	1244573	OK	
24/01/2017 5:32	64 33.33	116 55.43	in2017_v01_002	Deep blue	1244569	OK	
29/01/2017 4:19	64 15.80	116 00.86	in2017_v01_003	Deep blue	1244574	Bad	
29/01/2017 4:24	64 15.81	116 01.58	in2017_v01_004	Deep blue	1244570	OK	
29/01/2017 7:25	64 15.86	116 23.97	in2017_v01_005	Deep blue	1244566	OK	Start of seismic line MCS-07B.
29/01/2017 9:03	64 15.96	116 37.1	in2017_v01_006	Deep blue	1244575	OK	
31/01/2017 22:34	63 56.15	120 13.93	in2017_v01_007	Deep blue	124457	OK	
	64 57.43	120 38.53	in2017_v01_008	Deep blue		OK	
3/02/2017 23:22	64 35.71	117 34.65	in2017_v01_009	Deep blue	1244572	OK	
4/02/2017 1:54	64 35.7	117 34.43	in2017_v01_010	Deep blue	1244568	OK	
4/02/2017 4:33	64 43.86	119 27.22	in2017_v01_011	Deep blue	1244576	OK	
4/02/2017 6:52	64 37.3	119 38.53	in2017_v01_012	Deep blue	1244556	OK	
6/02/2017 6:02	64 28.95	118 50.19	in2017_v01_013	Deep blue	1244560	Bad	
6/02/2017 6:06	64 28.98	118 50.12	in2017_v01_014	Deep blue	1244564	OK	Start of seismic line MCS-09B
6/02/2017 8:47	64 29.02	118 50.02	in2017_v01_015	Deep blue	1244569	OK	Middle MCS-09B.
6/02/2017 10:38	64 29.05	118 49.95	in2017_v01_016	Deep blue	1244559	OK	Middle seismic line MCS-09B.
14/02/2017 0:53	64 31.64	119 07.81	in2017_v01_017	Deep blue	1244555	OK	Start seismic line MCS-010
14/02/2017 4:58	64 37.40	119 37.56	in2017_v01_018	Deep blue	1244554	OK	Centre seismicline MCS-010B.
14/02/2017 7:08	64 40.5	119 53.69	in2017_v01_019	Deep blue	1244558	OK	Middle seismic line MCS-010B
14/02/2017 8:14	64 42.03	120 01.93	in2017_v01_020	Deep blue	1244562	OK	End seismic line MCS-010B.

18/02/2017 0:10	64 35.68	117 33.82	in2017_v01_021	Deep blue	1244553	OK	
18/02/2017 1:54	64 35.61	117 31.66	in2017_v01_022	T5	371945	OK	
24/02/2017 6:03	64 43.11	118 50.48	in2017_v01_023	T5	371941	OK	Start seismic line MCS012.
24/02/2017 6:59	64 42.11	118 43.61	in2017_v01_024	T5	371937	OK	Centre seismic line MCS012.
24/02/2017 9:26	64 39.71	118 28.54	in2017_v01_025	T5	371936	OK	End seismic line MCS012.

XBT profiles within the survey zone were relatively homogeneous, with profiles characteristic of polar waters.

Three XBTs at voyage commencement were mislabelled as originating from voyage in2016_v06. This was corrected, and numbers allocated to in2017_v01 from the fourth XBT on.

Operations evaluation
XBTs can experience thermal shock if taken from an internal ambient temperature to the sub-zero Antarctic temperatures they were asked to endure. This thermal shock manifested itself as spikes in the data, which render the data unusable. To prevent this, XBTs were taken to an external store and allowed to equilibrate to the weather for at least 12 hours prior to deployment.

SHIP ADCP - 75KHZ/150KHZ

Equipment/Method
Both permanently mounted shipboard ADCPs were operated for the duration of the voyage.

The ADCPs are RDI Teledyne Ocean Surveyor 75Khz and 150Khz models. Data acquisition is performed by the University of Hawaii’s UHDAS system. In2017_v01 is the first full voyage that UHDAS has been used – previous voyages have been operated using RDI’s VMDAS software. Remote support was provided by Jules Hummon from the University of Hawaii, who monitored data quality throughout the voyage.

Both transducers are located on the ship’s drop keels, which were lowered to approximately 8m below the waterline for the duration of the voyage.

Operations evaluation
Both ADCPs generally operated well throughout the voyage, with the following issues noted:

- Both ADCPs suffer from interference from the CTD wire during deployments. Unless a LADCP is installed on the CTD rosette frame, this has minimal impact on overall data coverage. A plan is in place to mitigate this in port by rotating the ADCP transducers so all four beams are clear of the CTD deployment area.

- Both ADCPs suffer from ringing in their top data bins. A plan is in place to resolve this in port by lining the ADCP wells with neoprene or similar noise absorbing material.

- More seriously the OS150 device appeared to stop functioning altogether just after the transit home (26-Feb). From interrogating the data, it appears that two beams on the transducer may have failed. Further investigation is needed, and potentially the instrument will need to be serviced by RDI.

- The new UHDAS software worked extremely well, and remote monitoring by on shore experts was highly beneficial.

Summary
Except for the issues noted above, the ADCPs performed well with good data coverage throughout the voyage, and complete coverage of the survey areas. The data will be processed on shore and published along with a report via the CSIRO Data Centre.

HYDROCHEMISTRY

Equipment/Method
Hydrochemical measurements included dissolved oxygen (DO), salinity and nutrients (silicate, phosphate, nitrate, nitrite, ammonia). For DO measurements, pre-numbered 140 mL iodine determination flasks were triple rinsed with sample water, filled bubble-free to the top of the flasks and 1 mL of 3M manganese (II) chloride and 1 ml of 4M sodium iodide + 8M sodium hydroxide solution were added to the water. The flasks were sealed air-tight with a stopper and Milli-Q around the flask necks. Samples were arranged in boxes excluding light in the Hydrochemistry lab and analysed within 48 hrs. Nutrient samples were collected in triple-rinsed 50 ml HDPE bottles and stored at 4°C (depending on whether analysis was conducted < or > 24 hrs after sampling, respectively). Salinity samples were collected in triple-rinsed pre-numbered 200 ml volume OSIL bottles made of type II glass (clear) with disposable plastic insert and plastic screw cap. Samples held in Salt Room (in Hydrochemistry lab) for 7-8 hrs to reach 22 °C before analysis.

Casts and Profiles
Hydrochemical sampling and measurements were conducted on CTD Niskin water of the same depth as biological sampling. Within the Dalton polynya, more sampling depths than for biological sampling were analysed (approximately in 200-500 m intervals). The latter sampling depths were decided on depending on the downward cast profile (in particular, changes in temperature) to capture changes in water masses with depth.

Nutrients
CSIRO Oceans and Atmosphere Hydrochemistry nutrient analysis is performed with a segmented flow auto-analyser (Seal AA3 HR) to measure silicate, phosphate, nitrite, nitrate plus nitrite (NOx), and ammonium.

Silicate analysis was based on a modified Armstrong et al. (1967) method. Silicate in seawater was reacted with acidified ammonium molybdate to produce silicomolybdic acid. Tartaric acid was added to remove the phosphate molybdic acid interference. Tin (II) chloride was then added to reduce the silicomolybdic acid to silicomolybdous acid and its absorbance measured at 660nm.

Phosphate analysis was based on the original Murphy and Riley (1962) method with some modifications developed at the NIOZ-SGNOS Practical Workshop 2012 optimising the antimony catalyst/phosphate ratio and the reduction of silicate interferences by pH. Phosphate in seawater forms a phosphomolybdenum complex with acidified ammonium molybate. It was then reduced by ascorbic acid and its absorbance measured at 880 nm.

Nitrate is determined by first reducing it to nitrite via a basic buffered copperised cadmium column before the colour reaction (Wood et al., 1967). Nitrite in seawater reacted with sulphanilamide under acidic conditions to form a diazo compound. This compound couples with 1-N-naphthly-ethylenediamine di-hydrochloride to produce a reddish purple azo complex and its absorbance is measured at 520 nm.

The ammonia method, developed by Roger Kérouel and Alain Aminot, IFREMER (1997 Mar.Chem.57), is based on the reaction of ammonium with orthophtaldialdehyde and sulfite at a pH of 9.0-9.5 producing an intensely fluorescent product. Its emission is measured at 460nm after excitation at 370nm.

Dissolved O_2
This is the current SCRIPPS method based on a whole-bottle modified-Winkler titration of Carpenter (1965) with modifications by Culberson et al (1991) using an Automated Photometric Oxygen system (accuracy 0.01 ml/L + 0.5%). Manganese chloride followed by alkaline iodide, was added to the sample, and the precipitated manganous hydroxide was distributed evenly throughout the bottle by shaking. At this stage, the dissolved oxygen oxidises an equivalent amount of Mn(II) to Mn(IV). The sample was then acidified, converting the Mn (IV) back to the divalent state liberating an amount of Iodine equivalent to the original dissolved oxygen content of the water. The Iodine was titrated with thiosulphate solution. The endpoint was determined by measuring changes in the UV absorption of the tri-iodide ion at 365 nm. The point at which there was no change in absorbance was the endpoint.

Before each run of samples, the thiosulphate concentration was determined by titrating of a 10 mL aliquot of standard potassium iodate primary standard. Similarly, a blank correction is determined from the difference between two consecutive titres for 1 mL aliquots of the same potassium iodate solution.

Salinity
Salinity was measured using a Guildline Autosal Laboratory Salinometer 8400(B) with nan accuracy of ± 0.001 salinity units.

Other
The same scheme of hydrochemical sampling was conducted for water from the trace metal free underway intake (see section 5.2 Intake water line), nutrient samples were kept at -20°C before the analysis and, except DO (as water was exposed to air before sampling) for multicore Niskin and bottom water (see section 3.4.3.4.2 Multicore water sampling).

Operations evaluation
Hydrochemical measurements were conducted prior to any other water sampling, which was not a problem as the CTD rosette was equipped with 24 Niskin bottles and a separate bottle could be assigned to hydrochemistry only in most instances.

Summary
A total of 250 nutrient, 240 salinity and 241 dissolved oxygen (DO) samples were analysed. These were based mainly on CTD cast (196-197), underway (44) and multicore (9) water. Final data will be made available via the online MNF/CSIRO Data Portal.

UNDERWAY MEASUREMENTS

The underway temperature and salinity are measured by an SBE21 thermosalinograph (:http://www.seabird.com/sbe21-seacat-thermosalinograph). This is calibrated in the CSIRO NATA (National Association of Testing Authorities) certified calibration laboratory in Battery Point to provide coefficients to use to calculate salinity and temperature based on the raw output from the sensor.

The salinity is calculated using the 1978 practical salinity scale which is documented in Seabird Application Note 14(: http://www.seabird.com/sites/default/files/documents/appnote14.pdf).

The salinity is further calibrated against the output of the SBE9/11 lowered CTD after the voyage as part of the underway data processing. This process will be documented in the processing report after it is released.

Temperature is calculated using the ITS-90 temperature scale which is documented in Seabird Application Note 42(: http://www.seabird.com/document/an42-its-90-temperature-scale).

Fluorescence is measured by a WETLbas WETStar Fluorometer (: http://www.seabird.com/wetstar). This measures the fluorescence of Chlorophyll-a but the instrument was uncalibrated as of in2017_v01 and the measurement in the underway data is just a percentage of the full-scale output of the instrument, i.e. 0 would be no fluorescence and 100 would be the maximum fluorescence the instrument can measure.

Therefore, the measured output from the instrument is not an exact measurement of chl, to co-relate the measurement from the instrument to the actual amount of chl in the underway seawater requires taking regular samples though out the voyage to calibrate the instrument. Samples were taken and are being processed at Macquarie University post-survey.

All underway data will go through a QA process before the final dataset is released by CSIRO. Data collected on the survey for the survey area are presented in Figures 66, 67 and 68.

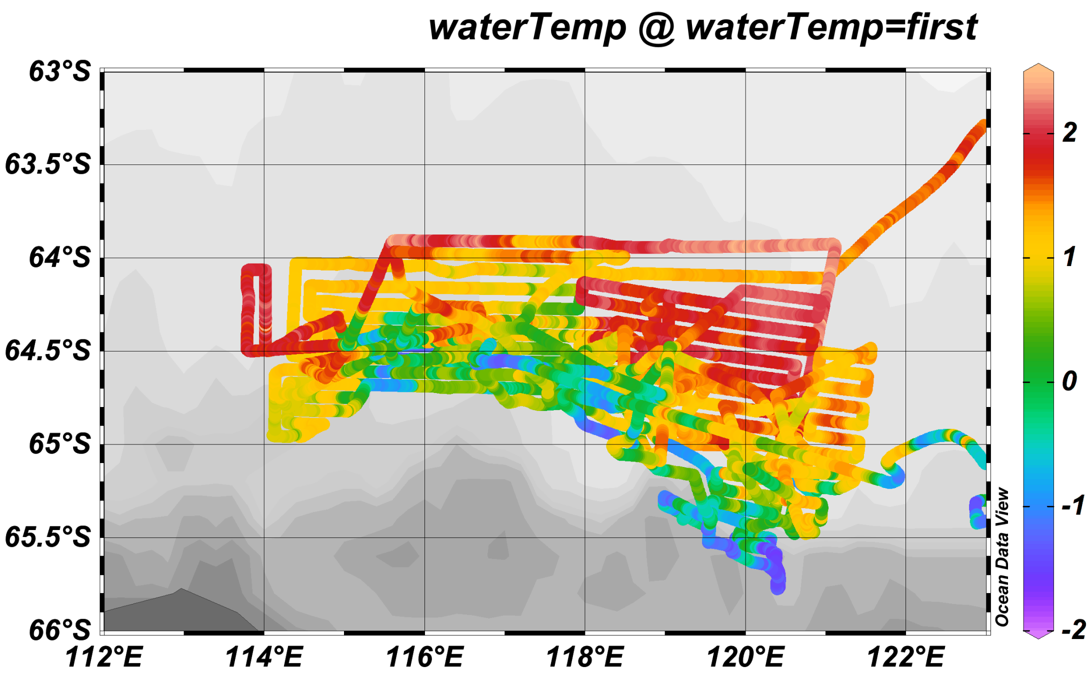

Figure 66. Underway water temperature plot.

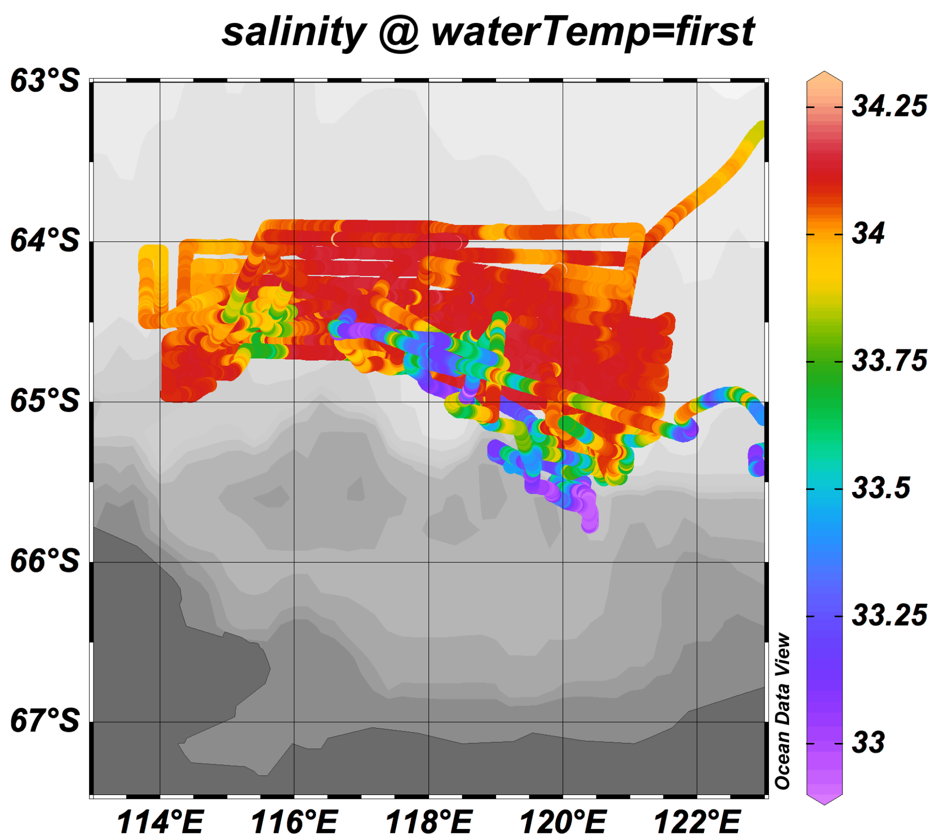

Figure 67. Underway salinity plot.

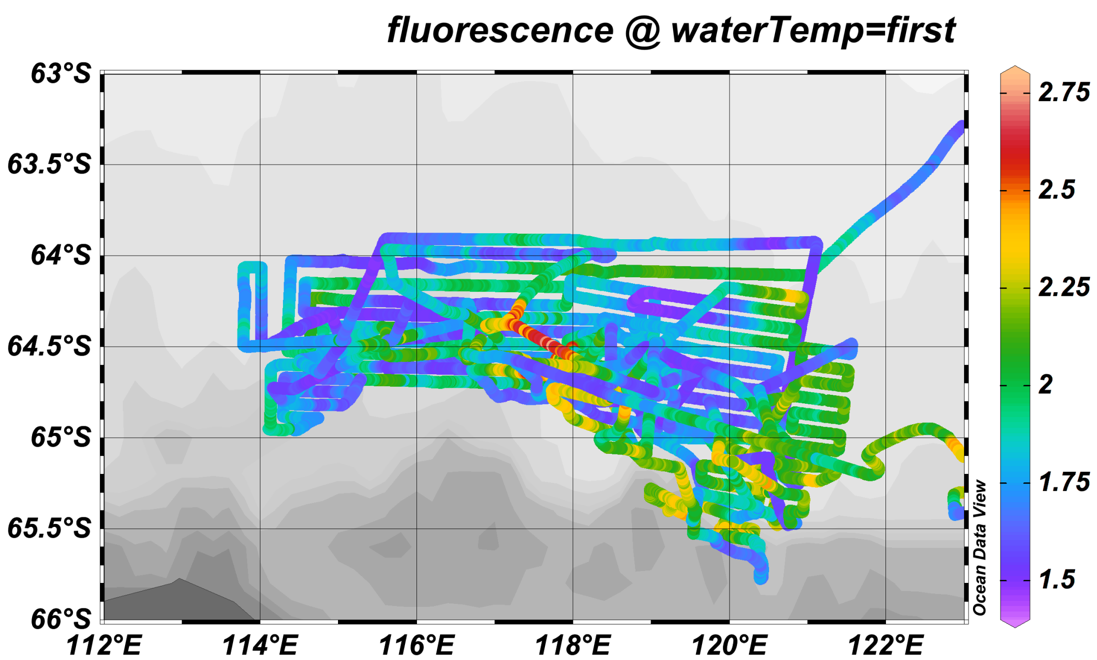

Figure 68. Underway fluorescence plot.

SEA-ICE SATELLITE OBSERVATIONS

Dr Jan Lieser

The Sabrina Seafloor Survey was supported by the Antarctic Gateway Partnership's Sea-Ice Service with mission-relevant sea-ice information in the form of satellite image data and expert analysis reports of sea-ice conditions. Images and reports were sent directly to the ship and available to the master and officers, as well as voyage management and the science party. Twenty-four reports were prepared while the ship was underway, which means that effectively an update on sea-ice conditions around the vessel was available every other day of the cruise (Appendix 8). Large scale sea-ice concentration charts were analysed in concert with visible image data from MODIS sensors on-board NASA's TERRA and AQUA spacecraft, as well as high-resolution Synthetic Aperture RADAR (SAR) data from ESA's Sentinel-1a and 1b satellites, where available. The synoptic interpretation of all available data sets with near-real time position data from the vessel was summarised in above mentioned reports, which enabled strategic decisions by all relevant parties at sea to select potential target areas of scientific interest with respect to current (and changing) sea-ice conditions.

While pan-Antarctic sea-ice extent and area were breaking new record low values almost daily, during the 2016/17 summer, the region between Law Dome and the Dalton Iceberg Tongue (the area of operation of the vessel) showed almost average sea-ice extent and considerably more sea ice compared to early 2016, when the Sabrina Coast was almost entirely free of sea ice. A more or less neutral sea-ice concentration anomaly established itself between 90 E and 130 E, during December 2016, while a strongly positive anomaly was found only centred around 140 E. The only other, albeit lower, positive sea-ice extent anomaly around Antarctica was only found along about 70 W, in the western Antarctic Peninsula.

SECTION 7. Marine Biology

PLANKTON NET

Method

A small plankton net of 30 µm mesh size was fitted within the mouth of a large plankton net with a 100 µm mesh size window within the cod end and 355 µm mesh size net (Figure 69). A 15-kg weight was attached to the bottom of the large net to keep it in position. After the first failed attempts to sink the small plankton net, a weight was attached to the collection bottle of the small net. The locations of the phytoplankton samples taken are illustrated in Figure 70 (location details in Appendices 6.2 and 1.1, 1.2, 1.4, and 1.5).

Figure 69. Plankton nets (30 and 100 µm).

Both nets were lowered together at a descend rate of 30 m/min, kept at 100 m depth for ~10 seconds and then brought back up at 20 – 30 m/min.

The volumes of the water samples were recorded. As the large net consistently retained lots of material, we recorded the volume before and after re-filtering through a 1000 µm sieve. The >1000 µm pellet was examined on-board for phytoplankton composition.

The material from the small net and the 1000 µm filtrate from the large net were processed for the following analyses:

- phytoplankton composition (~5 mL live samples plus all remaining material for on-board microscopy by A. Leventer and M. Duffy), filtered through a 22-mm diameter 0.45 µm HAWG gridded cellulose acetate filter, dried and mounted in immersion oil for microscopy
- phytoplankton abundance (~30 – 200 mL, Lugol's preservation for microscopy by Armand/Armbrecht),
- single cell isolations (5 mL live samples for on-board isolations by L. Armbrecht), Drawn out Pasteur pipettes were used to wash each cell by transferring it from a drop of sample to a drop of 0.22 µm filtered seawater, and then to another two drops of filtered seawater. Each cell was transferred into a separate well of a 98-well plate (Greiner Bio-One) filled with 20 µL F/2 media (made from 30 kDa filtered Antarctic (local) seawater and a nutrient stock provided by ANACC, CSIRO Hobart, Tasmania) and frozen at -80 °C.

Individual cells were also isolated and grown in 50 ml vented culture flasks (Corning®) with F/2 medium in an incubator at 1 or 4 °C under 25-50 µmol photons m^{-2} s^{-1} (depending of rather northern or southern origin of the isolates). At the end of the voyage cultures processed as follows: 1/3 of the culture was filtered onto GFF filters (Whatman) for HBI analysis (by S. Belt), 1/3 was concentrated by centrifugation, preserved in 4%, pH7 formaldehyde and kept at 4°C for spectroscopy analysis (by P. Heraud), 1/3 was filtered onto polycarbonate filters stored in 15 mL Falcon tubes at -80 °C for molecular analysis of HBI genes (by C. Bowler). Triplicates of one cell per culture were isolated for single cell genomics (by L. Armbrecht and M. Ostrowski).

- Planktonic foraminifer preservation (5 mL, frozen at -80 °C for analysis by W. Majeski),
- HBI analysis (~20 mL on a GF/F filter paper, and 2-5 mL stock, frozen at -80 °C for analysis by S. Belt),
- planktonic radiolarian analysis (re-sieved through a 63 µm net and permanent slide preparation by K. Lawler).

All samples that will be taken back to shore were photographed. A full record of samples taken can be found in the Armbrecht, Leventer and Lawler Quarantine records (Appendices 1.1, 1.2).

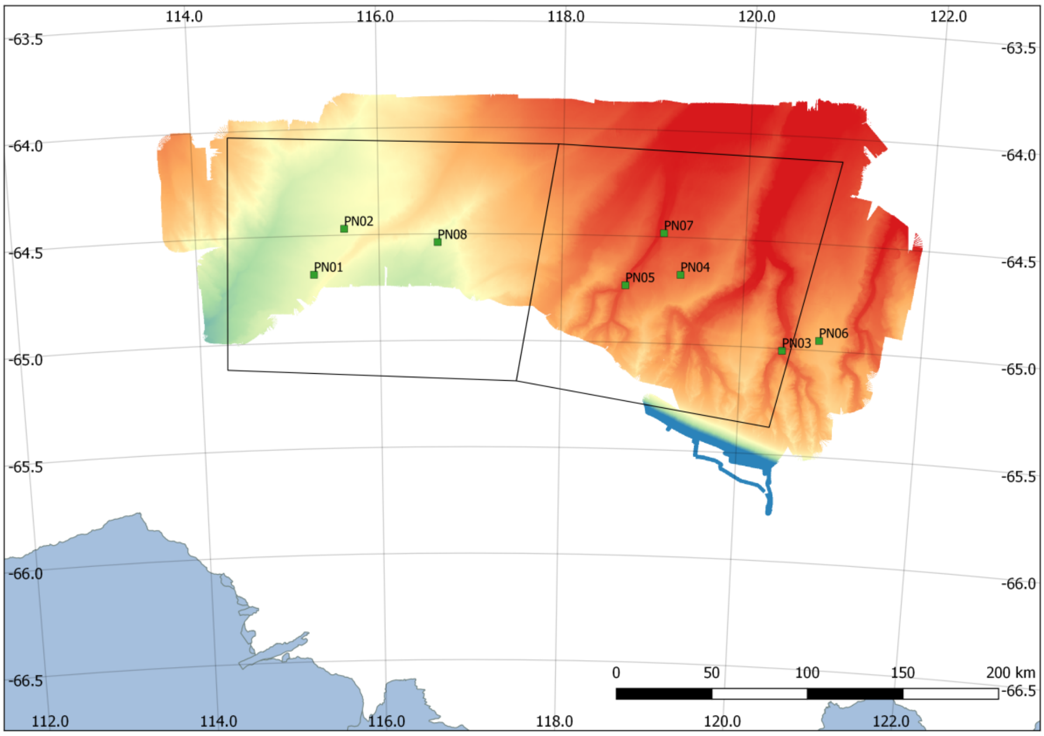

Figure 70. Map showing plankton net sampling sites in and next to the survey areas A and C. *Created in qgis by Kelly-Anne Lawler, March 2017.*

Preliminary Results

i Phytoplankton composition

Preliminary on-board microscopy at 400x magnification was conducted on both the 30 µm mesh size and 100 µm mesh size samples. In every sample, *Chaetoceros criophilus* and *Corethron pennatum* dominate the samples, likely due to their large size and the presence of long setae and spines, facilitating entanglement in the nets. Other diatoms commonly observed include *Rhizosolenia spp*., *Proboscia spp*. and chains of *Fragilariopsis*. Seawater samples taken from the uncontaminated seawater line at the same time as the plankton tows had much higher relative abundances of tiny *Fragilariopsis* (*F. cylindrus* and/or *F. pseudonana*), indicating that these small species are under-sampled via plankton tows.

We observed a difference in the planktonic material retained by the 30 and the 100 µm net (especially PN06-PN08), as in that the 30 µm net seemed to sample was more species-rich than the 100 µm sample, which mainly consisted of *Chaetoceros criophilus* and *Corethron* *pennatum*. In addition to these two species we observed *Thalassiothrix*, *Codonellopsis gaussi,* dinoflagellates, silicoflagellates, and pennate diatoms.

ii. Microscopy analyses will be conducted at Macquarie University by L. Armand and/or L. Armbrecht.

iii. A total of 126 single cells were isolated for single cell genomics under an inverted microscope. The single cells were mainly diatoms potentially producing highly-branched isoprenoids (HBI's, a sea-ice proxy), abundant dinoflagellates, tintinnids and unidentified organisms. A list of species including a photo of each isolated individual is given in Appendix 6.3.

Of a total of 57 attempted cultures, 15 cultures grew fast enough for on-board processing. These include the diatoms *Fragilariopsis* spp. (six cultures), *Pseudo-nitzschia* spp. (three cultures), *Nitzschia* sp. (one culture), *Odontella* sp. (two cultures), and *Navicula* sp. (one culture). Triplicate single cells isolated from these cultures are shown in Appendix 6.3 (marked by a "C" and culture ID number preceding the species name).

iv-v. All analyses will be conducted on land by the above indicated researchers. Foraminifer samples were taken in order to enable comparisons to sediment surface assemblages. Plankton net samples for HBI analyses are complementary to HBI samples taken from the underway intake and will provide new information on the distribution and concentration of this sea-ice proxy in the Sabrina coast region.

vi. Permanent slides were created from samples from plankton nets PN06, PN07 and PN08 for radiolarian analysis. No quantitative analysis was conducted, however it was found that only one radiolarian specimen was found in both PN06 and PN08, while PN07 contained multiple specimens of more than twenty different radiolarian species (See Appendices 6.4 and 1.4).

All samples taken back to the laboratory were photographed. A full record of samples taken can be found in the Appendices 6 and 1.1, 1.2, 1.4 and 1.4.

Operations evaluation

Figure 71. Re-sieving of 100µm plankton net sample.

Plankton nets were relatively easy to deploy, usually only took about 20 minutes to a depth of 100 m and retained a lot of material. This is of particular advantage to the HBI-analyses, which rely on high sample material. The first deployments required some testing of the 'double-net' approach, however, after attaching weights to both nets no entanglements occurred and both nets brought up concentrated plankton material.

The difference in phytoplankton composition between the 30 and 100 µm net sample might be due to the different mesh sizes but could also result from the re-sieving of the 100 µm net sample through a 1000 µm sieve, retaining a large pellet (Fig. 71). The sieved sample and the pellet were kept and processed by A. Leventer and M. Duffy and future analysis might provide more clarity in this regard.

Summary

A total of eight plankton net deployments were conducted, using a 'double-net' approach by simultaneously using a 30 µm and a 100 µm mesh size plankton net. Seven deployments were made to 100 m, and one deployment to 350m depth. After weights were attached to both nets and prevented entanglement, the nets brought up high amounts of plankton material.

Preliminary results suggested differences in plankton communities in the 30 and 100 µm samples, however, *Chaetoceros criophilus* and *Corethron pennatum* seemed to dominate communities at all locations. A total of 126 single cells were isolated, providing a unique data set for single cell genomics on Antarctic phytoplankton. Additionally, 15 cultures were grown from potentially HBI-producing diatoms and processed for a suite of targeted HBI-analyses on single species. Detailed future analyses of preserved material are anticipated for microscopy by A. Leventer, M. Duffy, L. Armbrecht, K. Lawler and L. Armand, for HBI analyses by S. Belt, and for foraminifer composition by W. Majewski.

INTAKE WATER LINE (GEAR AND METHODS)

Method

Samples were collected from the underway (UW) seawater intake (~9 m depth) during the transit and in both survey areas (Fig. 72, 73). During the transit the main idea was to sample at every degree of latitude until reaching the survey area. Except for some missing samples at the beginning of the transit, from 50° S and southward, every degree of latitude was sampled.

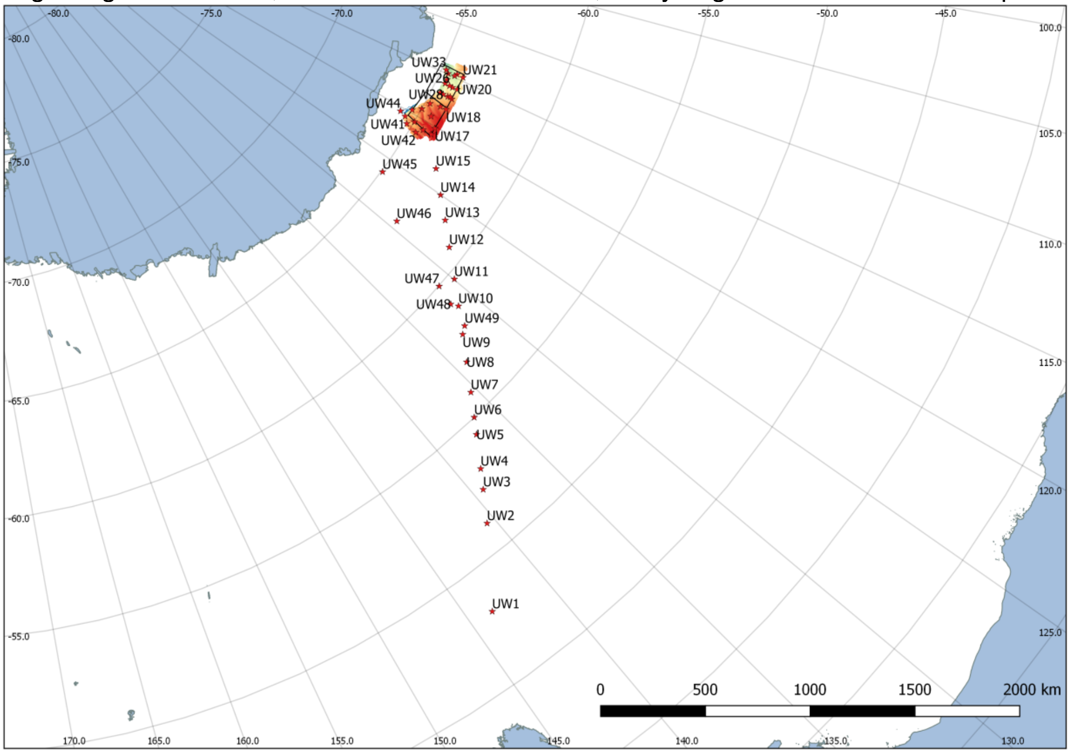

Figure 72. Map of the underway (UW) sampling locations on the N-S-N transect and in the survey area. *Created in qgis by Kelly-Anne Lawler, March 2017.*

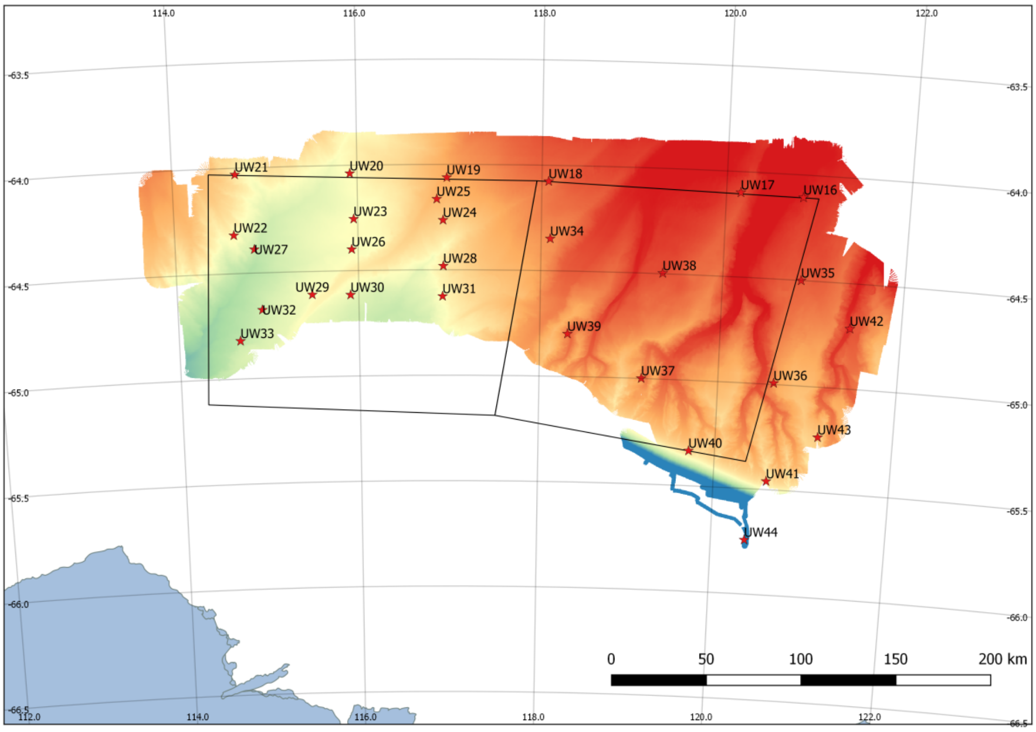

Figure 73. Map showing the underway (UW) sampling grid in and next to the survey areas A and C. *Created in qgis by Kelly-Anne Lawler, March 2017.*

At all UW locations samples were taken for the following analyses:

1. Hydrochemistry
2. Chlorophyll *a*
3. phytoplankton abundance (Lugol's preservation)
4. phytoplankton composition (microscope slides)
5. DNA
6. flow cytometry
7. virus (almost all)
8. HBI analyses
9. single cell isolations
10. dilution experiment (UW6)

A detailed record of the samples taken and volumes used was kept in a paper log sheet, an excel log sheet (Appendix 1.4) and the *Investigator* E-log. All samples that will be transported back to the lab were photographed. A more detailed description of the individual sample types is given in the following description sections.

Figure 74. Underway seawater lab sampling set-up. *From top left to bottom right: 25 µm plankton net; 3-head Watson and Marlow peristaltic pump used for DNA, HBI filtration; vacuum pump for Chlorophyll, phytoplankton; Watson and Marlow peristaltic pump with a 142mm filter holder.*

Hydrochemistry
Hydrochemical sampling has been undertaken for all UW samples and included: dissolved oxygen (DO), salinity, temperature, nutrients (NOX, nitrate, ammonia and phosphate).

Chlorophyll a
Water samples of 1 L were filtered onto 25 mm GF/F filter papers (Whatman) under darkened conditions, using a vacuum pump. Filter papers were folded in half, wrapped in aluminium foil and frozen at -80 °C until further analysis
Extractions of the first 23 were conducted following (Jeffrey and Humphrey, 1975), with slight modifications to enable on-board extractions. The filter papers were cut into six pieces, placed in a 15-mL centrifugation tube (Falcon), covered with 3 mL 100% Acetone (HPLC grade, Sigma Aldrich), shaken vigorously and kept in the dark at 4°C for at least 15 h. Then, 200 µL Milli-Q were added, followed by 1 mL 90% Acetone. The extract volume was recorded, 1.5 mL of the extract transferred into a 1.5 mL centrifugation tube (Eppendorff) and centrifuged for at least 5 min. at 7,000 rpm. The supernatant was transferred into a 1 cm cuvette and absorption was measured in a spectrophotometer at 750, 664, 647 and 630 nm. Chl a was calculated using:

$$[\text{chl-}a] \text{ in sample} = [((11.85*(A664-A750))/l) – ((1.54*(A647-A750))/l) – ((0.08*(A630-A750))/l)] * (V_{EXT}/V_{FILT})$$

With l being the path length of the measurement cell (cuvette = 1 cm), V_{EXT} the volume of the extract being measured, and V_{FILT} the volume of sample filtered (1L) (Jeffrey and Humphrey, 1975).

Phytoplankton abundance
Water samples of 1 L were filtered onto 25 mm SSWP filter papers (Millipore), transferred into a sterile 5 mL tube and covered with 5 mL 0.2 µm filtered seawater and 15 drops of Lugol's solution. After using all SSWP filter papers, 200 mL were collected in brown glass amber bottles and preserved with 8 mL Lugol's solution (final concentration 4%).

Phytoplankton composition
Underway water samples of 500 mL were filtered onto 25 mm HAWG 0.45 µm filter papers (Millipore) and transferred into a small petri dish. The filter papers were allowed to dry for 24 hours, then were mounted on top of a few drops of immersion oil on a microscope slide, allowed to dry for another 24 hours, covered with another 2 drops of immersion oil, and then covered by a 25-mm square coverslip. This process results in clarification of the filter and results in a filter that can be analysed for phytoplankton composition at 1000X. Assemblages were evaluated in a preliminary fashion on board, at 400X. The same procedure was used for CTD samples, using 2 L of water from each observed depth.

Phytoplankton composition also was observed by sieving water from the uncontaminated seawater system through a 20-micron mesh screen, for a period of 5 minutes. The collected material was pipetted into a Sedgewick Rafter Counting Cell and observed immediately on the inverted microscope at 400X. In addition to qualitative observations (Appendix 6.2), photographs were used to document the microflora and fauna. Species identifications were documented on a pdf on the science drive, sample data, IN2017_V01_Diatom_Photos_Meghan_Duffy.

DNA (Bacteria and Eukaryotic)
Microbial communities represent 90% of the ocean's biomass including bacteria, archaea and small eukaryote. They play a crucial role in the ocean ecosystem as they are at the basis of the marine food web, involved in all marine biogeochemical cycles from carbon fixation to sulphur degradation. Understanding their distribution and the role that environmental variables play in influencing on their abundance is crucial in order to model their distribution with future climate change.

Water samples of 2 – 4 L were filtered through a Sterivex filter (Millipore) 0.22 µm cut off, using a peristaltic pump (Watson and Marlow) set to 110 rpm. After the filtration, the two tube-adapters were sealed with parafilm and the Sterivex frozen at -80 °C after filtration.
DNA samples collected from the transit from Hobart until the beginning of the survey area will be analysed for bacteria and eukaryotic communities by Swalison Swan and Dr. Levente Bodrossy at CSIRO,Hobart, with the focus on understanding the changing in the bacteria communities in the Southern Ocean in relation with a physical and chemical gradient.

Samples collected within the survey area were be shipped on dry ice to Macquarie University, where the DNA will be extracted by A. Focardi and the 16s and 18s region will be sequenced within one year to understand the microbial (pro- and eukaryotic, respectively) community composition (Appendix 1.4).

Flow Cytometry
Water samples of 2 mL were fixed with 0.1 % Paraformaldehyde in a 2 or 5 mL Cryovial tube (Corning), frozen in liquid nitrogen for 15 min. and then transferred in -80 °C. Those samples will be analysed to understand the abundance of viruses, picocyanobacteria, small picoplankton and heterotrophic bacteria in different water masses.

Viriome composition
Seawater was collected each time to study the composition and distribution of the Southern Ocean Viriome. Accounting for the highest abundance in the marine environments viruses have a considerable influence on the ecology and the biogeochemical cycles of the ocean. Viral–induced mortality can influence the flux of nutrient in the oceanic microbial food webs and alter the species composition through horizontal genes transfer.

Briefly 15 L of seawater were filtered through a PES 0,22 µm filter (Millipore) using a peristaltic pump (Watson and Marlow) set at 30 rpm and equipped with a Gelman science filter holder (Fig. 75). Water for the last 11 samples was pre-filtered with a 0.22 µm Sterivex using a peristaltic pump (110 rpm). Samples were then incubated at room temperature for 1 hour with Iron Chloride 0.01 % following John et al. (2011) and filtered again through a Polycarbonate 0.8 µm filter (Millipore) to recover viral communities. Filters were stored in a 50-mL centrifugation tube sealed with parafilm and kept at 4 °C until further analysis on shore (Appendix 1.4).

Dilution Experiment
The aim of the dilution experiment is to determine the daily rates of picoplankton mortality by grazing and viral infection. To better model the influx for primary production, 15 L of seawater were collected and divided into 2 carboys. Seven litres were filtered through a sterivex 0,22 µm filter (Millipore). The other 7 L were filtered through a 60 µm mesh. Three and a half litres of filtered seawater (0.2 µm) was added to different concentration of 60 µm filtered seawater from surface to decrease the probability of encounter between prey and predator as per the Landry Protocol (Landry et al., 1995; Worden and Binder 2003). The other 3.5 L were filtered again using a 30 kDa cutoff cassette to remove viruses, and then added to 60 µm filtered water as before. Experiments were performed in 500 mL bottles and run in triplicate. 2 mL of each sample were collected at time zero and after 24 h followed an on-deck incubation and cryopreserved for subsequent analysis.

Experiments were performed in 500 mL bottles and run in triplicate. Of each sample, 2mL were collected at time zero and after 24h on-deck incubation, where incident light was measured as the one at surface water and temperature was maintained equal to seawater temperature thanks to a continuously running of seawater. Sample were then flash frozen in liquid nitrogen and cryopreserved at -80°C for later analysis. Between experiments bottles were washed with 3% hydrochloric acid and then rinsed 3 times with milliQ water.

Samples will be shipped in dry ice to Macquarie University and analysed by A. Focardi using flow cytometry before August 2017. The aim is to understand the impact of virus infection and organisms grazing on picoplankton, to better model the nutrient influx for primary production. Especially in Antarctic waters viruses are thought to be the primary mortality cause for pico eukaryotic organisms, which in turn are responsible for the majority of primary production. The rates of grazing and viral infection will be inferred through a regression analysis of the instantaneous growth of each single groups calculated over 24 hours and the relative dilution applied.

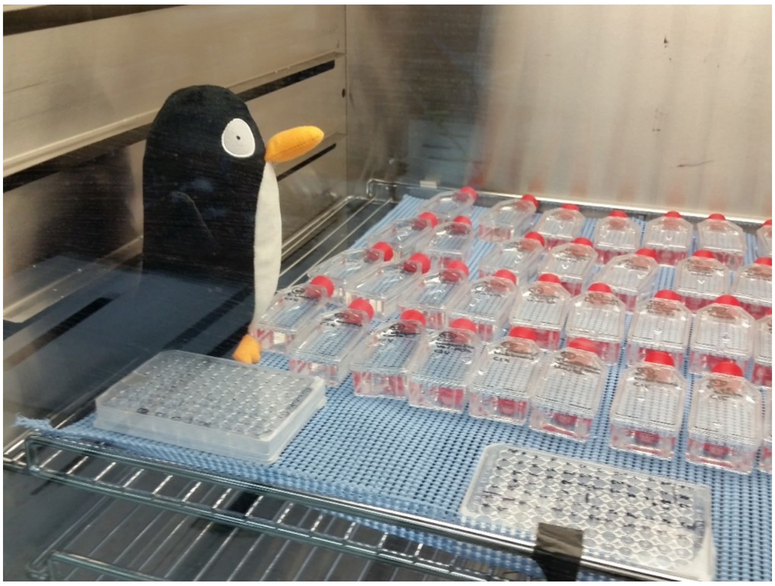

Figure 75. Samples in the Incubator.

Highly branched isoprenoids (HBIs)
Water samples of 2-4 L were filtered onto 25 mm GF/F (Whatman) filter papers, folded in half, wrapped in aluminium foil and frozen at -80 °C. Additionally, a 25 µm plankton net was attached to the seawater intake tap for 10 minutes. The sample was concentrated to ~20 mL of which 2 mL were transferred into a centrifugation tube (Eppendorff) tube and frozen at -80 °C. The remaining ~18 mL were kept in the fridge and used to isolate single cells. The aim of HBI

analysis from the underway intake will be to determine the distribution and concentration of diatom-produced HBI's, which act as a sea-ice proxy (analysis to be undertaken by S. Belt, complementary to HBI sampling from Plankton nets).

Single cell isolation
About 18 mL concentrated sample from the 25 µm plankton net that was attached to the underway seawater line were used to isolate single cells. Isolation was conducted, using drawn-out Pasteur pipettes, under an inverted microscope (Olympus IMT-2). Each cell was washed on a microscope slide by transferring it from a drop of sample to a drop of 0.22 µm filtered seawater, and then to another two drops of filtered seawater. Subsequently each cell was transferred into a separate well of a 98-well plate (Greiner Bio-One) filled with F/2 media made from 30 kDa filtered Antarctic (local) seawater and a nutrient stock provided by ANACC, CSIRO Hobart, Tasmania. Cultures were kept at 1 °C and 20 µm photons m^{-2} s^{-1} or at 4 °C under 50 µm photons m^{-2} s^{-1}, depending on isolation location (survey areas A/C or transit, respectively).

A strong focus was placed on species that are assumed to produce highly branched isoprenoids (HBIs). Good growing clones of the isolates were cultured and, at the end of the voyage, processed as follows:

- 1/3 of the culture was filtered onto GFF filters for HBI analysis (Belt),
- 1/3 was concentrated by centrifugation and preserved in 4 % formaldehyde kept at 4 °C for spectroscopy analysis (Heraud),
- 1/3 was filtered onto polycarbonate filters for molecular analysis of HBI genes (Bowler),
- 1 mL was kept for experimental in-vitro analysis of HBI pathways (Beardall), and
- one cell was isolated for single cell genomics (Ostrowski).

For the latter purpose, we also isolated individual cells from seawater directly without culturing. For detailed sample listings refer to Appendices 1.4 and 1.5. Sites sampled in addition to underway and plankton net samples are listed in Table 17.

Table 17. Cell isolation (CI) locations during IN2017_V01, in addition to underway and plankton net sampling locations.

Cell isolation ID	Date (UTC)	Latitude (°S)	Longitude (°E)
CI1	19.01.2017	60 35.81	128 24.32
CI2	20.01.2017	63 31.86	122 31.15
CI3	20.01.2017	64 06.32	120 40.27
CI4	12.02.2017	64 42.74	117 43.05
CI5	17.02.2017	65 28.23	120 51.30

Preliminary Results

Hydrochemistry
All Hydrochemistry data will be made available via the MNF/CSIRO data portal once finalized.

Chlorophyll a (Chl a)
113 samples were collected for Chl *a*, we extracted and measure just the first 23 samples because we encountered difficulties with the absorbance measurements, e.g. negative absorbance readings (See Table 18). These unrealistic reading might be due to the sensitivity of the spectrophotometer on a moving vessel or as extraction time being too short. It was decided to complete the Chl *a* extraction and measurements at Macquarie University.

Table 18. Chlorophyll a readings for underway samples.

Underway samples	ug/L
1	1,305144
2	-1,963752
3	2,513116
4	0,965448
5	-0,634164
6	3,8557
7	0
8	27,399248
9	0,025008
10	-3,26436
11	8,37006
12	0
13	28,181604
14	0,58186
16	3,289892
20	1,104016
20	-2,184396
21	0,285024
22	0,60638

Phytoplankton composition
During transit, the diatom assemblage, as expected, varied with water temperature. From about 52-58° S, water temperature averaged 6 °C; the flora was diverse, with contributions from larger species of *Chaetoceros*, *Rhizosolenia*, *Proboscia*, *Fragilariopsis kerguelensis* and *Pseudonitzschia*. In addition, we observed many species of dinoflagellates and larval stages of zooplankton.

From 58-62° S, water temperatures cooled, from 6 °C down to 2 °C, and the waters are distinguished by a change in diatom assemblage, to one dominated by long chains of *F. kerguelensis* and small (<15-micron) unidentified centrics. Within this zone, the contribution of small centric diatoms decreased southward with a proportionally increased contribution of the sea ice associated *Fragilariopsis*.

Finally, south of 62° S, sea ice *Fragilariopsis* were generally most abundant, particularly the tiny forms, *F. cylindrus* and *F. pseudonana*, which were very difficult to distinguish in girdle view. Other common *Fragilariopsis* include *F. curta*, *F. separanda* and *F. rhombica*. However, the floral assemblage patterns are complex, with some sites are co-dominated by *Chaetoceros criophilus* and others by *Corethron pennatum*. Due to their large size, these species potentially contribute significantly to silica and carbon cycling. Other common species include: *Corethron inerme*, *Guinardia cylindrus* and *G. tubiformis*, *Dactyliosolen*, *Proboscia inermis* and *P. truncata*, and several species of *Rhizosolenia*.

In addition to the diatoms, we observed low abundances of the silicoflagellate *Dichtyocha speculum*, tintinnids, dinoflagellates, rare pteropods (*Limacina helicina antarctica*) and rare foraminifera. The diatom *Fragilariopsis pseudonana* was often observed attached to the tintinnids in the polar waters south of 64° S. While many of the forams are the planktonic species *Neogloboquadrina pachyderma*, we have also observed a variety of biserial planktic species. Forams were observed at 64° S between 114° E and 129° E with only one sieve sample at 117° 14' E containing more than a few specimens.
For complete listing refer to Appendix 6.2.

From CTD samples, initial microscopic observations document a diatom assemblage that is dominated by sea ice associated *Fragilariopsis*, *Chaetoceros criophilus* and *Corethron pennatum* in the surface waters (Fig. 76). The deeper water samples collected during CTD casts show increasing abundance of the diatom *F. kerguelensis*, silicoflagellates, chrysophyte cysts, and single cells of *Phaeocystis*. Deeper chlorophyll maxima also have higher concentrations of *Chaetoceros* resting spores. The near absence of their vegetative counterparts suggests that these are the sinking remnants of phytoplankton that bloomed prior to our cruise, as the ice initially retreated.

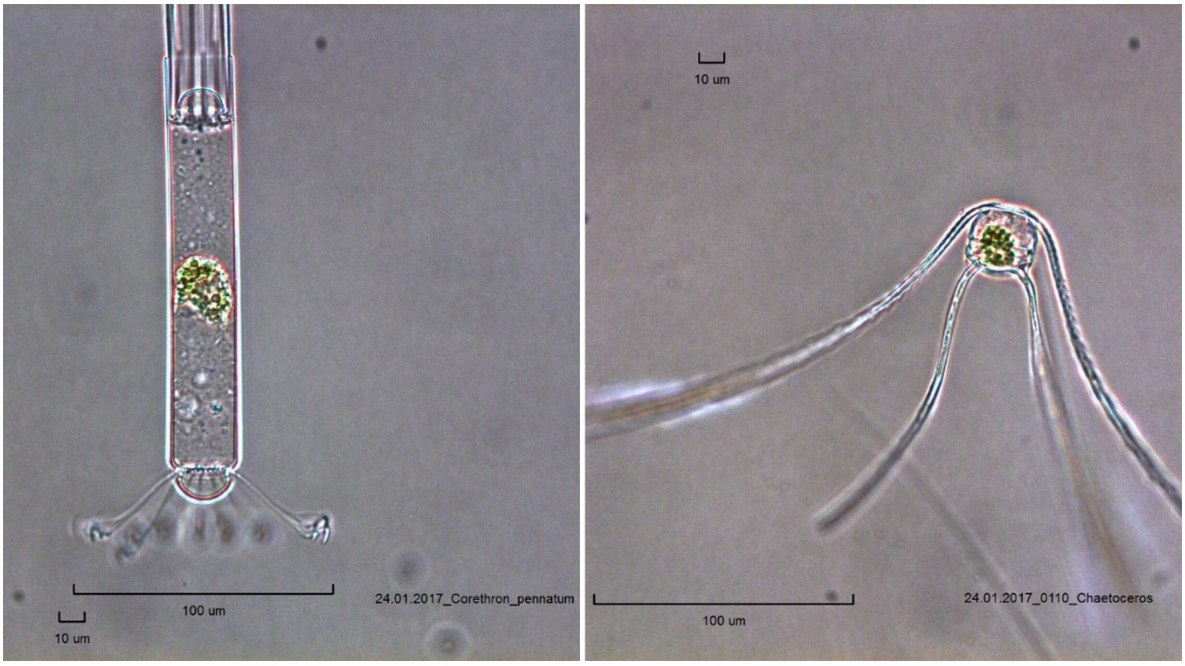

Figure 76. Corethron pennatum (left) and Chaetoceros criophilus (right) are commonly observed in underway sieved samples.

Operations evaluation

The underway seawater lab on board the Investigator is ideally equipped for an underway sampling suit as conducted during this voyage. Sampling is very convenient as water is led from the intake at ~9 m depth directly to the lab via several taps subject to different pre-filtrations (clean, trace metal-free etc.). All necessary technology is easily accessible, such as 24 hrs active screens and displays with underway physico-chemical underway data, enabling rapid sampling in physico-chemically and biologically interesting locations. No improvements to the underway intake can be thought of at this time.

Summary

A total number of 51 underway samples were collected during IN2017_V01, along a N-S-N transect and an along- and across-shore grid in the survey areas A and C. Underway sampling included a suite of sampling for chlorophyll *a*, phytoplankton abundance and composition, single cell isolations, and DNA, flow cytometry, HBI and hydrochemical analyses. Most samples will be analysed on land by A. Focardi, A, Leventer, M. Duffy, L. Armand, L. Armbrecht and S. Belt. However, preliminary observations suggest a N-S transition in phytoplankton communities, with the diatoms *Chaetoceros*, *Rhizosolenia*, *Proboscia*, *Fragilariopsis kerguelensis* and *Pseudo-nitzschia* dominating north of 58°S, *Fragilariopsis kerguelensis* and small centric diatoms dominating between 58-62°S and small sea-ice associated *Fragilariopsis* spp. dominating south of 62°S. High numbers of *Chaetoceros criophilus* and *Corethron pennatum* were also consistently encountered south of 62°S.

CONDUCTIVITY TEMPERATURE DEPTH (CTD) WATER SAMPLING

Method

During each CTD casts, the real-time profiles were followed during the downward cast. Based on the profiles of fluorescence, temperature, salinity, oxygen, photosynthetically active radiation (PAR) and turbidity, sampling depths were decided on when the CTD arrived at ~10 m above the bottom. During each CTD cast, water samples were collected in 12L Niskin bottles, usually including at least the bottom and the deep chlorophyll maximum depths as well as the surface.

Immediately after securing the CTD on board samples for hydrochemical analysis by P. Hughes were collected from the Niskin bottles for each depth sampled. Subsequently, 10L carboys were triple-rinsed and filled with seawater and transferred into the underway seawater lab for processing.

From the 10L carboys, we then subsampled for the following analysis:

1. Hydrochemistry,
2. Chlorophyll *a*,
3. phytoplankton abundance (Lugol's preservation),
4. phytoplankton composition (microscope slides),
5. DNA (microbial communities)
6. flow cytometry,
7. Viriome composition

For detailed information on the methods used for each different analysis please refer to the underway sampling section above.

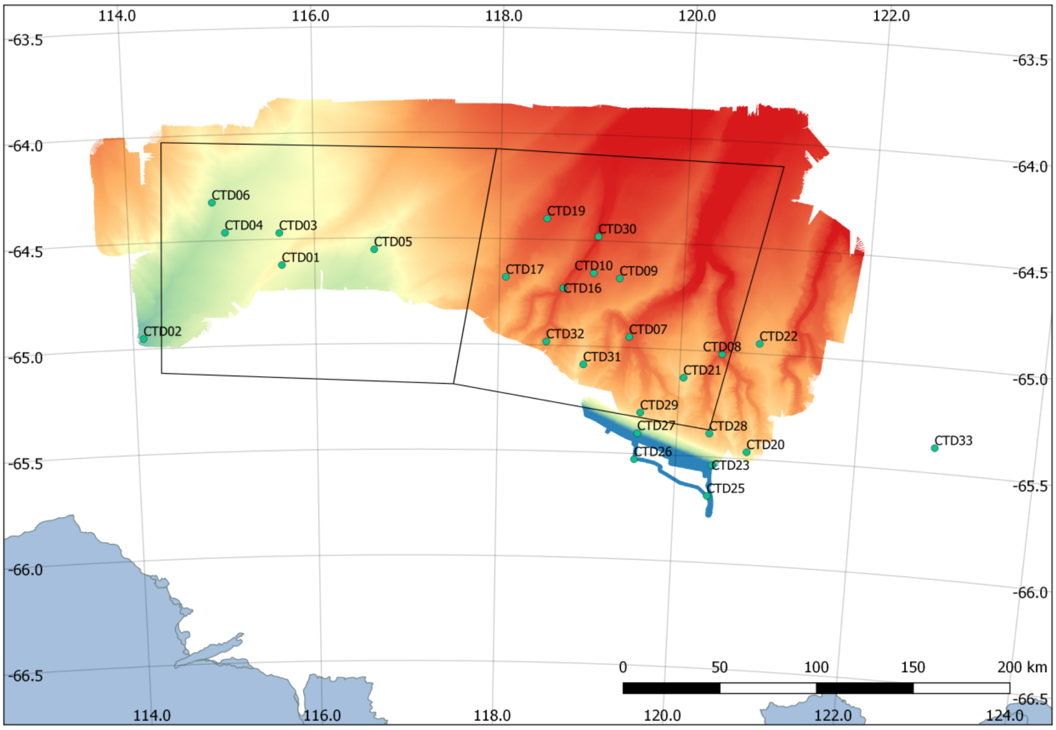

Figure 77*. Map showing CTD sample sites in and next to the survey areas A and C (created in qgis by Kelly-Anne Lawler, March, 2017).*

Preliminary Results

Phytoplankton composition

From CTD samples, initial microscopic observations documented a diatom assemblage that is dominated by sea ice associated *Fragilariopsis*, *Chaetoceros criophilus* and *Corethron pennatum* in the surface waters. The deeper water samples collected during CTD casts showed increasing abundance of the diatom *F. kerguelensis*, silicoflagellates, chrysophyte cysts, and single cells of *Phaeocystis*. Deeper chlorophyll maxima also have higher concentrations of *Chaetoceros* resting spores. The near absence of their vegetative counterparts suggests that these are the sinking remnants of phytoplankton that bloomed prior to our voyage, as the ice initially retreated.

From CTD samples, initial microscopic observations document a diatom assemblage that is dominated by sea ice associated *Fragilariopsis*, *Chaetoceros criophilus* and *Corethron pennatum* in the surface waters (Fig. 76). The deeper water samples collected during CTD casts show increasing abundance of the diatom *F. kerguelensis*, silicoflagellates, chrysophyte cysts, and single cells of *Phaeocystis*. Deeper chlorophyll maxima also have higher concentrations of *Chaetoceros* resting spores. The near absence of their vegetative counterparts suggests that these are the sinking remnants of phytoplankton that bloomed prior to our cruise, as the ice initially retreated.

MARINE MAMMAL OBSERVATIONS

Method

Marine mammal operations

All marine mammal observations conducted during seismic activity were undertaken under seismic permit 2016-0005 and as per the EPBC Act Policy Statement 2.1- Interaction between offshore seismic exploration and whales (also referred to as ‘the policy’). As part of the policy, three precaution zones (Fig. 78) were used to determine appropriate action to be taken by the marine mammal observer (MMO) to minimise harm to cetaceans during seismic activities. As per the EBPC Act Policy Statement 2.1:

For proposed seismic surveys that can demonstrate through sound modelling or empirical measurements that the received sound exposure level for each shot will not likely exceed 160 dB re 1 $\mu Pa^2 s$, for 95 % of seismic shots at 1 km range, the following precaution zones were used:

- *Observation* zone: 3+ km horizontal radius from the acoustic source.
- *Low power* zone: 1 km horizontal radius from the acoustic source.
- *Shut-down* zone: 500 m horizontal radius from the acoustic source.

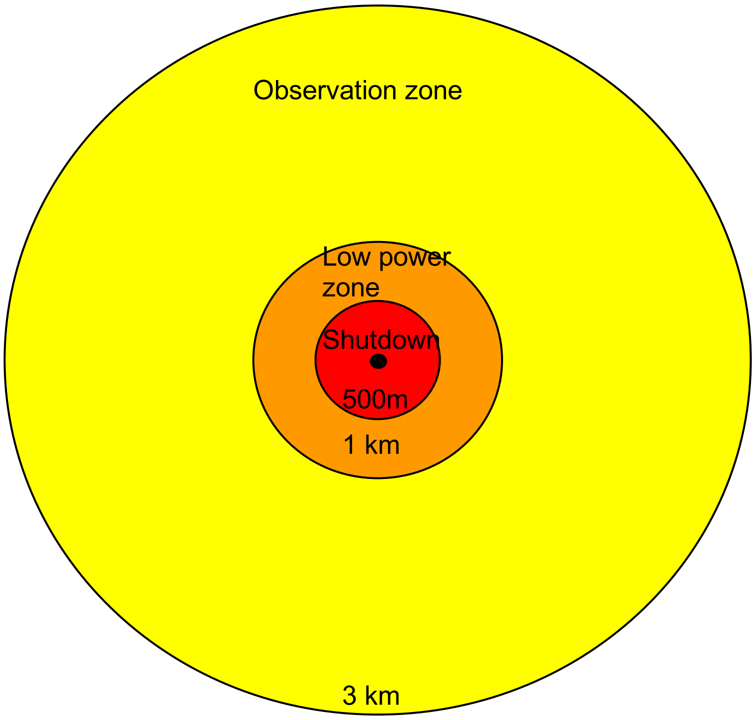

Figure 78. Precaution zones used during seismic activity. *Image from the EPBC Act Policy Statement 2.1.*

Observations
All marine mammal observations during seismic activity were conducted during daylight hours and as per the permit and policy.
The following operations were undertaken as required:

- Pre-start-up visual observation
- Soft start
- Start-up delay
- Operations
- Power- down and Stop work

The following is a brief summary of each operation adapted from the policy:
Pre start-up visual observation
During daylight hours, visual observations (using binoculars and the naked eye from the bridge) for the presence of whales were undertaken by a suitably trained crew member (the MMO) for at least 30 minutes before the commencement of the Soft Start Procedure.
Note: To ensure 360-degree observations around the ship, the MMO circled the entire bridge to make sure observations included areas behind the stern of the vessel. The seismic buoy at the end of the streamer was used as a permeant visual of distance used to indicate 400 m from the standing position on the wings of the bridge during all seismic operations.

Soft start
If no whales were sighted within the Low power and Shut-down zones during the pre-start-up procedure, the soft start procedure outlined below commenced.
Soft start procedures were used each time the acoustic sources were initiated, gradually increasing power over a 30-minute period. A total of two air guns were used in seismic activity. Soft start during seismic operations consisted of firing a single gun to 70 bar over the first five minutes. The next five minutes consisted of the firing of the second gun, also to 70 bar. Over the next 20-minute period, the seismic team gradually increased the pressure of both guns to a final pressure of 140 bar.

Start-up delay procedure
If a whale was sighted within the 3-km observation zone during the soft start, an additional trained crew member or scientific crew member assisted the MMO on the bridge. If a whale was sighted within or was about to enter the Low power zone, the acoustic source was powered down to the lowest possible setting (e.g. a single gun). If a whale was sighted within or was about to enter the Shut-down zone, the acoustic source was shut down completely.
Soft start procedures only resumed after the whale had been observed to move outside the Low power zone, or when 30 minutes had elapsed since the last whale sighting.

Stop work procedure
If a whale was sighted within the 3-km observation zone, the MMO continuously monitored the whale whilst in sight on the bridge.
If a whale was sighted within or was about to enter the Low power zone, the acoustic source was powered down to the lowest possible setting. If a whale was sighted or was about to enter the Shut-down zone, the acoustic source was shut down completely.

Power-up of the acoustic source with soft-start procedures only occurred after the whale was observed outside the Low power zone, or when 30 minutes had elapsed since the last whale sighting.

During times of low visibility
Start-up commenced according to the Soft-Start Procedure provided that there had not been 3 or more whale instigated power-down or shut-down situations during the preceding 24-hour period.

Operations proceeded provided that there were 3 or more whale instigated power-down or shut-down situations during the preceding 24-hour period.
At times of low visibility, continuous observations were maintained with a particular focus on the low power and shut-down zones. If whales were detected, stop work procedures applied.

Marine mammal observation location: the bridge
The bridge provided the best viewing platform on the vessel. The ship has a purpose-built observation platform known as the monkey island, which was not chosen for observations due to restricted visibility from two large communication balls. Alternatively, approval to use the bridge for all marine mammal observations was granted by the ship's master. The bridge is located 20 metres above sea level and provides a 360-degree view around the vessel, with port and starboard wings. The bridge also offers a comfortable viewing environment for long periods of observations, with a bathroom and desk space for paper/laptop work. Clear communication between the master, seismic team, operations room and MMO were kept throughout all seismic surveys. The MMO was able to speak directly to the master/crew, who relayed information directly to the seismic team in real time.

Equipment used:
1x Binocular 7x50
1x Laser range finder
1 x 100-400 mm lens for species ID shots
Distance measurements were primarily based using known distances from positions on the wings and use of a range finder. Distance estimates prior to seismic work were conducted on the bridge using a sextant to determine known distances of icebergs at various distances. The seismic buoy at the end of the streamer was used as a constant/known distance (400 metres from the wings) to help determine individuals within 500 metres from the acoustic source.

MMO assistance
The dedicated MMO was always assisted by crew members on the bridge and a second person from the scientific team. This allowed for the MMO and assistant to be positioned on both port and starboard wings. The MMO frequently moved around the bridge to ensure that 360-degrees of the ship was monitored. Windows at the back of the bridge allowed for sightings directly behind the ship, in addition to the wings. During the transit to the study site, the MMO briefed assistants on basic whale biology, permit requirements, the EPBC Act Policy Statement 2.1, as

well as what to look for when whale watching (e.g. blow, breach). A marine mammal field guide was also provided to assistants. Assistants were rotated every hour, which enabled the MMO to take frequent breaks every 1.5 to 2 hours. During short breaks, the MMO was contactable by the bridge and chief scientist. All seismic activity was overseen by the chief scientist/s who were present throughout every survey.

Record keeping
Records of all seismic activity and marine mammal sightings were taken throughout observations. Forms were taken directly from the Australian Antarctic Division Cetacean Sighting Application (CSA) program. The four main types of reporting forms included:

1. Observer effort form- records observer effort and weather.
2. Operations form- records operations and latitude/longitude e.g. soft start, full power, shut downs etc.
3. Cetacean sightings form
4. Non-cetacean sightings form

Hard copies of forms were printed before and during the voyage. Hard copy records were manually transferred into the CSA program after each seismic line, which generated a single report (10 reports in total, one for each seismic line). Completed forms, in addition to this report, will be provided to the Federal Government as per permit requirements.

Preliminary Results
Summary of seismic survey activities
Seismic survey activities were undertaken from 21 January 2017 to 24 February 2017. A total of 10 seismic surveys were conducted across both sites A and C. Table 19 provides a summary of each seismic survey undertaken, including the date, start and end time of each seismic survey, number of shut downs and power downs and total number of whales observed. See Appendix 9 for seismic daily review and general observations.

A graphical representation of all seismic activities and cetacean sightings is provided below (Figure 79, 80).

Table 19. Summary of seismic surveys undertaken in Antarctic waters during the Sabrina Seafloor survey. Seismic surveys were numbered based on the seismic teams numbering system.

Seismic survey line	Start date (UTC)	Start time (UTC)	End time (UTC)	Survey length (time hrs)	No. of shut downs	No. of power downs	No. whales seen
1	21/1/2017	21:00	03:19	6hrs 19mins	2	1	9
2	23/1/2017	21:00	04:42	7hrs 42mins	1	1	17
3	24/1/2017	21:00	00:35	3hrs 35mins	0	0	3
6	27/1/2017	02:26	10:12	7hrs 46mins	1	1	20
7	29/1/2017	03:30	09:04	5hrs 34 mins	4	1	20
8	3/2/2017	20:30	07:01	10hrs 29mins	0	2	20
9	6/2/2017	03:30	10:55	7hrs 25mins	3	3	15
10	13/1/2017	23:14	08:29	9hrs 15mins	1	1	15
11	18/2/2017	20:47	02:08	6hrs 21mins	1	0	3
12	24/2/2017	03:00	09:23	6hrs 23mins	2	0	3
Total				68.89 hrs	16	10	125

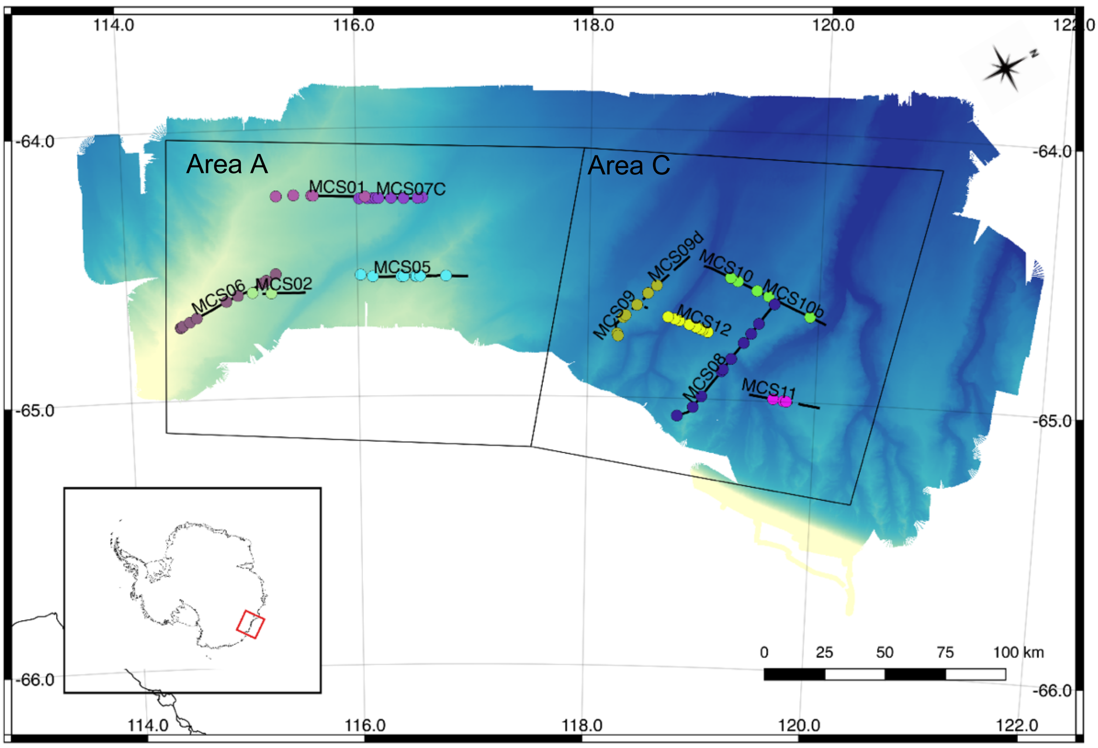

Figure 79. Summary of all seismic lines conducted in areas A and C. *Seismic lines are indicated by black lines. Coloured dots represent location of initial whale sightings. Different coloured whale sightings correspond to different seismic lines. Gaps in black seismic lines indicate shut downs.*

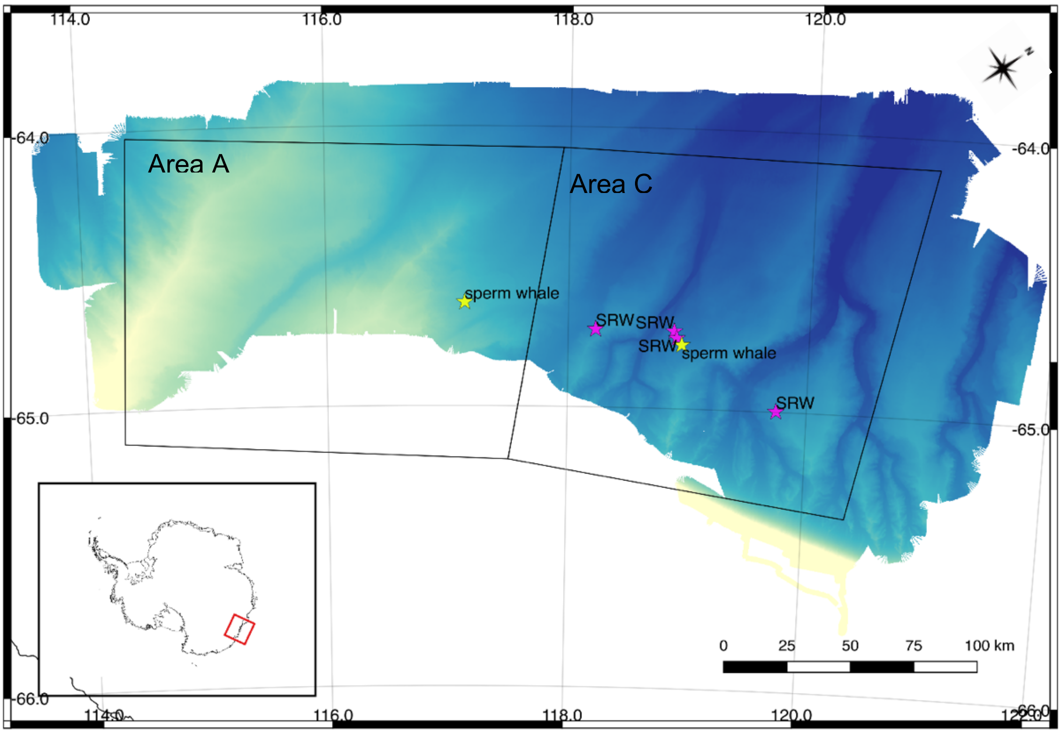

Figure 80. Other large cetacean sightings. *Sperm whales and southern right whales observed during seismic activity and during transit. In addition to humpback whales, these were the only other large whale species observed.*

Operations evaluation

Overall, marine mammal operations were successful during seismic activities. All marine mammal operations were conducted as per permit requirements and the prescribed Australian EPBC Act Policy Statement 2.1. Communication between the ship's crew and seismic team ran smoothly. An understanding of the policy and permit by the ship's crew and seismic team was greatly appreciated and made working within the team environment enjoyable. As this was the first-time seismic operations were conducted on the *RV Investigator,* a small number of recommendations have been made for future MMOs.

The following recommendations are applicable to future MMOs during seismic operations and can also be used as an overview for general marine mammal observations on the *RV Investigator*.

Communication

It is essential for the MMO to have good communication between:

- the master/ship crew
- chief scientist/s
- seismic team
- general scientific team

A briefing at the start of the voyage was provided to the crew and scientific team (including seismic team). This provided information on the role of the MMO, policy information, permit guidelines and operations. This established a primary understanding of the role of the MMO in detail and allowed people to ask questions.

Recommendation one: The MMO should provide a pre-seismic briefing to crew and scientific team (including the seismic team) before operations start.

Discussion with the bridge team before seismic operations took place was very helpful. This allowed the ship's crew to be briefed about the standard operation procedures during marine mammal observations, actions to take in the case of a power down and shut down and ask questions. The master/ship crew also assisted the MMO to weather and directional information using the ship's navigational displays and equipment (e.g. gyroscopes for ship's heading). Operational terminology was also discussed. A list of short terms was compiled for ease of communication during operations. These were also relayed to the seismic team and logged by the operations room via the ship's e-log. The master/crew were vital to the communication between the MMO and seismic team. This was a successful component of marine mammal observations.

Recommendation two: Establish a list of operation action terminology with definitions. This can then be used by the bridge team to communicate to the seismic team and operations room to e-log. For example, if the MMO allows the seismic team to progress to soft start, the bridge can then communicate approval to soft start to the seismic team. This information would then be acknowledged by the ship's operations room.
Communication between the seismic team and MMO was also important, especially as the seismic team was Italian and not familiar with the Australian permit and policy.

Recommendation three: Discuss permit operation procedures with seismic team before operations begin. This will provide the seismic team with an opportunity to ask questions and become familiar with operations and terminology. In addition, this will also provide the team with a better understanding of the MMOs role and the level of protection that Australia provides to cetaceans to help minimise the potential impacts from seismic activities.

MMO familiarity with the bridge
As all marine mammal observations took place on the bridge, it was important that the MMO became familiar with the best vantage points for scanning all operation zones (e.g. observation zone, low power zone and shut down zone).

Recommendation four: The MMO should inspect the bridge for all best vantage points prior to official observations. It is also important that the MMO respects the workspace of the master and crew. The MMO is to keep paper work, camera, range finder and binoculars in an accessible yet tidy fashion. If unsure about best location to setup paper work, the MMO should ask the master or person in charge at the time.

Summary
Seismic activity during this voyage was a success. From an operational point of view, communication between the bridge, seismic team and the MMO made operations run smoothly. The pre-seismic operations briefing by the MMO was important to ensure that the role of the observer and the permit requirements were understood and followed. This was particularly important for the Italian seismic team, who were not familiar with the Australian EPBC Act Policy Statement 2.1.

A range of whale behaviours during seismic activities were observed. On multiple occasions (seismic lines 6, 7, 9 and 12), humpback whales approached the vessel and seismic buoy during seismic operations. This resulted in a number of power downs and shut downs. The most memorable seismic line was also the last attempted, which was unsuccessful in data collection due to a single, very entertaining humpback whale. The individual left two other whales to circle (mug) the vessel for a few hours. Observations of whale behaviour during the use of seismic airguns during this voyage was important. Records, photographs and anecdotal evidence will help add to our knowledge of whale interactions and behaviour towards seismic operations in Antarctica.

The *RV Investigator* provided a comfortable environment for all marine mammal observations during seismic operations. The master and crew were understanding of the MMOs role, which enable the successful implementation of permit requirements. Future seismic operations should take into account the recommendations made here in this report.

Acknowledgments
Thank you to the following who assisted with seismic operations:
The bridge crew - Master Mike, Rod, Adrian and Andrew.
The seismic team - Roberto, Andrea and Diego.
Chief scientists - Leanne and Phil.

Engine room - Genna
The scientific team.

POST-SURVEY PHYSICAL SAMPLE MANAGEMENT

Samples of sediment, water and organisms were returned to most of the institutions represented by the science party. A full quarantine record of sample movements from the ship is held by Leanne Armand. The major sediment repository is the Geoscience Australia marine sediment archive (MARS: http://dbforms.ga.gov.au/pls/www/npm.mars.search).

SECTION 8. The Polar Cell Aerosol Nucleation Project

INTRODUCTION

The Polar Cell Aerosol Nucleation Project (PCAN) was a piggyback voyage on board IN2017-V01 led by Dr Ruhi Humphries of CSIRO O&A, with on-board operations handled by Jack Simmons of the University of Wollongong. Atmospheric aerosol populations in the Antarctic and Southern Ocean regions are key components of the global radiative balance and represent one of the few places on earth relatively untouched by anthropogenic influence. Recent investigations have shown that the region of the Polar Cell just north of the Antarctic continent is atmospherically distinct from those both further north in the Southern Ocean and on the continent itself. This region has only been measured a handful of times previously, and remains largely uncharacterised, yet the small number of observations showed unexpected properties uncharacteristic of the greater region. Therefore the objectives of this study were therefore to:

1. Increase the number and quality of atmospheric observations in the region.
2. Characterise the chemical and physical properties of atmospheric aerosol populations in the northern region of the Antarctic Atmospheric Polar Cell.
3. Understand the seasonal changes of the Polar Cell aerosol populations by comparing to springtime measurements at the same location taken in 2012 (AAD project 4032).
4. Observe the aerosol formation processes in the pristine atmosphere of the Antarctic polar cell.

Appendix 10 details logs and information related to the PCAN piggy-back project on IN2017-V01.

Methods

The PCAN project utilised a suite of instruments to characterise aerosol populations in the northern polar cell off the Sabrina coast of Antarctica. Permanent instrumentation (owned by MNF) was utilised as well as additional instrumentation added specifically for this voyage. All instruments were running continuously throughout the voyage unless noted, except for periods of malfunction as described in the Operations section. Flow corrections, inlet efficiency corrections and data filtering (e.g. for periods of sampling exhaust) are required for all instrument datasets.

All instruments except the Tekran and the reactive mercury filters were plumbed into existing permanent sample manifolds in either the air chemistry laboratory or the aerosol sampling laboratory (Figs. 81 and 82).

Permanent Instrumentation

CCNC

Cloud condensation number concentration was measured using a Cloud Condensation Nuclei Counter (CCN100, Droplet Measurement Technologies, Longmont, Colorado, USA). This instrument continuously measures the concentration of particles forming cloud condensation nuclei at supersaturation percentages ranging from 0.2-1% (Droplet Measurement Technologies, Inc., 2009). The CCNC is permanently mounted in the aerosol sampling lab. Data was exported hourly as .csv files at a temporal resolution of one second, by the 'Single CCN.exe' software.

Nano SMPS

Fine fraction aerosol size distributions were measured using the Grimm nano Scanning Mobility Particle Sizer (SMPS). This instrument continuously scans through particle size bins and measures the number concentration associated with each size range, resulting in a particle size distribution. It is capable of detecting particles from approximately 3nm to 3000nm, depending on the chosen configuration (GRIMM Aerosol Technik GmbH & Co. KG, 2011). During this voyage, the median column was installed, providing complete scans from 4nm through 430nm every five minutes throughout the voyage. Data was output in daily .raw and .cpc (ASCII file types) files by the 'GRIMM Nano Software' used for data acquisition. Sample flowing into this instrument was first passed through an Ecotech Nafion dryer, supplied by five litres per minute of desiccant dried ambient air as backflow. The nano SMPS is permanently mounted in the aerosol sampling lab.

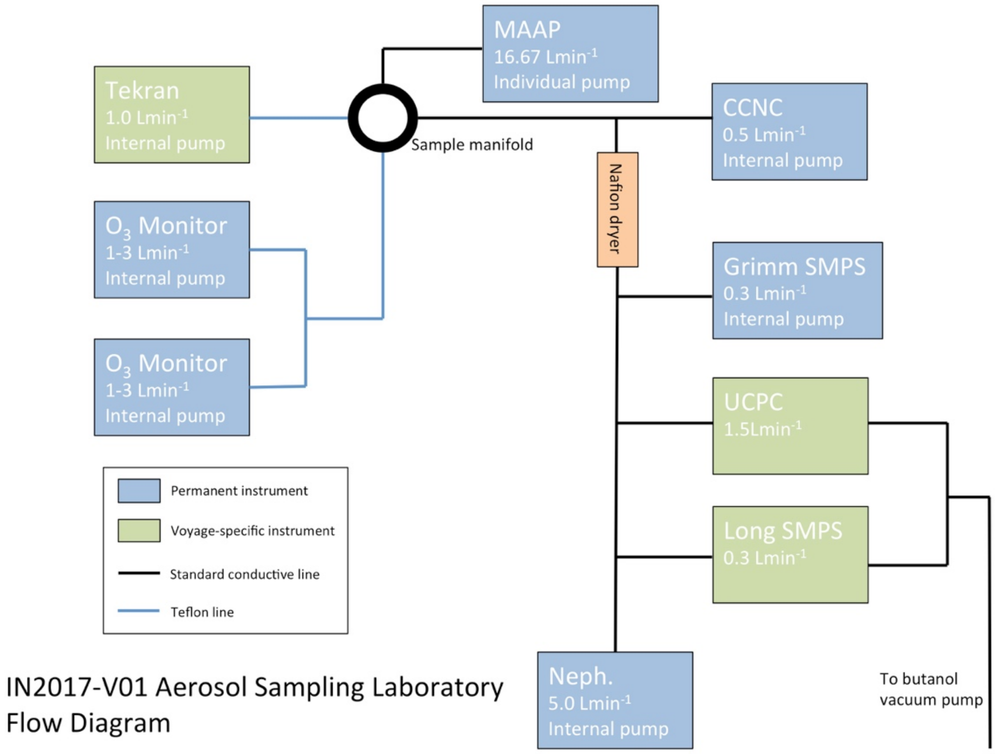

Figure 81. Summary flow diagram with instrument flow rates of the aerosol sampling laboratory as set up for IN2017-V01.

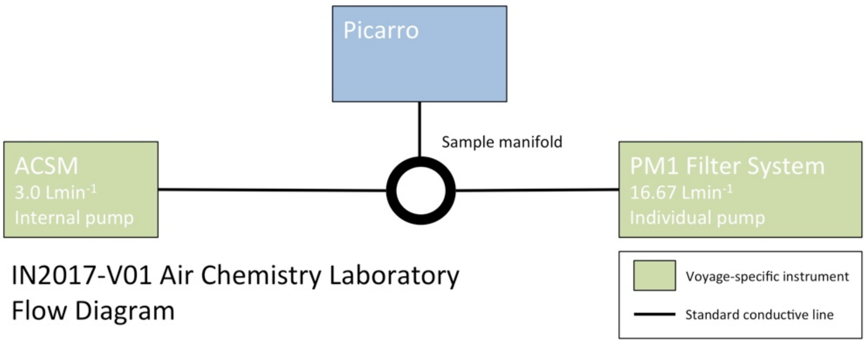

Figure 82. Summary flow diagram with instrument flow rates of the air chemistry laboratory as set up for IN2017-V01.

Nephelometer
The ecotech Aurora 4000 nephelometer measured scattering caused by particles at 450nm, 525nm and 635nm (Ecotech Environmental Monitoring Solutions, 2011). Scatter at angles from 0° to 90° was measured in 5° increments. Data was logged directly by the CSIRO data acquisition system. Sample flowing into this instrument was first passed through an Ecotech Nafion dryer, supplied by five litres per minute of desiccant dried ambient air as backflow. The nephelometer is permanently mounted in the aerosol sampling lab.

MAAP
The Thermo Scientific Model 5012 Multi-Angle Absorption Photometer monitored black carbon concentration on the voyage by measuring interaction of radiation with aerosol sample collected on glass fibre filter paper (Thermo Fisher Scientific Inc., 2009). Data was logged directly by the CSIRO data acquisition system. The MAAP is permanently mounted in the aerosol sampling laboratory.

Voyage Specific Instrumentation
Long SMPS
The Long SMPS (Scanning Mobility Particle Sizer, TSI, USA) measured the distribution of particles between 14 and 685 nm (TSI Incorporated, 2009). It is comprised of a TSI Model 3081 long differential mobility analyser (DMA) column with a TSI Model 3080 controller connected to a TSI Model 3772 Condensation Particle Counter. An impactor was attached to the inlet for the duration of the voyage. Particle distributions for 298 second scans were output as daily .S80 files (readable in the Aerosol Instrument Manager software). The long SMPS was located in the aerosol sampling laboratory during IN2017-V01. The instrument used belongs to CSIRO Oceans and Atmosphere, Aspendale.

UCPC
The total number of particles greater than three nanometres were measured using the TSI 3776 Ultrafine Condensation Particle Counter (UCPC). One second averages of 10 Hz measurements are output by the instrument (TSI Incorporated, 2006). Sample air was drawn through the instrument at 1.5 litres per minute. Aerosol Instrument Manager 10.2 was used to output daily .C76 files containing particle counts per cubic centimetre for the first part of the voyage. Following a computer change (detailed in Operations), Aerosol Instrument Manager 10.2 was used. Sample flowing into this instrument was first passed through an Ecotech Nafion dryer, supplied by five litres per minute of desiccant dried ambient air. The UCPC was located in the aerosol sampling laboratory during IN2017-V01. The instrument used belongs to CSIRO Oceans and Atmosphere, Aspendale.

Tekran
The Tekran Model 2537B Ambient Mercury Vapor Analyzer was used on IN2017-V01 to monitor ambient total gaseous mercury concentrations. The instrument measures elemental mercury in the atmosphere at concentrations of less than one nanogram per cubic metre (Tekran Instruments Corporation, 2012). The instrument was plumbed using Teflon tubing directly from the sampling inlet to reduce metal contamination and line losses. Argon carrier gas was used at a line pressure of 50psi. Measurements were taken every five minutes and exported daily as text files by ‘Hg logger’ software. The Tekran was located in the aerosol sampling laboratory during IN2017-V01. The instrument used belongs to Grant Edwards of Macquarie University.

ACSM
The Aerodyne Time-of-Flight Aerosol Chemical Speciation Monitor (ToF-ACSM) provided real-time chemical composition of sampled aerosol on IN2017-V01. The ACSM uses time-of-flight mass spectrometry to determine relative abundance of chemical species in sampled particulate matter. A dryer was attached to the instrument. The software ‘IgorDaq’ logged sample data daily as text files as well as producing daily error matrices. ‘DryerStats‘ logged dryer data at a temporal resolution of five seconds, also as text files. The ACSM was located in the air chemistry laboratory for IN2017-V01. The instrument used belongs to CSIRO Oceans and Atmosphere, Aspendale.

PM1 Filters

All particulate matter smaller than one micron (PM1) in diameter was collected on quartz filters. The PM1 filter system was installed in the air chemistry lab. A line ran from the main sample manifold to a vacuum pump via the filter cartridge and a mass flow controller. Flow rate was set at 16.67 litres per minute (1000 litres per hour). The pump was connected to a switching unit that automatically switched off when the air sampling inlet was facing the ship's exhaust stack for the second part of the voyage. Filters were changed every 24 hours. When less than 12000 litres of air passed through a filter in 24 hours, the filter was left on the system for another 24 hours. Both used and unused filters were stored in a -20° freezer when not in use. Blanks were taken weekly. A clean sample was loaded into the cartridge and placed on the system before being immediately removed and stored. The PM1 filter system was set up in the air chemistry lab and is the property of CSIRO Oceans and Atmosphere, Aspendale.

Reactive mercury filters

The Active Reactive Mercury System is designed to provide a robust, low maintenance, and easily deployable method to sample ambient air reactive gaseous mercury (RGM) concentrations. The system utilizes two types of filter media to capture RGM, cation exchange membranes (CEM), and nylon membranes. Each filter type is deployed in sets of three for a two-week sampling period. Filters are housed in 47 mm Teflon® two-stage filter holders, providing a primary upstream collection filter. A secondary downstream filter captures breakthrough RM. Ambient air is pulled through the filter assemblies using flow controlled vacuum pumps, and total volumetric flow is recorded via in-line gas meters. Grant Edwards of Macquarie University provided the reactive mercury filter system for IN2017-V01. The system was mounted on a rail under cover on the port side of 05 Deck for the voyage. Used filters were stored at -20°C.

MicroTops Sun Photometer

The MicroTops II sun photometer is a portable instrument used for determining aerosol optical depth. It consists of a GPS unit and the sun photometer itself. Measurements require a clear view of the entire solar disc. Therefore they were performed sporadically throughout the voyage, due to incidence of consistent cloud cover. Measurements were taken in sets of 5-10 scans at approximate intervals of two hours. Changing weather conditions made this sampling interval difficult. Sun photometry measurements were taken from various places on ship, influenced by the position of the sun, and the ship's exhaust plume. Alexander Smirnov of NASA provided the MicroTops II sun photometer used on IN2017-V01.

Cloud Lidar

The cloud lidar data was logged directly by CSIRO data acquisition, The lidar is owned by Alain Protat of the Bureau of Meteorology. The SITS team completed maintenance of this instrument.

PRELIMINARY RESULTS

Preliminary results from the PCAN project are promising. Initial data processing was begun on board, but the majority of results will not become clear before more significant and robust data processing is completed. Logged events impacting measurements, such as flow checks, will have to be removed from the dataset. Periods during which ship exhaust was sampled during the voyage also have to be removed. Exhaust sampling during the voyage was relatively common. Sampling of exhaust occurs when the relative wind speed at the ship is greater than zero knots with wind blowing to the bow of the ship.

Aside from these events, periods of very low aerosol concentrations were observed. This was noted on the CCNC (Fig. 83), the UCPC and both SMPS instruments. The CCNC displayed especially low counts during precipitation events. During the transit south to the main survey area, precipitation fell as rain. When at latitudes greater than approximately 60°S, precipitation fell mostly as snow and sleet.

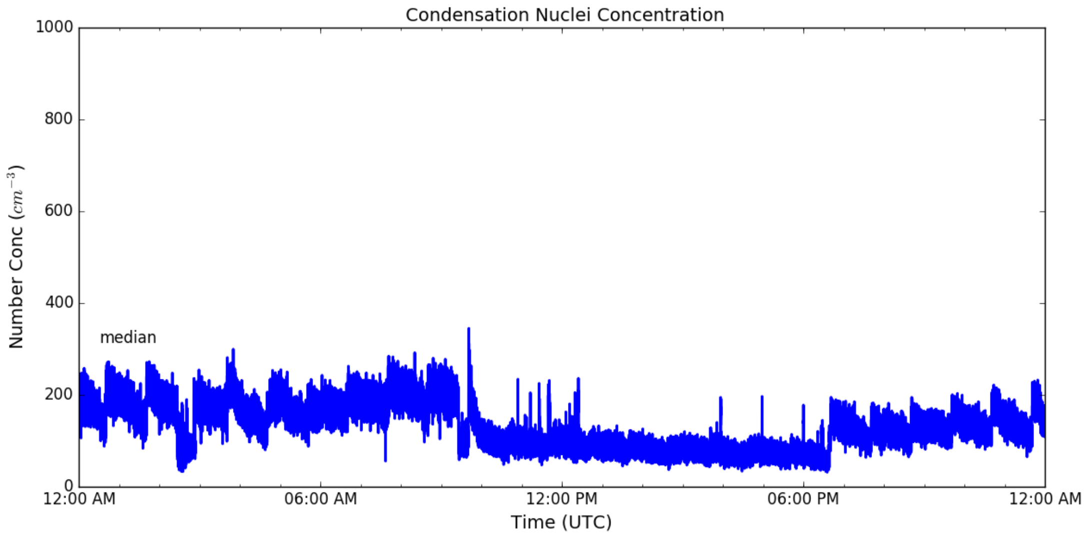

***Figure 83: Raw data showing cloud condensation nuclei (CCN) counts (number of CCN per mL) from the CCNC on January 24th demonstrating low counts.** Each hour the instrument goes through a cycle of supersaturations, starting at 1% and decreasing to just 0.3% (i.e. 101% and 100.03% relative humidity). The higher supersaturations result in more of the aerosol population being able to grow to detectable sizes.*

Relatively stable ambient mercury concentrations were observed from the Tekran, mostly between 0.4 and 0.8 ngm^{-3}. A script was written on board capable of resampling data to hourly resolution, and plotting the hourly mean plus/minus one standard deviation. An example plot from this plot is presented as Figure 84.

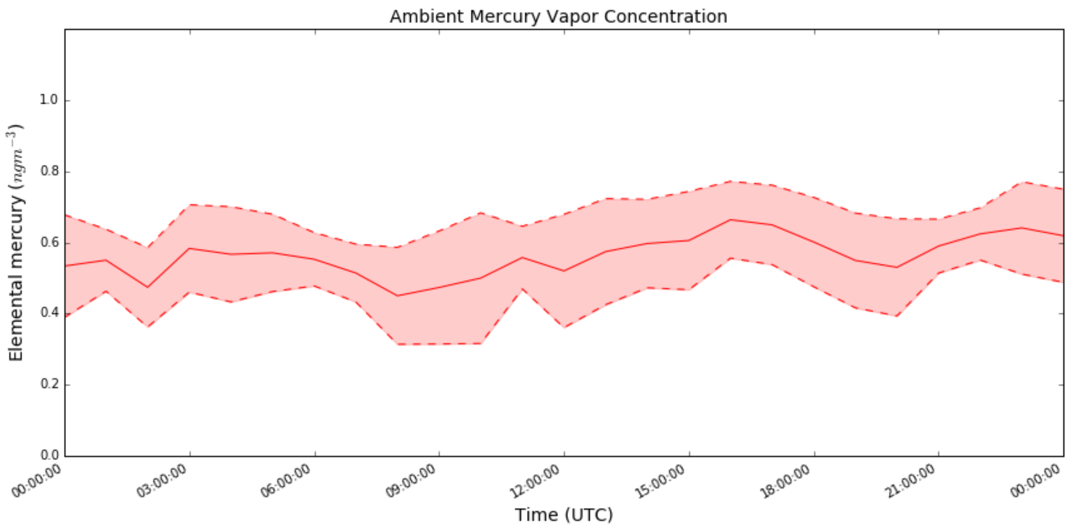

Figure 84: Mean hourly ambient mercury vapor concentration for the 11th of February, plus and minus one standard deviation.

The ACSM measured aerosol populations dominated by sulphate for the majority of the voyage (Fig. 85). This is expected due to the large source of DMS (a precursor for sulphate aerosol) produced by polar marine phytoplankton.

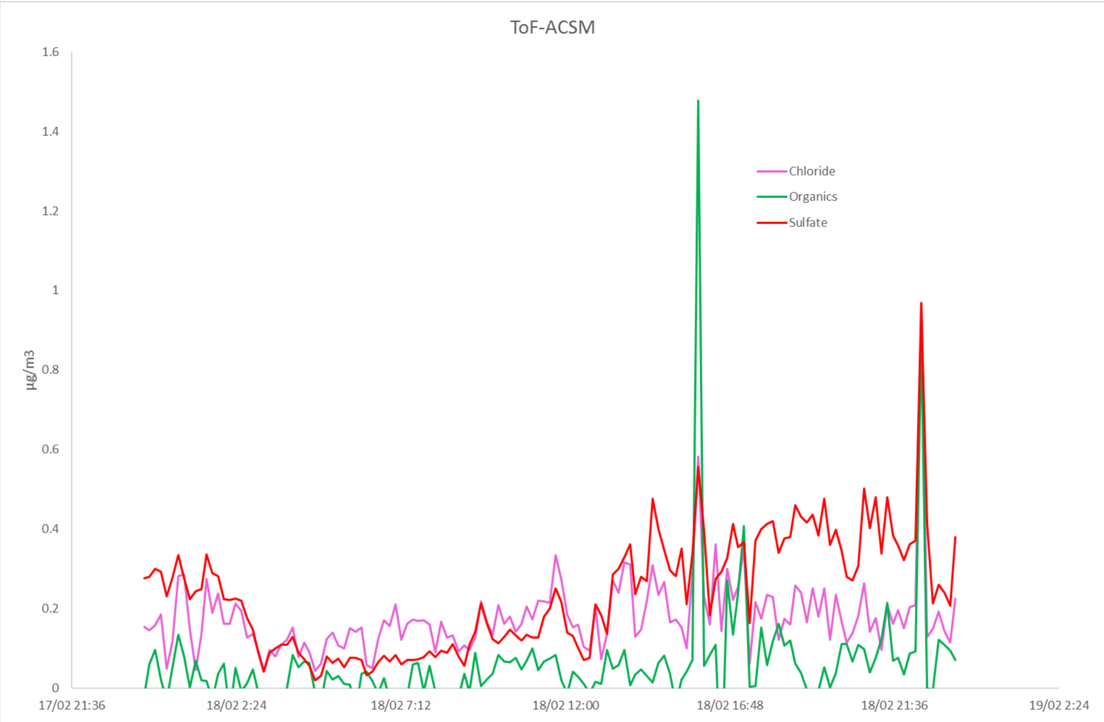

Figure 85: Real-time aerosol chemical composition as measured by the aerosol chemical speciation monitor. *Large spikes within the data represent periods of measuring ship exhaust.*

MicroTops sun photometry measurements measured aerosol optical thickness. Although measurements were less frequent than would have been ideal, it is hoped that measurements taken on IN2017-V01 can provide a valuable contribution to the Marine Aerosol Network component of NASA's global AERONET program. Locations at which MicroTops measurements were taken are presented in Figure 86. Filter samples are awaiting analysis in laboratories ashore.

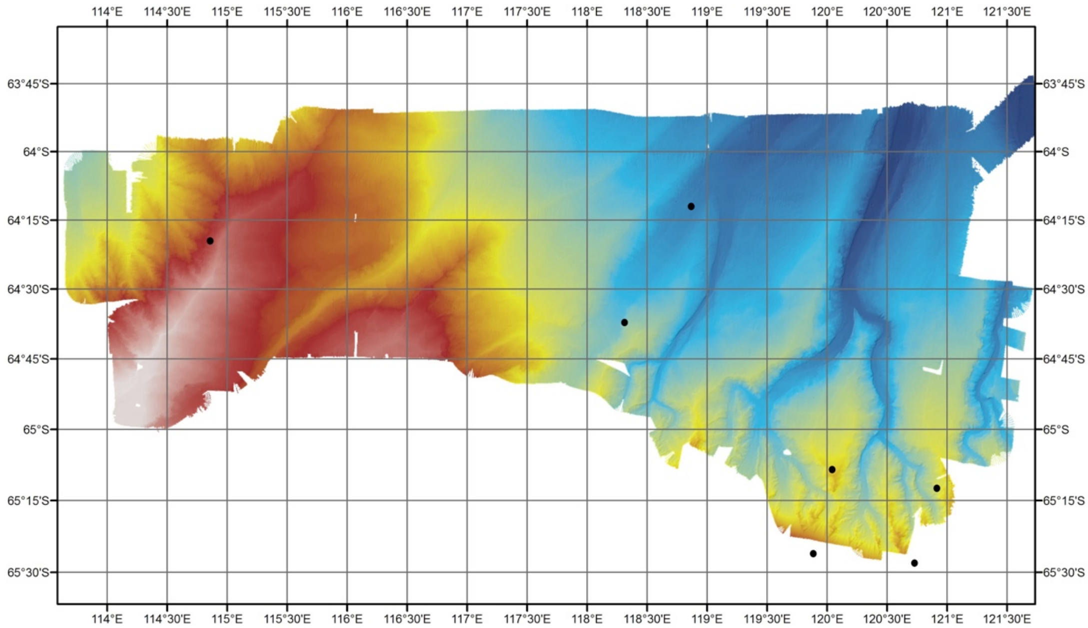

Figure 86: Locations of MicroTops measurements taken on IN2017-V01 overlayed on bathymetry mapped on the voyage.

OPERATIONS EVALUATION

The PCAN instrument suite was assembled and deployed during the week of the 9th of January, before the departure of the RV Investigator from Hobart on the evening of Saturday the 14th local time. Details of the instrument suite are presented in the Methods. Presented below is a summary of major PCAN operational challenges experienced during IN2017-V01. More comprehensive documentation can be found in the e-log and Appendix 10. All dates and times in UTC unless noted.

Instrument function is summarised in the timeline below (Fig. 87).

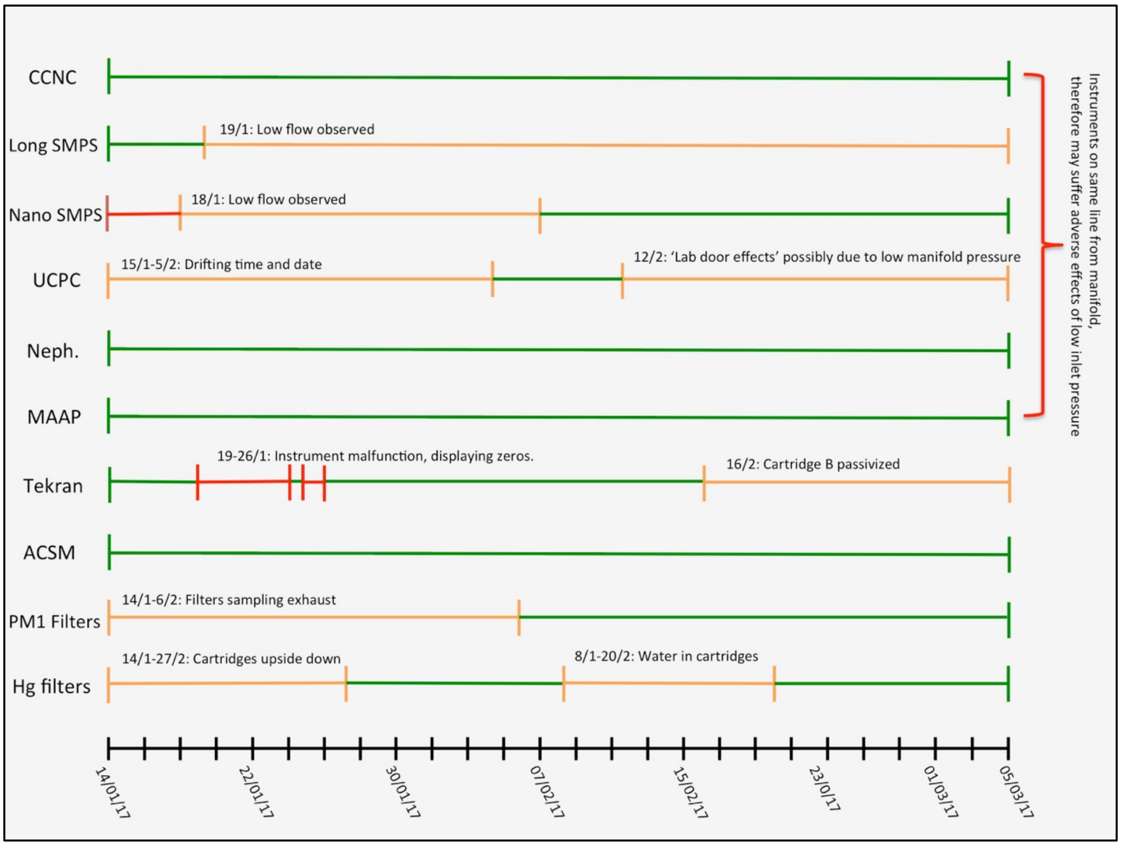

Figure 87. Summary timeline of instrument function throughout the voyage. *Green lines indicate usable data. Orange lines indicate data requiring significant processing. Red lines indicate no data collected or unusable data.*

Tekran Malfunction

During deployment, the 3772 CPC experienced a major malfunction and caused a butanol spill in the aerosol sampling laboratory. The lab was evacuated and ventilated until the spill was cleared. The instrument fault was unable to be repaired in time for voyage departure. The instrument was therefore shipped back to CSIRO Oceans and Atmosphere for repair.

Following the butanol spill, the Tekran Ambient Mercury Vapor Analyzer began displaying null readings. Prior to departure on the 14th, a lamp replacement was undertaken. This immediately improved instrument function.

A routine lamp optimization was performed on the Tekran on the 18th of January. Following this optimization, all instrument output including calibration peak values displayed zero. Multiple recalibrations were performed, with no improvement over the following days. With remote assistance from Grant Edwards ashore, checks of lamp voltage, heater function and solenoid switching were undertaken. During a check of solenoid function on the 22nd, the lamp warning LED came on. A breakthrough was achieved on the 23rd of January, when the performance of a lamp optimisation led to a successful calibration. Data collection was begun and ran as expected, barring a period on the 24th in which the instrument PC ran out of battery after the power cable was not reconnected. Further lamp optimisations were performed throughout the voyage (1/2/17, 10/2/17, 22/2/17) without issue. On the 17th of February, a significant difference in reported ambient mercury concentrations was noticed between cartridge A and cartridge B on the Tekran. This is hypothesised to be due to cartridge B becoming passivized. Only the data from cartridge A should be used from the point in which the difference in reported concentrations becomes significant.

AIM for UCPC Time Drift

On the 22nd of January it was also noted that the AIM software for the UCPC was not aligned with UTC. The computer was re-synced to the ship's time server, with no change. A reinstall of AIM was suggested, but advised against by DAP, due to limited ability to recover the program if corrupted during install. Instead, a new sample was opened manually on the 27th of January. This reset the time and date, but after a few days it had drifted again. Another new sample was manually opened on the 31st. Drift was characterised, and found to be irregular. Therefore, on the 2nd of February, AIM 10.2 was installed on Field PC2 (an alternate PC), and the UCPC set to run on this computer. Time and date did not drift from this point onward. A number of computer restarts were performed, forcing the creation of a number of new sample files, but the new system ran without issue from the 6th of February.

Reactive Mercury Filter System

Reactive mercury filters were first changed on the 26th of January. All filter cartridges bar one were installed upside down. Water was present in the cartridges. Cartridges were dried in the fume hood. Once dry, the cartridges were reloaded and reinstalled with O-rings in an attempt to minimise water intake into cartridges. The filters were changed again on the 8th of February. The cartridges were much drier. Again, flows were unable to be adjusted due to heavy seas. Filters were replaced for a third time on the 20th of February. On this replacement, it was noted a line between a cartridge and the pumps had disconnected. The clear flexible tubing used in the system had become very hard in the cold, and therefore it was extremely difficult to maintain a leak-free system. Large amounts of water were present in some filters. It is hypothesised a large, very wet snowstorm the preceding day caused the water in the cartridges. Again, the cartridges were placed in the fume hood to dry before reinstallation.

PM1 Filter System

It was noted on the 6th of February that the PM-1 filter system was not connected to the pump switching system in the air chemistry laboratory. This caused filters numbered 1 through 23 to be contaminated with ship exhaust. Aside from this case of operator error, the system worked well.

Low Manifold Pressure

Low flow was first observed through both SMPS instruments on the 18th of January (both measured <200cc/min where 300cc/min is expected). This was the first symptom of the most operationally challenging aspect of PCAN on this voyage. The flow in the GRIMM SMPS recovered to 283cc/min on the 8th of February. Aside from one brief period on the 14th of February, the TSI SMPS did not return to normal flow. When no line was connected to the inlet of the TSI SMPS (i.e. non-inline inlet flow) flow was as expected. A multitude of checks and tests were performed to diagnose this problem. The impactor on the TSI SMPS was removed, cleaned, and the orifice checked before reinstallation. The conductive tubing between the instrument and the sample line was replaced. The instrument was connected to other ports off the main line, swapped with the UCPC port and the valves replaced. The instrument was connected directly to the manifold. Inline inlet flow was monitored throughout these tests and demonstrated no consistent improvement. Flow to other instruments on the same line from the manifold was tested and found to be as expected. Flow to the nephelometer was not measured due to a lack of the appropriate connections.

On the 11th of February, a spike in particle concentrations was noticed upon opening the lab door was noticed on the UCPC particle concentration. Following this observation, a number of thorough line inspections were performed, including one with Nicole Morgan from the SITS team. The Energy Recovery Valve (ERV) was set to ensure maximum air in and minimum air out, in an attempt to ensure positive pressure inside the aerosol sampling lab. Lab pressure was measured as positive on the 18th of February using the barometer in the watch of Jason Fazey. Each instrument in which lab air could enter the system and contaminate the UCPC data was isolated. It was found that removing the Grimm SMPS and CCNC from the system did not remove the 'door effect' on UCPC concentration. The test for the nephelometer was inconclusive. At the time of writing, it is hypothesised that low atmospheric pressure, in conjunction with low pressure in the manifold, is causing the butanol vacuum pump (for the UCPC and the TSI SMPS) to draw lab air through the nephelometer exhaust when the lab pressure changes suddenly (such as when the lab door is opened). Attempts are being made to measure sample manifold pressure to test this.

Other instruments

The Grimm nano SMPS, CCNC, MAAP and nephelometer functioned as expected for the duration of the voyage. The CCNC working fluid (milliQ water) was routinely changed without issue. However, these instruments were all located on the problematic sample line described above. Therefore care must be taken in data processing to ensure all contamination by laboratory air is removed.

The ToF-ACSM functioned as expected for the duration of the voyage. A brief hiccup was experienced just prior to departure, as an accidental IP address change limited communication between instrument and PC. This was quickly resolved with assistance from the manufacturer. An error was frequently experienced in the saving of dryer parameters (the data backup job and instrument trying to access the same file simultaneously). This did not impact on the logging of dryer data except for the 26th of January.

MicroTops sun photometry measurements were taken infrequently throughout the cruise. Scans were taken in sets of five to ten. Measurements are summarised in the below table. One measurement set on each the 9th and the 16th of February may be contaminated by ship exhaust. More frequent measurements were impossible due to the dominance of cloudy conditions, including high cirrus clouds obscuring the solar disc.

Table 20. Summary of MicroTops measurements taken throughout the voyage.

Date	Number of Scan Sets
17/01/2017	1
02/02/2017	1
09/02/2017	2
16/02/2017	3
23/02/2017	1
25/02/2017	2

Throughout the voyage, the on-board analyst would call the bridge before entering the aerosol sampling lab, and upon return. The analyst was accompanied to the lab on every visit. The installation of a CCTV camera in the aerosol sampling lab allowed the analyst to take short solo visits if the bridge was notified the analyst would be alone.

Suggestions for Future Campaigns

From the above operational report, a number of suggestions for future campaigns are proposed.

A portable barometer would be useful to monitor the pressure of spaces in the ship, such as the aerosol sampling lab. It would also be much easier to diagnose and solve the type of pressure problem described above if a pressure measurement inside the sampling manifold was available. Another possibility would be to split the instruments onto a number of sample lines from the manifold, to reduce the draw on any one line.

Some alterations to the reactive mercury filter system are also proposed. A more robust connection between the end of the lines and the top of the filter cartridges is required, as the clear flexible tubing becomes very hard and has potential for leaks in the cold. The issue of water in the cartridges also needs to be considered. Despite being located well above the sea spray zone and out of direct precipitation, water still entered the cartridges. This issue could potentially be solved by installing the cartridges in a screened box or similar. Finally, the mechanism of flow measurement was difficult to perform. Running a power lead out the external door on 05 Deck was not ideal when the ship had any kind of roll. A simple fix to this would be the use of a battery-operated flow meter.

The policy of calling in and out of the aerosol sampling lab worked well. The installation of the camera should make it possible for those working in the lab to visit alone in the future should they be unable to find accompaniment.

Summary

The PCAN project has been greatly successful on board IN2017-V01. It is hoped data from this voyage can contribute to increased understanding of aerosol populations in the Antarctic polar cell. Operational challenges were faced, as with any fieldwork. However, data processing is expected to remove any contamination and lead to useful and exciting products.

SECTION 9. CSIRO Educator at Sea

Educator on Board – Stuart Gifford

BACKGROUND:
The CSIRO Educator on Board is an initiative run by the CSIRO Marine National Facility. The program offers Australian school teachers the opportunity to join research voyages on board the RV *Investigator* to work alongside scientists as an 'Educator on Board'. The program used the Totten Glacier voyage as a pilot, with the formal Educator on Board intended to be launched later in 2017. The purpose of this program is to turn the RV *Investigator* into a floating classroom for both teachers and students.

The Marine National Facility (MNF) which operates the RV *Investigator* has as one of its business objectives to provide student training opportunities, promote marine science, as well as STEM (science, technology, engineering and mathematics) studies and support the development of future generations of marine researchers.

To help achieve this objective, the MNF is offering Australian school teachers the opportunity to join research voyages on board RV *Investigator* and work alongside scientists as an 'Educator on Board'.

The Educator on Board program seeks to promote real-world application of STEM studies to Australian students, and highlight the importance and opportunities within the marine sciences. Teachers selected for the program will coordinate, develop and deliver a range of educational and outreach activities, including during the voyage by delivering live video broadcasts from the ship to classrooms across Australia. They will use the MNF website and CSIRO social media channels as an outreach base to share the story of the ship and its research with students, families, and the community.

Teachers selected will also develop curriculum resources to allow other teachers across Australia to use the ship and its research in teaching and learning programs within their own STEM curriculum.

Stuart Gifford of Taroona High School, Tasmania, was selected as the first 'Educator on Board'. He participated in many science activities to gain experience then conducted lessons with classrooms in Australia via a tablet computer and the ship's wifi internet connection (Fig. 88). Stuart moved around the vessel talking to scientists and crew while filming activities. His observations and experience is detailed below.

Figure 88. Stuart in action on the RV Investigator experiencing microscopic observation of living phytoplankton samples at sea (left) and sediment description and sampling (middle) and in action during a direct link to Primary school classes (right). *Photos D. Thost/MNF.*

PERSONAL OBSERVATIONS AND EXPERIENCE:

Being a part of the pilot program was something that I never thought would be possible, so to be asked to apply and eventually win my spot on the ship was a privilege. Being the first teacher to be on an 'Educator on Board' voyage certainly had its successes, as well as challenges.

Due to the multidisciplinary nature of the voyage, I was able to observe and assist in a wide range of scientific fields that occurred throughout the expedition. The sciences included atmospherics, geoscience, hydrochemistry, sedimentology, as well as meteorology. My role also gave me the opportunity to help with the deployment and retrieval of the equipment, which provided a first-hand view of the process of data collection, from the launching of the gear to the final stages of collecting and storing of the samples.

What I learnt working alongside the students and scientists will be something that I can bring back to my own classroom, especially in sedimentology, as I had minimal experience in this before the mission. Understanding the process in testing seawater will also help my own classes, as this helped to consolidate my prior knowledge of this particular science. Working under the calibre of scientists such as Assoc. Prof. Leanne Armand and her team was a career highlight, and the opportunities for me to learn new skills was endless.

Maintaining a daily blog about my personal experiences was an important part of my role as Educator on Board, and knowing that it was reaching out to a wide ranging audience meant that I was bringing the science and life on board to a number of interested stakeholders. I enjoyed writing them, and everyday there were moments where I thought that would be a good blog topic. I was never short of things to write about, and the positive feedback from the blogs also inspired me to help promote STEM to the wider community. I am very appreciative of the efforts put in by Asaesja Young, who had to proof read and edit every blog before it was posted

Developing resources based on the science conducted, and in particular different units on types of sediments, and what that means in relation to the history of the Earth, will also benefit classes around Australia, especially as it helps to fill a void in geoscience; there aren't many educational units based on this particular field. Working in conjunction with Dr. Ben Arthur with what I was developing was extremely beneficial as it would have been very difficult to produce these plans without his guidance.

Another successful aspect of the pilot program was the use of WebEx conferencing. When it worked, it was a unique way to present the ship and the science back to the classrooms. I certainly had fun hosting these, and from the feedback I received from the teachers they were also very impressed with the ship, the science and delivery of the content. The following is a list of organisation and schools who signed up to a WebEx conference:

- BHP Billiton Science and Engineering Awards Camp – Participants from all over Australia
- Antarctic Experience – Participants from all over Australia
- Taroona High School – Tasmania
- Ithaca Creek State School – Queensland
- Fadden Primary School – Australian Capital Territory
- Mercedes College – Western Australia
- Clarence High School – Tasmania
- Reddam House School – New South Wales
- Hughes Primary School – Australian Capital Territory

Other schools also showed an interest, however due to time constraints, and issues beyond our control, we didn't get a chance to do a linkup. However, they will be locked in on the next voyage where there is an educator on board.

In addition to these schools, I also got to conduct an experiment, as well as answer questions which were emailed to me from other schools. Vaucluse Public School's 5/6 class asked me to see how long it would take for boiling water to freeze on the deck of the ship. It was an informative and interesting experiment. Combined this and the use of WebEx is just another example of how technology can play such a huge role in the Educator on Board program.

Of course, there were a number of issues that I encountered, the internet access being one of the biggest. It was always going to be difficult, in terms of where we were in the Southern

Ocean, to consistently conduct WebEx conferences due to the availability of satellite coverage, therefore some schools missed out on their live link up with the ship, although we dealt with that as best we could.
Being the only teacher on board the vessel, it was also difficult to bounce ideas of people, although there were some scientists who I found to be very helpful in the designing of the lessons, and for that I'm very grateful for. Also knowing Ben was only a phone call away helped, as he made sure I was on the right track with my approaches to the pilot program. These concerns were more of an inconvenience, rather than a hindrance to the overall program. The benefits outweighed any negatives by a large margin, and being the pilot, there were always going to be a few teething issues.

I feel that after this expedition, I am better equipped to educate my students about Antarctic science and the research that is being undertaken. This experience cannot be replicated on land (although I will do my best to convey my new found knowledge to others). To be involved in this voyage, and all aspects of it, from working the deck, assisting in the lab, even communicating with the crew makes the Educator on Board program a once in a lifetime opportunity. Collecting the data is a vital part of the process; however the outreach adds priceless benefits.

Based on feedback from schools and Ben, the pilot program has been a success; certainly from my point of view it has been a very successful 51 day voyage, and one I will never forget. Being a part of this ground breaking study of the Sabrina coastline is something that I am truly grateful for. A big thank you has to go to Assoc. Prof. Leanne Armand, Chief Scientist, and Doug Thost, Voyage Manager, for delivering this expedition, and also to Matt Marrison, Max McGuire, and Dr. Ben Arthur and all the CSIRO and MNF staff involved for giving me the opportunity to be the pilot Educator on Board.

SECTION 10. CSIRO Communicator on board

INTRODUCTION

A CSIRO communication advisor was placed on board the ship to help promote the voyage and underway science. Interviews conducted with the principal investigators and other senior scientists on board helped identify suitable stories for media. Utilising photographs and video footage, story ideas were pitched to journalists which lead to more than twenty interviews and strong media coverage. Social media was also utilised to share facts about the voyage and announce milestones, as well as to promote the 11 students on board.

Methods

Communication channels used were mainstream media, ECOS, CSIRO blog, Sabrina Seafloor blog, Twitter, Facebook and Instagram.

RESULTS

More than twenty interviews were conducted from the date of departure to arrival. Media coverage included both international, national, state and local media, across both online, print, radio and television. Social media posts received good pick up and at least two tweets were within the top three in Australia for their specific day.

Table 21. Tally of Communication Events.

TV/radio/print/online items: 71 TV/radio/print/online audience reach*: 2,600,000 (*estimate only due to limitations of media monitoring) Facebook reach: 779,844 Twitter impressions: 4.8M with 954 tweets LinkedIn reach: 7,883 Instagram: 56,154 reach with 2,762 engagements	CSIRO blog hits: *Women in Science:* 1,378 views average time on page 4m9s (CSIRO av 3.05) *Ancient DNA:* 969 views, 3m18s ECOS story on aerosols: 205 views External research blog: 21,260 views CSIRO Intronaughts podcast: listened 428 times

Discussion

Overall the voyage received strong promotion via mainstream and social media. A catalogue of photographs and video footage was collected and will remain on file with the Marine National Facility to use in future communication. A number of short videos will also be produced, highlighting the excellent science the ship enables.

SUMMARY AND HIGHLIGHTS

The voyage received strong international, national, state and local coverage as well as high interest and engagement on social media. Highlights included:

- Strong mainstream and social media reach, with a number of national and international stories, including multiple stories in Fairfax and Guardian mastheads.
- Voyage departure story in The Guardian attracted an international audience and was shared more than 1600 times
- National television coverage for voyage departure and return.
- Regular radio segments delivered throughout duration of voyage.
- High-impact story delivered about organisms living on the East Antarctic sea floor.
- Engaging and reusable photographic and video content produced.
- More than 250,000 audience captured with two Triple J interviews.
- Well-received social media campaign highlighting student scientists delivered.
- 10+ future marine scientists received comprehensive media training package and communication exposure.

SECTION 11. Summary of survey results and operations

The Sabrina Sea Floor Survey (IN2017-V01) was highly successful in obtaining long cores that probably contain paleoclimate records covering several glacial cycles, which was the main component of the science proposal. It was also highly successful at obtaining multiple supporting data sets and the piggy back atmospheric aerosol program PCAN was also successful. The long list of “firsts” and success has already been given above.

The survey benefited from good weather in the survey area, however, this was balanced by drifting pack ice that prevented access to all of our highest priority area. The pack was light but the low ice rating of the vessel meant avoidance was a priority. The piston coring equipment proved difficult to deploy and this is the subject of post-survey work by the MNF. We also encountered a number of issues with the laboratories, which have also been described in internal reports to the MNF.

In summary, the *RV Investigator* and its crew, MNF staff and the science party performed very well in the vessel’s first dedicated Antarctic geoscience voyage.

SECTION 12. The Last Word

As the Chief Scientist, I would like to acknowledge here the efforts of ALL who sailed and participated on this first voyage to Antarctica on the RV *Investigator*. It was truly the best of research voyages to have led and benefitted through the good will and support of many, including those who did not sail but supported the voyage from Australia or elsewhere in the world. To the students who sailed for the first time, you were all brilliant and my hope is that you will all find your own successful research pathways to get you back on board investigating the Earth's oceans and seafloor; we need your talents and enthusiasm to continue discovering and understanding our blue planet. To my colleagues on board, your support, expertise and good humour made this voyage a pleasure to lead and I thank you for your confidence in my role debut. To both Phil, my co-chief, and Mike, the Captain, thanks for letting me work out this Chief Scientist gig and guiding me especially when the Antarctic conditions or equipment didn't always work in our favour.

Finally, we lost a colleague recently who backed this voyage from the start. Gene Domack was a friend and colleague to many of us, and a principle researcher and ideas man on Antarctic geology and climatic evolution. May he rest in peace.

SECTION 13. References

AITKEN, A. R. A., YOUNG, D. A., FERRACCIOLI, F., BETTS, P. G., GREENBAUM, J. S., RICHTER, T. G., ROBERTS, J. L., BLANKENSHIP, D. D. & SIEGERT, M. J. 2014. The subglacial geology of Wilkes Land, East Antarctica. *Geophysical Research Letters,* 41**,** 2390-2400.

ALLEY, R. B., MAROTZKE, J., NORDHAUS, W. D., OVERPECK, J. T., PETEET, D. M., PIELKE, R. A., PIERREHUMBERT, R. T., RHINES, P. B., STOCKER, T. F., TALLEY, L. D. & WALLACE, J. M. 2003. Abrupt climate change. *Science,* 299**,** 2005-2010.

CHURCH, J. A., CLARK, P. U., CAZENAVE, A., GREGORY, J. M., JEVREJEVA, S., LEVERMANN, A., MERRIFIELD, M. A., MILNE, G. A., NEREM, R. S. & NUNN, P. D. 2013. Sea level change. *In:* STOCKER, T. F., QIN, D., PLATTNER, G.-K., TIGNOR, M., ALLEN, S. K., BOSCHUNG, J., A., N., XIA, Y., BEX, V. & MIDGLEY, P. M. (eds.) *Climate Change 2013: The Physical Science Basis. Contribution of Working Group I to the Fifth Assessment Report of the Intergovernmental Panel on Climate Change* Cambridge, United Kingdom and New York, NY, USA: Cambridge University Press.

COFAIGH, C. O., DOWDESWEL, J. A., EVANS, J. & LARTER, R. D. 2008. Geological constraints on Antarctic palaeo-ice-stream retreat. *Earth Surface Processes and Landforms,* 33**,** 513-525.

COOK, C. P., VAN DE FLIERDT, T., WILLIAMS, T., HEMMING, S. R., IWAI, M., KOBAYASHI, M., JIMENEZ-ESPEJO, F. J., ESCUTIA, C., JAIRO GONZALEZ, J., KHIM, B.-K., MCKAY, R. M., PASSCHIER, S., BOHATY, S. M., RIESSELMAN, C. R., TAUXE, L., SUGISAKI, S., LOPEZ GALINDO, A., PATTERSON, M. O., SANGIORGI, F., PIERCE, E. L., BRINKHUIS, H. & SCIENTISTS, I. E. 2013. Dynamic behaviour of the East Antarctic ice sheet during Pliocene warmth. *Nature Geoscience,* 6**,** 765-769.

Droplet Measurement Technologies, Inc. (2009). *Cloud Condensation Nuclei Counter (CCN-100) Operator Manual.* Boulder: Droplet Measurement Technologies, Inc.

Ecotech Environmental Monitoring Solutions. (2011). *Aurora 4000 Polar Nephelometer User Manual.* Ecotech Environmental Monitoring Solutions.

GRIMM Aerosol Technik GmbH & Co. KG. (2011). *Manual for CPC Model 5.420.* Dorfstraße: GRIMM Aerosol Technik GmbH & Co. KG.

GWYTHER, D. E., GALTON-FENZI, B. K., HUNTER, J. R. & ROBERTS, J. L. 2014. Simulated melt rates for the Totten and Dalton ice shelves. *Ocean Science,* 10**,** 267-279.

JEFFREY, S. W. & HUMPHREY, G. F. 1975. NEW SPECTROPHOTOMETRIC EQUATIONS FOR DETERMINING CHLOROPHYLL A CHLOROPHYLL B CHLOROPHYLL C-1 AND CHLOROPHYLL C-2 IN HIGHER PLANTS ALGAE AND NATURAL PHYTO PLANKTON. *Biochemie und Physiologie der Pflanzen (BPP),* 167**,** 191-194.

JENKINS, A., DUTRIEUX, P., JACOBS, S. S., MCPHAIL, S. D., PERRETT, J. R., WEBB, A. T. & WHITE, D. 2010. Observations beneath Pine Island Glacier in West Antarctica and implications for its retreat. *Nature Geoscience,* 3**,** 468-472.

JOHN, S. G., MENDEZ, C. B., DENG, L., POULOS, B., KAUFFMAN, A. K. M., KERN, S., BRUM, J., POLZ, M. F., BOYLE, E. A. & SULLIVAN, M. B. 2011. A simple and efficient method for concentration of ocean viruses by chemical flocculation. *Environmental Microbiology Reports,* 3**,** 195-202.

KHAZENDAR, A., SCHODLOK, M. P., FENTY, I., LIGTENBERG, S. R. M., RIGNOT, E. & VAN DEN BROEKE, M. R. 2013. Observed thinning of Totten Glacier is linked to coastal polynya variability. *Nature Communications,* 4.

LANDRY, M. R., PETERSON, W. K. & LORENZEN, C. J. 1995. Zooplankton grazing, phytoplankton growth, and export flux: inferences from chlorophyll tracer methods. *ICES Journal of Marine Science*, 52, 337-345.

MACKINTOSH, A., GOLLEDGE, N., DOMACK, E., DUNBAR, R., LEVENTER, A., WHITE, D., POLLARD, D., DECONTO, R., FINK, D. & ZWARTZ, D. 2011. Retreat of the East Antarctic ice sheet during the last glacial termination. *Nature Geoscience,* 4**,** 195-202.

MASSON-DELMOTTE, V., SCHULZ, M., ABE-OUCHI, A., BEER, J., GANOPOLSKI, A., GONZÁLEZ ROUCO, J., JANSEN, E., LAMBECK, K., LUTERBACHER, J. & NAISH, T. 2013. Information from paleoclimate archives. *In:* STOCKER, T. F., QIN, D., PLATTNER, G.-K., TIGNOR, M., ALLEN, S. K., BOSCHUNG, J., A., N., XIA, Y., BEX, V. & MIDGLEY, P. M. (eds.) *Climate Change 2013: The Physical Science Basis. Contribution of Working Group I to the Fifth Assessment Report of the Intergovernmental Panel on Climate Change.* Cambridge, United Kingdom and New York, NY, USA: Cambridge University Press.

NBP1402 SCIENTIFIC PARTY, 2014, NBP1402, Sabrina Coast, Marine Record of Cryosphere-Oean Dynamics, 467 pp.

POLLOCK, R. 2002. *South Tasman Rise* [Online]. Geoscience Australia. . Available: http://www.ga.gov.au/provexplorer/provinceDetails.do?eno=20917 [Accessed 28.2.2017].

PRITCHARD, H. D., ARTHERN, R. J., VAUGHAN, D. G. & EDWARDS, L. A. 2009. Extensive dynamic thinning on the margins of the Greenland and Antarctic ice sheets. *Nature,* 461**,** 971-975.

PRITCHARD, H. D., LIGTENBERG, S. R. M., FRICKER, H. A., VAUGHAN, D. G., VAN DEN BROEKE, M. R. & PADMAN, L. 2012. Antarctic ice-sheet loss driven by basal melting of ice shelves. *Nature,* 484**,** 502-505.

QUILTY, P. G., KERRY, K. R. & MARCHANT, H. J. 1985. A SEASONALLY RECURRENT PATCH OF ANTARCTIC PLANKTONIC DIATOMS. *Search,* 16**,** 48-48.

ROBERTS, J. L., WARNER, R. C., YOUNG, D., WRIGHT, A., VAN OMMEN, T. D., BLANKENSHIP, D. D., SIEGERT, M., YOUNG, N. W., TABACCO, I. E., FORIERI, A., PASSERINI, A., ZIRIZZOTTI, A. & FREZZOTTI, M. 2011. Refined broad-scale sub-glacial morphology of Aurora Subglacial Basin, East Antarctica derived by an ice-dynamics-based interpolation scheme. *Cryosphere,* 5**,** 551-560.

SMITH, J. A., HILLENBRAND, C.-D., KUHN, G., LARTER, R. D., GRAHAM, A. G. C., EHRMANN, W., MORETON, S. G. & FORWICK, M. 2011. Deglacial history of the West Antarctic Ice Sheet in the western Amundsen Sea Embayment. *Quaternary Science Reviews,* 30**,** 488-505.

Tekran Instruments Corporation. (2012). *Model 2537B Ambient Mercury Vapor Analyzer User Manual Rev: 3.12.* Tekran Instruments Corporation.

Thermo Fisher Scientific Inc. (2009). *Model 5012 Instruction Manual Multi Angle Absorption Photometer (MAAP).* Franklin: Thermo Fisher Scientific Inc.

TSI Incorporated. (2006). *Model 3776 Ultrafine Condensation Particle Counter Operation and Service Manual.* Shoreview: TSI Incorporated.

TSI Incorporated. (2009). *Series 3080 Electrostatic Classifiers Operation and Service Manual.* Shoreview: TSI Incorporated.

WEBER, M. E., CLARK, P. U., RICKEN, W., MITROVICA, J. X., HOSTETLER, S. W. & KUHN, G. 2011. Interhemispheric Ice-Sheet Synchronicity During the Last Glacial Maximum. *Science,* 334**,** 1265-1269.

WILLIAMS, G. D., MEIJERS, A. J. S., POOLE, A., MATHIOT, P., TAMURA, T. & KLOCKER, A. 2011. Late winter oceanography off the Sabrina and BANZARE coast (117-128 degrees E), East Antarctica. *Deep-Sea Research Part II-Topical Studies in Oceanography,* 58**,** 1194-1210.

WORDEN, A. Z. & BINDER, B., J. 2003. Application of dilution experiments for measuring growth and mortality rates among Prochlorococcus and Synechococcus populations in oligotrophic environments. *Aquatic Microbial Ecology*, 30, 159-174.

YOUNG, D. A., WRIGHT, A. P., ROBERTS, J. L., WARNER, R. C., YOUNG, N. W., GREENBAUM, J. S., SCHROEDER, D. M., HOLT, J. W., SUGDEN, D. E., BLANKENSHIP, D. D., VAN OMMEN, T. D. & SIEGERT, M. J. 2011. A dynamic early East Antarctic Ice Sheet suggested by ice-covered fjord landscapes. *Nature,* 474**,** 72-75.

SECTION 14. Appendix List

Appendices are downloadable separately to this Post-cruise report. Please see the ANU library website related to this doi for details.

Appendix No.	Sub Appendix No.	Title
1		IN2017_V01 Sample lists
	1.1	IN2017_V01 Quarantine Sediment sample lists
	1.2	IN2017_V01 Quarantine Sediments and slides for USA lists
	1.3	IN2017_V01 Kasten Core u-channel record
	1.4	IN2017-V01 Quarantine Filtered seawater sample lists
	1.5	IN2017_V01 Quarantine Seawater Sample lists
2		IN2017_V01 Voyage manager situation reports
3		IN2017_V01 Seismic acquisition system
4		IN2017_V01 Core logs and data
5		IN2017_V01 Core coarse fraction descriptions
6		IN2017_V01 Phytoplankton Observations
	6.1	IN2017_V01 Kasten Core Smear Slide Diatom Observations
	6.2	IN2017_V01 Underway Sieved Samples Diatom Observations
	6.3	IN2017_V01 SingleCellSeq
	6.4	IN2017_V01 Radiolarian_photos_PN07
	6.5	IN2017_V01 Piston Core Smear Slide Diatom Descriptions
	6.6	IN2017_V01 Radiolarian photos from Kasten cores
7		IN2017_V01 CTD_metadata
8		IN2017_V01 Sea ice reports (combined)
9		IN2017_V01 Cetacean sitings
10		IN2017_V01 PCAN event log